International Conference on Calcium Aluminates 2026

Proceedings of the 2026 International Conference on Calcium Aluminates

Lausanne; 8 – 11 June 2026

Editors: Matthew P. Adams, Elsa Qoku, and Jason H. Ideker

The Proceedings of the 2026 International Conference on Calcium Aluminates

Co-Edited by:

Matthew P. Adams, Associate Professor, New Jersey Institute of Technology, Newark, NJ, USA

Elsa Qoku, Research Group Leader, Technische Universität Braunschweig, Braunschweig, Germany

Jason H. Ideker, Professor, Oregon State University, Corvallis, OR, USA

Held in Lausanne, CH 8 – 16 June, 2026

Cover photos ourtesy of papers contained in this proceedings

Top Left: Hizballah et al.; “Understanding Biodeterioration Mechanisms of a Calcium Aluminate-Based Coating Affected by Substrate Cracking”

Top Right: Katagiri et al.; “Ultra-Rapid Hardening Repair Mortar with Amorphous Calcium Aluminates for Frezer Floor Applications at -25 ℃”

Middle: Valix et al.; “Performance Assessment of Specialty Cements for Manhole Construction in Australian Sewer Infrastructure”

Table of Contents

Topic: Ettringitic Systems

Topic: Biogenic Corrosion

Topic: Carbon Footprint

Topic: Durability

International Conference on Calcium Aluminates 2026

Conventional and potential alternative non-conventional raw materials for the production of calcium aluminates-based cements of different hydraulic activity.

Dominika Madej[1*], Wojciech Kagan[2], Piotr Palichleb[2] and Michał Karolczyk[2]

[1]AGH University of Krakow, Faculty of Materials Science and Ceramics, Department of Ceramics and Refractories, al. A. Mickiewicza 30, 30-059 Krakow, Poland
*dmadej@agh.edu.pl

[2]Górka Cement Sp. z o.o., ul. Lipcowa 58, 32-540 Trzebinia

Abstract: Calcium aluminate cements (CACs) are well known for their rapid setting characteristics and refractory performance, owing to their significant early strength gain and excellent thermal stability. The properties of CACs vary based on their alumina content. Global demand for CACs has shown consistent growth in recent years. However, this projected rise in production is likely to intensify the demand for natural raw materials such as limestone and bauxite, thereby increasing the environmental impact-particularly due to emissions associated with limestone calcination. Numerous conventional and alternative raw materials have been identified and studied within CAC technology, owing to their multiple advantages, including cost reduction, lower carbon emissions, and enhanced sustainability. This study tackles the combined challenges of incorporating alternative raw materials and developing hydraulic binders exhibiting diverse hydration characteristics.

Keywords: calcium aluminate cement, hydration, raw materials, high-temperature processes, refractory castables

1. INTRODUCTION

The current development of engineering and technology is strongly dependent on the type and availability of binding materials, particularly those designed for specialized applications such as unshaped refractories and building materials. aluminate cement from bauxite and limestone [1-2].

Calcium aluminate cements (CACs) are a class of hydraulic binders characterized by rapid strength development, high refractory performance, and good resistance to chemical attack. They are typically synthesized from alumina- and calcium-rich raw materials, most commonly bauxite and limestone. Bauxite serves as the primary source of Al_2O_3, while limestone provides CaO upon thermal decomposition.

The production process generally involves the homogenization of raw materials followed by high-temperature treatment, during which a series of solid-state reactions and partial melting phenomena occur. These processes lead to the formation of key calcium aluminate phases, such as $CaAl_2O_4$ (CA) and $CaAl_4O_7$ (CA_2), which are primarily responsible for the hydraulic properties of CAC. The phase composition and microstructure of the final product depend strongly on factors such as the Al_2O_3/CaO ratio, impurities (e.g., SiO_2 and Fe_2O_3), and the applied thermal regime.

During synthesis, the presence of silica and iron oxides may result in the formation of secondary phases, including calcium aluminosilicates and ferrites, which can influence both the melting behavior and the mechanical performance of the cement. Therefore, careful control of raw material composition and processing conditions is essential to tailor the properties of CAC for specific applications, particularly in refractory and high-temperature environments.

In recent years, increasing attention has been paid to the use of alternative alumina sources in the production of calcium aluminate cements, driven by the limited availability and rising cost of high-grade bauxite. Among these alternatives, electrocorundum has emerged as a promising raw material due to its high Al_2O_3 content and well-defined phase composition, which can enhance the formation of desired calcium aluminate phases [3-4].

Additionally, secondary industrial by-products, such as return dusts generated during clinker production, are being explored as supplementary raw materials. These dusts often contain significant amounts of reactive oxides, including Al_2O_3, CaO, SiO_2, and Fe_2O_3, and can contribute to the formation of complex phase assemblages during high-temperature processing. Their utilization not only reduces the consumption of natural resources but also supports waste valorization and circular economy approaches.

However, the variability in chemical composition and the presence of minor impurities in such alternative materials require careful characterization and process optimization to ensure consistent phase development and desirable performance of the final cement product.

The aim of this study is to investigate the synthesis of calcium aluminate cement using alternative alumina-bearing raw materials, specifically metallurgical electrocorundum and secondary return dusts from clinker production, as substitutes for conventional bauxite. The work focuses on evaluating the influence of raw material composition on phase formation, high-temperature behavior, and the resulting phase evolution of the synthesized materials. Particular attention is given to the development of key calcium aluminate phases and the potential formation of secondary phases associated with impurity elements.

Additionally, the study seeks to assess the feasibility of utilizing industrial by-products as sustainable raw material sources, with the objective of reducing

dependence on primary resources while maintaining or improving the functional properties of calcium aluminate cement.

In this work, Górka Cement company has developed and commercialized a new class of hydraulic binders utilizing alternative raw materials derived from local and recycled sources. This innovative approach not only improves application performance but also enhances process efficiency and reduces overall production costs.

2. METHODOLOGY

2.1 Materials

A commercially produced cement clinker composition and four laboratory-developed clinker compositions were created and produced using alternative raw materials. The batch compositions of the samples were as follows: *Sample 1* (as reference) was composed of bauxite and limestone; *Sample 4* was composed of metallurgical electrocorundum, limestone and return dust from GÓRKAL 40 clinker production with reduced SiO_2 content; *Sample 5* was composed of metallurgical electrocorundum, limestone and return dust from GÓRKAL 40 clinker production with increased content of SiO_2; *Sample 6* was composed of metallurgical electrocorundum, limestone and bauxite with reduced content of SiO_2; *Sample 7* was composed of metallurgical electrocorundum, limestone and bauxite with increased content of SiO_2. The samples were wet-milled to obtain suspension, thoroughly homogenized, and then dried to produce a fine powder. In the next step, the dry powder was pressed into cylindrical samples and then fired at 1350°C for 2 hours.

2.2 FACTSAGE 8.4 thermodynamic simulation

Thermodynamic evaluations of the sinterability of cement clinkers were performed using FactSage (version 8.4). The simulations utilized the FTmisc 8.4, FToxid 8.4, and FactPS 8.4 databases in combination with the EQUILIB module to establish equilibrium conditions. The chemical compositions of the mixtures were determined based on the data presented in Table 1. Calculations were conducted under an air pressure of 1 atm across a temperature range of 1000°C to 1700°C, with increments of 50°C. The results provided insights into the temperature-dependent evolution of the liquid phase content.

Table 1. Chemical composition of samples.

Oxides	Sample 1	Sample 4	Sample 5	Sample 6	Sample 7
SiO_2	4.79	2.99	5.02	3.36	4.26
TiO_2	2.23	0.38	0.37	0.34	0.33
Al_2O_3	53.96	51.55	51.15	50.41	50.69
Fe_2O_3	2.01	2.72	2.66	2.84	2.63
CaO	37.00	42.35	40.80	43.06	42.08

2.3 Heating Microscope Thermal Analysis (HMTA)

Laboratory-scale heating microscopy thermal analysis (HTMA) was used to examine the dimensional changes of mixtures derived from raw materials during thermal treatment. Homogenized powder mixtures were formed into cubic specimens with a height of 3 mm using a manual press. The samples were heat treated from room temperature up to 1500°C at a heating rate of 10°C/min. The measurement were carried out using Linseis L74 Heating Microscope. Sample height measurements were collected at 1°C intervals, from which shrinkage curves were derived. The relative height change (δh) was calculated according to Eq. (1).

$$\delta_h(T) = \frac{h(T)}{h_0} \times 100, \% \qquad (1)$$

where:
h_0 – initial height of the sample,
$h(T)$ – height of the sample at elevated temperature T.

2.4 Phase composition (XRD)

X-ray diffraction (XRD) patterns were recorded using the PANalytical X'Pert Pro diffractometer over a 2θ range of 15°–50°, with Cu Kα radiation (λ = 1.54060 nm) at an operating voltage of 45 kV and a step size of 0.008°. Phase identification was performed using HighScore Plus in conjunction with the ICDD PDF-2 and JCPDS databases (Powder Diffraction Files, Philadelphia, PA, USA, 1997). Prior to analysis, the castable samples were ground in a ball mill to obtain fine powders with particle sizes below 63 μm.

3. RESULTS AND DISCUSSION

3.1 FACTSAGE 8.4 thermodynamic simulation and Heating Microscope Thermal Analysis (HMTA)

The synthesis of cement clinker is a highly complex, multidimensional process, making its accurate reproduction under laboratory conditions inherently difficult. One experimental approach that approximates this process is Heating Microscope Thermal Analysis (HMTA), which is now often supplemented with thermochemical modelling. The FactSage software was used to model the quantity of the liquid phase as a function of temperature. The results of modelling are presented in Fig. 1. Figure 2 illustrates the relative change in sample height, $\delta_h(T)$, for the tested materials. Based on the results from the high-temperature microscope, it can be observed that up to 1300°C the curves follow a similar trend. However, above 1300°C, Sample 1 exhibits the highest thermal stability. As shown in Figures 1 and 2, the shrinkage curve of these samples is closely correlated with the liquid phase content determined in FactSage thermochemical calculations. This relationship is most clearly observed for the two extreme samples, 1 and 6, as well as for sample 5. In contrast, no clear correlation is found for samples 4 and 7, which may be

related to the viscosity of the liquid phase. Images of the samples at 1350 °C recorded during *in situ* measurements clearly confirm shrinkage in Samples 1, 4, and 5, as well as softening in Sample 7 and melting in Sample 6 (Fig. 3).

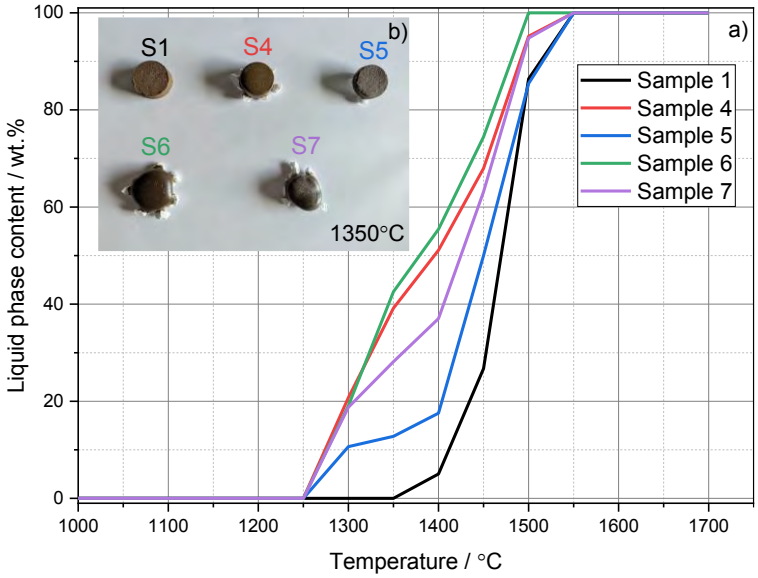

Fig. 1. Liquid phase content of the individual samples as a function of temperature, calculated by the FactSage software, additionally pictures of the samples after heat-treatment at 1350°C.

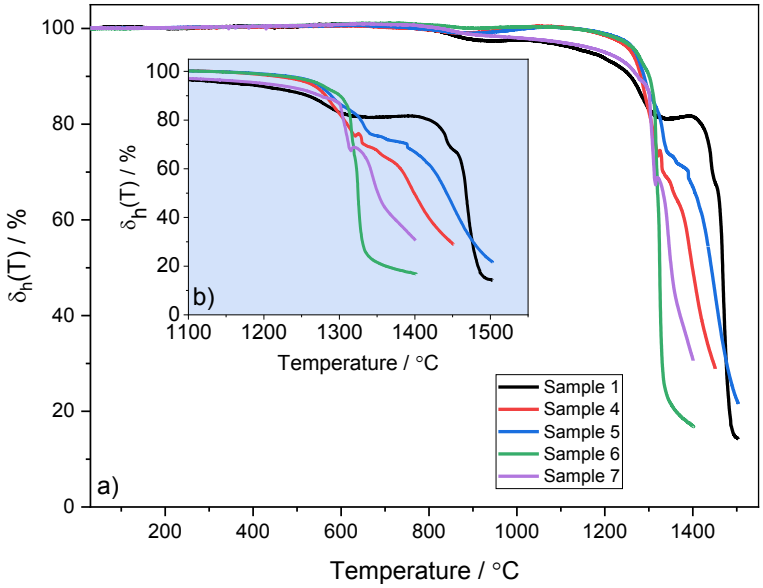

Fig. 2. Relative change in height $\delta_h(T)$ of the tested samples during heating.

Sample 1		
	cam0_img0	cam0_img7611
Sample 4	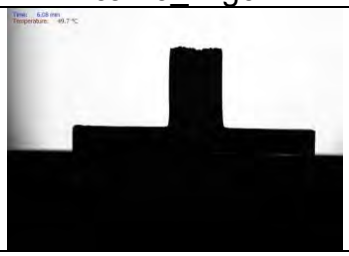	
	cam0_img0	cam0_img7603
Sample 5	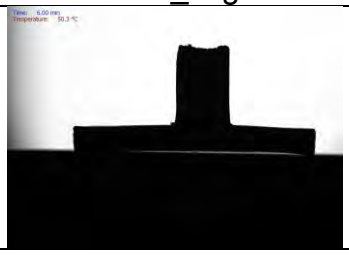	
	cam0_img0	cam0_img7601
Sample 6	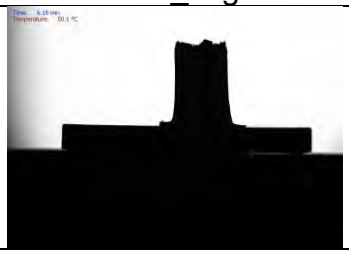	
	cam0_img0	cam0_img7600
Sample 7	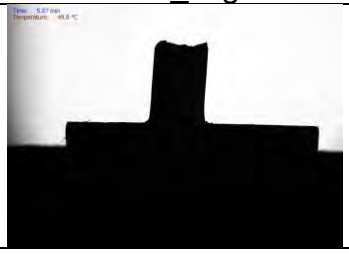	
	cam0_img0	cam0_img7599

Fig. 3. Images of the samples at 1350°C (right) recorded during *in situ* measurements. On the left-hand side, the sample is shown at room temperature.

3.2 Phase composition (XRD)

A XRD-based phase-composition analysis of (Fig. 4) shows the presence of $CaAl_2O_4$ (CA) and $Ca_2Al_2SiO_7$ (C_2AS) in Sample 1; $CaAl_2O_4$ (CA), $Ca_{12}Al_{14}O_{33}$ ($C_{12}A_7$), $Ca_2Al_2SiO_7$ (C_2AS), Ca_2SiO_4 (C_2S) and $CaAl_{0.5}Fe_{0.5}O_{2.5}$ (C_4AF) in Samples 4, 6 and 7; $CaAl_2O_4$ (CA), $Ca_{12}Al_{14}O_{33}$ ($C_{12}A_7$), $Ca_2Al_2SiO_7$ (C_2AS) and Ca_2SiO_4 (C_2S) in Sample 5.

The results indicate a clear variation in phase assemblage depending on the sample composition, particularly with respect to the presence of iron-bearing phases. The occurrence of C_4AF in Samples 4, 6, and 7 suggests the incorporation of Fe into the crystal structure, which may significantly influence the high-temperature behavior of these materials, including their melting and softening characteristics. In contrast, the absence of this phase in Samples 1 and 5 points to a comparatively simpler phase composition.

Furthermore, the coexistence of calcium aluminate (CA, $C_{12}A_7$) and calcium aluminosilicate (C_2AS) phases across most samples indicates partial interaction between alumina- and silica-rich components. The presence of C_2S in selected samples (4, 5, 6, and 7) may also contribute to the formation of a liquid phase at elevated temperatures, thereby affecting densification, shrinkage, and viscosity during thermal treatment.

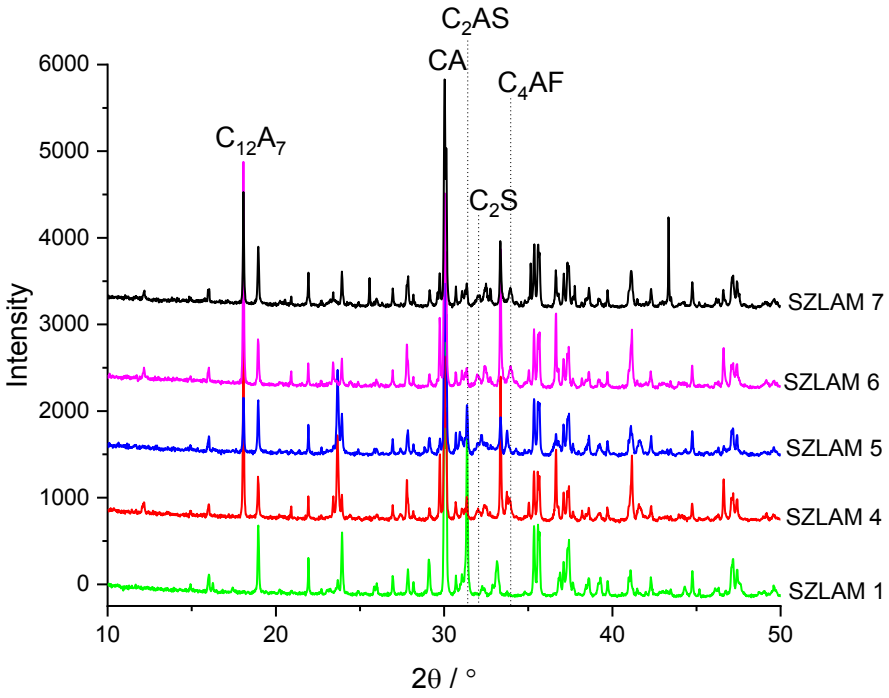

Fig. 4. X-ray diffraction patterns of the samples.

Conclusions

The results of this study demonstrate that the unique raw material composition has a significant influence on the phase assemblage of the investigated materials. Variations in the proportions and types of alumina- and calcium-bearing components, as well as the presence of minor constituents such as iron and silica, lead to noticeable differences in the formation and stability of crystalline phases. In particular, the use of alternative alumina sources and secondary raw materials promotes the development of complex phase systems, including calcium aluminate, calcium aluminosilicate, and ferrite phases.

These findings confirm that the specific chemical and mineralogical characteristics of the starting materials play a decisive role in determining the final phase composition, and consequently the high-temperature behavior and potential performance of the synthesized products.

Importantly, the application of secondary raw materials enabled a reduction in the firing temperature required for material synthesis. This effect is attributed to the presence of admixtures, which promote earlier liquid-phase formation and enhance solid-state diffusion processes during thermal treatment. As a result, densification and phase formation occur at lower temperatures compared to compositions based solely on conventional raw materials.

Acknowledgements

This work is supported by Górka Cement Sp. z o.o. Company. This work was also partly supported by the statutory funds of the Faculty of Material Science and Ceramics AGH University of Krakow, Poland with the Agreement no. 16.16.160.557. This research was also supported by the "Research project „Excellence initiative – research university" for the AGH University" grant ID 13447.

References:

1. An overview of practical challenges and current advances related to calcium aluminate cement systems, *Journal of Building Engineering* (2025).
2. Roy et al., "Beyond Bauxite or Alumina: A Review of Alternative Alumina Rich Sources for Calcium-Sulfo Aluminate Cement Production," *Nordic Concrete Research* (2025).
3. Calcium aluminate cement production and raw material considerations, *ScienceDirect Topics / Cement Clinker Overview*.
4. Hewlett, P.C. (Ed.), *Lea's Chemistry of Cement and Concrete*, 4th ed., Arnold.

International Conference on Calcium Aluminates 2026

PRECIZE: A NOVEL APPROACH TO DECARBONIZING SPECIALTY BINDERS THROUGH HYDROGEN COMBUSTION

Kumar, Bela[1], Elorza Ricart, Enrique[1], Maach, Nicolas[1], Lenfant, Pascal[1], Parr, Chris[1]

[1]ITC (Imerys Technology Center) Lyon, 1, rue Le Chatelier, 38090, Vaulx Milieu, France, bela.kumar@imerys.com

Keywords: decarbonization, hydrogen fuel, calcium aluminate cements (CACs), CO_2 Emissions, performance

ABSTRACT

Addressing the significant CO_2 emissions from calcium aluminate cement (CAC) production is a critical challenge for the building and infrastructure sectors, with fossil fuels accounting for a large portion of the greenhouse gas (GHG) footprint. To tackle this, we initiated the PRECIZE *(PRocédé ÉCologique et Innovant de liants de spécialité Zéro Émission)* project, a strategic collaboration with Air Liquide, “Laboratoire de Génie Chimique” (LGC) in Toulouse, and “Conditions extrêmes et Matériaux: Haute Température et Irradiation” (CEMHTI) in Orléans. Funded by the French state as part of the France 2030 program and operated by ADEME, this initiative is a strategic component of our commitment to science-based targets. One of the key objectives of this project is to demonstrate a scalable pathway to decarbonize CAC production by replacing fossil fuels with a carbon-free alternative like hydrogen. Our study presents the methodology and findings of a successful 12-day pilot trial conducted at our Dunkerque site, detailing the progressive transition from a mixture of 100% natural gas to a 100% hydrogen. The results of this extensive pilot trial will be presented in this paper. We will provide a comprehensive analysis of the impact on CAC quality and performance, as well as on kiln behavior and stability.

INTRODUCTION

The PRECIZE project, a France 2030 initiative led by Imerys Aluminates and supported by ADEME, aims to decarbonize calcium aluminate production using hydrogen combustion. Central to this project is the validation of the proprietary Furnace Innovative Technology (FIT), following a successful 12-day industrial trial at the Dunkirk pilot plant in May 2025. Beyond fuel substitution, the study evaluates the impact of H_2/O_2 combustion on clinker mineralogy, refractory corrosion, and the calibration

*bela.kumar@imerys.com

of 3D CFD models. This paper details the trial methodology and provides a technical assessment of hydrogen's viability as a primary energy source. These findings establish the foundational scaling laws required to transition this low-carbon technology to full-scale industrial manufacturing.

METHODS

FIT pilot Operating principle

The FIT pilot is located at the Imerys Aluminates site in Dunkirk. This patented[1] furnace, developed over several years, has validated the production of calcium aluminates using alternative fuels. It also demonstrates the feasibility of producing clinker from alternative decarbonated raw materials sourced from the circular economy.
As part of the PRECIZE project, the pilot has been re-engineered with new refractories to accommodate a hydrogen combustion process. The process involves precisely dosing and conveying raw materials (limestone and bauxite with a small correction with sand) into the furnace via a screw feeder. A specialized multi-fuel burner was developed by consortium partner Air Liquide. Before injection, the hydrogen pressure is reduced to the required levels. The combustion sequence begins with the introduction of natural gas and/or hydrogen, using pure oxygen as the oxidizer for both. The burner targets the material pile to produce a molten clinker that exits the furnace in a liquid state, while combustion and reaction fumes are evacuated through the chimney.

Campaign

The campaign began and concluded with natural gas to establish a baseline. The hydrogen proportion was increased in 25% increments every two days, with a proportional decrease in natural gas, reaching 100% H_2 as shown in Figure 1., with a temporary return to natural gas on Day 7 due to supply logistics (Sunday). Although volumetric CO_2 emissions in the flue gas decreased as expected, residual CO_2 remained present even at 100% H_2 injection, due to the calcination of limestone within the process.

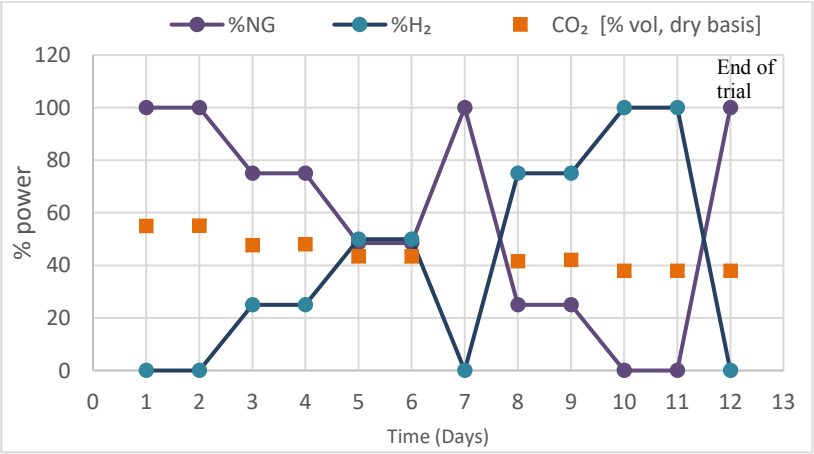

Figure 1. Evolution of Hydrogen and Natural Gas Power Consumption vs. Volumetric CO_2 Percentage

Air Liquide supplied the gaseous hydrogen via semi-trailers Figure 2, with an on-site pressure-reduction station regulating the flow. For the oxygen supply, a large-capacity storage tank was refilled throughout the campaign. To ensure precise monitoring during these transitions, a rigorous sampling protocol was implemented : samples were collected three times per shift. This systematic approach provided representative data to validate the material's consistency as the hydrogen ratio increased. The size of the sampler Figure 3 was designed and validated to obtain similar results to our Fusion plants.

Figure 2. Hydrogen semi-trailers secured by chain-link fencing and mandatory safety clearance distances

Figure 3. Clinker cooling in sampler

KEY FINDINGS

Product Quality: The clinker's chemistry, mineralogy, and color remained entirely unaffected by the switch to hydrogen/oxygen combustion, ensuring a seamless transition for existing applications. Chemical analyses under 75% and 100% H_2 atmospheres demonstrate the same proportions of major oxides—lime, alumina, iron, and silica—as observed in commercial calcium aluminate (Ternal Fondu). Regarding mineralogy, phase distributions remained consistent with reference values. Chemical compositions were accurately measured using X-ray Fluorescence (XRF), while mineralogical phases were determined via X-ray Diffraction (XRD) and quantified using the Rietveld refinement method.

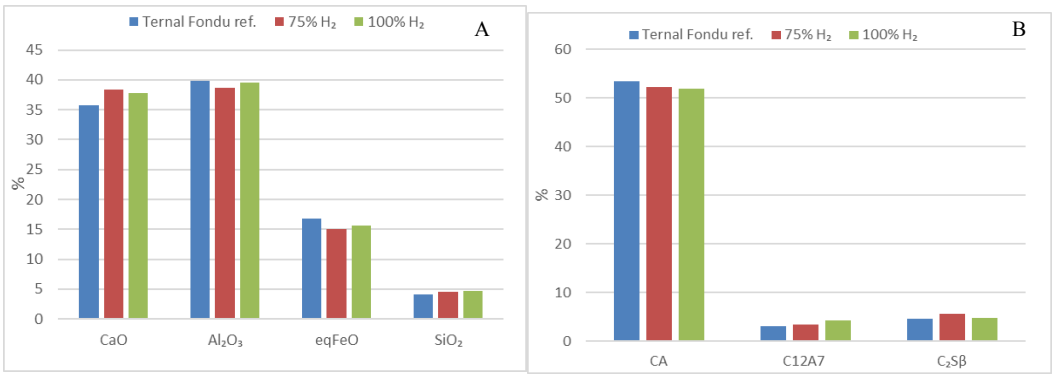

Figure 4. Comparison of major chemical oxides (A) and mineralogical phases (B): Clinker produced with 75% and 100% H_2 vs. standard Fondu.

Product Performance : Extensive application tests confirmed that the product works exactly as expected. Setting times and mechanical strengths (flexural and compressive) are equivalent (75% to 100%) to our traditional commercial calcium aluminate product (Ternal Fondu). These results were strictly validated according to international standards and internal protocols:

- Mortar Preparation: According to EN 14647.
- Setting Time : Measured via Vicat needle under demineralized water with an additional 700g mass, according to EN 196-3.
- Mechanical Strength: Test bars prepared according to EN 196-3.

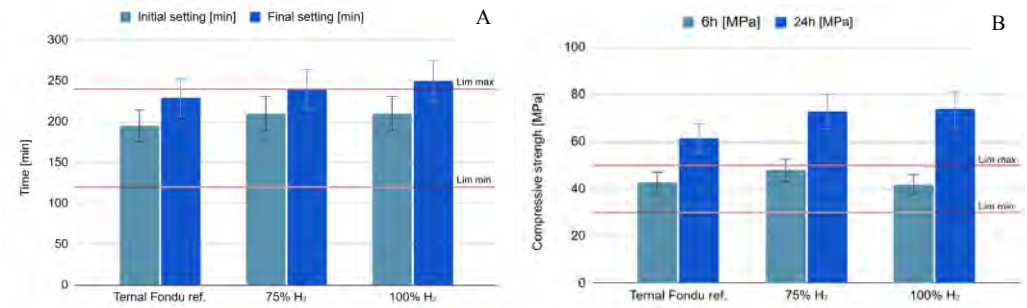

Figure 5 : Comparison of setting times (A) and compressive strengths (B) of clinker produced with 75% and 100% hydrogen vs. standard Fondu.

Kiln stability: The furnace performed reliably throughout all project phases. Furthermore, a post-mortem analysis confirmed that the refractory materials showed no signs of degradation despite the tough, hydrogen-rich and H_2O atmosphere.

CONCLUSION

The pilot tests for FIT technology, conducted as part of the Precize Project, have successfully validated the use of oxy-hydrogen combustion for the production of calcium aluminates at the Imerys Aluminates site in Dunkirk. Experimental results demonstrate that performance remains consistent, with the product's physicochemical properties staying strictly unchanged compared to conventional methods. This study represents a world-first demonstration of oxy-hydrogen as a primary fuel source for calcium aluminate fusion, offering a significant breakthrough for the decarbonization of high-temperature industrial processes.

REFERENCES

[1] Patent Publication No. WO/2017/009581, filed under the title « Process for manufacturing Calcium Aluminates ».

International Conference on Calcium Aluminates 2026

HYDRATION AND CONVERSION REACTIONS OF CALCIUM ALUMINATE CEMENT WITH REACTIVE CALCITE AT VARIABLE TEMPERATURES

Goetz-Neunhoeffer*, Friedlinde & Goergens, Julian, FAU Erlangen-Nürnberg, GeoZentrum Nordbayern, Mineralogy, Erlangen, Germany

Keywords: Calcium Aluminate Cement, Reactive Calcite, Quantitative XRD, Monocarbonate, Conversion

ABSTRACT

The reaction and potential transformation behaviour during hydration of a calcium aluminate cement (CAC) mixed with reactive calcium carbonate (Cc) were investigated at different temperatures.

By introducing CO_3^{2-} into the pore solution of the hydrating CAC through calcite dissolution, a promising way was investigated to avoid or limit the metastable hydrate phases (CAH_{10}, C_2AH_x) that typically occur during the early hydration of pure CAC. Instead, the precipitation of mainly monocarbonate (Mc = $C_3A*Cc*11H$), is favoured. Analysis of the extensive data base (10-90°C) has shown the general conditions and temperature limits under which Mc is formed and stabilized. At 60°C, no thermodynamic stability or formation limit of Mc is found. In closed systems studies no conversion of Mc to C_3AH_6 (or dissolution-precipitation) was observed up to 80°C. This probably only occurs above a critical temperature, which is specified in databases as approximately 90°C.

We were able to show in a large number of measurements that C_2AH_X acts as a precursor for Mc formation in the early hydration of mixtures of CAC and Cc. Below 20°C no or only a small amount of C_2AH_x and thus also no or only minor Mc should initially form in CA-dominated CAC-Cc pastes. Here, CAH_{10} is prevailing. At elevated temperatures (40°C and 60°C), at which CAH_{10} does not initially precipitate, Mc is formed as a result of the rapid conversion of the precursor phase C_2AH_X.

INTRODUCTION | BACKGROUND

CACs are mainly used in refractory applications and - together with OPC and calcium sulphate and/or CSA cement - in ternary mixtures (e.g. self-levelling screeds and grouts), as the addition of CACs promotes early setting and reduces shrinkage. White CACs contain mostly CA along with CA_2, often with minor amounts of $C_{12}A_7$ or Al_2O_3. However, CA is mostly domi-

*friedlinde.goetz@fau.de

nant and greatly determines the hydration behaviour. The frequently mentioned problem of "conversion" is unfortunately still very often interpreted as a disadvantage for the use of CAC in binder formulations.

The prevention of subsequent, often harmful conversion was investigated for mixtures of CAC with silicate-containing materials such as blast furnace slag, micro silica or fly ashes[1-3] or limestone-containing additives[4,5] or both[6-8]. Studies on these mixtures have shown that much lower amounts of metastable hydrate phases were formed in the presence of Si- or CO_2-containing materials. The mechanical properties of many of these mixtures also showed significantly better results compared to reference mixtures without. Among the materials added, limestone proved to be the most suitable [6,8].

CAH_{10}, Monocarbonate (Mc) and C_3AH_6, the stable phases that can form in CAC-Cc pastes, play a particularly interesting and crucial role here. However, some ambiguity remained regarding their formation and stability. Several authors reported differing temperature or stability limits[9,10] of Mc, others the potential conversion of Mc to C_3AH_6 (the reverse is also possible).

Since the formation of Ca-Al-hydrate phases during CAC hydration were reported to be highly temperature-dependent, the investigations were carried out at four different temperatures (10, 23, 40, and 60 °C). Despite many individual studies, there is a lack of comprehensive research and deeper understanding of very early hydrate phase formation in combination with long-term stable hydrate phase contents for a single type and source of CAC. We therefore chose mixes of Fe-free CAC with reactive calcite in order to specifically improve the state of knowledge. Within the scope of the investigation, all experimental parameters, such as the w/c ratio, storage conditions, sample size, parameters for XRD analysis, etc., were kept unchanged and only modified for specific questions.

METHODS

We mainly performed time-resolved QXRD on the hydration of a commercial CAC mixed with reactive calcite (Cc) (w/CAC ratio = 1.1) stored for periods ranging from 1 d to 12 months and analyzed them in terms of their absolute phase fraction using the Rietveld method and G-factor quantification Thermodynamic calculations using GEMS modeling were used to indicate which hydrate phases are the predicted stable phases under the respective conditions.

KEY FINDINGS

The results of the extensive study are summarized for early hydration (0-16 h, Figure 1) and long-term hydration (up to 12 months, Figure 2).

Summary of early hydration (Fig. 1)

Dissolution of CA, CA_2, and calcite during early hydration is shown by in-situ XRD at different temperatures as upper part of the diagrams in Fig. 1. At 10°C and 23°C, main hydration begins shortly before 4 h, with CA rapidly dissolving to a residual level. At 40°C, the induction period is shorter, while at 60°C, CA is completely dissolved within the first 16 h. Hydration of CA_2 is

not detected at 10°C, but at 23°C and above CA_2 starts dissolving simultaneously with CA, albeit at a slower rate.

The formed hydrate phases are presented in the lower part of Fig. 1. At 10°C, "metastable" CAH_{10} is the first and only hydrate phase. At 23°C, both CAH_{10} and C_2AH_x precipitate. While CAH_{10} is not re-dissolving within the first 16 h, the initially formed C_2AH_X decreases and Mc is formed instead.

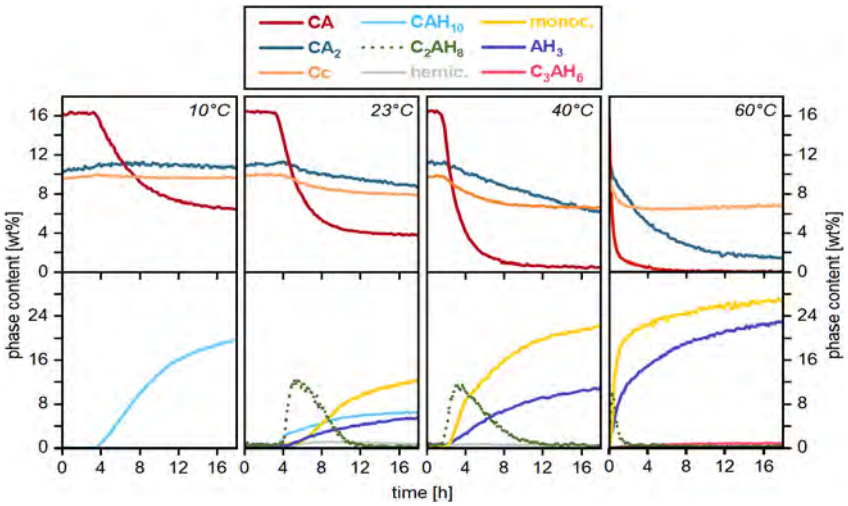

Figure 1: Mean values of the in-situ QXRD of the CAC-Calcite mixture with a w/CAC ratio of 1.1 of the first 16 h of the hydration are shown [12]. Rietveld scale factors of C_2AH_8 are plotted in dotted lines.

Overview of long-term hydration (Fig. 2)

Results of the CAC-Cc long-term tests demonstrated stable phase compositions and thus a high potential for applications in construction chemistry. At 5°C CAH_{10} remained the predominant hydrate phase until the end of the experiment after one year, with no signs of conversion. The coexistence of $AH_{3(am)}$ appears to condition CAH_{10}.

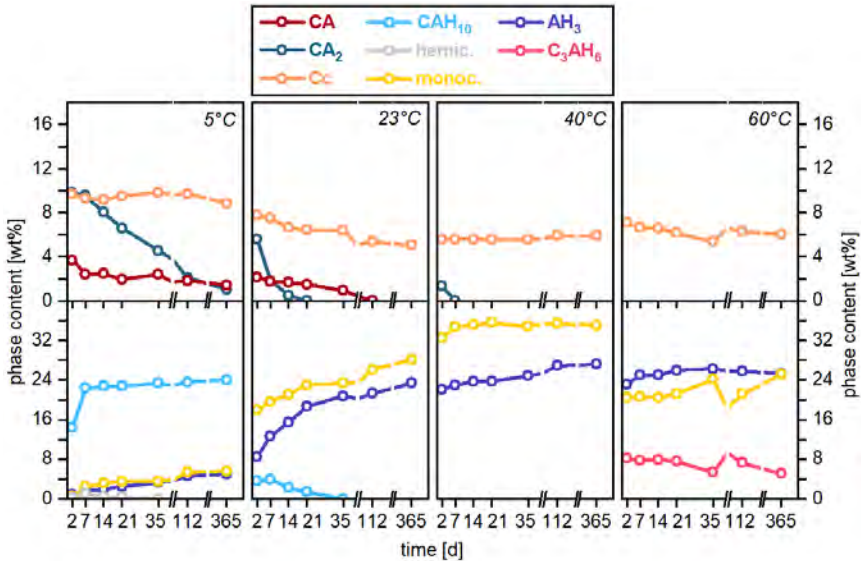

Figure 2: Mean values of the long-term sample QXRD (0-365 d) of the CAC-calcite mixture with a w/CAC ratio of 1.1 [13,14]

After the first day of hydration, C_2AH_x was no longer observed at any temperature in our investigations.
Mc was found to be stable[13,14] alongside AH_3 (Gibbsite) as the dominant phase across the entire temperature range from 5 to 60 °C. The conversion of Mc to C_3AH_6 could not be observed in a closed system at temperatures up to 80°C. However, evaporation of mixing H_2O in the early hydration stage stabilizes C_3AH_6 with a stoichiometric lower H_2O requirement than Mc.

CONCLUSIONS

- CA and CA_2 were completely dissolved within 365 days - at different rates - but only in the 5 °C samples were residues of <2 wt% detected.
- CAH_{10} is a “stable” hydrate phase at low temperatures for up to 365 d.
- The formation of Mc from CA in early hydration is preceded by precipitation of the precursor phase C_2AH_x.
- The AH_3 phase precipitates at all temperatures.
- No thermodynamic instability or formation limit of Mc was observed up to 60 °C.
- The evaporation of mixing H_2O at elevated temperatures shifts hydrate phase stability towards C_3AH_6 (lower w/Ca-ratio) instead of Mc.

REFERENCES

(1) Majumdar, A.J., Edmonds, R.N., Singh, B. (1990) “Hydration of calcium aluminates in presence of granulated blastfurnace slag”, in: R.J. Mangabhai (Ed.), Calcium Aluminate Cements, pp. 259–271.
(2) Fentiman, C.H., Rashid, S., Bayoux, J.P., Bonin, A., Testud, M. (1990) “The effect of curing conditions on the hydration and strength development in Fondu: slag” in: R.J. Mangabhai (Ed.), Calcium Aluminate Cements, pp. 272–281.
(3) Bentsen, S., Seltveit, A., Sandberg, B. (1990) “Effect of microsilica on conversion of high alumina cement, in: R.J. Mangabhai (Ed.), Calcium Aluminate Cements, pp. 294–319.
(4) Kuzel, H.J., Baier, H. (1996) “Hydration of calcium aluminate cements in the presence of calcium carbonate”, Eur. J. Mineralogy 8 129–141.
(5) Darweesh, H.H.M. (2004) “Limestone as an accelerator and filler in limestone-substituted alumina cement”, Ceram. Int. 30 145–150. https://doi.org/10.1016/S0272-8842(03)00073-7.
(6) Cussino, L., Negro, A. (1980) “Hydratation du ciment alumineux en presence d’agregat siliceux et calcaire”, in: /E Congr. Int. La Chim. Des Ciments, Commun. pp. 62–67.
(7) Puerta-Falla, G., Kumar, A., Gomez-Zamorano, L., Bauchy, M., Neithalath, N., Sant, G. (2015) “The influence of filler type and surface area on the hydration rates of calcium aluminate cement, Constr. Build. Mater. 96 657–665. https://doi.org/10.1016/j.conbuildmat.2015.08.094.
(8) Adams, M.P., Ideker, J.H. (2017) “Influence of aggregate type on conversion and strength in calcium aluminate cement concrete”, Cem. Concr. Res. 100 284–296. https://doi.org/10.1016/j.cemconres.2017.07.007.
(9) Midgley, H.G. (1984) “Measurement of high-alumina cement-calcium carbonate reactions using DTA”, Clay Miner. 19, 857–864. https://doi.org/10.1180/claymin.1984.019.5.13.
(10) Luz A.P., Pandolfelli V.C. (2012) “$CaCO_3$ addition effect on the hydration and mechanical strength evolution of calcium aluminate cement for endodontic applications”, Ceram. Int., 38, 1417–1425. https://doi.org/10.1016/j.ceramint.2011.09.021.
(11) Klaus, S.R., Neubauer J., Goetz-Neunhoeffer, F. (2013) “Hydration kinetics of CA_2 and CA - Investigations performed on a synthetic calcium aluminate cement”, Cem. Concr. Res. 43 62–69. https://doi.org/10.1016/j.cemconres.2012.09.005.
(12) Goergens, J., Manninger, T., Goetz-Neunhoeffer (2020) "In-situ XRD study of the temperature-dependent early hydration of calcium aluminate cement in a mix with calcite", Cem. Concr. Res. 136, 106160 https://doi.org/10.1016/j.cemconres.2020.106160.
(13) Goergens, J. (2024) “Hydration of calcium aluminate cement in mixtures with calcite: Investigations at different temperatures and CA_2/CA ratios, PhD thesis, FAU Erlangen-Nürnberg, https://doi.org/10.25593/open-fau-341.
(14) Goergens, J., Goetz-Neunhoeffer, F. (2021) “Temperature-dependent late hydration of calcium aluminate cement in a mix with calcite – Potential of G-factor quantification combined with GEMS-predicted phase content”, Cement 5, 1-13. doi.org/10.1016/j.cement.2021.100011

International Conference on Calcium Aluminates 2026

Influence of the type and amount of calcium sulfate on the hydration of a C12A7-based cement

Wolf, Julian[1], Polat, Buket[2], Avcioğlu, Berrak [1]

[1]Sabanci Technology Center GmbH, Freisinger Landstraße 50, Garching bei München, 85748, Germany, julian.wolf@sabancibs.com*,

[2]ÇİMSA ÇİMENTO
SANAYİ VE TİCARET A.Ş, TOROSLAR MAH. TEKKE CAD.
YENİTAŞKENT – AKDENİZ, Mersin, 33013, TÜRKIYE

Keywords: self-levelling underlayment, C12A7, calcium aluminate cement, calcium sulfates

ABSTRACT

Mayenite based cements allow for reduction of the global warming potential of dry-mix recipes compared to typical ternary binder system. With this technology you can achieve the same early age properties at a lower total binder content of the recipe compared to conventional ternary dry-mix recipes. Typically, these formulations are poor in Portland cement and calcium sulfates are added to maximize the early ettringite yield during hydration. The type and amount of calcium sulfate plays a critical role in the hydration behavior of mayenite-based systems and not a lot of research has been performed on this topic. In this work we investigated the influence the types and amounts of calcium sulfates have on the hydration of a C12A7-based cement. We investigated both a model system as well as a self-leveling underlayment recipe based on this technology.

It is shown that the reactivity of the calcium sulfate plays a significant role in the early strength build-up and ettringite formation rates. In addition, long term expansion is also significantly influenced by changes in the calcium sulfate types and different hydrate phase assemblages are observed.

This work provides a basis for further investigations within this system, in which, for example, the influence of various retarders and the amount of Portland cement on the hydration behavior and mechanical performance will be examined.

*email address of corresponding author

INTRODUCTION | BACKGROUND

In several special mortar applications rapid strength build-up and drying of the product is required. Conventionally ternay blends composed of calcium aluminate cement, ordinary Portland cement and calcium sulfates are used. The calcium aluminate cement used in these applications is generally based on monocalcium aluminate (CA). New calcium aluminate cements based on the more reactive C12A7 offer alternative formulation pathways where the same mechanical properties can be reached in an eco-optimized mix design.

Only little research has been published so far on these binders. This study aims to contribute to a better understanding of the underlying mechanisms determining success in application. Varying amounts and types of calcium sulfates have been dosed to a C12A7-based cement in a self-levelling underlayment recipe. The mechanical performance and dimensional stability of these blends was investigated over 28 days.

METHODS

The basis for the investigation is an application like binder formulation consisting of a C12A7-rich cement (Recipro 40-S by Çimsa), a commercial beta hemihydrate and a commercial natural anhydrite. In addition, two different grades of limestone fillers (ultrafine and fine) and a quartz filler are used.

The chemical composition & Blaine values of these materials are given in Table 1. The chemical composition was determined via energy dispersive XRF.

Table 1: Blaine & chemical composition of the used binders and fillers. XRF results in wt.-%, for clarity only the main oxides are listed.

Material	Recipro 40-S	b-hemihydrate	natural anhydrite	limestone filler UF	limestone filler F
Al2O3	37.2	0.1	0.1	0.1	0.1
SiO2	4.2	1.2	0.1	0.3	0.6
SO3	0.1	52.7	58.7	0.0	0.0
CaO	46.5	38.4	41.6	56.4	56.4
TiO2	1.8	-	-	-	-
Fe2O3	7.5	0.1	-	-	0.1
LOI	0.3	6.4	0.2	42.9	42.4
Blaine (cm^2/g)	3200	7100	3700	9900	7100

The mix design of the investigated self-levelling recipes is given in Table 2. The employed water to solid ratio is 0.25. All experiments were performed at 20°C. The used additive package is identical for all mixes. It contains Li2CO3 as accelerator, tartaric- and citric acid as retarders, a VAE based polymer powder, a PCE based superplasticizer, a high molecular weight copolymer thickener, a defoamer and an air entraining agent.

Table 2: Mix design of the five investigated recipes.

components	100% b-HH	70% b-HH	70% b-HH & 30-% anhydrite	50% b-HH & 50-% anhydrite	30% b-HH & 70-% anhydrite
Recipro 40-S	16.0%	16.0%	16.0%	16.0%	16.0%
beta hemihydrate	12.8%	9.0%	9.0%	6.4%	3.8%
natural anydrite	0.0%	0.0%	3.8%	6.4%	9.0%
ultra fine limestone filler	7.0%	10.8%	7.0%	7.0%	7.0%
fine limestone filler	24.4%	24.4%	24.4%	24.4%	24.4%
sand filler	36.5%	36.5%	36.5%	36.5%	36.5%
dispersion polymer powder & additives	3.3%	3.3%	3.3%	3.3%	3.3.%
Pot-life (min)	25	25	29	34	35

For each mix mortars 4x4x16 cm³ mortar moulds were prepared, and strength was measured based on the methodology described in EN 196-1. The moulds were stored at > 90% r.H. and 20°C for 6 h. Then the prisms were demoulded and subsequently stored at >90% r.H. / 20°C. The dimensional stability was measured according to EN 12617-4.

KEY FINDINGS | FUTURE RESEARCH NEEDS | CONCLUSIONS

The compressive strength results are shown in Figure 1. After 6h the 100% b-HH shows 40 – 50% decreased strength compared to all other blends. For the 100% b-HH strength even further decreases with ongoing storage until 24h. At the same time a significant expansion is evident for this blend (see Figure 2).The dimensional change between 6h and 24h translates to an expansion of 3.9 mm/m, which likely results in the formation of microcracks and thus reduced strength. All other systems show further increase in strength with further hydration progress from 6 to 24 hours. The 100% b-HH system cannot recover from the significant expansion occurring in the early hydration stages and shows the worst performance at all times. After 7d of curing the 70% b-HH system falls short compared to the systems with a mix of calcium sulfate types. This blend is also the only blend showing continuous shrinkage from the point of demoulding on. The total calcium sulfate content in this system thus is too low to utilize the full reactive potential of the binder system. For all blends only minor changes in strength between 7 to 28 days is observed, highlighting the early reactive potential of the binder system. The three blends comprising mixtures of b-HH and anhydrite show the best, comparable mechanical performance up to 28 days of hydration. They also follow a similar trend in the dimensional

changes over 28 days. In the early stages minor expansion is observed, which is compensated in all systems by subsequent shrinkage between 7 to 14 days. After 28 days these systems show a net dimensional change of < 0.1 mm/m.

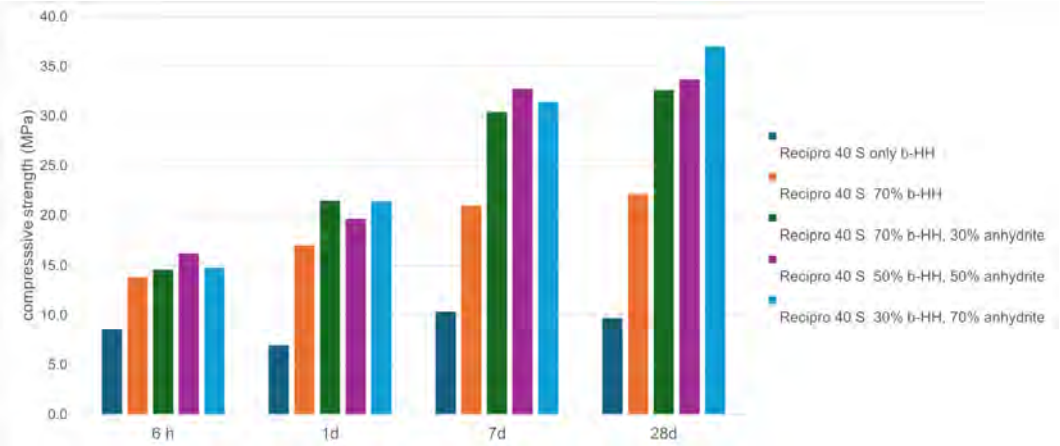

Figure 1: Compressive strength measured on 4x4x16 cm³ mortar prisms. Each data point corresponds to the average of three individual measurements.

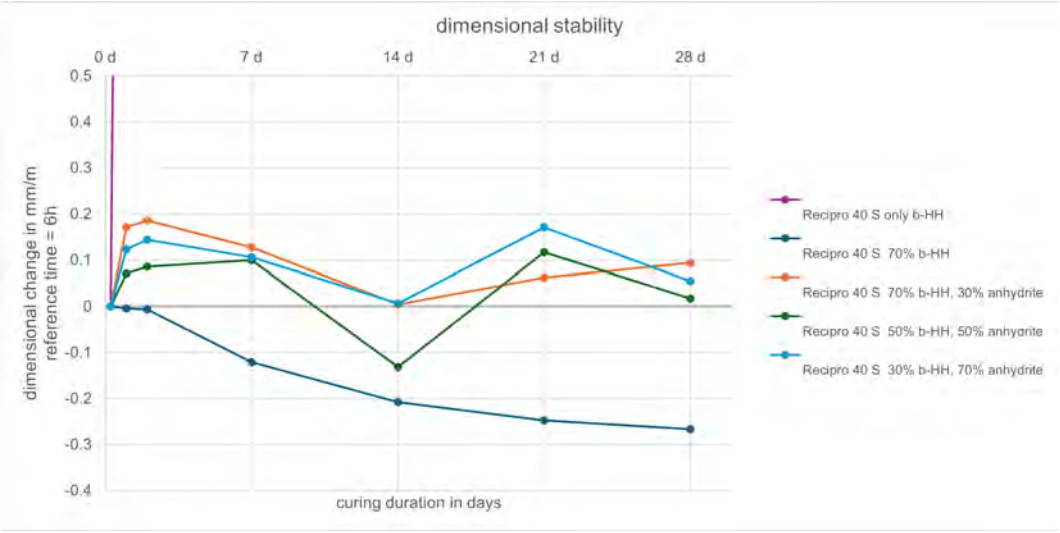

Figure 2: Dimensional stability of the mortar prisms cured at 20°C and > 90% r.H. The reference time for the dimensional stability is after 6h of hydration which corresponds to the time of demoulding. Each data point corresponds to the average of three individual measurements.

In conclusion: the amount and mix design of calcium sulfates play a key role in application success when formulating with C12A7 based cement. Too high amounts of highly reactive calcium sulfates result in severe expansion and long-term reduced strength. Too low amounts of calcium sulfates reduced the potential strength of the binder system. The data indicates that the best practice is a mix of calcium sulfates with varying reactivity.

International Conference on Calcium Aluminates 2026

THE ROLE OF SLAG AND CALCINED CLAY IN THE HYDRATION AND CONVERSION OF CALCIUM ALUMINATE CEMENT

Bašić, Alma-Dina[1] , Serdar, Marijana[1], Gerz, Alexandra[2]
[1] University of Zagreb, Faculty of Civil Engineering, Department of Materials, Fra Andrije Kačić-Miošić 26, 10000 Zagreb, Croatia, [2]Calucem d.o.o., Revelanteova 4, 52100 Pula, Croatia

Keywords: slag, calcined clay, hydration, microstructure, conversion

ABSTRACT

One of the widely accepted approaches to decarbonizing the cement sector is the partial replacement of clinker with supplementary cementitious materials (SCM), such as slag, limestone, fly ash. Previous studies have shown that slag helps to inhibit the conversion of calcium aluminate cement. Due to the problems with the availability and cost of slag, there is a need to investigate other possible SCMs and their application potential in CAC. Calcined clay with medium kaolin content available in the region was used in this study. The evaluation of the hydration and conversion process was monitored by analyzing the microstructure and compressive strength up to 56 days. The results show the influence of strätlingite hydrate formation on the conversion process of CAC.

INTRODUCTION

The specificity of CAC is that it undergoes a conversion process depending on the temperature and humidity of the environment, which leads to a decrease in strength[1]. The conversion process is accelerated when the temperature exceeds 30°C, and rapid formation of stable C_3AH_6 and AH_3 occurs[2]. Several previous studies[3, 4] have confirmed that the conversion process can be mitigated by the use of ground granulated blast furnace slag (GGBFS). The reaction of silicon dioxide in the slag with CAC cement hydrates leads to the formation of the stable phase strätlingite (C_2ASH_8)[5].
Despite all the advantages of using slag as a partial replacement for CAC cement, there are certain challenges in using slag in the cement industry. More than 90% of the available slag is already used in the production of cement or as an additive to cementitious mixtures. Moreover, the availability of slag does not follow the trend of global cement production. In the case of OPC, calcined clay (CC) in combination with limestone (LC3) has been shown to be a possible solution to reduce the environmental footprint of cement without compromising the mechanical properties and durability of OPC[6]. Unlike industrial by-products, the availability of calcined clay is not dependent on industrial production volumes, making it a more reliable and

*marijana.serdar@grad.unizg.hr

sustainable alternative. The research question remains whether calcined clay could be a promising material for use in combination with CAC, to inhibit the conversion process in a similar way to the addition of slag already confirmed in the literature.

METHODS

Calcium aluminate cement with 52.67 % Al_2O_3 produced by Calucem company from Pula, Croatia was used. To evaluate the effects on conversion process, slag (S) and calcined clay (CC) supplied from South-East Europe region were used. Slag used in this study was received industrially milled with Blaine size 4580 cm^2/g, while clay was received as raw material without prior processing. Prior to mixing, clay was first dried for 24h at 60°C to remove the moisture, then ground (for 90s) to Blaine size of 5980 cm^2/g, and at the end calcined at 850 °C for one hour. Used clay was investigated by the authors in previous research, where detailed analysis of clay is given[6].

To access conversion process of CAC cement, three different mixes were prepared. One reference mixture (labelled CAC100), one mixture with 30% replacement of CAC by slag (labelled CAC70S30), and one mixture with 30% replacement of CAC by calcined clay (labelled CAC70C30). The replacement level of 30% was used to ensure that any changes induced by the addition of SCM are visible in properties and microstructure. The mixes were prepared according to EN 14647.

First 24 h samples were covered and stored in humidity chamber at 20 °C with 95% of relative humidity. After 24 h samples were demoulded. To access conversion process one set of samples was cured in water bath at 20 °C, and one set in water bath at 38 °C. The compressive strength was measured according to EN 196-1:2016. Impact of elevated curing temperature on microstructural changes of CAC cement in combination with slag or calcined clay were evaluated by thermogravimetric analysis (TGA), qualitative powder analysis (XRD), and mercury intrusion porosimetry (MIP) after 28 days of curing at 20°C and 38°C.

RESULTS

The development of compressive strength over 56 days for specimens cured at 20°C and 38°C is shown in Figure 1 a) and b) respectively. During curing at 20°C, the mixture with slag exhibited a lower initial compressive strength. However, at the end of the measurements, after 56 days of curing, the compressive strength was higher than that of the reference mix. When cured at 20°C, the mixture with calcined clay had a lower compressive strength than the reference mixture throughout the test period. All mixtures showed an increase in compressive strength during the 56-day curing period at 20°C. However, the mix in which 30% of the CAC cement was replaced with calcined clay showed slightly lower strength compared to the other two mixes.

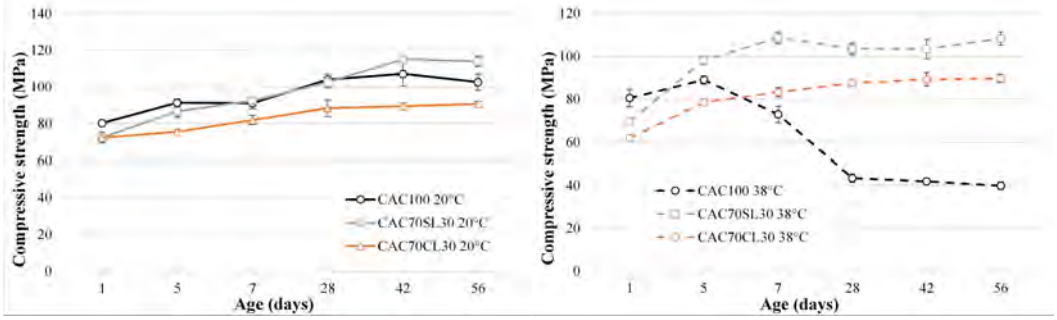

Figure 1. Development of compressive strength over 56 days for samples cured at: a) 20 °C, b) 38 °C

After curing at 38°C, the compressive strength of the reference CAC mix started to decrease after five days, indicating a conversion process. With longer curing, the speed of the conversion process increased and the compressive strength began to decrease rapidly. After 28 days of curing, the compressive strength of the CAC mixture reached the lowest value, indicating that the conversion process was complete. In contrast, both mixtures with slag and calcined clay showed a continuous increase in compressive strength after curing at 38°C compared to the initial values.
The comparison of DTG for mixtures cured at 20°C and 38°C is shown in Figure 2.

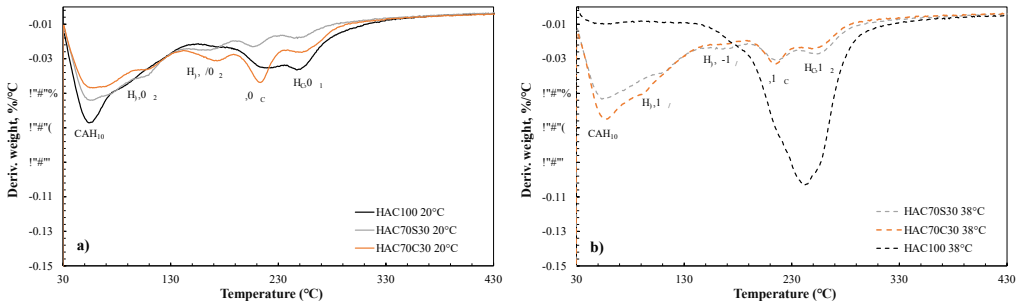

Figure 2 Comparison of DTG for mixtures cured at: a) 20°C and b) 38°C

For sample with 30% replacement of CAC by slag for both curing regimes dehydration of a new peak designated to strätlingite hydrate (C_2ASH_8) was detected. Similarly, for sample with calcined clay, metastable (CAH_{10} and C_2AH_8), stable hydrates (C_3AH_6) and strätlingite (C_2ASH_8) did occur, but the intensities of the mass loss peaks attributed to each of these hydrates were different compared to the intensities of the same peaks in the case of mixture with slag. The formation of strätlingite in CAC with slag and in CAC with clay was additionally confirmed in XRD (results not shown in the abstract)[7].
Figure 3 shows capillary pore classification according to Mehta (2005). In this case, capillary pores were divided into three groups, micro (0.01 – 0.1 μm), meso (0.1 – 1 μm), and macro (1 – 10 μm) capillary pores. The reference mix cured at 38°C, where conversion process occurred, had a higher proportion of larger capillary pores than the reference mixture cured at 20°C. Therefore, once metastable phases were transformed into stable phases, critical pore entry diameter increased, and capillary pores became larger.

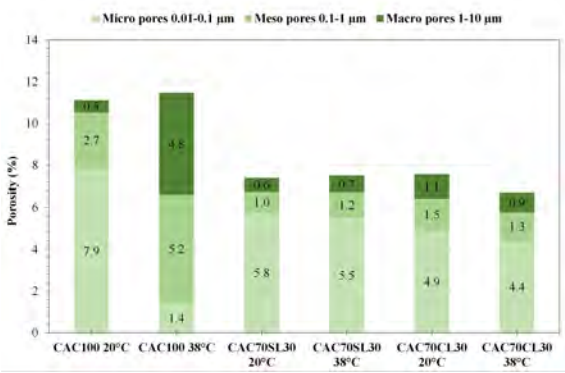

Figure 4. Capillary pores classification for all three mixes after 28 days of curing at 20 °C and 38 °C

KEY FINDINGS

Exposure of CAC mortar to elevated temperatures (38 °C) resulted in the conversion of metastable hydrates to stable hydrates, leading to the formation of new macro capillary pores (1 – 10 µm), a significant increase in critical pore diameter and a loss of 60% of compressive strength. The substitution of 30% CAC with calcined clay resulted in a slight reduction in 1-day compressive strength (15% reduction in compressive strength compared to pure CAC cured at the same temperature), but a reduction in compressive strength was avoided when curing was carried out at a higher temperature. The formation of strätlingite in the calcined clay mix densified the structure and reduced the critical pore entry diameter, especially during curing at 38°C.

REFERENCES

[1] Adams, M.P., Lute, R.D., Moffatt, E.G., Ideker, J.H. 2018. “Evaluation of a Procedure for Determining the Converted Strength of Calcium Aluminate Cement Concrete”, Journal of Testing and Evaluation 46, 4, 1659-1672.

[2] Pacewska, B., Nowacka, M. 2014. “Studies of conversion progress of calcium aluminate cement hydrates by thermal analysis method”, J. Therm. Anal. Calorim., 117, 653–660.

[3] Kirca, Ö., Özgür Yaman, I., Tokyay, M. 2013. “Compressive strength development of calcium aluminate cement-GGBFS blends”, Cem. Concr. Compos., 35, 163–170.

[4] Yang, H.J., Ann, K.Y., Jung, M.S. 2019. “Development of strength for calcium aluminate cement mortars blended with GGBS”, Adv. Mater. Sci. Eng.

[5] Ideker, J.H., Scrivener, K.L., Fryda, H., Touzo, B. 2019. ”Calcium aluminate cements”, in. P. Hewlett, M. Liska (Eds.), Lea`s Chemistry of Cement and Concrete England, Elsevier Science Publishers Ltd., 537-584.

[6] Ram, K., Serdar, M., Londono-Zuluaga, D., Scrivener, K. 2022. “The effect of pore microstructure on strength and chloride ingress”, Cas. Stud. Constr. Mat., 17

[7] Basic, A-D., Serdar, M. 2025 Substituting Slag with Calcined Clay to Mitigate Conversion in Calcium Aluminate Cement, Journal of Materials in Civil Engineering, Volume 38, Issue 2

International Conference on Calcium Aluminates 2026

QUANTIFICATION OF THE METASTABLE CALCIUM ALUMINATE PHASES C_2AH_X USING AN EXTENDED PONKS METHOD

Goergens, Julian, Hilti Entwicklungsgesellschaft mbH, Hiltistrasse 6, 86916 Kaufering, Germany: julian.goergens@hilti.com
Goetz-Neunhoeffer, Friedlinde, Friedrich Alexander-University Erlangen-Nürnberg, 91054 Erlangen, Germany

Keywords: Hydration, Hydrate phase, Conversion, X-ray diffraction, XRD

ABSTRACT

The calcium-aluminate-hydrate C_2AH_8 ($2CaO \cdot Al_2O_3 \cdot 8H_2O$) is the most prominent representative of the so called C_2AH_x phases, which are described in XRD studies on hydrated calcium aluminate cement (CAC). The "x" in the formula stands for the moles of H_2O content of the unit cell. Due to problems of structure determination using XRD—in early hydration, often several metastable C_2AH_x phases with different basal spacing appear in XRD diagrams—no structural data are available for quantification using the Rietveld method. This paper presents an hkl model for quantifying these phases based on an extended PONKS methods [1,2]. An F-factor corresponding to the product of the volume square and density of C_2AH_x was determined herewith. The underlying hkl-model enables quantifications based on XRD diffractograms.

INTRODUCTION | BACKGROUND

C_2AH_x plays an important role in the hydration of calcium aluminate cement (CAC), as it is a metastable hydrate phase and thus affected by the phenomenon of conversion as a thermodynamically metastable hydrate phase. Quantification of this phase is essential for evaluating the progress of conversion, both for academic and industrial applications. Important crystallographic research on C_2AH_x was carried out by [3–9]. During the hydration of CAC, not only C_2AH_8 but also $C_2AH_{7.5}$ and, secondarily, the form $C_2AH_{8.2}$ (with the highest basal spacing) are usually visible in XRD diffractograms as two or three reflections with d-values of their different (00l)-lattice plane. No structure for the Rietveld refinement of C_2AH_x has been published to date. However, in a diffractogram of pure C_2AH_x (where x can be attributed to a known value), a so-called "hkl-model" can be created with a Rietveld analysis software [1]. The scale factor of this model (the integrated area of the peaks, considering effects such as preferred orientation and reflection multiplicity) must then be proportional to the crystalline content of the phase in the sample, provided that the amorphous fraction approaches zero. To

meet this requirement, numerous syntheses are necessary, ultimately leading to an error-free evaluation of the crystallinity of the C_2AH_x phase in the sample.
This scale factor is the decisive parameter (eq. 1) that enables absolute quantification of the crystalline phases and is later required for the G-factor approach [30]. When cell volume and density of a phase are unknown, which is the case when using an hkl-phase-model, an F-factor must be determined to replace this term (eq. 2). The procedure has previously been explained in a similar way for a C-S-H hkl-phase-model [1,2]. The newly calculated C_2AH_x hkl-phase-model then must be calibrated via the mass balance (knowledge of the amount of hydrated reactant) and stoichiometric balance and ultimately delivers the scale factor.

METHODS

$C_{12}A_7$ in combination with CH from lab-syntheses was selected for the synthesis of all C_2AH_x calibration samples investigated. CH and $C_{12}A_7$ were synthesized and evaluated as pure (>97%) by XRD. The $C_{12}A_7$-CH powder was mixed with deionized and decarbonated water (water/powder = 10) in a CO_2-free glove box. Immediately afterwards, the sealed containers with the suspensions were left for their early hydration in different temperature-controlled environments: 23 °C or 29 °C ± 2 °C or 10°C or combinations of temperatures. After reaction times of 2–24 hours, depending on the reaction temperature, the samples were centrifuged and dried at room temperature in a CO_2-free glove box over a $CaCl_2$ solution and then stored further at the corresponding temperature. In total, more than 100 recorded diffractograms from 42 C_2AH_x syntheses with variations in temperature and hydration and storage times were compiled and evaluated in this work to approximate the maximum scale factor and thus the crystallinity of C_2AH_x for calibration. The term “crystallinity” in connection with XRD evaluations is used synonymously with the C_2AH_x content in this work and therefore with the scaling factor of C_2AH_x, provided that the other parameters in Equation 1 do not change. The G-factor method was used for all XRD quantifications [10].

$$xi = \frac{\mathrm{si} \cdot \rho\mathrm{i} \cdot \mathrm{V}^2\mathrm{i} \cdot \mu\mathrm{i}}{\mathrm{G}} = \frac{\mathrm{si} \cdot \mathrm{Fi} \cdot \mu\mathrm{i}}{\mathrm{G}} \qquad \text{eq. 1}$$

$$Fi = \rho i \cdot \mathrm{V}^2\mathrm{i} = \frac{\mathrm{xi} \cdot \mathrm{G}}{\mathrm{Si} \cdot \mu\mathrm{z}} \qquad \text{eq. 2}$$

G is the G-factor determined with an external standard [10]. The content of the phase of interest $C_2AH_x = x_i$ can be calculated if F_i is known (eq.1). F_i can be calculated indirectly from eq. 2, without knowing the density and cell volume of C_2AH_x, if x_i is known. The value for x_i in eq. 1 is at most 100 w% minus all quantified minor phases in the powder. The maximum possible content of precipitates, like minor CAH_{10} or monocarbonate, is added up, considering a stoichiometric mass balance to account for amorphous AH_3. The difference between this sum and 100 w% is then the correct x_i.

KEY FINDINGS | CONCLUSIONS

For $C_2AH_{7.5}$, an hkl-model was generated based on the samples with the highest x_i value (fig.1, fig 2). For the transfer of the model to the other two phases, C_2AH_8 and $C_2AH_{8.2}$, the c-lattice parameter must be adjusted in the Rietveld evaluation software according to their corresponding value [11]. Each diffractogram was analyzed and refined using the Rietveld analysis software TOPAS, Bruker AXS, V5: The 2θ range between 7◦ and 40◦ was selected. The first reflection of C_2AH_x occurs at approximately 8◦ 2θ, while no C_2AH_x peaks of significant intensity are found at angles >40◦ 2θ. First, a "peaks phase model" is created in the evaluation software, and peaks of smaller hydrate phases (monocarbonate, CAH_{10}, and C_3AH_6) are excluded. The indexing solutions of different space groups were compared in terms of their goodness of fit (GOF) as well as the volume and lattice parameters a_0 and c_0 for a hexagonal unit cell (and a_0, b_0, and c_0 as well as β for a monoclinic unit cell). The indexing solution with a P6 space group was selected and the required parameters (space group, a_0, c_0, volume of unit cell) were used for the generated "hkl-phase-model". The primitive hexagonal space group (P6) provided the best GOF and thus an optimized fit for Rietveld quantification. All synthesized samples of C_2AH_x were subsequently evaluated with the generated hkl-model.

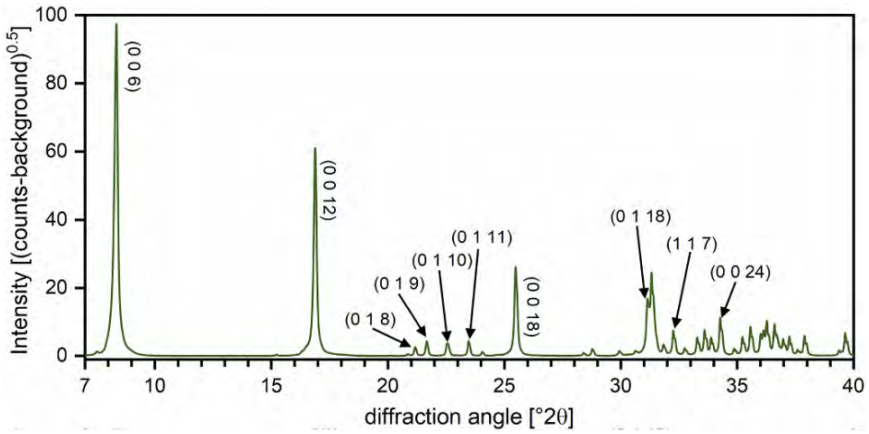

Figure 1: Plot of the hkl-model determined for $C_2AH_{7.5}$ (C_2AH_x with a lattice spacing that fits samples, were C_2AH_x with x=7.5) and the lattice plains indexing.

After all samples had been evaluated with respect to their non-determinable content (so the hypothetical C_2AH_x-content plus the potential over-all amorphous content of the sample) which is achieved by considering minor phase contents and an internal error analysis (errors for G factors, quantified phases, evaluation routines and microstructure limitations), a assumed x_i, initially neglecting amorphous contents (eq. 2) could be plotted for all samples (fig. 2). It becomes visible that this value – regardless of the hydration condition and storage time – approaches a value that must be considered a 100% benchmark (fig. 2). No C_2AH_x crystallinity achieves a higher value, so it is concluded that this must be the maximum content of C_2AH_x with no or marginal amorphous content in the sample and therefore equals x_i (eq. 2) within the scope of this study. Based on this x_i (red, dotted line in fig. 2),

a final F_i of 262.565 for eq. 2 is determined: Together with the hkl-model, as published in [11], this factor enables a correct quantification of C_2AH_x in hydrated CAC.

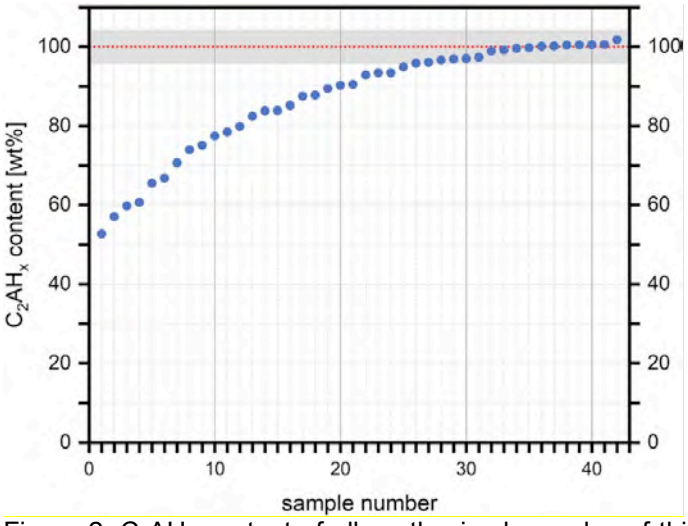

Figure 2: C_2AH_x content of all synthesized samples of this study, quantified with the hkl-model in fig. 1. A maximum value for crystallinity of C_2AH_x is approached.

REFERENCES

[1] N.V.Y. Scarlett, I.C. Madsen, Quantification of phases with partial or no known crystal structures, Powder Diffract. 21 (2006) 278–284, https://doi.org/10.1154/1.2362855.

[2] S.T. Bergold, F. Goetz-Neunhoeffer, J. Neubauer, Quantitative analysis of C-S-H in hydrating alite pastes by in-situ XRD, Cem. Concr. Res. 53 (2013) 119–126, https://doi.org/10.1016/j.cemconres.2013.06.001

[3] N. Richard, N. Lequeux, P. Boch, EXAFS study of refractory cement phases: CaAl2O14H20, Ca2Al2O13H16, and Ca3Al2O12H12, J. Phys. III 5 (1995) 1849–1864.

[4] N. Ukrainczyk, T. Matusinovic, S. Kurajica, B. Zimmermann, J. Sipusic, Dehydration of a layered double hydroxide-C2AH8, Thermochim. Acta 464 (2007) 7–15, https://doi.org/10.1016/j.tca.2007.07.022.

[5] M.H. Roberts, New calcium aluminate hydrates, J. Appl. Chem. 7 (1957) 543–546, https://doi.org/10.1002/jctb.5010071004.

[6] G. Geng, J. Li, Y.S. Yu, D.A. Shapiro, D.A.L. Kilcoyne, P.J.M. Monteiro, Nanometerresolved spectroscopic study reveals the conversion mechanism of CaO·Al2O3·10H2O to 2CaO·Al2O3·8H2O and 3CaO·Al2O3·6H2O at an elevated temperature, Cryst. Growth Des. 17 (2017) 4246–4253, https://doi.org/10.1021/acs.cgd.7b00553.

[7] F. Hueller, J. Neubauer, S. Kaessner, F. Goetz-Neunhoeffer, Hydration of calcium aluminates at 60◦C – development paths of C 2 AH x in dependence on the content of free water, J. Am. Ceram. Soc. 102 (2019) 4376–4387, https://doi.org/10.1111/ jace.16314.

[8] B. Raab, Synthese und Charakterisierung nanoskaliger hydraulisch hochreaktiver Phasen des Portland- und Tonerdezements IX, in: G. Borg, K. Friedrich, M. Frühauf, C. Glasser, H. Heinisch, W. Kühling, C. Lempp, H. Pöllmann, K.-H. Schmidt, W. Thomi, P. Wycisk (Eds.), Hallesches Jahrb. Für Geowissenschaften, Beih. 26, Halle (Saale), 2011 pp. IX–147.

[9] W. Gessner, D. Müller, H.-J. Behrens, G. Scheler, Zur Koordination des Aluminiums in den Calciumaluminathydraten 2CaO•Al2O3•8H2O und CaO•Al2O3•10H2O, Z. Anorg. Allg. Chem. 486 (1982) 193–199.

[10] D. Jansen, F. Goetz-Neunhoeffer, C. Stabler, J. Neubauer, A remastered external standard method applied to the quantification of early OPC hydration, Cem. Concr. Res. 41 (2011) 602–608, https://doi.org/10.1016/j.cemconres.2011.03.004.

[11] J. Goergens, A. Koehler, F. Goetz-Neunhoeffer, Calibration and quantitative analysis of C2AHx (2CaO·Al2O3·xH2O) by Rietveld refinement combined G-factor method, Cement and Concrete Research, Volume 158,
2022, https://doi.org/10.1016/j.cemconres.2022.106854

International Conference on Calcium Aluminates 2026

INFLUENCE OF CURING TEMPERATURE ON THE PHASE COMPOSITION AND MICROSTRUCTURE OF CALCIUM ALUMINATE CEMENT BOND CASTABLES SUBJECTED TO HYDROTHERMAL CONDITIONS

Koehler*, Andreas, Almatis GmbH, Ludwigshafen, Germany;
Klaus, Sebastian, Almatis GmbH, Ludwigshafen, Germany;
Kuiper, Stefan, Almatis BV, Frankfurt, Germany;
Buhr, Andus, Almatis GmbH, Frankfurt, Germany;
Goetz-Neunhoeffer, Friedlinde, Friedrich-Alexander Universität Erlangen-Nürnberg, Erlangen, Germany

Keywords: Cement, Refractory Castable, Hydrothermal, Drying, Hydrate phases

ABSTRACT

Calcium aluminate cement is widely used as a binder in refractory castables because it enables shaping complex geometries and allows the material to withstand extreme temperatures. Their typical manufacturing process consists of mixing, curing, demoulding, drying and firing. In modern dense and highly dispersed castables with very low permeability, water remains in the castable body during the drying up to 200°C and beyond. This leads to an increase in internal pressure and hydrothermal conditions occur. Consequently, problems such as cracking and explosive spalling can arise.

Different temperatures during hydration of CAC lead to the formation of distinct hydrate phases and consequently, different microstructures can develop in the hardened material. Hydrothermal conditions lead to the transformation of the original hydrate phases, while still preserving microstructural features inherited from the initial hydration stage. This study presents the influence of curing temperature (5, 23, and 40 °C) on phase development and porosity in a refractory castable model system subjected to hydrothermal conditions.

Quantitative X-ray diffraction measurements revealed that CAH_{10}, C_2AH_x, C_3AH_6 and AH_3 are formed during curing at different temperatures and that the degree of hydration also varies. When hydrothermal conditions occur, the remaining clinker phases react and the already formed hydrate phases first transform to AH_3 and C_3AH_6. While C_3AH_6 remains stable with increasing temperature and pressure, AH_3 converts to boehmite above 140 °C.

Although the final mineralogical phase composition is the same, microstructural analyses via SEM and mercury intrusion porosimetry revealed differences in the three initially differently cured materials. While the total porosity is comparable, the samples that were cured at 40 °C have a higher proportion of large pores and a different appearance of C_3AH_6. The study could show that the initial microstructure that is created during curing is preserved after hydrothermal conditions induce additional reactions and phase conversions.

andreas.koehler@almatis.com

INTRODUCTION

Refractory castables undergo several manufacturing steps during production. In the first step, the dry raw materials, consisting of calcium aluminate cement, different aggregates, fillers and additives are mixed with water and poured into a mould. In the following curing step, the cement starts to dissolve and hydrate phases are formed which leads to an increase in green strength. The kind of hydrate phase as the reaction speed are strongly temperature dependent[1]. When a sufficient strength is reached, the castable can be demoulded. Afterwards the material is first dried to evaporate the unbound water before firing at high temperature where the crystalline bound H_2O is removed. In the drying and firing step problems such as cracking or explosive spalling can occur which makes it the most critical part of the manufacturing process. These problems can occur because modern, highly dispersed castables are so dense that water cannot readily escape from the green body during heating, and the resulting steam buildup can cause an increase in pressure. These hydrothermal conditions can change the phase composition and microstructure of the castable. This study aims help to understand problems during the drying/heating step by determining how a different phase composition and microstructure after curing at low, moderate and high temperature affects the mineral phases and porosity after hydrothermal conditions.

METHODS

All samples had the same initial composition (40 wt.% calcium aluminate cement and 60 wt.% alumina filler). A higher cement content than typically used in modern castables was selected to better visualize the effects of cement and hydrate phase formation during hydration and after being exposed to hydrothermal conditions. The cement was a commercial 70% Al_2O_3 CAC (Almatis CA14-S), mainly composed of CA and CA_2 with some α-Al_2O_3. The alumina filler (Almatis tabular alumina T60/T64 <45 µm) consisted primarily of corundum with traces of β-Al_2O_3 ($NaAl_{11}O_{17}$). The dry mixture was homogenized with deionized water, poured into a sealed plastic mould and cured for 48 h at 5, 23, or 40 °C respectively. Afterwards the plastic was removed and the tablet was transferred to a PTFE-lined autoclave for hydrothermal treatment. The maximum temperature and pressure investigated were 180 °C/~11 bar. After autoclaving, the samples were analyzed using X-ray diffraction (XRD), scanning electron microscope (SEM) and mercury intrusion porosimetry (MIP). The quantitative phase composition was determined by XRD by applying the G-factor method[2] to Rietveld data[3] using quartz as an external standard. A more detailed description of the sample preparation and methodology can be found in Koehler et al. 2022[4,5].

KEY FINDINGS AND CONCLUSIONS

After hydrating the samples in a closed system at 5, 23 and 40 °C for 48 h respectively, a different degree of hydration was reached and different hydrate phases were formed (Figure 1). At low temperatures (5 °C) the clinker phases, especially CA_2, only partially reacted and CAH_{10} was formed as the only crystalline hydrate phase. Hydration at moderate temperatures (23 °C) led to the formation of CAH_{10} next to C_2AH_x and AH_3. While higher amounts of CA and CA_2 reacted at 23 °C, still 9.6 wt.% unreacted clinker phases were left after 48 h of hydration. Curing at 40 °C resulted in a complete reaction of CA and CA_2. At 40 °C hydration temperature, C_3AH_6 and AH_3 are formed. Those differently cured samples were placed in the autoclave afterwards to simulate the hydrothermal conditions that can occur during the drying/heating step.

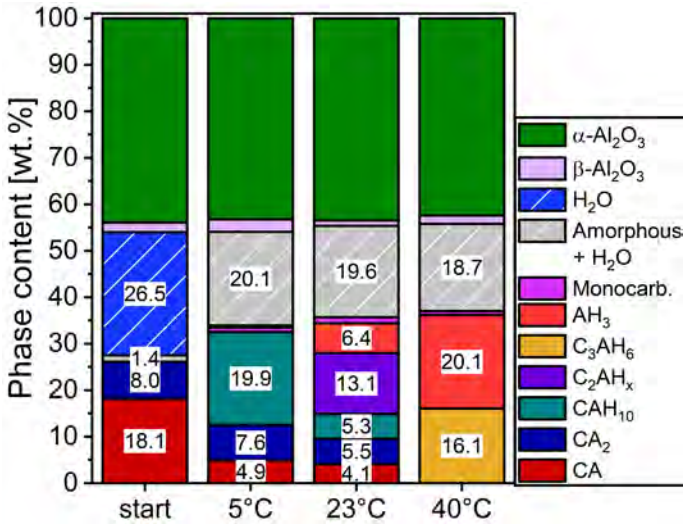

Figure 1. Phase compositions of the samples after curing for 48 hours at 5, 23 and 40 °C. Start column: Initial phase composition of the paste (water, cement and Al_2O_3 filler)

While all samples have a different phase composition after curing at different temperatures, hydrothermal conditions lead to exactly the same phase composition. Remaining clinker phases react and all existing hydrate phases convert to C_3AH_6 and Boehmite. While C_3AH_6 is already present after curing, it is freshly formed from unreacted clinker phases and conversion of CAH_{10} and C_2AH_x. Boehmite is freshly formed in all three samples. However, similar to C_3AH_6 it is formed from conversion of different hydrate phases and reaction of unreacted CA/CA_2 in the 5/23 °C curing samples. In the 40 °C sample it is purely formed by conversion of AH_3. Although samples subjected to hydrothermal conditions (180 °C/~11 bar) reach the same final phase composition, the path leading to it differs.

Investigations with SEM and MIP revealed that while the phase composition is the same, the microstructure differs after autoclaving. Large-area BSE segmentation showed distinct differences between the 40 °C–cured samples and those cured at 5 and 23 °C after autoclaving. The pores in the 40 °C samples are in general bigger and more heterogeneously distributed. Find more information in the publication by Koehler et al[6]. To verify those findings, MIP measurements were performed on the samples after autoclaving. The measurements show that the bulk density (~1.69 g/cm³) and total porosity (~43%) is the same in all samples. The pore size distribution shows that all samples have a dominant pore diameter near ~1 µm. However, the samples cured at 40 °C show a markedly lower intensity at this peak and instead displays a secondary maximum around ~3 µm (Figure 2). Compared with the 5 and 23 °C samples, the 40 °C sample contains fewer fine pores and a higher fraction of larger pores, which are absent in the lower-temperature samples. Although hydrothermal treatment yields the same phase composition, the resulting microstructures differ. This indicates that the curing conditions, particularly temperature, establish an initial microstructural framework whose “footprint” persists despite subsequent hydrothermal exposure and phase transformations.
The higher fraction of large pores (2–10 µm) observed only in the 40 °C autoclaved samples can be attributed to the mineral phases formed during hydration. At high curing temperatures, substantial amounts of C_3AH_6 and AH_3 form rapidly. Among calcium aluminate hydrates, C_3AH_6 incorporates the least water and has the highest density (2.53 g/cm³)[6], leaving water either bound in crystalline phases or as free pore water. Under hydrothermal conditions, preformed C_3AH_6 remains stable, while AH_3 transforms to boehmite, releasing additional water and

generating extra porosity. Thus, hydrothermal treatment does not substantially change the microstructure. In contrast, samples cured at low or moderate temperatures initially contain CAH_{10} (1.78 g/cm^3), C_2AH_8 (1.95 g/cm^3)[6], poorly crystalline AH_3, and unreacted clinker. These less dense phases produce a finer, less permeable pore network. When hydrothermal conditions arise, the phases convert to C_3AH_6 and boehmite, but the finer microstructural framework largely persists. Castables cured at low or moderate temperature can therefore be considered more susceptible to explosive spalling and other pressure-related failures. More results can be found in Koehler et al. 2022[5].

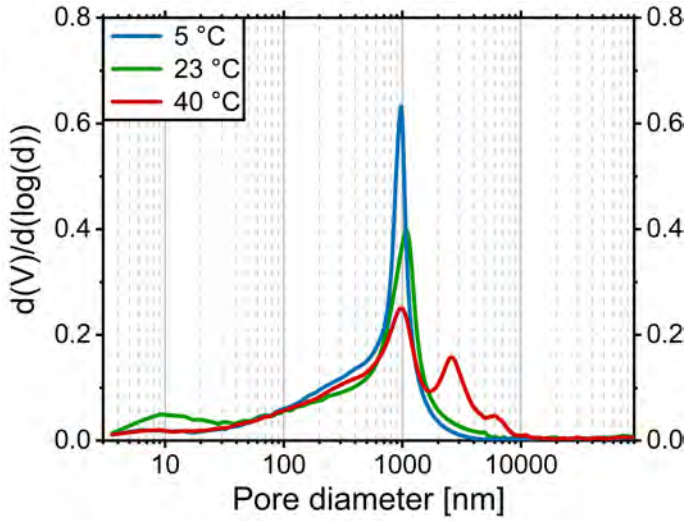

Figure 2. Pore size distributions of the samples after autoclaving First derivative of the MIP pore volumes as function of pore diameter.

REFERENCES

[1] B. Lothenbach, L. Pelletier-Chaignat, F. Winnefeld, Stability in the system CaO-Al_2O_3-H_2O, Cem Concr Res. 42 (2012) 1621–1634.

[2] D. Jansen, F. Goetz-Neunhoeffer, C. Stabler, J. Neubauer, A remastered external standard method applied to the quantification of early OPC hydration, Cem Concr Res. 41 (2011) 602–608.

[3] B.H. O'Connor, M.D. Raven, Application of the Rietveld refinement procedure in assaying powdered mixtures, Powder Diffr. 3 (1988) 2–6.

[4] A. Koehler, J. Neubauer, F. Goetz-Neunhoeffer, Phase changes during the drying of calcium aluminate cement bond castables–the influence of curing and drying conditions, Cement. (2022) 100020.

[5] A. Koehler, C. Rößler, J. Neubauer, F. Goetz-Neunhoeffer, Phase and porosity changes in a calcium aluminate cement and alumina system under hydrothermal conditions, Ceram Int. 49 (2023) 4659–4667.

[6] W. Kurdowski, Cement and concrete chemistry. Springer Science & Business, 2014.

International Conference on Calcium Aluminates 2026

REDUCING THE RISK OF EXPLOSIVE STEAM SPALLING OF CALCIUM ALUMINATE BONDED REFRACTORY CONCRETES THROUGH A MODIFIED HYDRATION PATH

Auvray* Jean-Michel, Lacoue Frédéric, Wöhrmeyer Christoph, Parr Christopher, Imerys Technology Center, Vaulx-Milieu,(France)

Keywords: CAC, Hydration, Castable, Permeability, Dry-out

ABSTRACT

High-performance (HP) refractory concretes utilize dense matrix systems and micro-powders to achieve superior durability. However, their extremely low permeability creates a significant industrial challenge: during the initial heat-up, trapped water cannot escape easily. This leads to internal pressure build-up, risking structural cracks or explosive spalling if the heating process is not strictly controlled. This paper explores how to improve permeability without sacrificing the benefits of a low-porosity structure. The key lies in the hydration path of the calcium aluminate cement. By triggering the formation of gel-like hydrates instead of traditional crystalline hydrates (such as CAH_{10}, C_2AH_8, C_3AH_6, AH_3, and AH), the material's behaviour changes fundamentally. This specific gel releases its water at much lower temperatures between 100°C and 150°C. Thus, the system becomes more permeable before high-pressure hydrothermal conditions can develop. This allows for a safer, faster, and more economical dry-out process for industrial furnace linings.

INTRODUCTION

Explosive spalling remains a critical issue in the refractory industry when the dry-out stage is poorly managed. This failure is caused by excessive steam pressure build-up within the material[1]. To prevent this, increasing the permeability of the castable is essential. While polymeric fibers are systematically added to create permeable networks upon burning out (between 180°C and 250°C), the choice of the bonding system is equally decisive for drying sensitivity. Traditionally, Calcium Aluminate Cements (CAC) are the preferred hydraulic binders due to their predictable properties and high green strength. However, they require strict, slow heating schedules up to 600°C to safely remove water. Alternatives like Colloidal Silica (CS) offer faster dry-out capabilities through increased permeability with the decomposition of the silica gel at 100°C, yet they suffer from storage difficulties and low green strength. Conversely, Hydratable Alumina forms a boehmite-like gel that densifies the structure, unfortunately reducing permeability and raising the risk of explosive failure. To bridge these gaps, a recent development of a proprietary permeability enhancing active compound, an organo-mineral powder (abbreviated here as code MP30

*jeanmichel.auvray@imerys.com as corresponding author

Imerys) offers a hybrid solution[2]. It combines the mechanical advantages of CAC with the drying efficiency of gel/sol technologies. This paper investigates the hydration characteristics of CAC+MP30 compared to a standard 70% Al_2O_3 CAC. By proposing a specific reaction mechanism, this study demonstrates how MP30 modifies the hydration path responsible for a highly permeable microstructure at 110°C.

MP30 Concept

MP30 is a hydraulic binder that can be combined with a large range of CAC and already contains a deflocculating system adapted to most of castable formulation types. The recommended dosage is 2.5% by weight of castable by replacing all other dispersants and additives, as well as the balance of 2.5 wt.% of the matrix (mainly the binder). Table 1 gives the chemical compositions of MP30 and CAC.

Table 1. Main compositions of CAC (70%Al_2O_3) and MP30 binders.

Chemistry (%wt.)	Al_2O_3	CaO	MgO	SiO_2	LoI (950°C)
MP 30	34-38	16-18	16-20	< 0.9	24-30 %
CAC	68.7-70.5	28.5-30.5	< 0.5	0.2-0.6	< 1%

METHODS

A specific apparatus to measure the electrical conductivity was used to analyse the typical stages of dissolution and precipitation of the hydrates from CAC and MP30 containing diluted suspensions Solid/Liquid=1/10 at ambient temperature. Neat pastes (calcined alumina+CAC+MP30) have been prepared to follow the hydration evolution with CAC up to 7 days. Exothermic profiles, DSC and XRD measurements were performed to characterise the hydration behaviour of the two systems. Last, an example of applicative performance is given by measuring the drying behaviour of a refractory castable composition.

KEY FINDINGS

Hydration characteristics

Whilst a sharp increase of conductivity attributed to the partial dissolution is observed in Fig. 1.a for CAC suspension, it is seen a plateau of conductivity up to 7 hours before observing an increase of conductivity C for the MP30 containing suspension. This later is associated with a pH increase of the suspension from 9 to 12. The massive precipitation of hydrates, as characterised by a sharp decrease in the C curve is observed at 5 hours for the CAC suspension whilst never observed for CAC+MP30 suspension up to 24h. Fig. 1.b shows the exothermic profiles of neat pastes comprising of CAC as reference compared to the same material but with addition of two dosages of MP30. At very low dosage, it can be considered a high retarding effect of MP30 on the CAC hydration (peak located at 80h). At higher dosage, a first peak is observed during the first hours whilst a second peak appears later at around 60h that could be attributed to alumina hydrates formation.

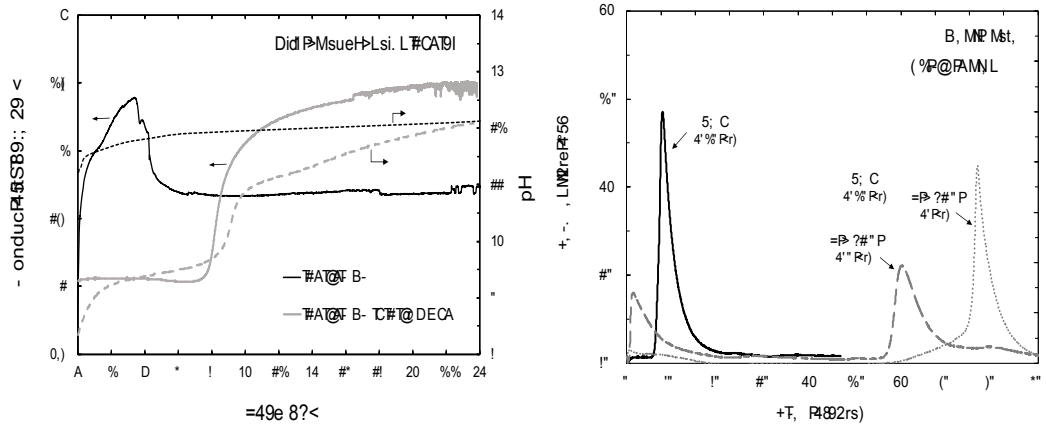

(a) (b)

Figure 1. Conductivity / pH curves vs. time (a) and Exothermic profiles (b) for CAC and CAC+MP 30 neat pastes.

DSC and XRD measurements have been performed on the same neat pastes containing CAC vs. CAC+MP30 (150gr CAC+10gr MP30) to follow the hydration until 7 days from the casting (see Fig. 2). At 24h, it is suggested that MP30 inhibits the hydration of the CAC since only alumina gel is observed (that decomposes at around 100°C according to the DSC curve).

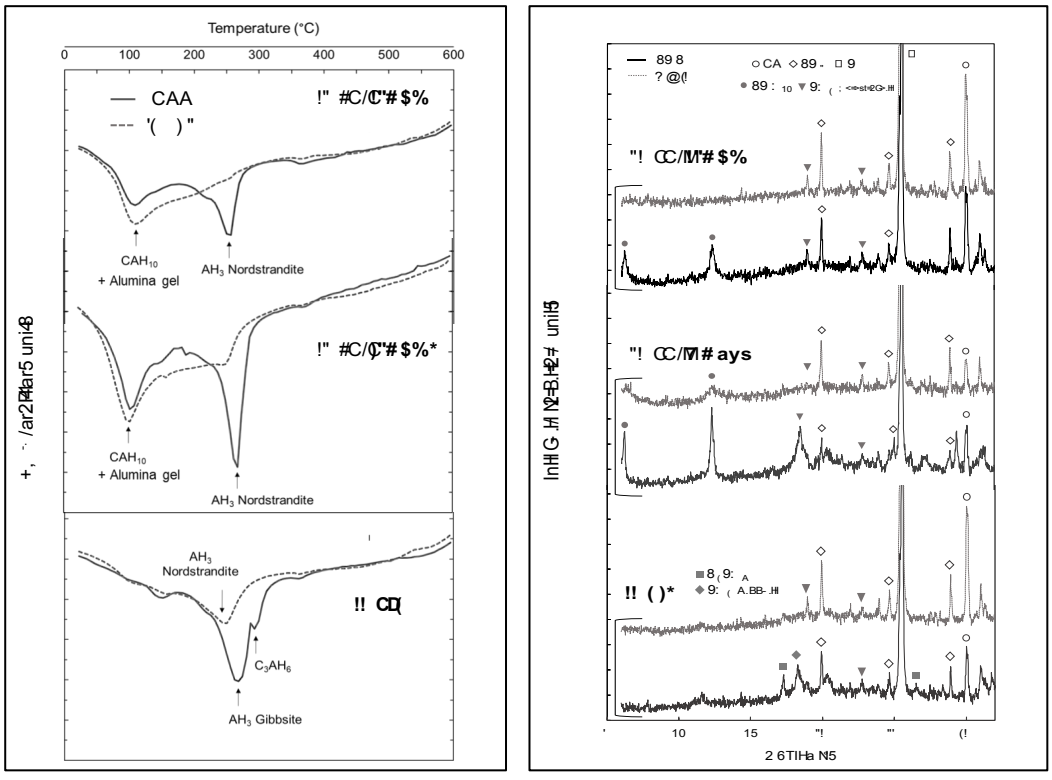

(a) (b)

Figure 2. DSC (a) and XRD (b) measurements for CAC and CAC+MP30.

After 7 days, a marginal amount of CAH_{10} is detected with MP30. This suggests that MP30 significantly inhibits or reduces the formation of these crystalline calcium aluminate hydrates, likely through a gelling mechanism.

At 110°C, whilst C_3AH_6 and AH_3 Gibbsite are formed for CAC paste, only AH_3 Norstrandite is obtained for MP30. It is assumed that it derived from the removal of water from the aluminous gel during this first drying stage.

Applicative performances

An example of the drying ability of a refractory alumina castable is given in Fig. 3. In CAC castables (5%wt. CAC with and w/o PP fibers), dry-out typically spans a broad range from 100°C to 400°C (Fig. 3.a). However, MP30 castable (2.5%wt CAC+2.5%wt MP30) releases water much earlier (100-150°C) due to a unique hydration/dehydration mechanism that creates a highly permeable microstructure according to the permeability values measured at 110°C, facilitating a faster mass transfer during heating. The advantage of this behaviour is that internal pressure build-up is largely decreased (Fig. 3.b) and reducing the risk of explosive spalling of the castable.

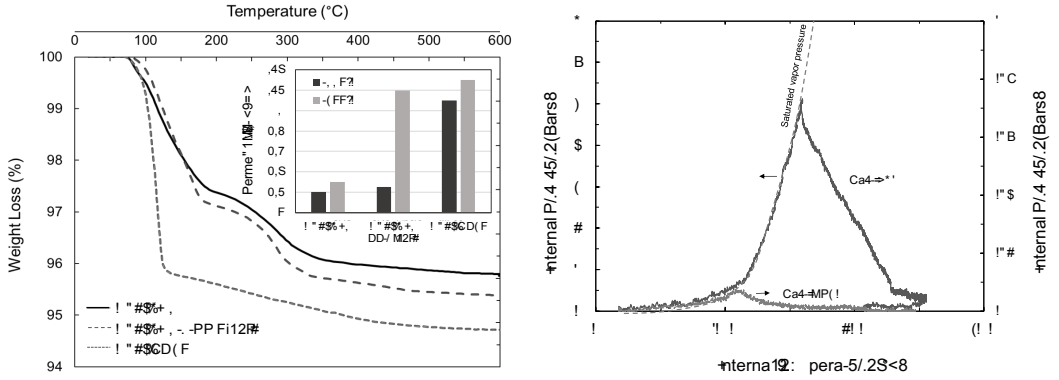

Figure 3. TGA (a) and pore pressure (b) measurements vs T°C for CAC and MP30 castables.

CONCLUSION

The new binder MP 30 significantly reduces the risk of explosive steam spalling in refractory concretes by modifying the hydration path of calcium aluminate cement. By triggering the formation of gel-like hydrates instead of traditional crystalline structures, the material releases water at lower temperatures (100°C–150°C). This early dehydration creates a highly permeable microstructure that minimizes internal pressure build-up, enabling a faster, safer, and more economical industrial dry-out process.

REFERENCES

1. R. Salomao, V.C. Pandolfelli, “Dry-out temperature-vapor pressure profile of polymeric fiber containing refractory castables”, Journal Tech. Asso. Refract., Japan, 24 [2], pp 115-19 (2004).

2. C. Zetterström, J.M. Auvray, C. Wöhrmeyer, C. Parr, “Enhanced permeability for a rapid dry-out of refractory castables”, Proc. UniteCr 2015, Vienna.

International Conference on Calcium Aluminates 2026

Calcium Aluminate Cement Hydration under the Influence of Mineral Acids

Deffner, Lukas[1] , Collin, Marie[1] , Gädt, Torben[1]*

[1]Chair for the Chemistry of Construction Materials, TUM School of Natural Sciences, Technical University of Munich, Lichtenbergstraße 4, 85748 Garching, Germany

Keywords: Calcium Aluminate Cement, Hydration, Mineral Acids, Thermodynamic Modeling

ABSTRACT

In technical applications, the hydration kinetics of calcium aluminate cement (CAC) are commonly modified by chemical admixtures. In this phenomenological study, we investigate the influence of five strong acids - HCl, HNO_3, $HClO_4$, H_2SO_4, and H_3PO_4 - on CAC hydration in dilute suspensions (w/s = 100). In-situ pH and conductivity measurements show that all acids inhibit the initial dissolution of monocalcium aluminate (CA). Thermodynamic modeling suggests that early precipitation of $Al(OH)_3$ plays a key role. Notably, the acids differ in their inhibiting efficiency at equivalent proton dosages. Phosphoric acid stands out, which is attributed to the simultaneous formation of hydroxylapatite and $Al(OH)_3$. For the other acids, the inhibition follows the order SO_4^{2-} > Cl^- > NO_3^- > ClO_4^-. This sequence is in line with the Hofmeister series, indicating that anion-specific effects influence calcium solvation. At the same time, the anion influence may also result from differences in the solubility of anion-containing aluminum hydroxide phases that form in the presence of the respective acid. In summary, this work provides new insights into acid-specific mechanisms during initial CAC dissolution by combining experimental data with thermodynamic modeling.

INTRODUCTION | BACKGROUND

Calcium aluminate cement (CAC) is widely applied in refractory systems and chemically resistant construction materials due to its rapid strength development and distinct hydrate assemblage [1]. Hydration is initiated by dissolution of monocalcium aluminate (CA), followed by a dormant period. During the main reaction, metastable hydrates such as CAH_{10} and C_2AH_8 precipitate, which later convert to stable phases including C_3AH_6 and

*torben.gaedt@tum.de

AH_3 [2]. Additives significantly influence CAC hydration kinetics. Lithium salts strongly accelerate the reactions, while hydroxides [3] and polymers like alginates [4] show smaller acceleration. In contrast, phosphates and various organic acids act as retarders [5,6], with effects linked to calcium complexation, salt solubility, surface precipitation, or formation of amorphous $Al(OH)_3$ layers. The mechanisms by which retarders interact with different cement types during hydration remain unclear, and no consensus exists on the rate-determining steps or overall process.
This study investigates the influence of five strong acids (HCl, HNO_3, $HClO_4$, H_2SO_4 and H_3PO_4 as a reference [5]) on the initial dissolution to focus on the role of pH and solubility of the different phases involved. Therefore, simple yet rigorous methods are applied. We combine in situ CAC dissolution experiments (high dilution) monitored by pH and conductivity measurements in combination with thermodynamic modeling to clarify the fundamental interactions between strong acids and calcium aluminate cement.
The objective of this work is to differentiate between proton-controlled thermodynamic effects and anion-specific mechanisms governing early CAC hydration.

MATERIALS AND METHODS

A commercial calcium aluminate cement (64.0% CA; 15.2% CA_2; 20.8% Al_2O_3) was used as the reactive phase. Hydration experiments were performed at high dilution (w/s = 100) in acidic solutions. The five strong acids - HCl, HNO_3, $HClO_4$, H_2SO_4 or H_3PO_4 - were dosed to achieve defined proton concentrations. The high dilution allowed the use of pH and electrical conductivity sensors, which track the pore solution conditions from the beginning of the hydration with high time resolution over two hours.
Supporting pore solution analysis was carried out by ICP-OES to determine the calcium and aluminum concentrations.
Thermodynamic calculations were performed using GEM-Selektor v.3.6 (GEMS) and the Cemdata18 database. Assuming only the reactive phase CA reacts in the studied timeframe, we modelled the phase development over the CA reaction degree.

RESULTS AND DISCUSSION

Compared to a reference (CAC in water), we found that pH and conductivity increase are delayed after binder addition to the stirring acidic solution. The temporal accordance with the delayed increase of calcium and aluminum concentrations in the pore solution confirms the observations from the sensors. This proves that the acid-introduced CA dissolution inhibition can be accurately tracked with the two sensors. Based on thermodynamic calculations, the inhibition of CA reactivity could be triggered by the rapid precipitation of $Al(OH)_3$ (whose solubility minimum occurs in mildly acidic

conditions). One possible explanation is that $Al(OH)_3$ precipitates directly on the surface of the reacting calcium aluminate phase(s), blocking active dissolution sites and thereby slowing further dissolution. Alternatively, the saturation state with respect to $Al(OH)_3$ restricts the aluminum transport from the CA phase in solution, which in turn reduces the overall dissolution rate.

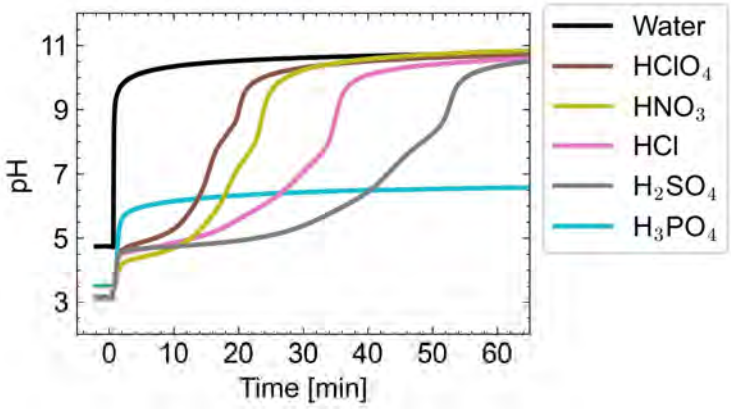

Figure 1. Influence of different mineral acids at equimolar proton concentrations of 82 µmol on the course of pH during hydration of CAC at w/s = 100.

At identical proton dosages (see Figure 1), pronounced acid-specific differences are observed. H_3PO_4 exhibits the strongest inhibition, consistent with additional precipitation of hydroxylapatite, which further reduces calcium activity in solution. For the remaining acids, the retarding efficiency follows the order: $SO_4^{2-} > Cl^- > NO_3^- > ClO_4^-$. Thermodynamic calculations suggest that this ion specific inhibition effect cannot be explained with calcium salts or anion incorporated AFm phases precipitation, since they do not form under the given conditions. However, it was found that these anions can be incorporated into the aluminum hydrate phase [7,8]. Unfortunately, solubility data are only available for the sulfate-containing phase (basaluminite) [8]. Yet, the experimentally determined solubility of the three phases that precipitate immediately after neutralization increases in the following order: $Al(OH)_{2.5}(Cl)_{0.5}\cdot xH_2O$ < $Al(OH)_{2.5}(NO_3)_{0.5}\cdot xH_2O$ < $Al(OH)_{2.95}(ClO_4)_{0.05}\cdot xH_2O$ [7]. The formation of phases with lower solubility has been shown to be associated with stronger inhibition of dissolution. Accordingly, in our systems, anion incorporation into the aluminum-containing phase may modify the solubility of the rate-limiting phase, leading to distinct inhibition times.

At the same time, we note that the observed sequence – $SO_4^{2-} > Cl^- > NO_3^- > ClO_4^-$ – aligns with the Hofmeister Series [9]. The series ranks ions by their effects on aqueous processes, with kosmotropes stabilizing water structure and chaotropes disrupting it. In mineral dissolution, stronger water-cation binding lowers the entropy of dissolution and slows the process. Electrolyte anions can stabilize the hydration shell of dissolving cations, reducing the entropy gain and decreasing dissolution rates. Thus, kosmotropes tend to inhibit dissolution, while chaotropes promote faster dissolution.

Although the exact understanding of the mechanism is incomplete, the results indicate the coupled impact of protons and anions on the hydration kinetics of CAC.

KEY FINDINGS | FUTURE RESEARCH NEEDS | CONCLUSIONS

- The addition of strong mineral acids inhibits early CA dissolution.
- Proton concentration governs early $Al(OH)_3$ precipitation and dissolution inhibition.
- H_3PO_4 exhibits the strongest retardation due to combined formation of $Al(OH)_3$ and hydroxylapatite.
- The anion-specific inhibition trend ($SO_4^{2-} > Cl^- > NO_3^- > ClO_4^-$) might be related to anion-influence on the stabilization of calcium ion solvation, or anion-incorporation into the aluminum-containing phase, thereby altering the solubility of the rate-limiting phase.

Conclusion:
Early CAC hydration is controlled by coupled dissolution–precipitation equilibria in which both proton activity and anion identity play decisive roles. The integration of in-situ measurements and thermodynamic modeling provides a mechanistic framework linking solution chemistry to practical hydration kinetics.

REFERENCES

[1] J.H. Ideker, K.L. Scrivener, H. Fryda, B. Touzo, in: P.C. Hewlett, M. Liska (Eds.), Leas Chem. Cem. Concr. Fifth Ed., Butterworth-Heinemann, 2019, pp. 537–584.
[2] F. Götz-Neunhoeffer, Modelle Zur Kinetik Der Hydratation von Calciumaluminatzement Mit Calciumsulfat Aus Kristallchemischer Und Mineralogischer Sicht, Universitätsbund Erlangen-Nürnberg: Universitätsbibliothek Erlangen-Nürnberg, Erlangen, 2006.
[3] B.R. Currell, R. Grzeskowlak, H.G. Mldgley, J.R. Parsonage, Cem. Concr. Res. 17 (1987) 420–432.
[4] A. Engbert, J. Plank, Mater. Des. 195 (2020) 109054.
[5] T. Manninger, D. Jansen, J. Neubauer, F. Goetz-Neunhoeffer, Cem. Concr. Res. 122 (2019) 83–92.
[6] R. Kaden, H. Poellmann, in: H. Pöllmann (Ed.), Cem. Mater., De Gruyter, 2017, pp. 159–190.
[7] G.J. Ross, R.C. Turner, Soil Sci. Soc. Am. J. 35 (1971) 389–392.
[8] D.K. Nordstrom, Geochim. Cosmochim. Acta 46 (1982) 681–692.
[9] Y. Zhang, P.S. Cremer, Annu. Rev. Phys. Chem. 61 (2010) 63–83.

International Conference on Calcium Aluminates 2026

HYDRATION OF CAC-ALUMINA SYSTEMS IN THE PRESENCE OF DIFFERENT SILICA FUMES

Schramm*, Tillmann; Neubauer, Jürgen; Goetz-Neunhoeffer, Friedlinde

Friedrich-Alexander-Universität Erlangen-Nürnberg, GeoZentrum Nordbayern, Mineralogy, Schlossgarten 5a, 91054 Erlangen, Germany

Keywords: Calcium aluminate cement, Silica fume, Refractory cement, Hydration, Setting

ABSTRACT

The study is focused on how the hydration of a refractory binder system consisting of commercial white CAC and tabular alumina is changed by the addition of different silica fumes. Four silica fumes, two each of identical quality grade, but obtained from different batches, were selected and characterized by their physical and chemical properties. Then they were added to the system with a SF/CAC ratio of 1 and w/c of 1.4 at 23 °C. Even though no clear differences could be observed between the fumes of the same grade regarding chemical bulk analysis and specific surface area, they exhibited different rheological behavior after paste preparation.

To examine this, the hydration was followed via heat flow calorimetry, in-situ XRD and pore solution analysis. Additionally, hardness development within the first hours of hydration was measured with a Gillmore-needle device (IMETER).

It was found that the mixes with lower viscosity show an additional heat flow event located between the initial heat flow after mixing and the main reaction. This intermediate event is likely correlated to an initial dissolution of CA, which occurs directly after water addition in the mixes without this event. Also, an increased rate of hardness development was observed during the intermediate event. A potential link to the amount of dissolved silicon provided by the silica fumes shown in the pore solution data was examined by adding solutions containing low amounts of sodium silicate to the mixes. By this, the event could be induced in the two systems previously not showing this reaction. Higher concentrated solutions retard the hydration until a critical point, where the main reaction is eventually suppressed for at least 48 h.

INTRODUCTION | BACKGROUND

White, iron-free calcium aluminate cements (CAC) are widely used as binding component in refractory castables, particularly due to their high Al_2O_3 content which contributes to heat resistance. In such systems low porosity is of utmost importance since open porosity increases infiltration e.g. during steel production which accelerates wear and reduces lifetime.

tillmann.schramm@fau.de

To counteract, fine materials such as silica fume (SF) are added to the matrix. Besides increased mechanical strength, this can also contribute to a reduction of the water demand by filling the pore space and improve flow behavior [1]. SF is a byproduct of the (ferro-)silicon industry and consists of fine, amorphous, SiO_2-rich powder, with spherical primary particles less than 1 µm in diameter. Past studies [2,3] have shown that SF can induce an additional heat flow event between initial period and main reaction. This intermediate event (IE) is correlated to a premature stiffening of the paste which can critically impair the flow of castables. It was observed that the appearance of the IE depends on the SF/CAC ratio in the mix (the higher, the later it begins) and that there may be a correlation to the readily soluble amount of Si initially released by SF upon first contact with mixing water. Therefore, different SFs were investigated regarding their influence on hydration kinetics and hardness development and were additionally mixed with Na_2SiO_3 solutions to evaluate the potential effect.

METHODS

The materials used were a pure white CAC (CA14-S by Almatis), tabular alumina (T60/T64 -45 micron LI by Almatis) and four silica fumes: quality grade “A”, batch “1” and batch “2”, and quality grade “B”, batch “1” and batch “2”. The chemical compositions of these components were analysed via XRF (Table 1). The investigated pastes were composed based on these 3 ratios: SF/CAC = 1, Alumina/CAC = 1.5 and water/CAC = 1.4 or 2.8 (the higher w/c was necessary to extract sufficient solution amounts via centrifugation). The $Na_2SiO_3 \cdot 5H_2O$ was added to the mixing water and the bound water was accounted for to keep the water/CAC constant (Table 2).

Table 1. XRF analysis and specific surface area (SSA) determined by BET of the materials used. Sulfate content was determined via nephelometry.

[wt%]	CAC	Alumina	SF(A1)	SF(A2)	SF(B1)	SF(B2)
CaO	29.2	≤0.1	0.3	0.3	0.3	0.5
Al_2O_3	69.4	99.2	≤0.1	≤0.1	≤0.1	≤0.1
Na_2O	≤0.1	0.2	0.6	0.4	0.6	0.5
K_2O	≤0.1	≤0.1	0.2	0.2	0.6	0.4
MgO	0.2	≤0.1	0.1	0.1	0.3	0.4
Fe_2O_3	0.2	≤0.1	0.1	0.1	0.1	0.1
SiO_2	0.2	≤0.1	97.4	97.5	95.5	95.5
SO_3	-	-	0.2	0.2	0.3	0.4
LOI	0.2	0.3	1.0	1.1	2.3	2.1
SSA [m^2/g]	0.8±0.1	1.5±0.1	26.1±0.2	25.7±0.2	20.4±0.2	20.0±0.2

Every experiment was executed at 23 °C. Heat flow calorimetry was performed for every mix with a TAM air calorimeter. Hardness measurements were executed with an automated Gillmore-needle device (“Imeter” by MSB Breitwieser). For selected SFs quantitative in-situ XRD measurements were performed over the course of 24 h with a D8 ADVANCE diffractometer by BRUKER-AXS. Pore solutions were extracted

via centrifugation, filtered with a 0.2 µm syringe filter and measured by ICP-MS.

Table 2. Composition of pastes. SF(X) is calculated to 100 g, $Na_2SiO_3 \cdot 5H_2O$ is added on top. Nomenclature: e.g. SF(A1)+0.1NaSi = To the mix containing SF(A1) 0.1 %bwoc (by weight of cement) $Na_2SiO_3 \cdot 5H_2O$ was added.

[g]	CAC	SF	Alumina	$Na_2SiO_3 \cdot 5H_2O$	Deion. H_2O
w/c = 1.4					
SF(X)	20.4082	20.4082	30.6122	-	28.5714
+0.4NaSi	"	"	"	0.0816	28.5368
+0.5NaSi	"	"	"	0.1020	28.5281
+0.6NaSi	"	"	"	0.1224	28.5194
w/c = 2.8					
SF(X)	15.8730	15.8730	23.8095	-	44.4444

KEY FINDINGS | CONCLUSIONS

The heat flow curves and hardness developments of samples with every investigated SF are shown in Figure 1. Independently of quality grade (A or B) pastes display a sharp heat flow peak after a few minutes of hydration (batches A1 and B1) or directly after water addition (batches A2 and B2). This makes paste preparation, especially in SF(B2), extremely hard, which is why SF(A1) and SF(A2) were chosen for further investigations on systems of "good" and "bad" initial rheology.

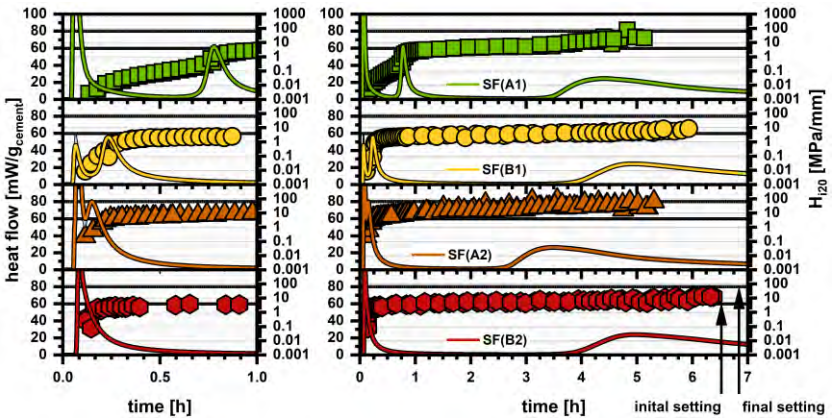

Figure 1. Heat flow curves and hardness development of mixes containing different SFs.

In the left section of Figure 2 the in-situ phase developments of SF(A1) and SF(A2) are shown. Precipitation of the hydrate phases CAH_{10} and C_2AH_x starts with the main reaction, and no crystalline precipitates are detected during the intermediate event. However, in SF(A1) it can be seen, that a small amount of CA is dissolved during the IE. This becomes more obvious in the pore solution data (Figure 2, right section). Before the IE in SF(A1), Ca and Al concentrations as well as pH (around 8-9) are comparatively low. During this period, Si present in solution is consumed until no Si is detectable anymore at the start of the IE. The initial CaO/Al_2O_3 ratio is very high (950/1 at the first measurement point after 5 min) and the dominant aqueous Si species at the given pH of 8.6 is $Si(OH)_4^0$. We therefore suggest

adsorption of $Si(OH)_4^0$ on a metastable Al-rich layer on CA surfaces formed due to incongruent dissolution is causing its stabilization and leading to a retardation of the initial CA dissolution.

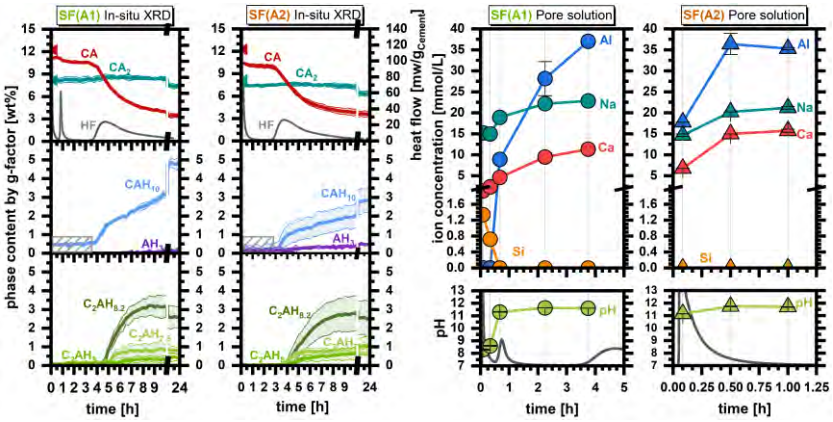

Figure 2. Phase development (left) and pore solution compositions of SF(A1) and SF(A2) (right).

Addition of $Na_2SiO_3 \cdot 5H_2O$ provides dissolved Si and is causing a retardation in the investigated mixes (Figure 3). This underlines the suggested mechanism of readily soluble Si provided by SF potentially being the reason for the observed hydration kinetics. Higher pH of these solutions could lead to different Si species which might explain e.g. the reduced hydration rates. Further investigations are needed to verify this hypothesis.

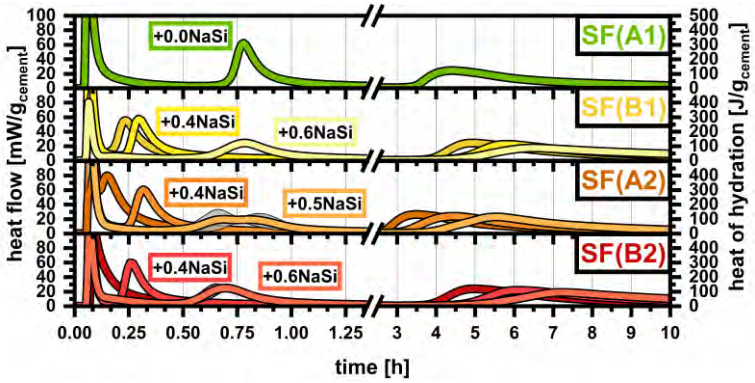

Figure 3. Heat flow curves of pastes containing $Na_2SiO_3 \cdot 5H_2O$.

REFERENCES

[1] M. Schnabel, A. Buhr, J. Dutton, Rheology of High Performance Alumina and Spinel Castables, Refractories World Forum 4 (2012) 95–100.

[2] S. Moehmel, W. Gessner, T.A. Bier, C. Parr, The Influence of Microsilica on the Course of Hydration of Monocalcium Aluminate, in: CAC: Calcium Aluminate Cements 2001, Edinburgh, 2001: pp. 319–330.

[3] T. Schramm, J. Neubauer, F. Goetz-Neunhoeffer, Influence of silica fume addition and content on the early hydration of calcium aluminate cement – The role of soluble silicon, Cem. Concr. Res. 184 (2024). https://doi.org/10.1016/j.cemconres.2024.107618.

International Conference on Calcium Aluminates 2026

Incorporation of metakaolin and limestone in ternary binders of Portland cement, calcium aluminate cement and calcium sulfate: Hydration, Phase development and Macroscopic properties

Qoku, Elsa[1*], Liu Liqiao [2], Bier Thomas[2],
[1]Institute of Building Materials, Concrete Construction and Fire Safety, Beethovenstrasse 52, 38106, Braunschweig, Germany
[2]Technical University of Freiberg, Institute for Ceramics, Refractories and Composite Materials, Leipziger Straße 28, 09599, Freiberg, Germany

ABSTRACT

This study examines the role of limestone and metakaolin as cement substitute in CAC-PC-calcium sulfate ternary binders. Combinations of CAC-PC-C$ with amounts of 5 up to 25% wt.% metakaolin/limestone were investigated in terms of heat evolution, setting time, phase formation, dimensional stability and strength development up to 90 days of hydration.

Within the first 24 hours of hydration both metakaolin and limestone lead to an acceleration of the heat of hydration, presumably serving as nucleation sites for both PC and CAC rich formulation.

Compressive strength increased by ~ 36%, in the metakaolin based compositions over 90 days compared to the control, while shrinkage was mitigated in the CAC rich samples. No major difference between samples with 5, 15 and 25 wt.% of substitution were observed, hence indicating that even small additions are sufficient to achieve an improvement in strength. Formation of AFm-carbonate equivalent phases was favored in presence of limestone. The content of AH_3 decreased with the increase of substitution level for CAC rich samples with metakaolin.

INTRODUCTION

Ternary binders composed of Portland cement (PC), calcium aluminate cement (CAC) and calcium sulphate have ($C\overline{S}H_X$) are widely applied as tile adhesives, self-leveling underlayment, and other technical formulations for repair work.

With the cement technology moving towards low embodied CO_2 cements, optimization of these systems that meet the sustainability need becomes relevant. Previous reports demonstrate that replacement of CAC by slag, silica fume or fly ash hinders the conversion process. Experimental evidence suggests that the silica present in the SCMs reacts with the calcium aluminates by avoiding the formation of C_2AH_8 and subsequently the conversion to C_3AH_6. Instead, formation of strätlingite occurs [1]. However, the incorporation of SCMs in PC-CAC- $C\overline{S}H_X$ ternary binders, has been overlooked and their role in such compositions has been hardly reported in the literature [2][3][4]. In the OPC rich quaternary formulations the limestone-based paste develops the highest compressive strength and lowest porosity, in respect to samples with fly ash and slag where a reduction in the compressive strength and increased in porosity was reported.

*Corresponding author: E.Qoku@ibmb.tu-bs.de

Similar results were observed in the CAC-rich quaternary binders. The increase of compressive strength in presence of limestone powder has been linked with formation of AFm-carbonate equivalents, thus leading to an increased volume of hydrates [3] [4].
In this work we expand the investigations and show selected results in terms of macroscopic properties as well as hydration for ternary systems composed of PC-CAC- $C\overline{S}Hx$ and limestone/metakaolin at different substitution levels.

MATERIALS

Table 1 shows the composition on the systems investigated in this work. CEM I 42.5 R was used as PC, along with Secar 51 as CAC. Anhydrite was used as sulphate source for the PC rich system and hemihydrate for the CAC rich formulations. Relatively pure limestone powder (LSP) and highly amorphous metakaolin (MK) at substitution levels of 5,15 and 25 wt.% of PC/CAC were varied through the study, whereas the sulphate content was kept constant.

Table1: Composition of the investigated systems.

System	PC	CAC	CSHx	LSP/MK
PC rich	92	0	8	0
	87	5	8	5
	77	15	8	15
	67	25	8	25
CAC rich	74.1	0	25.9	0
	69.1	5	25.9	5
	59.1	15	25.9	15
	49.1	25	25.9	25

Hydration was characterized though calorimetry measurements and vicat during the first 24 hours of hydration. All pastes were prepared at w/s = 0.55. Compressive strength was tested using 40 x 40 x 160 mm^3 prisms according to EN 196-1 up to 90 days of hydration storage conditions: 20 °C, 65% RH. Length change measurements in dry conditions were carried out up to 90 days of hydration. Additionally, qualitative analysis through TGA measurements was carried out at selected times of hydration.

SELECTED RESUTLS

Fig.1 shows results of the PC-rich formulation in presence of metakaolin in terms of calorimetry, compressive strength development and length change over 90 days of hydration. The use of metakaolin at substitution levels of 15 and 25 % slightly accelerates the hydration as shown in the calorimetry curve. Faster initial setting times were also measured, with the reference sample exhibiting an initial set time (data not shown herein) at 360 min vs 340 min, 300 min for the samples with 15 and 25 % substitution respectively.

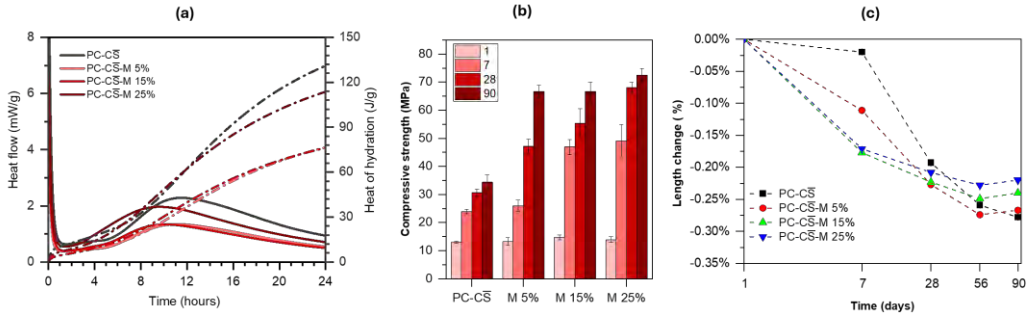

Fig 1: (a) Calorimetry heat flow measurement in presence of metakaolin (b) compressive strength measurements and (c) length change measurements up to 90 days of hydration for PC rich formulations.

An increase of compressive strength (Fig.1b) by ~ 36% in respect with the reference sample is observed across all substation levels at 90 days of hydration, whereas length change measurements in Fig.1c indicate that the use of metakaolin slightly mitigates shrinkage only at 90 days of hydration.

Fig 2 shows selected results for the CAC-rich formulations. The heat flow curves for each of the pastes in presence of metakaolin are depicted in Fig.2a. Almost three hydration peaks are evident in each of the curves, indicating a complex hydration behaviour. Most evident is the absence of the hydration event between 12-20 hours for compositions with 15 and 25% metakaolin substitution. In presence of liestone an acceleration of the main hydration peak by almost 4 hours was evident (data not shown here). In term of compressive strength (Fig. 2c), no major difference was observed across all samples with metakaolin in respect with the reference sample except the samples at 90 days of hydration. In presence of limestone an improved strength was identified only for samples with 5% substation. Finally, in contrast with PC-rich systems, in the case of CAC formulations, the use of metakaolin is found to mitigate shrinkage across all substitution levels (Fig 2b).

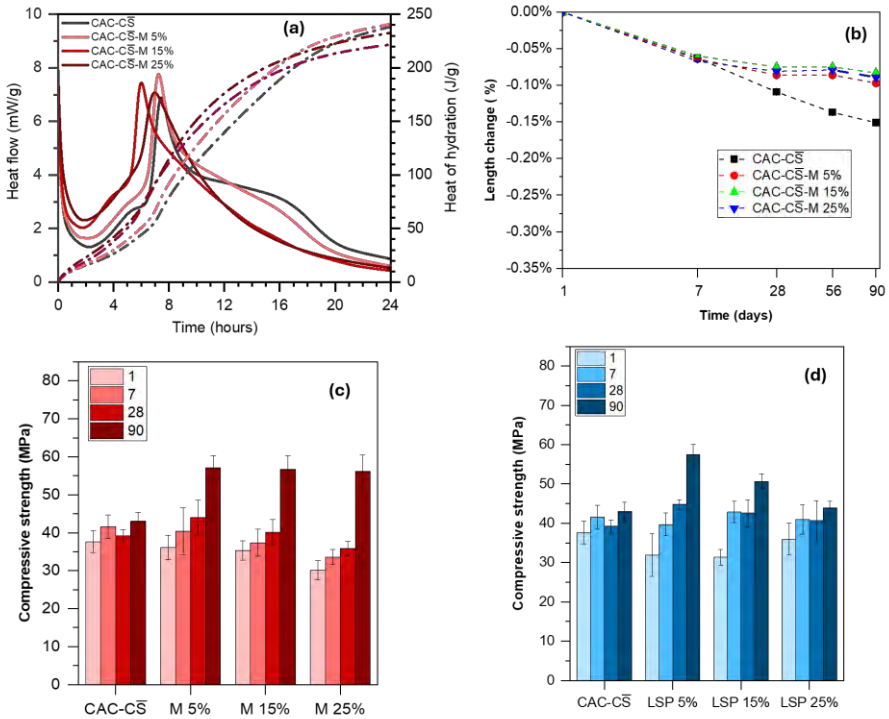

Fig. 2: (a) Calorimetry heat flow measurement in presence of metakaolin (b) length change measurements and (c) compressive strength measurements up to 90 days of hydration for CAC rich formulations.

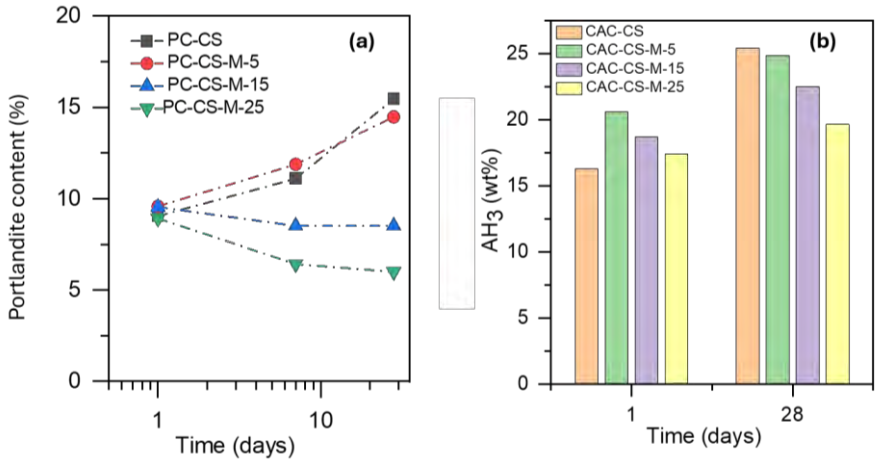

Fig.3: (a) Portlandite content in presence of metakaolin for the PC rich samples (b) AH_3 content in presence of metakaolin the CAC rich samples.

Finally, Fig. 3 shows semiqualitative results obtained from the TGA data for the portlandite and AH3 content of PC rich and CAC rich samples in presence of metakaolin up to 28 days of hydration. A decrease of Portlandite content is observed for the samples with 15 and 25 wt.% of metakaolin substitution, most likely due to pozzolanic reactions. For the CAC rich formulations, the AH_3 content decreases with the increase of substitution level. Formation of AFm-carbonate equivalent phases was favoured in presence of limestone (data not shown herein).

SUMMARY

- The use of metakaolin in both CAC and PC formulations leads to strength gain, mostly enhanced for PC based pastes.
- In the CAC rich formulations, the use of metakaolin leads to shrinkage mitigation.
- The presence of metakaolin influences the formation of portlandite in the PC-rich formulation as well as the formation of AH_3 in the CAC rich formulation.

REFERENCES

1. López A. H., et al. (2008) Microstructural evolution of calcium aluminate cements hydration with silica fume and fly ash additions by scanning electron microscopy, and mid and near-infrared spectroscopy J. Am. Ceram. Soc. 91 1258–65.
2. Fernández-Carrasco L. and Vázquez E. (2009) Reactions of fly ash with calcium aluminate cement and calcium sulphate Fuel 88 1533–8.
3. Bizzozero J. and Scrivener K. L. (2015) Limestone reaction in calcium aluminate cement-calcium sulfate systems Cem. Concr. Res. 76 159–69.
4. Bier T., et al. „Supplementary cementitious materials (SCM) in OPC and alkali activated binders" Industrial wastes – Characterization, Modification and Application of industrial residues. ISBN: 9783110674866

International Conference on Calcium Aluminates 2026

ENERGY-EFFICIENT 3D PRINTABLE MORTARS USING CAC–WPC BLENDS AND MICROENCAPSULATED PCMS

Sönmez, Sibel[1]; Sucu, Melike[1]; Engin, Ahmet S.[1]; Bundur, Zeynep B.[2]; Paksoy, Halime Ö.[3]

[1]Çimsa Çimento Sanayi ve Ticaret A.Ş., İstanbul, Turkey, 34750

[2] Özyeğin University, Faculty of Engineering, Civil Engineering Department, Istanbul, Turkey, 34794

[3] Çukurova University, Faculty of Science and Letters, Department of Chemistry, 01330 Adana, Turkey

Keywords: Calcium aluminate cement; White Portland cement; 3D printing; Microencapsulated PCMs; Energy-efficient mortars

ABSTRACT

Additive manufacturing (3D printing) continues to advance as an alternative to conventional construction techniques due to its numerous technical and operational advantages. This study aims to develop a mortar system incorporating Calcium Aluminate Cement (CAC), White Portland Cement (WPC), and microencapsulated Phase Change Materials (mPCMs) for 3D-printing applications. The inclusion of mPCMs provides latent heat storage capability, offering potential benefits for energy-efficient construction materials. The CAC used in the formulations contains a minimum alumina content of 50%, and the mineralogical characteristics of both CAC and WPC were determined by XRD–Rietveld analysis.

Printability requirements for extrusion-based additive manufacturing were evaluated through extrudability, buildability, workability loss, open time, green strength, and early-age compressive strength. The results demonstrate that the combined use of CAC and WPC induces the thixotropic behavior essential for maintaining structural stability during layer-by-layer deposition. The designed mortar mixtures exhibited sufficient flowability for extrusion while achieving high green strength to ensure dimensional stability. Furthermore, the incorporation of mPCMs was found to enhance buildability, indicating their potential to improve the performance of 3D-printed cementitious systems.

INTRODUCTION | BACKGROUND

Additive manufacturing has emerged as a promising alternative to traditional construction due to reductions in material waste, elimination of formwork, and improved labor efficiency.[1] For extrusion-based 3D printing, the performance of cementitious mortars relies on achieving an appropriate balance between pumpability during deposition and sufficient stiffness to sustain the load of subsequent layers.[2]

Calcium aluminate cement (CAC) has been investigated in printable binder systems because its rapid strength development and controllable setting

s.kurtsonmez@cimsa.com.tr

profile can support the early-age stiffening required for layer stability.[3] When blended with white Portland cement (WPC), CAC can contribute to thixotropic behavior, which helps maintain the geometry of printed layers by increasing structural build-up after extrusion.[4]

Parallel to fresh-state rheological requirements, there is a growing interest in developing energy-efficient cementitious materials for digital fabrication. Incorporating microencapsulated phase change materials (mPCMs) into printable mortars enables latent heat storage, improving thermal regulation in building elements without additional insulation layers.[9–11] These microcapsules can absorb and release heat during phase transitions, providing functional thermal performance in addition to structural behavior.

In this study, several CAC–WPC combinations were first screened to evaluate workability, open time, thixotropy, and green strength. Based on these assessments, two optimized formulations were selected: a control CAC–WPC mortar and a modified formulation containing 2% mPCM. Focusing on these two mixes allowed the investigation to isolate the influence of PCM incorporation on printability, setting behavior, and thermo-mechanical performance while maintaining suitability for extrusion-based additive manufacturing.

METHODS

Materials and Mix Selection

Several CAC–WPC mortar formulations were initially prepared to identify mixtures suitable for extrusion-based 3D printing. Based on fresh-state behavior—including flowability, thixotropic stiffening, open time, and green-strength performance—one optimized mix was selected as the control formulation, while a second mix was produced by incorporating 2% mPCMs to introduce latent-heat storage functionality. The microcapsules, consisting of polymer-coated organic PCM cores, were chosen for their spherical morphology, thermal stability, and durability documented in prior studies.[9–11] All mortars were prepared with standardized silica sand (maximum particle size 1 mm), and high-range water-reducer and polymer-based additives were used to achieve appropriate workability and rheological response during extrusion.

Workability evolution was evaluated using a flow table test (ASTM C230), where reductions in flow diameter over time served as indicators of early-age stiffening and thixotropy—two essential characteristics governing pumpability and shape retention in layered deposition.[1–2] Green strength, representing the structural stability of freshly deposited layers, was measured 30 minutes after mixing using a loading-to-failure procedure, and the resulting stresses allowed direct comparison of buildability between the control and PCM-modified mortars.[3] Setting behavior was examined using a modified Vicat needle protocol adapted from ASTM C191, and early-age mechanical performance was assessed through compressive and flexural strength testing at 1, 3, and 7 days according to EN 196-1 standards.

KEY FINDINGS | FUTURE RESEARCH NEEDS | CONCLUSIONS

Effect of mPCM on Workability and Early-Age Rheology

The control mix showed a gradual reduction in flowability, reflecting thixotropic stiffening beneficial for shape retention. The PCM-modified mix exhibited slightly faster workability loss, suggesting accelerated structural build-up—yet remained within printable limits.

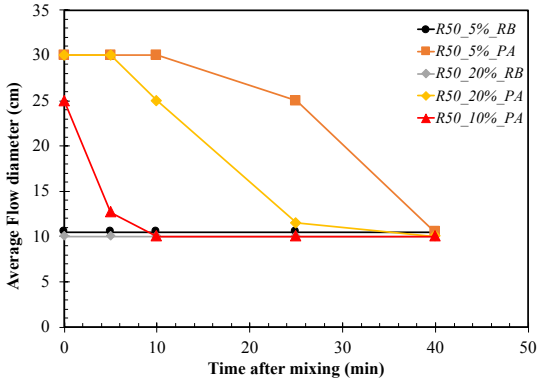

Figure 1: Flowability evolution of sWPC- Recipro 50 Blended mortars with time.

Green Strength and Buildability Performance

The PCM-modified mix demonstrated higher green strength at 30 minutes, indicating enhanced layer-support capability due to microcapsule-induced internal resistance.[3]

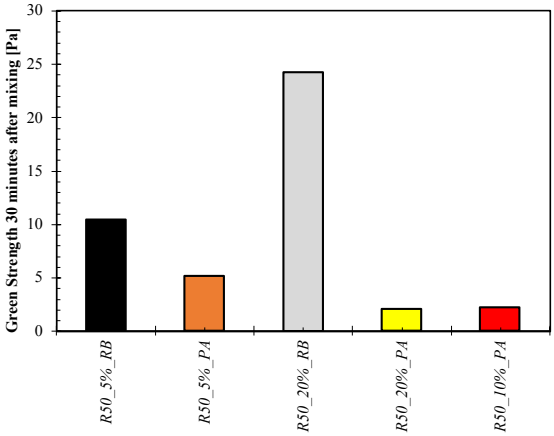

Figure 2: Green strength of sWPC- Recipro 50 Blended mortars 30 min after mix-ing.

Setting Behavior and Early-Age Strength Development

Both mixes achieved suitable setting times for extrusion processes. PCM addition caused moderate reductions in compressive/flexural strength but maintained acceptable structural capacity for printable mortars.

!"# A%("# C	CompreI I-. e !/ reMN2' (N4## RS			7%x/9+"%/ renN2'' (N4## RS			In-/-"%an; ' /-MN/-m
=NCP">S	?'	@	A'	?'	@	A'	In-/-"%
R5EFad FPA'	38.h'	53.a'	ahg@	hga'	13.i '	13.a'	155N
5EFad FPAFeF l Rd'	"Ragl '	@dgh'	"" 41.h'	7.i '	10.i '	12gi '	??EN

Table 1. Compressive and Flexural Strength values for mortar samples

Thermal Functionality and Latent Heat Contribution

Differential scanning calorimetry (DSC) results confirmed that the mPCMs provided a latent-heat storage capacity of approximately 50 J/g at a phase-change temperature near 24 °C, enabling the mortar to absorb and release thermal energy during the transition process.

This thermal functionality enhances the potential of the printed elements to regulate temperature fluctuations without the need for additional insulation layers. The microcapsules maintained their spherical morphology during mixing, and their integration did not disrupt fresh-state performance, demonstrating the feasibility of combining energy-storage capability with extrusion-based printability.

CONCLUSIONS

This study demonstrated that CAC–WPC mortars modified with microencapsulated PCMs can meet the fresh-state and mechanical requirements for extrusion-based 3D printing while offering energy-storage capability. PCM incorporation slightly accelerated rheological stiffening but improved buildability and maintained sufficient printability. Although early-age strength values were moderately reduced, structural integrity remained within acceptable limits. The combined thermal and mechanical performance highlights the potential of CAC–WPC–mPCM blends as multifunctional materials for energy-efficient 3D-printed construction. Future research may optimize PCM dosage and microcapsule properties to enhance durability and latent-heat performance.

REFERENCES

1. Paul, S.C., et al. Arch. Civ. Eng., 2018, 311–319.
2. Soltan, D.G., Li, V.C. Cem. Concr. Compos., 2018, 1–13.
3. Rahul, A., et al. Cem. Concr. Compos., 2019, 13–23.
4. Panda, B., Tan, M.J. Ceram. Int., 2018, 10258–10265.
5. Wangler, T., et al. RILEM Tech. Lett., 2016, 67–75.
6. Cellat, K., et al. Energy Build., 2015, 156–163.
7. Konuklu, Y., Paksoy, H.O. Sol. Energy Mater. Sol. Cells, 2017, 235–242.
8. Beyhan, B., et al. Int. J. Energy Res., 2017, 113–126.

International Conference on Calcium Aluminates 2026

EFFECTS OF SILICA NANO-PARTICLES ON HYDRATION PROPERTIES, MICROSTRUCTURE AND STRENGTH OF CALCIUM ALUMINATE CEMENT

Boris*, Renata; Antonovič, Valentin; Madej, Dominika; Kruk, Andrzej; Stonys Rimvydas; [1]Vilnius Gediminas Technical University, Linkmenų str. 28, Vilnius 08217, Lithuania
[2]AGH University of Kraków, A. Mickiewicza ave 30, Kraków 30-059, Poland
*E-mail: renata.boris@vilniustech.lt

Keywords: calcium aluminate cement, silica sol, hydration, microstructure, X-ray difraction

ABSTRACT

Hydration phenomena of a commercial white calcium aluminate cement (CAC (Górkal 70); Al2O3 – 69–72%) at 20°C was modified by adding silica nanoparticles addition in varying amounts and additives in the context of using CACs in the aspiration to achieve climate neutrality and the goal of net zero. The hydration process of CAC modified with silica sol (SS) was tracked by heat flow calorimetry, XRD and SEM experiments supplemented by mechanical strength determination at different curing ages. The findings demonstrate the potential to modify the traditional early (24 hours) hydration pathway of CAC-based systems by both SS and additives, leading to an accelerated process, in terms of the second exothermic peak of paste, and improved mechanical strength, even though no crystalline hydrates were formed. The results indicate that the evolution of the hydration is closely related to the effect of the SS content and additives on the densification and microstructure properties. CAC-based mortar containing 5 wt.% SS and additives exhibited the highest compressive strength, suggesting that early strength development may be attributed to silica nanoparticles acting as a filler. It is also evident that silica sol promotes the formation of CAH10 rather than C2AH8. All binder systems remain strength increase when exposed to 28-days curing conditions.

INTRODUCTION

Global carbon dioxide (CO_2) emissions remain at critically high levels, with the Global Carbon Project emphasizing the increasing vulnerability of natural carbon sinks to climate change. Cement production is a major contributor to these emissions due to both energy-intensive processes and inherent chemical reactions. In particular, the calcination of calcium carbonate ($CaCO_3$) during clinker production releases significant amounts of CO_2. Since emissions from cement-based composites are directly related to the proportion of Portland cement (PC)

*email address of corresponding author

used, reducing its content is essential for lowering the environmental impact of construction materials [1,2].

Portland cement dominates global clinker production, accounting for approximately 99.8% of total output. Its composition mainly includes calcium silicates (C_3S, C_2S), tricalcium aluminate (C_3A), and calcium aluminoferrite (C_4AF). In contrast, calcium aluminate cement (CAC), composed primarily of calcium aluminate phases such as CA, $C_{12}A_7$, and CA_2, is produced in much smaller quantities—around 1,000 times less than PC. However, CAC offers environmental advantages due to its lower calcium oxide content, resulting in reduced CO_2 emissions during production. As a result, CAC is increasingly considered a promising alternative binder for sustainable and potentially net-zero construction materials. The development of such alternative hydraulic binders is essential for reducing environmental impact while maintaining performance [3].

A key challenge associated with CAC is its hydration behavior, particularly the formation and transformation of hydrated phases. During hydration, metastable hydrates such as CAH_{10} and C_2AH_8 are formed, which can convert into the more stable C_3AH_6 phase depending on temperature, time, and water availability. This conversion process leads to increased density and often a reduction in mechanical strength. Since these transformations strongly influence long-term performance, understanding and controlling hydrate conversion is critical.

The hydration reactions of the CA phase are temperature-dependent. At low temperatures (below ~10–15°C), CAH_{10} is predominantly formed. At moderate temperatures (15–30°C), C_2AH_8 and aluminum hydroxide (AH_3) are produced, while at higher temperatures (above ~30–60°C), the stable hydrate C_3AH_6 becomes dominant. Although the exact temperature ranges vary across studies, it is generally accepted that higher temperatures accelerate the formation of stable hydrates and promote conversion.

To improve both sustainability and performance, various strategies have been explored, including the incorporation of supplementary cementitious materials such as microsilica, blast furnace slag, fly ash, metakaolin, and other pozzolanic additives. These materials not only reduce CO_2 emissions but also influence hydration processes and mitigate the negative effects of hydrate conversion [4-5].
Microsilica, an ultrafine amorphous silica with particle sizes around 150 nm, is particularly effective in modifying CAC hydration. It promotes the formation of additional hydration products, especially stratlingite (C_2ASH_8), which helps stabilize the microstructure and reduce the extent of conversion. An optimal replacement level of around 15% microsilica has been reported to enhance beneficial phase formation and improve long-term performance. However, microsilica does not completely prevent the formation of stable hydrates such as C_3AH_6.

The effect of microsilica on CAC hydration is multifaceted. It acts as a nucleation site for hydrate formation, refines pore structure, binds free water and ions, and participates in reactions that produce more stable microstructures. These effects generally improve long-term strength, although early-age strength may decrease due to accelerated reactions and shorter setting times [6-7].

Despite increasing interest in low-CO_2 CAC-based binders, systems incorporating nanocolloidal silica remain less studied. This is mainly due to challenges such as poor rheological properties, rapid setting, and low early strength.

These limitations are likely related to insufficient understanding of the interaction mechanisms between calcium aluminates and nanoscale silica, as well as the lack of suitable admixtures for such systems [8,9].

Various analytical techniques, including calorimetry, X-ray diffraction, thermal analysis and electron microscopy, have been widely used to investigate CAC hydration. These methods provide valuable insights into phase development, microstructure evolution, and reaction kinetics [10,11].

This study aims to advance the understanding of CAC systems modified with colloidal silica by investigating their hydration behavior, phase composition, and microstructural evolution. The findings are expected to clarify the mechanisms governing hydrate formation and conversion, and to support the development of more sustainable and high-performance CAC-based binders.

METHODS

CAC, grade Gorkal 70, was produced at the interprise Gorka Cement sp. z o.o in Trzebinia (Poland). The XRD spectrum of CAC are shown in Figure 1. The chemical composition and main phases, is shown in Table 1. As determined by XRD, the minerals monocalcium aluminate (CA) and calcium dialuminate (CA_2) were predominant. The phases α-Al_2O_3 and $C_{12}A_7$ were also identified and existed in small amounts in CAC.

Silica sol LITHOSOL 1540, additives GIESSFIX PT 88 (Additive 1) and DOLAPIX FF 44 (Additive 2) were provided by the Zschimmer & Schwarz (Lahnstein, Germany). The characteristics of silica sol LITHOSOL 1540 are: average particle size – approximately 15 nm, specific surface area – approximately 200 m^2/g and SiO_2 content – approximately 40%.

The CEN-NORMSAND according to the DIN EN 196-1 (Normensand GmbH, Beckum, Germany) was also used to prepare the CAC-based cement mortars bonded with silica sol [12].

Distilled water was used for making the samples.

For all experiments, the powder components (cement, additives), the liquid components (silica sol, water), and small laboratory equipment glass (baker, spatula) were equilibrated at 20°C for 24 h. The solid and liquid components were weighted according to the compositions listed in Table 2. This table also includes the nomenclature for all mixtures. Moreover, Additive 1 and Additive 2 were added in an amount of 0.2% by mass each to attain good rheology of CAC-based pastes

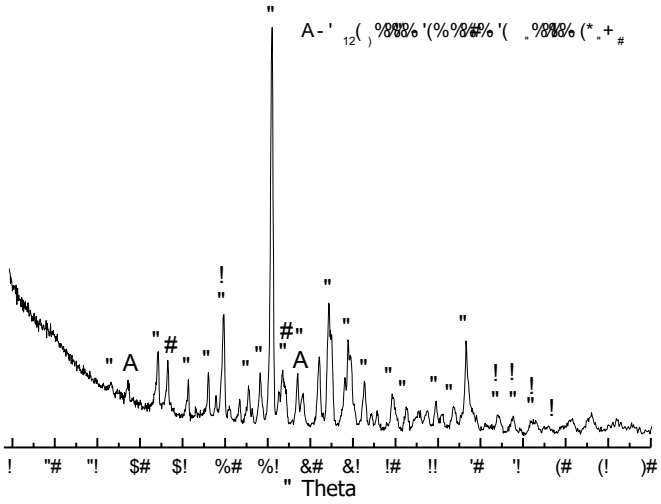

Fig. 1. XRD pattern of CAC Gorkal 70

Table 1: Composition and properties of the CAC used

Component	**Typical values (%)**	**Main phases**
Al_2O_3	69.0-71.0	CA: $CaO \cdot Al_2O_3$ CA_2: $CaO \cdot 2Al_2O_3$ Additional phases: $C_{12}A_7$: $12CaO \cdot 7Al_2O_3$ A: Al_2O_3
CaO	28.0-30.0	
SiO_2	<0.5	
Fe_2O_3	<0.3	
$Na_2O + K_2O$	<0.5	
Fineness Blaine (cm^2/g)	4000–4500	

Table 2. Composition and nomenclature of investigated CAC-based pastes bonded with silica sol.

No	**Sample name**	**Components / grams**			
		Dry CAC-G70	**Silica nano-particles**	**Total water content**	**W/(C+silica nano-particles) ratio**
1	G70C	10	-	5.0	0.5
2	G70_5SS_SP	10	0.2	5.1	0.5
3	G70_10SS_SP	10	0.4	5.2	0.5
4	G70_20SS_SP	10	0.8	5.4	0.5
5	G70_30SS_SP	10	1.2	5.6	0.5
6	G70_40SS_SP	10	1.6	5.8	0.5
7	G70_125SS	10	5.0	7.5	0.5

The cubic cement mortar samples of dimensions 40 × 40 × 40 mm^3 were used for compressive strength testing after curing periods of 1, 3, 7, and 28 days. Cube specimens were prepared in accordance with the EN

196-1 standard, using a W/(C+silica nano-particles) (water to cement and silica nano-particles ratio) of 0.5, with the mix proportions detailed in Table 3. Moreover, Additive 1 and Additive 2 were added in an amount of 0.2% by mass each to attain good rheology of CAC-based mortars

Table 3. Mix proportions and nomenclature of CAC-based mortars modified with silica sol mixed with different additives.

No	Sample name	Components / grams				
		Dry CAC - G70	Sand	Silica nano-particles	Water	W/(C+silica nano-particles) ratio
1	**M_G70C**	450	1350	-	225.0	0.5
2	**M_G70_5SS_SP**	450	1350	9.0	229.5	0.5
3	**M_G70_10SS_SP**	450	1350	18.0	234.0	0.5
4	**M_G70_20SS_SP**	450	1350	36.0	243.0	0.5
5	**M_G70_30SS_SP**	450	1350	54.0	252.0	0.5
6	**M_G70_40SS_SP**	450	1350	72.0	261.0	0.5
7	**M_G70_125SS**	450	1350	225.0	337.5	0.5

The heat generated during the binder hydration process and the rate of heat release are assessed using a TONICAL III calorimeter (Toni Technik GmbH, Berlin, Germany). A mixture consisting of 35g of water and 100g of solid material has been studied for 48 hours at a constant temperature of 20°C, the heat evolution curves being documented throughout the test.

The microstructure of samples was investigated with the scanning electron microscopy (SEM) device SEM JEOL JSM-7600F (Oxford Instruments, High Wycombe, UK). Electron microscopy parameters: Power 10 kW, distance to specimen surface from 7 to 10 mm. Characteristics of the microstructure was identified by testing the specimen splitting surface. Before testing, the splitting surface was coated with electrically conductive thin layer of gold by evaporating the gold electrode in the vacuum using the instrument QUORUMQ150R ES (Quorum, Laughton, UK).

The X-ray diffraction (XRD) analysis of the phase composition of materials was carried out upon applying diffractometer DRON-7 (Bourevestnik, St. Petersburg, Russia). In order to obtain X-ray radiation Cu Kα spectrum (λ = 0.1541837 nm), a graphite monochromator was used. The parameters of the tests were following: voltage - 30 kV; current - 12 mA; the range of the diffraction angle – from 4 to 60°, the detector movement step – 0.02°; the duration of the intensity measuring in a step – 0.5 s. Phase identification was carried out by decoding the XRD patterns according to International Centre for Diffraction Data (ICDD) diffraction databases. The quantitative changes in the XRD patterns were assessed according to the height of the peak of the main diffraction maximum of a mineral.

According to the standard EN 1015-11:2007, the compressive strength tests were carried out. A cement bonded with silica sol strength was determined using the H200KU hydraulic press (Tinius Olsen, Redhill, UK).

Results and Discussion

The hydration heat evolution of reference and silica sol-modified cement pastes (Figure 2 a–b) showed similar profiles with five stages: dissolution, induction, acceleration, deceleration, and stabilization. All samples exhibited an initial exothermic peak within minutes due to early hydration. The reference sample (G70C) showed the slowest reaction and lowest heat release, while silica sol-modified pastes displayed sharper peaks, indicating accelerated hydration due to nanoparticle-induced nucleation of C-A-H/C-A-S-H phases.

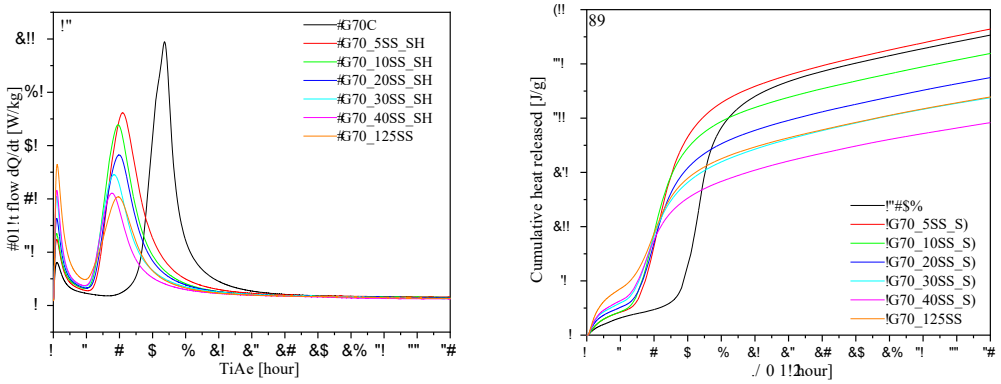

a) b)

Fig. 2. Variation in the (a) hydration exothermic rate and (b) cumulative hydration heat of samples G70C, G70_5SS_SP – G70_40SS_SP and G70_125SS with time.

Silica sol significantly shortened the induction period, from ~5 h for G70C to ~2 h for G70_125SS, with other samples showing ~2.5 h. During the acceleration stage, peak intensity increased with silica content, reflecting enhanced hydration kinetics, likely due to Ca^{2+} interactions with silica nanoparticles.

Despite faster reactions, modified systems exhibited lower total heat release, suggesting suppressed crystalline hydrate formation, confirmed by XRD after 24 h. After the second peak, hydration slowed, and all samples reached a stable state within 24 hours (Fig. 3, a).

The mineralogical evolution of the binders was evaluated by XRD at 1, 3, 7, and 28 days of curing. All samples consisted of unhydrated calcium aluminate phases (mainly $CaAl_2O_4$ and $CaAl_4O_7$) and newly formed hydrates. With increasing curing time, the intensities of $CaAl_2O_4$ ($2\theta \approx 30.0°$) and $CaAl_4O_7$ ($2\theta \approx 25.4°$) gradually decreased, confirming progressive consumption of anhydrous phases.

At 1 day, silica sol strongly influenced early hydration. The reference sample and G70_125SS showed lower $CaAl_2O_4$ intensity than mixes containing both silica sol and chemical additives, indicating a complex

interaction between silica and admixtures. G70_125SS favored the formation of $CaAl_2O_4 \cdot 10H_2O$, while the reference sample contained both $CaAl_2O_4 \cdot 10H_2O$ and $Ca_2Al_2O_5 \cdot 8H_2O$. Samples with combined silica sol and additives showed partially hindered early hydration.

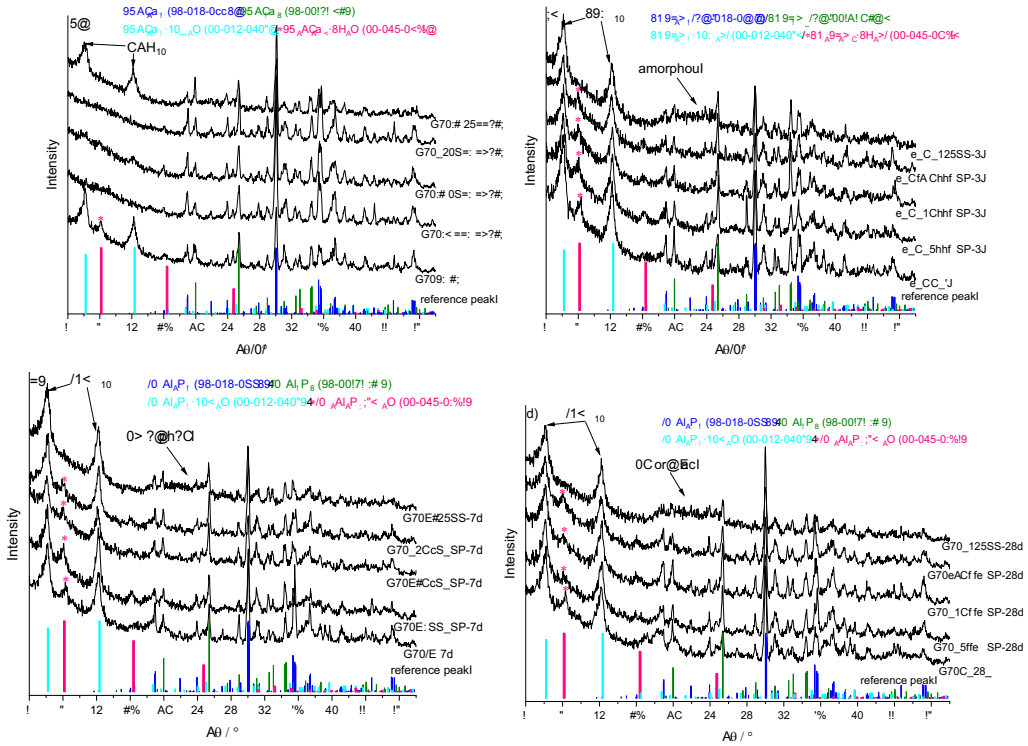

Fig. 3. XRD patterns collected on the reference paste and pasted modified with silica sol after 1, 3, 7 and 28 days of hydration (a-d)

At later ages (3–7 days), hydration progressed in all systems, but silica-containing samples exhibited reduced anhydrous phase content and altered hydrate formation. Increased amorphous content was observed in the reference paste. By 28 days, G70_125SS predominantly contained $CaAl_2O_4 \cdot 10H_2O$, whereas other mixes showed both $CaAl_2O_4 \cdot 10H_2O$ and $Ca_2Al_2O_5 \cdot 8H_2O$ alongside residual anhydrous phases.

Overall, silica sol promoted stabilization of $CaAl_2O_4 \cdot 10H_2O$ and inhibited formation of $Ca_2Al_2O_5 \cdot 8H_2O$, suggesting suppression of conversion toward stable C_3AH_6 and long-term modification of hydration pathways.

The microstructure of CAC pastes was investigated by SEM at 1, 7, and 28 days of curing, supported by EDS analysis. The control sample (G70C) showed well-defined CAH_{10} crystals at early ages, while C_2AH_8 was less clearly observed. Its microstructure remained relatively porous and disordered, indicating limited densification over time (Fig. 4).

In silica sol-modified samples, early-age (1 day) crystalline hydrates were difficult to distinguish, suggesting that silica nanoparticles promote the formation of very fine or partially amorphous hydration products. These nanoparticles likely act as nucleation sites, leading to a more compact and

homogeneous microstructure and accelerating hydration. The G70_125SS sample clearly contained CAH_{10}, consistent with XRD results. At 7 days, silica-containing systems exhibited a denser structure with tightly packed crystals. CAH_{10} and C_2AH_8 were identified in most modified samples, while G70_125SS predominantly contained CAH_{10} embedded in an amorphous matrix, which increased with silica content. At 28 days, the control sample showed formation of cubic C_3AH_6, confirming hydrate conversion (CAH_{10} → C_2AH_8 → C_3AH_6). In contrast, silica-modified samples exhibited a denser, more uniform microstructure with reduced conversion and a higher proportion of amorphous phases.

Overall, silica sol acted as a nucleation and structure-refining agent, producing a denser microstructure and improving mechanical performance, with 5 wt.% SS showing the most favorable results.

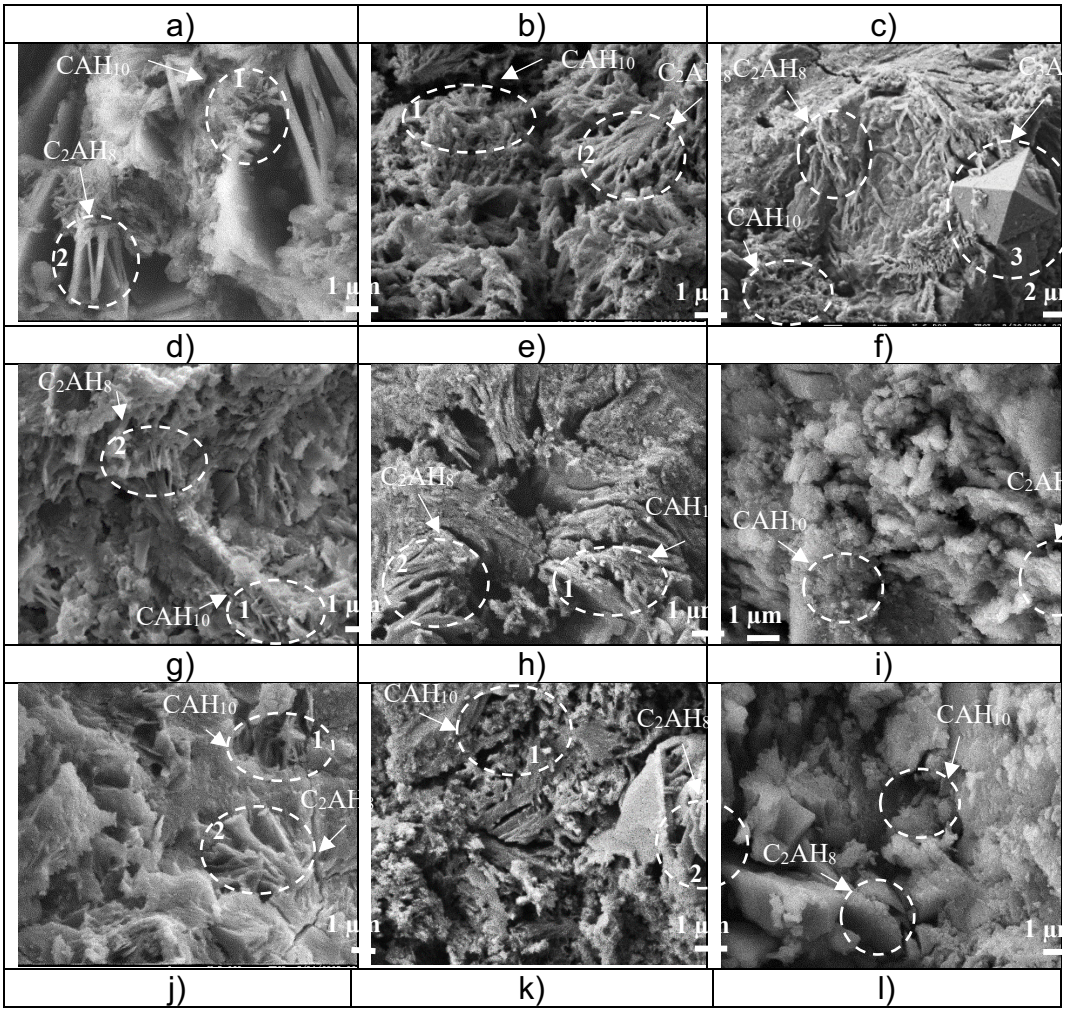

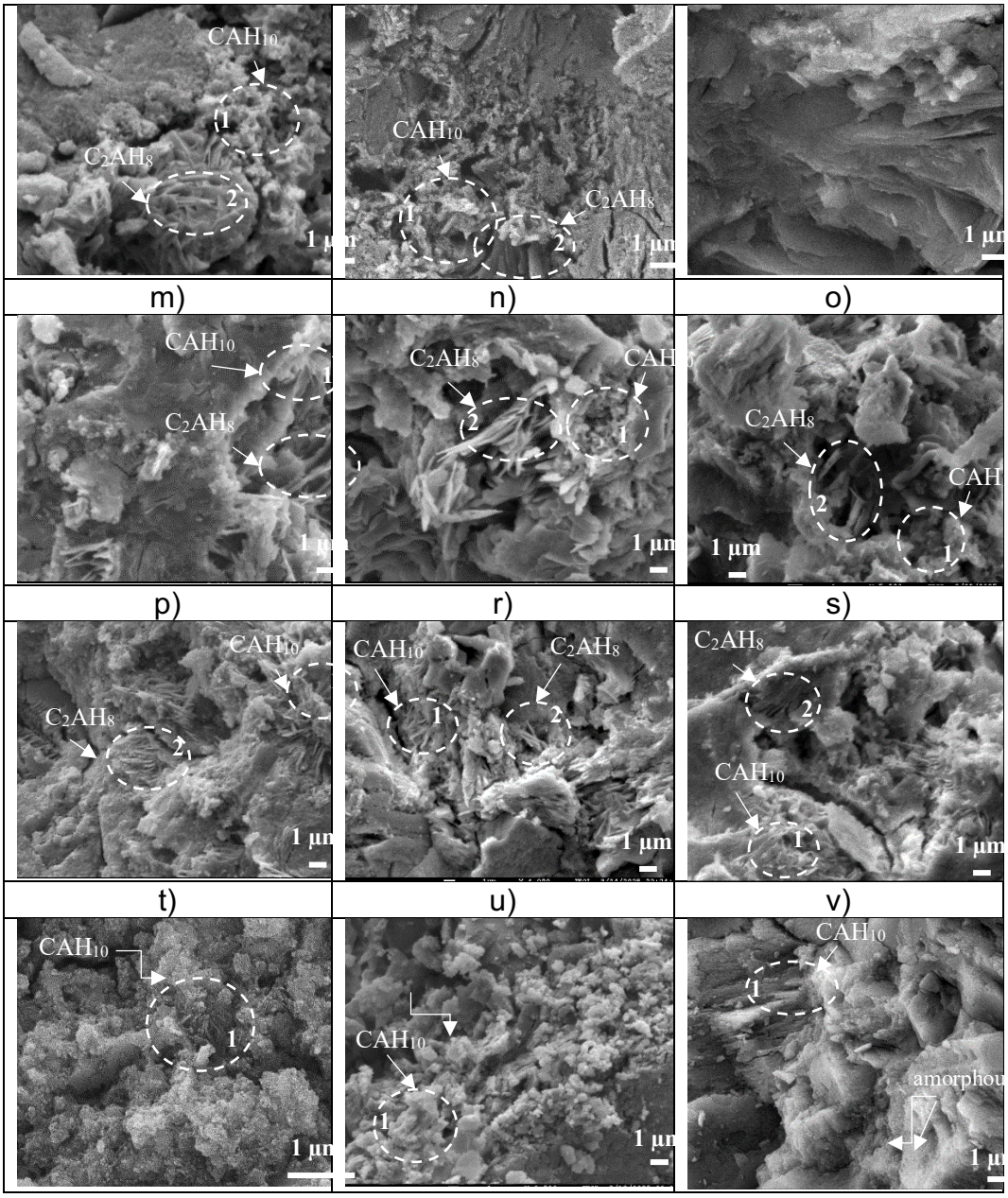

Fig. 4. The microstructure images of G70C (a-c), G70_5SS_SP (d-f), G70_10SS_SP (g-i), G70_20SS_SP (j,k,l), G70_30SS_SP (m,n,o), G70_40SS_SP (p,r,s) G70_125SS (t,u,v) after 1 (a,d,g,j,m,p,t); 7 (b,e,h,k,n,r,u) and 28 (c,f,i,l,o,s,v) days of curing.

The compressive strength results (Fig. 5) show that all mortars increased in strength with curing time. The highest early-age strength (56.5 MPa at 1 day) was achieved by the M_G70_5SS_SP mixture, attributed to the filling effect and nucleation activity of silica nanoparticles in the cement matrix. At 1 day, both M_G70_5SS_SP and M_G70_10SS_SP exhibited higher strength than the reference mortar, confirming the beneficial effect of low silica sol contents.

However, increasing silica sol content to 20 wt.% (M_G70_20SS_SP) reduced early strength to 38.9 MPa, indicating a detrimental effect at higher

dosages. At later ages (3, 7, and 28 days), all samples followed a similar trend, but mortars with 10 wt.% and 20 wt.% silica sol consistently showed lower compressive strength compared to both the reference and 5 wt.% modified mortar. Overall, results indicate that silica sol enhances compressive strength of CAC mortars only at optimal low contents, with 5 wt.% providing the most favorable performance.

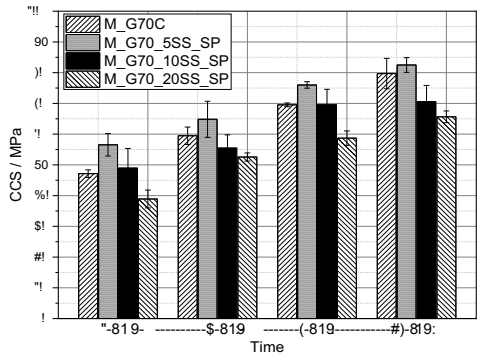

Fig. 5. Compressive strength of development in calcium aluminate cement-based mortars bonded with silica sol versus time

CONCLUSIONS

1. This study investigated the effect of silica sol on the hydration and performance of calcium aluminate cement (CAC). The results show that silica sol significantly modifies the hydration behavior, phase development, and microstructure of CAC systems up to 28 days of curing at 20°C.
2. At early ages, silica sol strongly influences hydration kinetics, shortening the induction period and accelerating exothermic reactions. This effect is most pronounced at low silica sol contents (5–10 wt.%), which also lead to enhanced early strength development. However, higher silica sol contents reduce the beneficial effect on compressive strength.
3. XRD and SEM results confirm that silica sol affects hydrate formation, promoting CAH_{10} development and contributing to a denser microstructure compared to the reference system. The modified pastes exhibit a more compact structure with refined hydration products and reduced porosity.
4. Compressive strength results show that the optimal performance is achieved at 5 wt.% silica sol, which provides the highest strength at both early and later curing stages. Overall, silica sol improves CAC hydration and mechanical performance when used at appropriate dosages, primarily by accelerating early hydration and refining the microstructure.

Acknowledgements

The Authors would like to thank Górka Cement Sp. z o.o. (Trzebinia, Poland) for providing high-quality calcium aluminate cement for this

research, as well as for their cooperation and support in attending the International Conference on Calcium Aluminates 2026.

REFERENCES

[1] NOAA Research, Global atmospheric carbon dioxide levels continue to rise. https://research.noaa.gov/article/ArtMID/587/ArticleID/2914/No-sign-of-significant-decrease-in-global-CO2-emissions, 2024 (accessed 10 December 2024).
[2] Window to the World News Chicago, Cement Carbon Dioxide Emissions Quietly Double in 20 Years. https://news.wttw.com/2022/06/22/cement-carbon-dioxide-emissions-quietly-double-20-years, 2024 (accesed 10 December 2024).
[3] K. Scrivener, M. Ben Haha, P. Juilland, C. Levy, Research needs for cementitious building materials with focus on Europe, RILEM Tech. Lett. 7 (2023) 220 – 252. https://doi.org/10.21809/rilemtechlett.2022.165
[4] N. Maach, J.F. Georgin, S. Berger, J. Pommay, Chemical mechanisms and kinetic modeling of calcium aluminate cements hydration in diluted systems: Role of aluminium hydroxide formation, Cem. Concr. Res., 143 (2021) 106380. https://doi.org/10.1016/j.cemconres.2021.106380.
[5] R. Boris, I. Wilińska, B. Pacewska, V. Antonovič, Investigations of the influence of nano-admixtures on early hydration and selected properties of calcium aluminate cement paste, Mater. 15 (2022) 49 – 58. https://doi.org/10.3390/ma15144958
[6] J.M. Rivas Mercury, X. Turrillas, A.H. de Aza, P. Pena, Calcium aluminates hydration in presence of amorphous SiO2 at temperatures below 90°C, J. Solid State Chem. 179 (2006) 2988 – 2997. https://doi.org/10.1016/j.jssc.2006.05.017.
[7] V. Antonovič, R. Stonys, I. Pundienė, I. Prosyčevas, E. Fataraitė, Investigation of structure formation in complex binder. Mater. Sc. 15(4) (2009) 343 – 348. https://etalpykla.vilniustech.lt/handle/123456789/125587
[8] F. Wang, P. Chen, X. Li, B. Zhu, Effect of colloidal silica on the hydration behavior of calcium aluminate cement, Mater. 11 (2018) 1849. https://doi.org/10.3390/ma11101849.
[9] F. Wang, P. Chen, B. Zhu, Effect of silica sol on microstructure and properties of corundum castables bonded with aluminate cement, J. Chin. Ceram. Soc. 46(03) (2018) 427–433.
[10] P. Faucon, T. Charpentier, D. Bertrandie, A. Nonat, J. Virlet, J.C. Petit, Characterization of calcium aluminate hydrates and related hydrates of cement pastes by 27Al MQ-MAS NMR, Inorg. Chem. 37 (1998) 3726–3733. https://pubs.acs.org/doi/epdf/10.1021/ic9800076?ref=article_openPDF
[11] J. Skibsted, E. Henderson, H.J. Jakobsen, Characterization of calcium aluminate phases in cements by 27Al MAS NMR spectroscopy, Inorg. Chem. 32 (1993) 1013–1027.
[12] D. Madej, R. Boris, R. Stonys, V. Antonovič, A. Kruk, Effects of silica sol on hydration properties, impedance response, microstructure and strength of calcium aluminate cement // Ceram. Inter. London: Elsevier BV. 51 (2025) 31176-31191. DOI: 10.1016/j.ceramint.2025.04.305

International Conference on Calcium Aluminates 2026

EFFECT OF CALCIUM SULFATE SOURCE AND CURING TEMPERATURE ON THE HYDRATION BEHAVIOR OF CAC-OPC-C$ TERNARY SYSTEMS

Demirdoğan, Özge[1], Meral Akgül, Çağla[2], Erbuğa Avcıoğlu, Berrak[3]

[1]Sabancı Technology Center GmbH, Freisinger Landstraße 50 Garching, Munich, Germany, 85748, ozge.demirdogan@sabancibs.com,
[2]Department of Civil Engineering, Middle East Technical University, Ankara, Türkiye, 06800,
[3]Sabancı Technology Center GmbH, Freisinger Landstraße 50 Garching, Munich, Germany, 85748

Keywords: phosphogypsum, calcium aluminate cement, hydration behavior, curing temperature, ternary binders

ABSTRACT

Ternary binder systems composed of calcium aluminate cement (CAC), ordinary Portland cement (OPC), and calcium sulfate (C$) can provide rapid setting, rapid hardening, and controlled expansion properties depending on the binder composition and the type of calcium sulfate source. In this study, the effect of calcium sulfate source and curing temperature on the hydration behavior of CAC–OPC–C$ ternary systems was investigated. Different calcium sulfate sources, anhydrite, α-hemihydrate, natural gypsum and phosphogypsum, were considered because they have different dissolution rates and sulfate release behavior. These differences are expected to influence reaction kinetics, setting behavior, and phase formation. The study also focused on understanding how the calcium sulfate source influenced the hydration process of CAC-based ternary systems under different curing temperatures. Since CAC hydration is sensitive to temperature, curing condition is also an important parameter affecting the reaction rate and stability of hydration products. Isothermal calorimetry was used as the primary technique to evaluate reaction kinetics and heat evolution characteristics. Complementary analyses including X-ray diffraction (XRD) and setting time measurements were conducted to support the interpretation of hydration mechanisms. The results indicate that the type of calcium sulfate source strongly affects the early-age hydration kinetics. Systems containing α-hemihydrate exhibited the highest initial reaction rate and fastest setting behavior due to rapid dissolution, whereas phosphogypsum-containing systems showed slower reaction kinetics but higher cumulative heat release, indicating prolonged hydration.

ozge.demirdogan@metu.edu.tr / ozge.demirdogan@sabancibs.com

Anhydrite and gypsum systems demonstrated intermediate behavior depending on their dissolution rates. These differences are directly linked to sulfate availability and ettringite formation mechanisms. Overall, this study aims to clarify the combined effect of calcium sulfate source and curing temperature on CAC–based ternary systems. The findings can contribute to the selection of suitable sulfate sources for designing ternary binders with controlled hydration and setting behavior.

INTRODUCTION | BACKGROUND

Ternary cementitious systems composed of ordinary Portland cement, calcium aluminate cement, and calcium sulfate are used to obtain systems having improved properties compared to their individual components. Depending on the ratio of the components, these systems can provide rapid setting, rapid hardening, rapid drying, and shrinkage or expansion compensation properties. Therefore, they can be used in different applications such as self-leveling mortars, tile adhesives, grout mortars, and rapid repair materials [1]. Hydration of CAC–OPC–C$ ternary systems is complex because different phases from OPC and CAC participate in hydration reactions at the same time. Formed hydration products change depending on the mixture ratio. While OPC-based systems generally include C-A-S-H, portlandite, and ettringite, CAC-based systems mainly include ettringite and gibbsite [2]. Ettringite formation is especially important because it affects early hydration, setting behavior, and volume stability of the system. Different calcium sulfate sources can be used in ternary systems. Gypsum, α-hemihydrate, anhydrite, and phosphogypsum provide calcium and sulfate ions, but they have different solubility and dissolution rates. Therefore, the type of calcium sulfate source influences hydration kinetics, ettringite formation, setting time, strength, and porosity of the system [3,4]. Previous studies showed that anhydrite can lead to longer setting time due to its slower dissolution rate compared with gypsum and α-hemihydrate, while α-hemihydrate can cause different expansion behavior compared with gypsum and anhydrite [5,6]. Phosphogypsum is also a potential alternative calcium sulfate source because it is a by-product of the phosphate fertilizer industry. However, impurities in phosphogypsum can affect hydration reactions and setting behavior. Therefore, its use in CAC–OPC–C$ ternary systems should be investigated carefully [7]. Curing temperature is another critical parameter because CAC hydration is highly temperature sensitive. Different hydrated phases can be formed at different temperatures, and this situation can influence reaction kinetics and performance [8]. For this reason, the combined effect of calcium sulfate source and curing temperature should be considered in the design of ternary CAC–OPC–C$ systems. Therefore, this study focuses on the hydration behavior of CAC–OPC–C$ ternary systems by changing the calcium sulfate source and curing temperature. The main aim is to understand the effect of sulfate source selection on hydration reactions and to generate reference systems for further studies.

METHODS

Calcium aluminate cement (CAC 40), ordinary Portland cement (CEM I 42.5 R), and four different types of calcium sulfate sources, namely anhydrite (A), α-hemihydrate (H), natural gypsum (G), and phosphogypsum (PG), were used to prepare CAC-based ternary binder systems. In order to investigate only the effect of sulfate source, the component ratios of the systems were kept constant, and only the type of calcium sulfate was changed. All cement paste samples were prepared with a constant water-to-binder ratio of 0.5. The hydration behaviour, phase evolution, and setting characteristics of the systems were investigated under different curing temperatures. Isothermal calorimetry was used to evaluate the hydration kinetics of the systems. In addition, X-ray diffraction (XRD) analysis was conducted to identify the phase assemblage and to monitor the evolution of hydration products. Setting time measurements were performed using automatic Vicat equipment to determine the initial and final setting behaviour of the systems. The selected experimental methods were used to establish the relationship between sulfate source and hydration behaviour under different curing conditions.

KEY FINDINGS | CONCLUSIONS

According to the isothermal calorimetry results, the type of calcium sulfate source has a significant effect on the hydration behavior of CAC–OPC–C$ ternary systems. Even though the binder composition was kept constant, changing only the sulfate type resulted in clearly different reaction kinetics. The system including α-hemihydrate (H) shows the highest initial peak at very early ages, indicating very fast dissolution and rapid reaction. This behaviour also explains the rapid consumption of sulfate ions and the relatively lower heat flow at later ages, suggesting a fast but short-lived hydration process. The anhydrite (A) containing system also shows high reactivity; however, its behaviour is more gradual, with multiple peaks indicating stepwise reactions and a slower but sustained sulfate release. The gypsum (G) containing system exhibits intermediate behaviour, with a slightly delayed main peak and a smoother heat flow curve, indicating a more balanced hydration process. On the other hand, the phosphogypsum (PG) system shows clearly delayed hydration behaviour, with a later main peak and lower early-age reaction rate. This indicates slower sulfate release, while the broader peak suggests a more prolonged hydration process. These observations are also consistent with the setting time results. The hemihydrate system shows the shortest setting time, while gypsum and phosphogypsum systems show longer setting times, and anhydrite shows intermediate behaviour. When all systems are compared, it can be concluded that the dissolution rate of the calcium sulfate source directly controls the hydration kinetics and setting behavior of CAC–OPC–C$ ternary systems. The order of reactivity can be summarized as:

α-hemihydrate > anhydrite > gypsum > phosphogypsum

REFERENCES

[1] T.A. Bier, Composition and properties of ternary binders, in: Cementitious Materials, 2017, pp. 353–376. https://doi.org/10.1515/9783110473728-013

[2] E. Qoku, T.A. Bier, G. Schmidt, J. Skibsted, Impact of sulphate source on the hydration of ternary pastes of Portland cement, calcium aluminate cement and calcium sulphate, Cem. Concr. Compos. 131 (2022) 104502. https://doi.org/10.1016/j.cemconcomp.2022.104502

[3] P.C. Hewlett, M. Liška, Constitution and specification of Portland cement, in: Lea's Chemistry of Cement and Concrete, Elsevier, 2019. https://www.sciencedirect.com/book/9780081007730/leas-chemistry-of-cement-and-concrete

[4] L. Noor, A. Tuinukuafe, J.H. Ideker, A critical review of the role of ettringite in binders composed of CAC–PC–C$ and CSA–PC–C$, J. Am. Ceram. Soc. 106 (2023) 3303–3328. https://doi.org/10.1111/jace.19014

[5] L. Xu, P. Wang, G. Zhang, Calorimetric study on the influence of calcium sulfate on the hydration of Portland cement–calcium aluminate cement mixtures, J. Therm. Anal. Calorim. 110 (2011) 725–731. https://doi.org/10.1007/s10973-011-1920-z

[6] S. Zhang, X. Xu, S.A. Memon, Z. Dong, D. Li, H. Cui, Effect of calcium sulfate type and dosage on properties of calcium aluminate cement-based self-leveling mortar, Constr. Build. Mater. 167 (2018) 253–262. https://doi.org/10.1016/j.conbuildmat.2018.01.146

[7] J. Li, J. Chang, T. Wang, T. Zeng, J. Li, J. Zhang, Effects of phosphogypsum on hydration properties and strength of calcium aluminate cement, Constr. Build. Mater. 347 (2022) 128398. https://doi.org/10.1016/j.conbuildmat.2022.128398

[8] B. Pacewska, M. Nowacka, Studies of conversion progress of calcium aluminate cement hydrates by thermal analysis method, J. Therm. Anal. Calorim. 117 (2014) 653–660. https://doi.org/10.1007/s10973-014-3804-5

International Conference on Calcium Aluminates 2026

ETTRINGITE SYSTEMS - MICROSTRUCTURE, PERFORMANCE AND CHARACTERIZATION TECHNIQUES

Qoku, E.[1*], Noor, L.[2], and Ideker, J.H[3],
[1]Institute of Building Materials, Concrete Construction and Fire Safety, Beethovenstrasse 52, 38106, Braunschweig, Germany
[2]Bauer Foundation Corporation, Tampa, Florida, United States
[3]Oregon State University - School of Civil and Construction Engineering 101 Kearney Hall, Corvallis, Oregon, USA

BACKGROUND

Ternary binders composed of Portland cement (PC), calcium aluminate cement (CAC) and calcium sulphate have ($C\bar{S}H_X$) are widely applied as tile adhesives, self-leveling underlayment, and other technical formulations for repair work. In the literature one can distinguish between PC-rich and CAC-$C\bar{S}HX$ rich formulations. The later ones are also known as ettringite systems, with ettringite being the main hydrate phase, whereas for PC-rich formulations the hydration mechanisms are to an extent similar to pure PC. The hydration and microstructure development of such binders is relatively complex and for a holistic understanding a multi-method approach with a wide range of analytical techniques is required. Such fundamental studies are limited. For instance, the work of (Lamberet, 2005), addresses the issue of microstructure development and durability mechanisms under controlled atmosphere and natural weathering in both PC and CAC rich formulations. In this work, the influence of the formulation was investigated with respect to hydration mechanism, porosity and transport properties. Later, a more quantitative study was carried out by (Qoku, 2019) investigating mineralogical development of hydrates ternary binder systems with a special focus on the characterization and quantification of hydrated X–ray amorphous phases. An in–depth study was conducted in selected formulations of the ternary diagram PC–CAC– $C\bar{S}HX$ by combining XRD, TGA, ^{27}Al NMR, ^{29}Si NMR spectroscopy and thermodynamic calculations (Qoku, 2019).In a recent review paper, research regarding conditions that influence ettringite stability in ternary binders composed of CAC–PC–C$ and CSA–PC–C$ were synthetized. The authors highlighted limitations of current analytical techniques and proposed techniques for further research. One special focus was the use of MAS NMR spectroscopy as well as Xray/Neutron imaging techniques (Noor et al., 2023a).

Environmental exposure studies are relatively limited in ettringite systems (Lamberet, 2005) and this remains an area for further work, particularly as interest in these systems grows for outdoor application. Mechanical properties and volume stability are amongst the most used techniques for investigation. Neutron radiography was recently used to investigate the efficiency of curing in high early strength systems (calcium sulfoaluminate, calcium sulfoaluminate – OPC blends, and accelerated OPC system).

*Corresponding author: E.Qoku@ibmb.tu-bs.de

Ettringitic systems were shown to develop a discontinuous microstructure at a smaller depth compared to OPC systems, have lower evaporable water, and that a surface coating of curing compound applied after finishing and near initial set was generally the most efficient curing technique. (Noor, 2023b).

In this short summary we show selected results related to microstructure and performance of CAC rich ternary binders, with a special focus on MAS NMR spectroscopy, thermodynamic modelling and performance-based data. For the performance-based study, these systems were investigated for stability (volume, strength, phase assemblage) under exposure to different conditioning regimes. A detailed review of the role of temperature and relative humidity (RH) on ettringite based systems can be found in (Noor et al., 2023a).

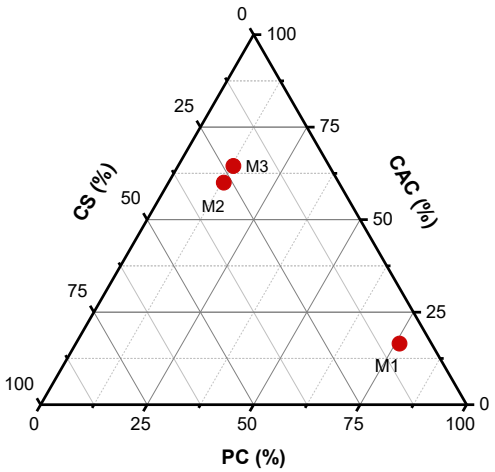

Fig.1: Composition of the systems in the ternary diagram described in this work.

A detailed description of each of the above compositions can be found in the literature (Qoku, 2019) and (Noor, 2023b).

KEY FINDINGS

The hydration and microstructure of ettringite based systems is depended on several factors, such as water to solid ration, OPC/CAC ratio, type of sulphate or mineralogical composition of the raw cements. For instance, Fig 2. shows data from thermodynamic modelling and ^{27}Al MAS NMR for a CAC rich composition (M3), with three different types of CAC cement. The main difference of the CAC cements is their chemical and mineralogical composition with (M3-c) having the highest content of alumina.

Modelled hydrate phase assemblage for formulations (M3-a) and (M3-b) predict the formation of ettringite, monosulphate, AH_3, and strätlingite, along with Si–hydrogarnet with iron incorporation. In both cases the amount of predicted ettringite, increased up to 7 days of hydration and afterwards decreases. Experimentally from QXRD, the content of ettringite was observed to decrease from day 1 of hydration. Hydrogarnet was experimentally observed only at 28 days of hydration. By comparing system M3(a) and the main difference is route of strätlinigte formation. In the first case (Fig.2a) it occurs through the consumption of AH_3, whereas in the

second system (Fig.2b) the precipitation of strätlingite is predicted earlier during hydration and is proposed that formation occurs through the hydration of gehlenite. These observations were supported from TGA and QXRD experimental data where decrease of AH_3 content and enhanced degree of hydration of C_2AS over time was observed respectively.
Fig.3b shows the ^{27}Al MAS NMR experimental spectra for M3-c hydrated compositions at 1 and 28 days of hydration. The anhydrous CAC is characterized by signals in the range of 75 − 80 ppm, which corresponds to the Al (IV) coordination of anhydrous phases such as CA, C_2AS, CA_2. Ettringite and other signals related to the Al(VI) coordination are also indicated. The signal at 10.5 ppm includes the contributions of AH_3, monosulphate and possibly C-A-H phases. Surprisingly for this system, strätlingite is also detected by the tetrahedrally coordinated aluminum sites ~68.5 ppm at 28 days of hydration. The detection of strätlingite in this case remains unclear, as AH_3 was found to increase experimentally over time whereas the content of gehlenite in high alumina CAC is relatively low.

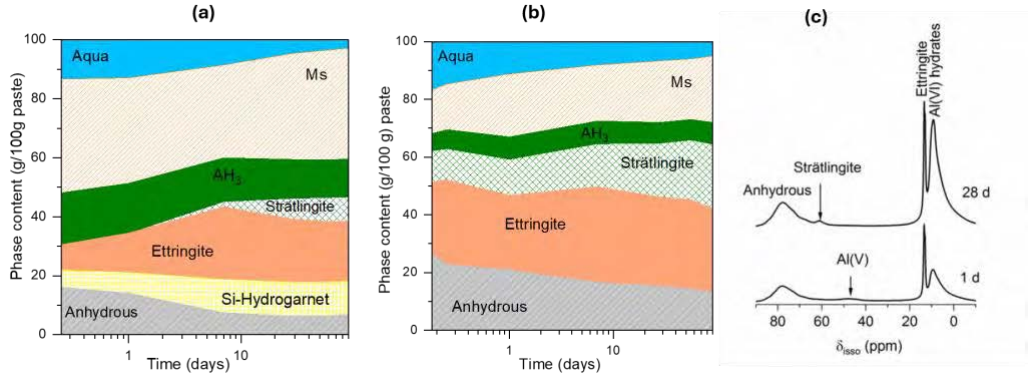

Fig.2: Thermodynamic modelling and ^{27}Al MAS NMR data for M3 ternary binder. The figure has been adapted from (Qoku, 2019).

To investigate the performance of these systems in simulated exterior conditions two main conditioning regimes were investigated: exposure at 23C and 50% RH; 60C and 50% RH. Selected results for dynamic vapor sorption after long-term conditioning are shown in Fig.3 for M1 and M2 controls and M1 and M2 with the addition of 1.5% styrene acrylic latex (SAL). In general, the CAC-rich system (M2) showed a higher quantity of ettringite formation compared to the OPC-rich system (M1) and this resulted in less shrinkage, and a more stable retention of ettringite quantity over the course of conditioning. It was noted that both systems experiences little to now compressive strength loss over time. However, at 50% RH the M2 system did show a decrease in flexural strength. The flexural strength in the M1 also showed a reduction in strength at elevated temperature; this system was less sensitive to RH changes than the M2 system.
Styrene acrylic copolymer latex (SAL) is often used in cementitious materials for building chemistry applications. The role of SAL on ettringite stability in these systems is not completely clear. A typical dosage rate is 1.5% SAL by mass of cementitious material and that was investigated as an addition in M1 and M2 systems following the same conditioning regimes

as previously outlined. Further, ettringite stability was also investigated using quantitative XRD and dynamic vapor sorption between 10-50% RH. In the most aggressive condition (60C and 0% RH) there was a decrease in ettringite content in the M2 system up to 7 days, with no further change noted after 28 days. In contrast, the ettringite content increased in the M1 system up to 7 days and then after 28 days did not show further change.
In the M1 system, the surface water adsorption was lower in 1.5%SAL samples at 60C-50%RH samples measured by dynamic vapor sorption (DVS) measurements. However, no significant improvement was observed in M2 systems.

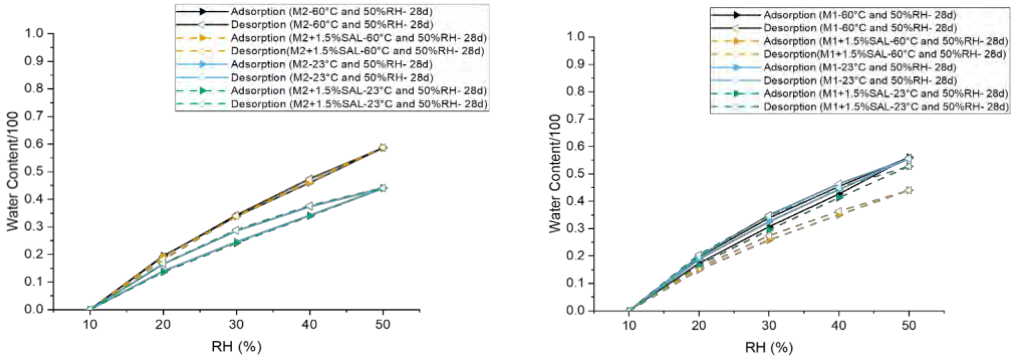

Fig.3: Dynamic vapor sorption isotherms for M1 and M2 systems with and without 1.5% SAL, after conditioning (from Noor, 2023b).

FUTURE RESEARCH NEEDS

- Ettringite systems exhibit complexity in the microstructure and only a multi-method approach allows for a full understanding of mechanisms that govern hydration, durability, and performance. These vary systems based on composition, exposure, and conditioning.
- Chemical thermodynamic modelling, reactive transport modelling and machine learning can help to optimize the systems and perhaps reduce or better focus experimental work.

REFERENCES

1. Lamberet S., “Durability of ternary binders based on Portland cement, calcium aluminate cement and calcium sulfate”, Dissertation, EPFL (2005)
2. Qoku E., “Characterization, and quantification of crystalline and amorphous phase assemblage in ternary binders during hydration”, Dissertation, TU Bergakademie Freiberg, (2019).
3. Noor, L., Tuinukuafe, A., and Ideker, J.H., (2023a) “A Critical Review of the Role of Ettringite in Binders Composed of CAC–PC–C$ and CSA–PC–C$,” Journal of the American Ceramic Society, https://doi.org/10.1111/jace.19014
4. Noor, L., (2023 b) “Investigations of Hygrothermal Stability and Curing Efficiency of Ettringite Accelerated Binders,” Dissertation, October 2023, Oregon State University, 235 pp.

International Conference on Calcium Aluminates 2026

Development of temperature-dependent phase composition during hydration of ternary OPC-CAC-C$ mixtures with two different CAC types

Rost, Pauline[1]; Bologna, Fabrizio[1]; Wolf, Julian[2], Avcioğlu, Berrak[2], Goetz-Neunhoeffer, Friedlinde[1]

[1]Friedrich-Alexander-Universität Erlangen-Nürnberg, Geozentrum Nordbayern, Lehrstuhl für Mineralogie, Schlossgarten 5a, Erlangen, 91052, Germany, pauline.rost@fau.de*,
[2]Sabanci Technology Center GmbH, Freisinger Landstraße 50, Garching bei München, 85748, Germany

Keywords: Calcium aluminate cement, Portland cement, Calcium sulfates, Hydration, X-ray diffraction;

ABSTRACT

Ternary mixtures composed of calcium aluminate cement (CAC), Portland cement (OPC) and calcium sulfates ($C\$H_X$) are commonly used as tile adhesives, self-levelling compounds, repair cements or technical mortars. Different setting and hardening times as well as expansion, shrinkage and early strength can be easily controlled by varying the proportions of the three components. Many studies have shown that formation of different hydrate phases in the mixtures is strongly influenced by both the OPC/CAC and the CAC/C$ ratio. In general, calcium aluminates (C_3A and/or CA) can react with the calcium sulfate, which is leading to formation of ettringite. However, the quality of the CACs, which is related to the reactive clinker composition, also influences the composition of the phase formed during and after hydration in the mixture. Depending on the CAC and C$ content or limestone addition (Cc), the conversion of ettringite to AFm (monosulfate or -carbonate) can also be accelerated or prevented.

The influence of two different CACs (iron-containing and iron-reduced) on the hydration of application-related ternary mixtures was therefore investigated. The reaction kinetics were determined using heat flow calorimetry and quantitative X-ray diffraction analysis (QXRD). Storage samples for up to 90 d at 10 °C and 23 °C were examined with G-factor method in order to clarify the influence of the CA and iron content of the respective clinker on the stable hydrate phase composition and on the amorphous phase content. It could be shown what differences in the phase composition occur during storage at 10 °C or 23 °C. In addition, strength measurements could provide further insights into the influence of the various CACs on the development of strength during hydration.

*email address of corresponding author

INTRODUCTION | BACKGROUND

The hydration behaviour and resulting properties of cementitious materials can be finely tuned by combining calcium aluminate cement (CAC), ordinary Portland cement (OPC), and calcium sulfates ($C\$H_X$). A decisive factor controlling hydrate phase development in these systems is the balance between OPC and CAC, as well as the amount of calcium sulfate relative to the aluminate phases [1]. In the presence of sufficient sulfate, reactive calcium aluminates such as CA or C_3A preferentially form ettringite during early hydration. Thereby, the mineralogical quality and reactivity of the CAC clinker can play a crucial role in determining which hydrate phases form and remain stable over time. Furthermore, depending on the availability of silicon and the relative calcium aluminate content left during the late hydration reaction the formation of straetlingite may occur [2]. The hydrate phase development of such a ternary mixture was therefore investigated in relation to the added CAC source, examining the role played by the iron and silicon contained in the CAC during hydration.

METHODS

An Fe-rich CAC (CAC 40) and an Fe-reduced CAC (CAC 50) were each examined in combination with OPC and hemihydrate ($C\$H_{0.5}$) with a w/s ratio of 0.65 (Table 1 and Table 2). An additional 0.003 wt.% citric acid was added to both pastes to delay the reaction and thus ensure good workability of the paste.

Table 1. XRF analysis of the components used, sulfate content was determined by nephelometry.

[wt.%]	CAC 40	CAC 50	OPC	Hemihydrate
CaO	35.1	36.7	65.1	39.2
Al_2O_3	39.6	53.3	4.9	0.2
SiO_2	4.2	3.9	19.9	0.7
Fe_2O_3	17.1	1.3	3.3	---
MgO	---	0.1	1.0	---
TiO_2	1.9	2.5	0.2	---
K_2O	0.2	0.3	0.6	---
SO_3	---	---	3.2	54.9
LOI	1.3	1.8	1.9	5.0

Table 2. Compositions of the used mixtures with w/s=0.65.

	CAC40mix	CAC50mix
CAC 40 (Fe-rich CAC)	31.8	---
CAC 50 (Fe-reduced CAC)	---	31.8
OPC	15.2	15.2
Hemihydrate ($C\$H_{0.5}$)	13.6	13.6
Water (H_2O)	39.4	39.4

The phase composition of storage samples after 1, 7, 28 and 90 d at 23 °C and 10 °C was examined using quantitative X-ray diffraction analysis. The samples were stored at 100% r.H., then sawn in half and a fresh surface was prepared using sandpaper. At least two samples were stored for each test point and each mixture, so that four samples per test point could be measured after sawing. A Rietveld analysis was performed using the TOPAS 5.0 software and the absolute crystalline phase composition and amorphous fraction were determined using G-factor analysis [3].

KEY FINDINGS | CONCLUSIONS

The QXRD analysis of the storage samples at 23 °C for both systems is shown in Figure 1. The upper section shows the development of the clinker phases, with the triangles near the left axis indicating the starting contents. The lower section displays the hydrate phases and the amorphous fraction. Only minor differences between the two systems and thus between the two CACs can be seen. In both systems, CA and hemihydrate in particular reacted within one day, forming ettringite. In CAC40mix, CA has completely reacted after 7 d, while in CAC50mix CA takes 90 d. C_2S and C_3S were dissolving in both systems within 90 d. C_3A and C_4AF dissolved in CAC40mix within 90 d. It is remarkable that gehlenite (C_2AS) reacted completely in both systems within the measurement period.

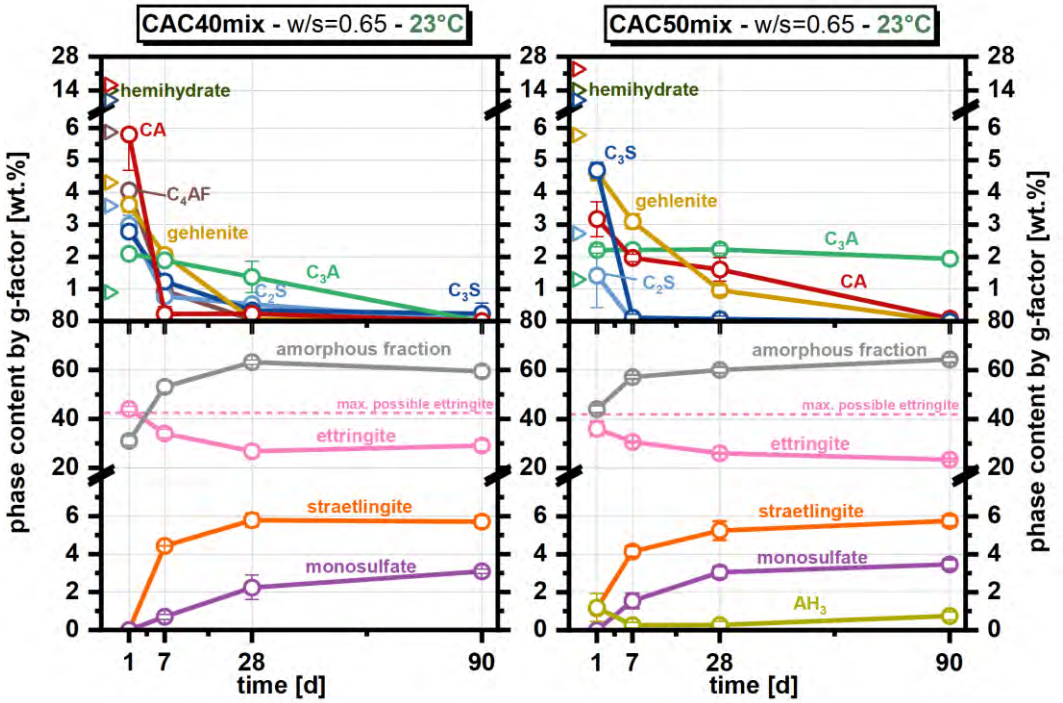

Figure 1. Main phase composition of stored samples determined with QXRD after 1, 7, 28 and 90 d at 23 °C; triangles on the left side of the upper sections indicate the starting values of the phases in the paste ($C\$H_{0.5}$ is not shown as it dissolves within 24 h).

After the maximum possible amount of ettringite (calculated based on sulfate content) has formed at the beginning of hydration, ettringite dissolved again during late hydration. Additionally, during the late hydration, monosulfate (partly from the dissolving ettringite) and straetlingite (from the

Si-containing clinker phases such as gehlenite) were precipitated. In the CAC50mix system, small amounts of crystalline AH_3 can also be detected. The results at 10 °C are shown in Figure 2, whereby the structure of the Figure is comparable to Figure 1. No significant difference in the (hydrate) phase development can be observed. Only a delay in the hydration reaction is visible, particularly with CAC40mix, as CA only dissolved significantly after 28 d, initially formed gypsum (from the hemihydrate) redissolved and only then the maximum possible amount of ettringite was detected.
In conclusion, it can be said that, despite different CACs, no significant differences occur during hydration at either 23 °C or 10 °C with regard to the phase development.

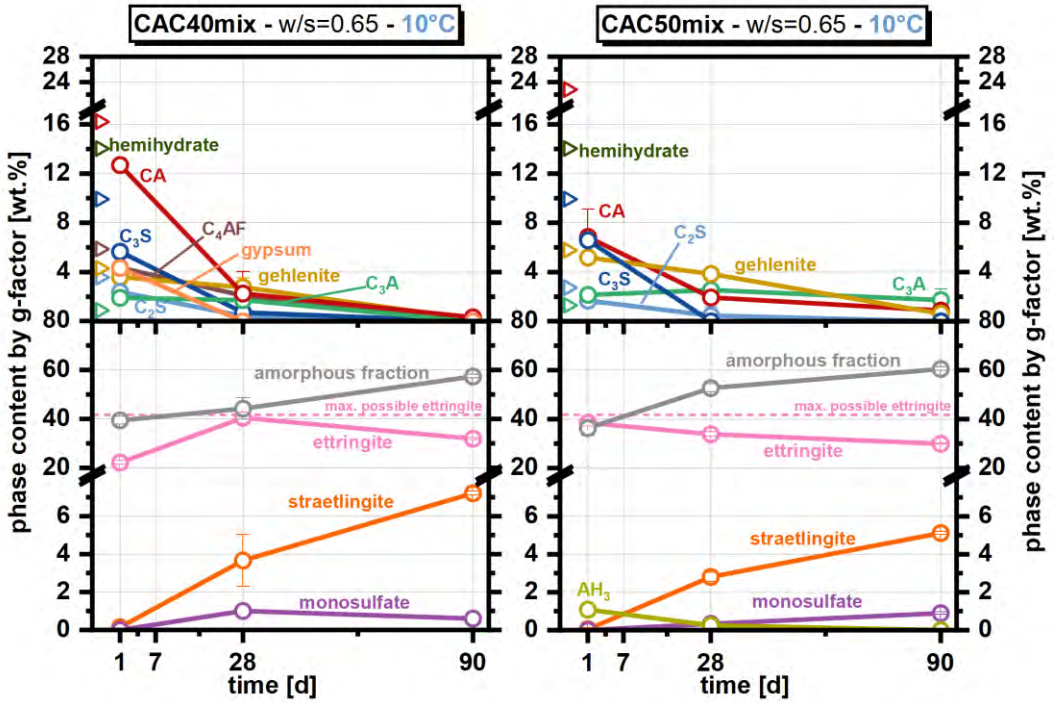

Figure 2. Main phase composition of stored samples determined with QXRD after 1, 28 and 90 d at 10 °C; triangles on the left side of the upper sections indicate the starting values of the phases in the paste ($C\$H_{0.5}$ is not shown as it dissolves within 24 h).

REFERENCES

[1] D. Torrens-Martín, F. Winnefeld, L.J. Fernández-Carrasco, Thermodynamic model for ternary OPC/CAC/Calcium Sulfate binders, Constr Build Mater 302 (2021). https://doi.org/10.1016/j.conbuildmat.2021.124120.

[2] J.J. Wolf, D. Jansen, F. Goetz-Neunhoeffer, J. Neubauer, Application of thermodynamic modeling to predict the stable hydrate phase assemblages in ternary CSA-OPC-anhydrite systems and quantitative verification by QXRD, Cem Concr Res 128 (2020). https://doi.org/10.1016/j.cemconres.2019.105956.

[3] D. Jansen, F. Goetz-Neunhoeffer, C. Stabler, J. Neubauer, A remastered external standard method applied to the quantification of early OPC hydration, Cem Concr Res 41 (2011) 602–608. https://doi.org/10.1016/J.CEMCONRES.2011.03.004

International Conference on Calcium Aluminates 2026

Controlled calcium sulfoaluminate synthesis and influence of superplasticizers on the formation kinetics

Ravindran*, Hari Priya, Laboratory for Energy Technologies and Innovation, PSI Center for Energy and Environment Sciences, Villigen, Switzerland, School of Materials Science and Engineering, EPFL, Lausanne, Switzerland ; Flatt, Robert J, Institute for Building Materials, ETH Zürich, Switzerland; Lothenbach, Barbara, Lab of Concrete & Asphalt, Empa, Dübendorf, Switzerland; Testino, Andrea, Laboratory for Energy Technologies and Innovation, PSI Center for Energy and Environment Sciences, Villigen, Switzerland, School of Materials Science and Engineering, EPFL, Lausanne, Switzerland

Keywords: Ettringite, monosulfate, PCEs, controlled synthesis, classical nucleation theory

ABSTRACT

Ettringite (AFt) is a key phase influencing the early-stage hydration and rheology of calcium aluminate, calcium sulfoaluminate and blended cements. However, a quantitative and mechanistic understanding of early-stage hydration - specifically nucleation and growth - remains unclear. Through a controlled titration-precipitation method, we synthesized AFt monitoring the physiochemical process through potentiometric techniques including ion selective electrodes (ISE). These data are further implemented to a model framework based on classical nucleation theory (CNT) and population balance model, estimating thermodynamic parameters such as solubility, interfacial energies alongside the nucleation kinetics. Addition of polycarboxylate ethers (PCEs) were observed to stabilize monosulfate (SO_4-AFm), in addition to causing nucleation delay. A concentration dependence of PCEs on this effect was also observed. Along with the model, crucial insights on the nucleation and growth stages could be obtained, even in presence of various admixtures. This could potentially open a new domain of design and development of various admixtures, optimizing the workability in blended cements.

*hari.ravindran@psi.ch

BACKGROUND

To advocate for the decarbonization of the construction sector, supplementary cementitious materials (SCMs)[1]are widely investigated as clinker replacement, as clinker production accounts for 8% of anthropogenic global CO_2 emissions. Such SCM containing blended cements often faces challenges maintaining durability and strength of concrete, necessitating the usage of superplasticizers (SPs). In the early stages of cement hydration, calcium sulfoaluminate hydrates, particularly ettringite (AFt) plays a key role in influencing the yield stress[2-4] due to its network of high aspect ratio needles, affecting the rheological behaviour[5]. While this could be mitigated through PCEs due to their dispersion abilities, their interaction and influence on the early formation stages are of extensive research[6–8] indicating a high affinity of PCEs to adsorb on AFt. Additionally, a delay of cement hydration in the presence of PCE has been widely reported with various mechanisms proposed.

Most of the previous studies have been carried out in (model) cements with the interference of other phases and often at uncontrolled (T, pH) conditions. A clear understanding of the interaction of PCEs in the early hydration stages requires isolation of the reacting phases and efficient monitoring. In our study, we focus on the calcium sulfoaluminates and their interaction with PCEs through a controlled titration-precipitation methodology. Dilute concentrations of the constituent ions allow sufficient timeframe to uncover the nucleation and growth effects of the solid formation, monitored through potentiometric measurements and subsequent model framework.

METHODS

AFt was synthesized in a controlled titration – precipitated method, where dilute solution of $CaCl_2$ was titrated to the solution containing excess $Al_2(SO_4)_3$ and NaOH at constant T (22^{o}C) and pH (12.4), to remain within the stability limit of AFt. The solid formation was monitored through Ca^{2+} ISE, conductivity and pH electrodes, correlating depletion of ionic species. Additionally, an optical electrode was used to monitor the evolution of solid. All these data are obtained in timestep of 5s throughout the experimental timeframe of 3-4 hours. To investigate the influence of PCEs, it was added in early addition mode i.e. before start of titration. PCEs with varying charge density and side chain lengths were used.

Further, these temporal data were introduced into a model framework. The activity coefficients of the species were estimated through extended Debye-Hückel approximation and further saturation of the system was estimated at each time step. For Ca^{2+} species, ISE potential was translated to activity. The kinetic model was formulated based on CNT assuming primary and true 3D secondary nucleation. A linear growth rate was estimated through assumption of Ca^{2+} diffusion growth validated through maintaining excess

of $Al_2(SO_4)_3$ in the starting solution. A monovariate population balance with non-linear class size distribution was implemented for modelling the evolving particles.

KEY FINDINGS

Preliminary thermodynamic model revealed the supersaturation of AFt, SO_4- AFm and gibbsite in our experimental conditions. The saturation of AFt was found to be 10^5 times higher than that of SO_4-AFm. In the experiments without PCEs, AFt was predominantly formed, with a small fraction of SO_4-AFm occurring in few experiments and no gibbsite formation. Notably, our experimental conditions are in the excess sulfate regime that should ideally favour AFt formation.

When PCEs are added, the system shifted towards forming SO_4-AFm as the predominant product. In some cases, minor amount of AFt was observed. The PCEs with lower sidechain lengths induced a higher delay of nucleation (delay ≈ 35 mins) as compared to the PCEs with higher sidechain lengths (delay ≈15 mins), even with the varying charge density of backbone. From the perspective of delay in nucleation, it is probable that PCEs with the higher side chain lengths might not effectively interact with the surface or evolving entities as compared to the ones with shorter side chain lengths.

When PCEs were dosed in varying amounts, delay in nucleation was observed to increase with concentration. Similarly, phase assemblage shifts from AFt dominated to SO_4-AFm dominated with increase in PCE concentration. However, the threshold concentration to shift towards SO_4-AFm also varies with PCEs. TEM analysis during the evolution of solid formation, in the absence of PCEs, validated the simultaneous presence of both the phases from the start, without intermediate transformation. However, to reveal the mechanistic influence of PCEs, further *in-situ* measurements during the solid growth are underway.

Thermodynamic parameters such as saturation, solubility of the freshly precipitated solid, interfacial energies corresponding to both primary and secondary nucleation are estimated based on model calculated wrt predominantly formed phases. Furthermore, based on the time resolved data, growth of the needles or SO_4-AFm platelets in case of PCE experiments are estimated. Thereby, we could obtain the fundamental information on the early stages and correlate physically significant parameters which are crucial for further design and development of various admixtures.

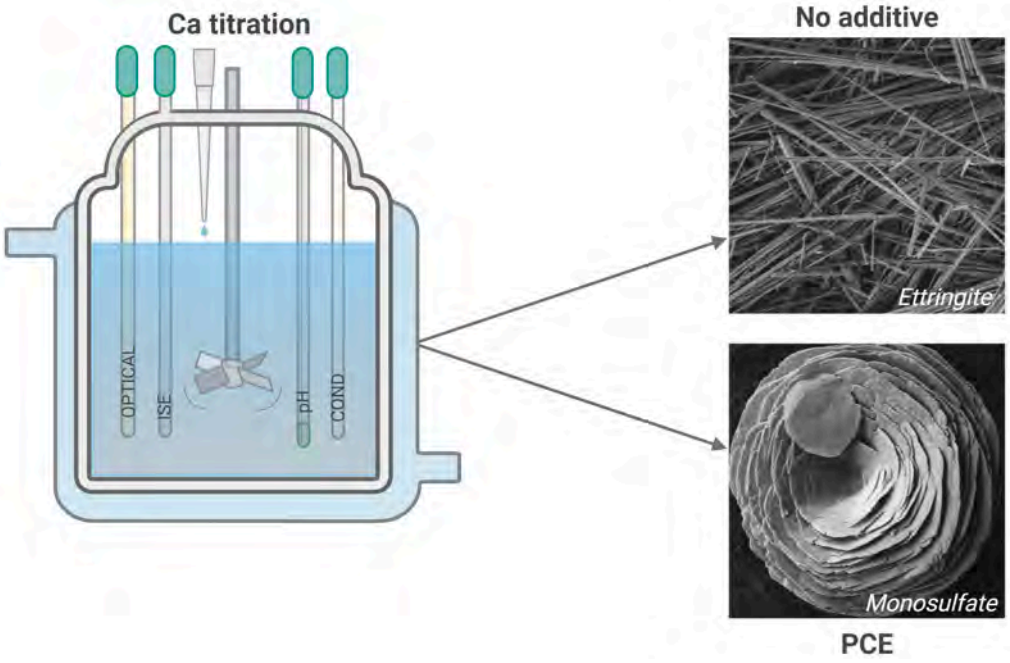

Figure 1. Influence of PCE on the solid formation in the controlled titration methodology

REFERENCES

[1] B. Lothenbach, K. Scrivener, R.D. Hooton, Supplementary cementitious materials, Cem. Concr. Res. 41 (2011) 1244–1256. https://doi.org/10.1016/j.cemconres.2010.12.001

[2] C. Jakob, D. Jansen, N. Ukrainczyk, E. Koenders, U. Pott, D. Stephan, J. Neubauer, Relating Ettringite Formation and Rheological Changes during the Initial Cement Hydration: A Comparative Study Applying XRD Analysis, Rheological Measurements and Modeling, Materials 12 (2019). https://doi.org/10.3390/ma12182957

[3] C. Jakob, D. Jansen, J. Dengler, J. Neubauer, Controlling ettringite precipitation and rheological behavior in ordinary Portland cement paste by hydration control agent, temperature and mixing, Cem. Concr. Res. 166 (2023) 107095. https://doi.org/10.1016/j.cemconres.2023.107095

[4] W. Mbasha, R. Haldenwang, I. Masalova, The influence of sulfate availability on rheology of fresh cement paste, 30 (2020) 54–63. https://doi.org/doi:10.1515/arh-2020-0106

[5] W. Prince, M. Espagne, P.-C. Aïtcin, Ettringite formation: A crucial step in cement superplasticizer compatibility, Cem. Concr. Res. 33 (2003) 635–641. https://doi.org/10.1016/S0008-8846(02)01042-6

[6] J. Plank, C. Hirsch, Impact of zeta potential of early cement hydration phases on superplasticizer adsorption, Cem. Concr. Res. 37 (2007) 537–542. https://doi.org/10.1016/j.cemconres.2007.01.007

[7] D. Marchon, R.J. Flatt, 12 - Impact of chemical admixtures on cement hydration, in: P.-C. Aïtcin, R.J. Flatt (Eds.), Science and Technology of Concrete Admixtures, Woodhead Publishing, 2016: pp. 279–304. https://doi.org/10.1016/B978-0-08-100693-1.00012-6

[8] D. Marchon, P. Juilland, E. Gallucci, L. Frunz, R.J. Flatt, Molecular and submolecular scale effects of comb-copolymers on tri-calcium silicate reactivity: Toward molecular design, Journal of the American Ceramic Society 100 (2017) 817–841.https://doi.org/10.1111/jace.14695

International Conference on Calcium Aluminates 2026

CALCIUM ALUMINATE CEMENT SAVING POTENTIALS IN BUILDING CHEMISTRY PRODUCTS

Gerz, Alexandra[1], Hartmann, Florian[1], Guillot Laurent[1]
[1]Calucem d.o.o., Revelanteova 4, 52100 Pula, Croatia

Keywords: Self-Levelling Compounds, In-Situ XRD, CO_2 Reduction

ABSTRACT

The incorporation of Calcium Aluminate Cements (CACs) into modern building chemistry products enable rapid set, fast hardening and quick drying. Apart from application demands, the CO_2 footprint of the products needs to be lowered as well to minimize climate impact. One avenue to reduce CO_2 is to decrease the cement content in the product formulation. The patented CAC Flex offers a solution due to its high reactivity and the cement saving potentials are demonstrated by a comparison with CAC50 and CAC505 in a Self-Levelling Compound (SLC). CAC505 offers increased cement fineness when compared to the reference CAC50, enabling a reduction of the CAC content by 10 % without sacrificing product performance. CACFlex combines the increased cement fineness with a higher content of the main reactive phase CA. As a result, SLCs containing CACFlex display better performance than the reference even after reducing CAC in the recipe by 20 %. The in-situ XRD and calorimetry investigations presented give insights in SLC phase development and reaction kinetics.

INTRODUCTION

The combination of CAC, Ordinary Portland Cement (OPC) and a sulfate source into a ternary system is characterized by ettringite formation, rapid hardening and quick drying and is the basis for SLCs [1]. The contribution of CAC to the SLCs' CO_2 footprint is not negligible as they are a main component of the binder system. More efficient CACs can be used at a lower dosage, thus improving the overall CO_2 balance. There are various ways to achieve higher efficiency of the CACs. Increasing the cement's fineness results in more small particles partaking in the early reaction with water. Klaus et al. [2] showed that the fineness of the main reactive phase monocalcium aluminate (CA) influences the degree of hydration with an increased CA fineness leading to a higher value. Further studies proved that highly efficient CACs enable the formulator to either boost overall performance or to reduce the CAC amount in the formulation without impairing physical-mechanical properties and with only slight formulation adjustments required [3][4]. The present study expands on these results and investigates how the cement content can be further reduced in SLC formulation by not only increasing the cement´s fineness but also increasing the amount of the reactive mineral phase CA.

*Alexandra.Gerz@calucem.com

METHODS

Three CACs with an Al_2O_3 content between 50-55% are included in this study: Reference CAC50 has a specific surface area of ~3500 cm^2/g, whereas the CAC505 and CACFlex offer higher fineness with a Blaine above 4000 cm^2/g. CAC505 has a reduced $C_{12}A_7$ content compared to CAC50. While CAC50 and CAC505 have similar CA content below 70%, CACFlex has a CA content above 70%. SLC mix designs are displayed in Table 1. Formulations are adjusted to an open time of approx. 30 min.

Table 1. SLC mix compositions

Sample name		SLC50	SLC505	SLCFlex
Binders [%]	CAC 50	20		
	CAC 505		18	
	CAC Flex			16
	OPC (CEM I 52.5 R)	6	6	6
	Sulfate (α-Hemihydrate)	6	6	8
Aggregates [%]	Quartz sand	39.4	41.4	41.4
	Limestone filler	28.6	28.6	28.6
Admixtures* [%]	Hydrated Lime	1.2	1.2	0.6
	Accelerator and Retarder	0.59	0.59	0.50
	Plasticizer, Stabilizer, Defoamer and Redispersible Polymer Powder	1.5	1.5	1.5
Water addition* [%]		22	22.5	22.5

*Admixtures and water are added on top of main components (binders + aggregates = 100%)

Cement hydration was characterized in a paste with w/c=0.7 using an isothermal microcalorimeter. Flowability was determined with a 68 x 35 mm flow ring. Compressive strength was tested using 40 x 40 x 160 mm prisms according to EN 196-1 after 4h, 6h, 24h and 28d (storage conditions: 20 °C, 65% RH). The hardening process was examined with ultrasonic measurements. SLC hydration was characterized by isothermal microcalorimetry at 20°C. In situ XRD was performed with a cooling stage at constant 20°C with the sample covered with Kapton® foil. Rietveld refinements were performed using Topas with external standard method. Results are considered semi-quantitative due to challenges in the experimental setup like e.g. short measurement times and sedimentation.

RESULTS

CAC50, CAC505 and CAC Flex calorimetry paste results are displayed in Figure 1. The initial heat release is associated with the dissolution of the binder in the mixing water and the additional energy uptake of the system during rapid stirring [2]. After the subsequent induction period the main asymmetrically shaped hydration peak of CAC50 and CAC505 starts to develop. CAC505 shows a delayed and more intense hydration reaction. On the other hand, CACFlex has a shorter induction period. The peak is narrow with a nearly symmetric rise and fall, indicating a punctuated and intense hydration reaction. Correspondingly, the total heat increases steeply and reaches 400 J/g within 5.2 h after the reaction starts.

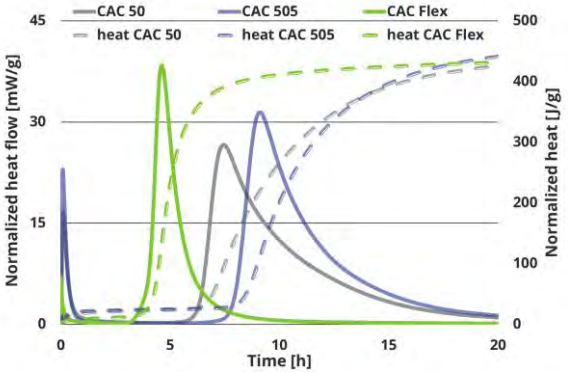

Fig. 1: Heat flow calorimetry of CAC50, CAC505, and CACFlex (paste with w/c = 0.7)

Calorimetry results of the SLCs are displayed in Figure 2, showing three reaction peaks P1, P2 and P3. P1 directly follows the start of hydration, due to the dissolution and stirring energy input. The shape of P2 is comparable for CAC50 and CAC505, but CAC505 reaches a higher maximum heat flow. A third broad reaction peak (P3) follows, which starts earlier in case of SLC505. The SLCFlex heat flow curve also shows three peaks but with different intensities and timings. P2 reaches its maximum earlier and overlaps with P3 reaction peak. The corresponding ultrasonic measurements show a similar hardening for SLC50, SLC505 and SLCFlex. Two major velocity increases can be observed concurrently with the heat flow reaction peaks P2 and P3. The main difference is the speed of the hardening process and the maximum velocity reached, in ascending order: SLC50<SLC505<SLCFlex. Corresponding phase development is qualitatively identical for all samples. In reactions P2 and P3 ettringite is formed. α-Hemihydrate (Bassanite) acts as a sulfate source for ettringite formation and continuously decreases due to its consumption in reactions P2 and P3. CA depletion mainly coincides with reaction peak P3. The major share of ettringite is formed in reaction P3 in all samples. The ratio between the determined ettringite values indicate an increased ettringite formation for SLCFlex, as compared to SLC505 and SLC50. The increased ettringite formation is likely not only due to the increased availability of CA, but also due to a higher sulfate content in the formulation.

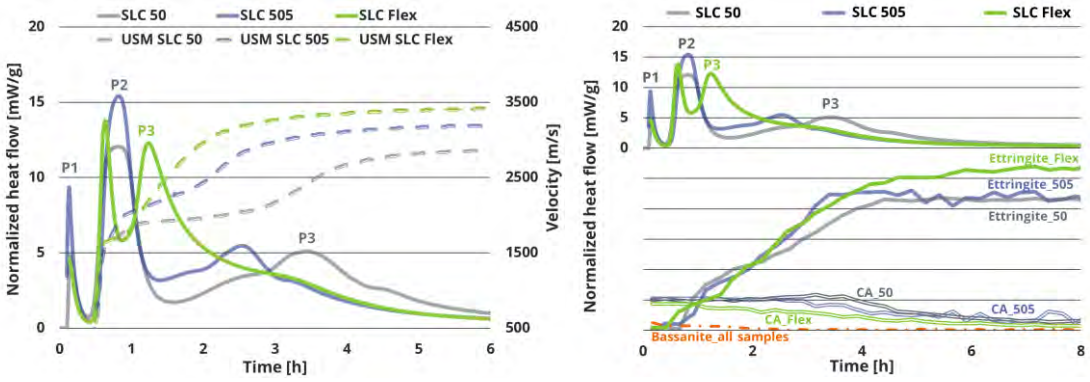

Fig. 2: Heat flow calorimetry of SLC50, SLC505, and SLCFlex with corresponding ultrasonic measurements (left) and corresponding semi-quantitative phase development – only phases involved in the reaction are included (right)

Application tests of the SLCs are displayed in Figure 3. SLC50 shows good initial flow and a slight flowability decrease after 15 min, caused by the start of the P1 reaction shortly before the 30 min flow. SLC505 and SLCFlex achieve stable and higher flows over 30 min. SLC50 and SLC505 show a comparable compressive strength development up to 28 d, though SLC505 contains 10 % less CAC. SLCFlex with 20 % less CAC in the recipe reaches slighter higher compressive strength after 4 h and 6 h due to an intense ettringite formation.

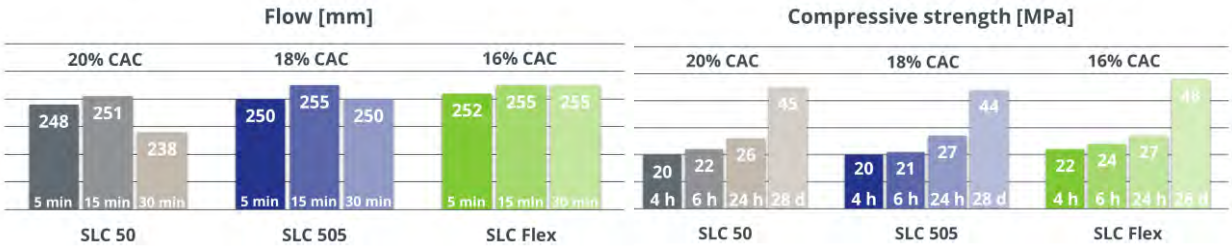

Fig. 3: Flowability [mm] after 5 min, 15 min, 30 min (left) and Compressive strength [MPa] after 4h, 6h, 24h, 28 d (right) of SLC 50, SLC 505 and SLCFlex

CONCLUSION

Results confirm the possibility of CAC reduction in the SLC formulation by using CAC505 (10 % less) and CACFlex (20 % less) without sacrificing application properties. Increased cement fineness leads to a higher early availability of CA for the ettringite formation. Only slight formulation adjustments are required when switching from CAC50 to CAC505. CACFlex combines higher cement fineness with increased CA content resulting in a punctuated, intense, and nearly symmetrical hydration peak, highlighting its high reactivity. To match the higher reactivity requires a sulfate increase in the SLC formulation but also allows to use less admixtures. The SLCFlex shows an enhanced ettringite formation which causes an overlap between the associated reaction peaks P2 and P3, leading to a homogeneous reaction. Within the first 6 h SLCFlex displays the highest heat evolution, velocity, and early compressive strength values even at 20 % reduced CAC content. This points out the possibility to reduce the CAC content even further and to save additional CO_2 in the overall SLC balance.

REFERENCES

[1] Ideker J. H., Scrivener K. L., Fryda H., Touzo B., Calcium Aluminate Cement. In: P C Hewlett, Martin Liska (ed), Lea´s chemistry of cement and concrete, 5th edition, 2019, 546-548

[2] Klaus, S., et al.: How to increase the hydration degree of CA – The influence of CA particle fineness, Cement and Concrete Research 67 (2015), 11-20

[3] Gerz A., Schmid M., Walenta G.: Highly efficient Calcium Aluminate Cements for modern building products, Drymix Mortar Yearbook 2021, 64-68

[4] Gerz A., Hartmann F., Walenta G.: Highly efficient Calcium Aluminate Cements for modern building products – Part 2, Drymix Mortar Yearbook 2022, 4-11

International Conference on Calcium Aluminates 2026

Understanding the strength development of self-compacting concrete formulation incorporating ettringite accelerator as strength booster

El Housseini, Sarra, Benevenuti, Barbara, Hervé, Fryda, Chambon, Muriel

Imerys Technology Center Lyon, 38090 Vaulx-Milieu, France,
sarra.elhousseini@imerys.com

ABSTRACT

One of the challenges of the precast industry is the ability to quickly increase productivity to face demand peak for specific job sites. Thermal curing is a classical option, but it can be limited by availability of heating devices and more challenging the effectiveness when an ultra-fast turnaround (4h) is required. Incorporating ettringite accelerator (EA) based on calcium aluminates as strength boosters is a more effective option[1,2]. A complementary study showed that incorporating such a type of EA in a self-compacting concrete (SCC) formulation for the precast industry led to an improvement of the resistance to chloride and had no significant effect on carbonation[3]. The focus of this study is to investigate the strength development of an SCC formulation including 50kg/m^3 and 100kg/m^3 of EA as Portland cement substitute.
Compressive strength can reach up to 17 MPa at 6h with 100 kg/m^3 of EA with 30 min workability, versus no strength at 6h for the non-accelerated formulation. Early strength is mainly due to early ettringite formation. No decrease in strength over time have been observed with EA, reaching the same or higher strength level at 1 year than the non-accelerated reference. The degree of hydration of C_3S remains more or less the same for all investigated systems. Pore structure assessment at 28d shows that the system incorporating 100kg/m^3 EA has the lowest total porosity.

INTRODUCTION

Heat curing effectiveness is physically limited when an ultra-fast turnaround (4h) is required. The necessity of a mandatory "preset period" to prevent thermal expansion damage, combined with strict limits on the rate of temperature rise to avoid cracking, makes it nearly impossible for heat-based systems to achieve release strength within such a narrow window. EA accelerators can bypass the delays of traditional curing cycles, achieving high early strength at ambient temperatures while eliminating the energy costs and infrastructure maintenance associated with steam production.

sarra.elhousseini@imerys.com

METHODS

Flow measurements on fresh concrete were carried out at 20°C according to EN 12350-8. Compressive strength measurements on concrete were carried out according to EN 12390-3. To understand the strength results, X-Ray Diffraction (XRD) measurements were carried out using a Bruker, D8 Advance device. The used program starts at 2Θ = 5° and ends at 80° with a step size of 0.01°. The Rietveld quantification method is used with the Topas V6.0. software from Bruker to quantify the ettringite and the unreacted C_3S contents. The external method was used to quantify the amorphous content. Thermogravimetric analysis (TGA) were carried out with NETZSCH device, open crucible. The measurement starts at 30°C and ends at 1000°C with a temperature ramp of 10°C/min under N_2 atmosphere to avoid carbonation. The bound water content is obtained from the differences between the mass losses between 30°C and 550°C. Pore structure was characterized by Mercury intrusion porosimetry (MIP) using a Porotec 140 and 440 devices. The contact angle between mercury and concrete is 140°.

Three systems are investigated: the reference and the reference accelerated with 50 and 100 kg/^{3} of EA (amorphous calcium aluminate and anhydrite Al_2O_3=23%, CaO=42%, SO_3=30% from Imerys).

RESULTS

Applicative results

Figure 1 (a) and (b) respectively show the flow measured at 5 and 30 minutes and the compressive strength results of concrete samples up to 1 year for the reference, the reference accelerated with 50kg/m^3 EA and -100kg/m^3. Results show that concrete accelerated with EA is still within the SF2 requirement needed for our SCC. Regarding the compressive strength, a clear acceleration of the compressive strength development at 6h thanks to the use of EA without compromising the long-term strength. The compressive strength at 6h increases with the % of EA. This is suitable for precast concrete applications where a rapid strength development is needed to increase production cycles.

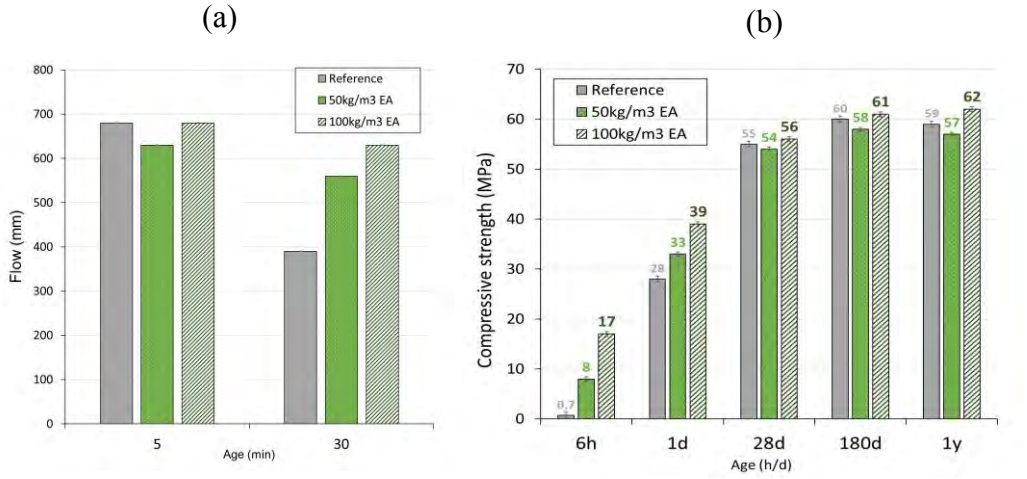

Figure 1 Flow values at 5 min and 30 min (a) and compressive strength development at 6h,1d, 28d,180d and 1 year (b) for the reference, reference with 50kg/m3 EA and -100kg/m3 EA.

Understanding the compressive strength results

Ettringite content and degree of hydration of C_3S by XRD

Figure 2 (a) and (b) show respectively the ettringite and the hydration degree of C_3S (DoH_{C3S}) calculated at 6 hours and 1 year on concrete samples. Results show that mixes incorporating EA leads to a higher ettringite content than the reference. The higher the EA content is the higher the ettringite content is both at 6h and 1 year. This explains the higher strength at 6h in systems incorporating EA. On the other hand, the hydration degree of C_3S at 6h is slightly lower than the reference with 50kg/m^3 EA. With 100kg/m^3 of EA, the difference in terms of DoH_{C3S} is not significant. XRD-Rietveld results are coherent with the compressive strength results. It is worth noting that no conversion products (C_3AH_6, C_2AH_8, CAH_{10}) have been detected by XRD. This is thanks to the presence of calcium sulfate that changes the phase assemblage and leads to ettringite formation instead.

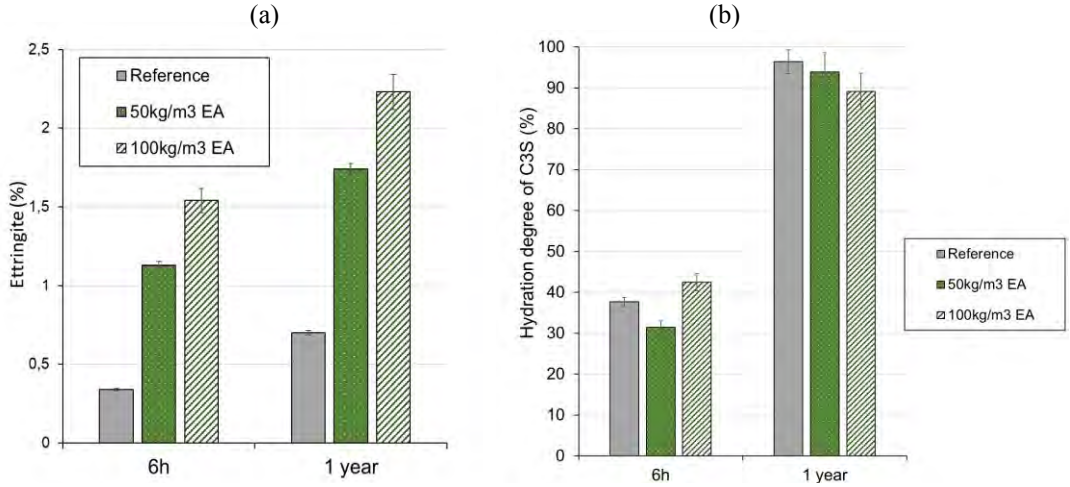

Figure 2 Ettringite content (a) and hydration degree of C_3S at 6h and 1 year for the reference, reference with 50kg/m^3 EA and -100kg/m^3 EA.

Bound water content by TGA

Figure 3 gives the bound water content from TGA for the reference, the reference with -50 and 100kg/m^3 EA at 6h and 1 year. Results show that the bound water content is higher at 6h for mixes incorporating EA compared to the reference. This could be explained by the fact of having comparable or only slightly lower degrees of hydration of C_3S with additional ettringite content from the EA reaction. At 1-year, comparable bound water values are obtained between the reference and the system with 50kg/m^3 EA. The concrete mix incorporating 100kg/m^3 EA have a higher bound water content. This could explain the slightly higher compressive strength obtained at 1 year with this dosage of EA.

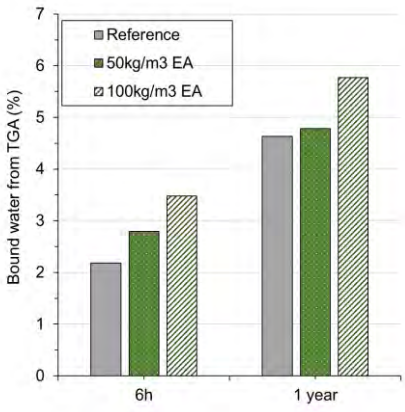

Figure 3 Bound water from TGA at 6h and 1 year for the reference, reference with 50kg/m³ EA and -100kg/m³ EA.

Pore structure characterization through MIP at 28d

To confirm that incorporating EA does not induce an increase of the porosity, the pore structure was characterized after 28d of hydration of concrete samples. Results are plotted in Figure 4. Similar total porosity with 50kg/m^3 compared to the reference is obtained. A reduction of the total porosity is observed with 100kg/m^3 of EA highlighting the positive effect of incorporating EA. The reduction of porosity is attributed to the additional ettringite formation and its good capacity to fill space. On the other hand, it can be seen that the reference has the smallest critical pore entry size followed by 50kg/m^3 then by 100kg/m^3 of EA.

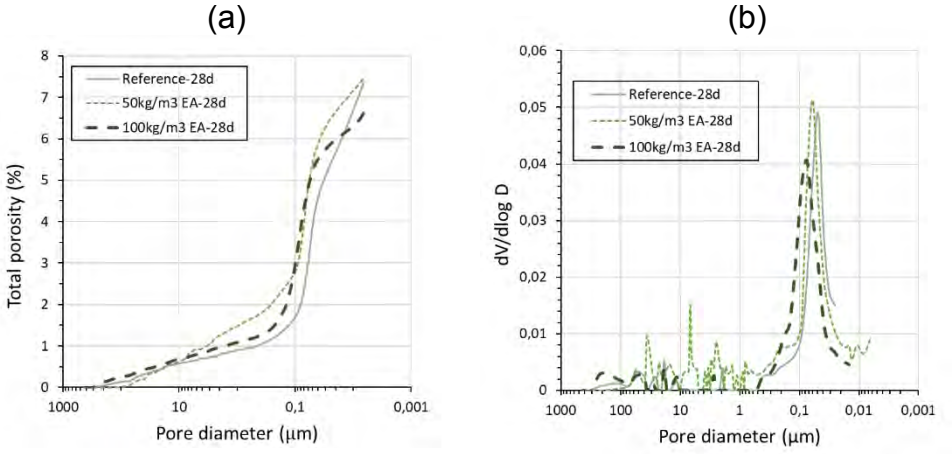

Figure 4 Total porosity (a) and cumulative pore volumes at 28d for the reference, reference with 50kg/m³ EA and -100kg/m³ EA.

CONCLUSIONS

The incorporation of EA as a partial Portland cement substitute (50 kg/m³ and 100 kg/m³) successfully accelerated the early-age strength development of the self-compacting concrete (SCC) formulation, achieving 6h compressive strength up to 17 MPa while maintaining long-term performance, with no detrimental strength decrease up to 1 year. This acceleration is primarily attributed to a higher early-age ettringite content, as confirmed by XRD-Rietveld analysis, with no

detection of conversion products. Furthermore, the 100 kg/m³ dosage positively impacted the microstructure, leading to a reduction in total porosity (MIP).

These findings demonstrate the feasibility of using EA based on calcium aluminates as Portland substitutes in a SCC precast formulation without major changes in the phase assemblage and with no long-term strength decrease.

REFERENCES

[1] S. El Housseini, Hydration and Durability of fast hardening binders incorporating supplementary cementitious materials, Thesis, EPFL, 2022.
[2] B. Benevenuti, S. El Housseini, N. Maach, H. Fryda, S. Perrot, M. Chambon, Improving the early age strengths of low CO_2 binders with a calcium aluminate cement-based accelerator, Rilem week, Toulouse, 2024.
[3] B. Benevenuti, A. Aboulela, S. El Housseini, Durability of concrete containing calcium aluminate based mineral accelerator, calcium aluminate cement 2026 conference proceedings, Lausanne, 2026.

International Conference on Calcium Aluminates 2026

HYDRATION BEHAVIOR OF QUATERNARY CAC-OPC-C$-SCM SYSTEMS INCORPORATING SUPPLEMENTARY CEMENTITIOUS MATERIALS UNDER VARIABLE CURING TEMPERATURES

Demirdoğan, Özge[1], Meral Akgül, Çağla[2], Erbuğa Avcıoğlu, Berrak[3]

[1]Sabancı Technology Center GmbH, Freisinger Landstraße 50 Garching, Munich, Germany, 85748, ozge.demirdogan@sabancibs.com,
[2]Department of Civil Engineering, Middle East Technical University, Ankara, Türkiye, 06800,
[3]Sabancı Technology Center GmbH, Freisinger Landstraße 50 Garching, Munich, Germany, 85748

Keywords: calcium aluminate cement, supplementary cementitious materials, hydration behavior, curing temperature, XRD

ABSTRACT

Quaternary cementitious systems consisting of calcium aluminate cement (CAC), ordinary Portland cement (OPC), calcium sulfate (C$), and supplementary cementitious materials (SCMs) can be designed to obtain systems having improved performance compared to individual binder components. The incorporation of SCMs is important not only for modifying hydration behavior and performance, but also for reducing clinker content and improving sustainability. In this study, the hydration behavior of CAC–OPC–C$–SCM quaternary systems was investigated under different curing temperatures. Ground granulated blast furnace slag (GGBFS) and natural pumice (NP) were selected as supplementary cementitious materials to observe their influence on hydration kinetics, phase development, setting behavior and strength progression. The effect of curing temperature was also considered because CAC-containing systems are highly sensitive to temperature changes. The study aims to understand how the incorporation of different SCMs affects the hydration behavior of CAC-based quaternary systems. Results showed that the type of SCMs has influences on the reaction mechanism depending on their chemical composition, physical properties, and reactivity. While slag can contribute to the system due to its latent hydraulic character, natural pumice can affect hydration through its pozzolanic nature and filler effect. Overall, this study focused on the interaction between SCM type and curing temperature in CAC–OPC–C$–SCM systems and provides a basis for optimizing these binders for rapid repair and specialty mortar applications.

ozge.demirdogan@metu.edu.tr / ozge.demirdogan@sabancibs.com

INTRODUCTION | BACKGROUND

In ternary systems, ordinary Portland cement (OPC), calcium aluminate cement (CAC), and calcium sulfate are combined to generate a system having superior properties compared to individual properties of their components. These systems can be used in different applications such as self-leveling mortars, tile adhesives, grout mortars, and rapid repair mortars because they can provide rapid setting, rapid hardening, shrinkage, or expansion compensation properties [1, 2]. In these systems, ettringite is formed as a major hydration product at early ages, which plays a key role in strength development and dimensional stability. A ternary system composed of OPC, CAC, and calcium sulfate can be prepared as OPC-based or CAC-based depending on the mixture ratio and application requirement. The formation mechanism of ettringite depends on the availability of sulfate ions and the reactivity of the aluminate phases present in the system [3]. Since CAC introduces additional reactive aluminate phases into the system, hydration kinetics and phase assemblage differ significantly from pure OPC systems. In CAC-based systems, ettringite and gibbsite are generally the main hydration products, and the formation of ettringite plays an important role in early-age behavior and volume stability [4]. Moreover, previous studies have shown that the stability of ettringite in OPC–CAC–C$ systems is strongly affected by environmental conditions such as temperature and relative humidity, which can influence phase assemblage and long-term performance [5]. Supplementary cementitious materials (SCMs) can be incorporated into these systems to improve performance and sustainability. The addition of SCMs can decrease clinker or cement amount, contribute to lower carbon dioxide footprint, and modify hydration reactions. Also, depending on their properties, SCMs can act as filler materials, participate in pozzolanic or latent hydraulic reactions, and influence the pore structure of the system. In previous studies, slag addition was reported to improve strength and durability of OPC–CAC–C$ systems, especially in aggressive environments [6, 7]. Furthermore, the stability of hydration products, particularly ettringite, has been shown to be closely related to moisture availability, pore structure, and phase assemblage, which can be influenced by SCM incorporation. Curing temperature is another important parameter for CAC-containing systems because hydration reactions of CAC are temperature sensitive. It has been reported that increasing temperature and decreasing relative humidity can significantly affect ettringite stability, leading to dehydration, phase transformation, and changes in mechanical and dimensional properties [8]. In this study, ground granulated blast furnace slag and natural pumice were selected as SCMs. Slag was chosen due to its latent hydraulic character and its potential contribution to additional hydration reactions. Natural pumice was chosen as an alternative pozzolanic material because it can contribute to sustainability and may affect hydration behavior through its fine particle size and reactive silica content. Therefore, the combined effect of SCM type and curing temperature should be investigated to understand the behavior of CAC–OPC–C$–SCM quaternary systems. Although there are studies related to ternary systems, the effect of different SCMs on CAC-based quaternary systems under different curing temperatures is still limited. Therefore, this study aims to investigate the hydration behavior of quaternary systems including SCMs and to provide information for further optimization of these binders.

METHODS

Calcium aluminate cement (CAC 40), ordinary Portland cement (CEM I 42.5 R), and four different calcium sulfate sources, anhydrite (A), α-hemihydrate (H), natural gypsum (G), and phosphogypsum (PG), were used to prepare CAC-based binder systems. In order to evaluate the effect of sulfate source, the binder composition was kept constant, and only the type of calcium sulfate was varied. Also, at the same ratio of SCMs was substituted for CAC-ternary binder systems by diluting the composition of CAC-ternary binder systems. Ground granulated blast furnace slag (GGBFS) and natural pumice (NP) was chosen as the types of SCMs. The physical properties of the materials used to generate quaternary systems are given in Table 1. All cement paste samples were prepared with a constant water-to-binder ratio of 0.5. To assess the temperature sensitivity of each formulation, curing was carried out at 5 °C, 23 °C, and 45 °C. The hydration behavior, phase evolution, setting characteristics and strength performances of the systems were investigated. Isothermal calorimetry was used to observe the hydration kinetics. In addition, X-ray diffraction (XRD) analysis was performed to identify the phase assemblage and to follow the evolution of hydration products. Setting time measurements were carried out using automatic Vicat equipment to determine the initial and final setting behavior. Early and long term compressive and the flexural strength performances were also conducted. The selected experimental methods were used to establish the relationship between sulfate source and hydration behaviour under different curing conditions.

Table 1. Physical properties of components

PSD Analysis [µm]	CAC	OPC	A	H	G	PG	BFS	NP
D10	1.43	1.43	1.34	1.61	1.58	1.15	1.56	1.17
D50	9.45	10.28	5.73	15.46	13.15	7.71	9.62	4.79
D90	46.66	36.98	14.97	52.99	39.64	35.5	34.82	26.85
Mean Size	18.66	16.30	7.53	23.28	18.35	15.5	15.33	10.00
Materials	**CAC**	**OPC**	**BFS**	**NP**				
Density g/cm^3)	3.25	3.11	2.91	2.36				
Blaine (cm^2/g)	3277	3250	5370	6011				

KEY FINDINGS | CONCLUSIONS

According to the calorimetry results, both the type of calcium sulfate source and the type of SCM have a significant effect on the hydration behavior of the systems. Even though the binder composition was kept similar, different sulfate sources resulted in clearly different reaction kinetics in both slag and pumice-containing systems. Both type of SCMs and curing temperature significantly influenced the hydration kinetics and product formation. In both systems, the α-hemihydrate-containing mixtures show the fastest reaction with a high initial heat flow, indicating rapid dissolution and accelerated early hydration. The anhydrite systems exhibit a more gradual behavior with multiple peaks, suggesting slower but sustained sulfate release. The gypsum systems show intermediate behavior, while phosphogypsum

systems clearly present delayed hydration with a later main peak and broader reaction profile. When the effect of SCM type is evaluated based on calorimetry results, slag-containing systems show higher early-age reactivity compared to pumice-containing systems. This indicates that slag contributes to hydration due to its latent hydraulic character, while pumice mainly influences the system through pozzolanic and filler effects. These observations are also consistent with the setting time results. The hemihydrate systems show the shortest setting times, while gypsum and phosphogypsum systems show significantly longer setting times. Anhydrite systems again show intermediate behavior. Slag enhanced early-age reactivity and caused earlier setting, particularly at elevated temperatures. On the other hand, delayed hydration happened at lower temperatures. The strength results also follow a similar trend for slag-containing systems. Systems with faster early hydration generally show higher early-age strength, while systems with delayed reactions show lower strength at early ages. Overall, it can be concluded that both calcium sulfate source and SCM type play a key role in controlling hydration kinetics, setting behavior, and strength development of CAC–OPC–C$ systems. Among the parameters studied, sulfate dissolution rate controls early-age behavior, while SCM type influences both reaction kinetics and mechanical performance.

REFERENCES

[1] T.A. Bier, Composition and properties of ternary binders, in: Cementitious Materials, 2017, pp. 353–376. https://doi.org/10.1515/9783110473728-013

[2] A.C. Rego, F.A. Cardoso, R.G. Pileggi, Ternary system Portland cement–calcium aluminate cement–calcium sulfate applied to self-leveling mortar: a literature review, Cerâmica 67 (2021) 65–82. https://doi.org/10.1590/0366-69132021673812929

[3] K.L. Scrivener, P. Juilland, P.J.M. Monteiro, Advances in understanding hydration of Portland cement, Cem. Concr. Res. 78 (2015) 38–56. https://doi.org/10.1016/j.cemconres.2015.05.025

[4] E. Qoku, T.A. Bier, G. Schmidt, J. Skibsted, Impact of sulphate source on the hydration of ternary pastes of Portland cement, calcium aluminate cement and calcium sulphate, Cem. Concr. Compos. 131 (2022) 104502. https://doi.org/10.1016/j.cemconcomp.2022.104502

[5] L. Noor, A. Tuinukuafe, J.H. Ideker, A critical review of the role of ettringite in binders composed of CAC–PC–C$ and CSA–PC–C$, J. Am. Ceram. Soc. 106 (2023) 3303–3328. https://doi.org/10.1111/jace.19014

[6] G. Li, A. Zhang, Z. Song, C. Shi, Y. Wang, J. Zhang, Study on the resistance to seawater corrosion of the cementitious systems containing ordinary Portland cement or/and calcium aluminate cement, Constr. Build. Mater. 157 (2017) 852–859. https://doi.org/10.1016/j.conbuildmat.2017.09.175

[7] G. Li, W. Wang, G. Zhang, Effects of slag on the degradation mechanism of ordinary Portland cement–calcium aluminate cement–gypsum ternary binder under multiple erosive ions, Constr. Build. Mater. 324 (2022) 126661. https://doi.org/10.1016/j.conbuildmat.2022.126661

[8] L. Noor, P. Rost, I. Kirchberger, F. Goetz-Neunhoeffer, J.H. Ideker, Hygrothermal stability of ettringite in blended systems with CAC–OPC–C$, Cem. Concr. Res. 184 (2024) 107590. https://doi.org/10.1016/j.cemconres.2024.107590

International Conference on Calcium Aluminates 2026

ETTRINGITIC ACCELERATORS: AN ADVANCEMENT FOR CEMENTITIOUS FOAMS

Bousseau, Jean-Noël*[1], Tichit, Emilie[1], Brigandat, Pierre[1], Berger, Stéphane[1], Fryda, Hervé[1] : [1]Imerys, Vaulx-Milieu, France

Keywords: mineral foam, ettringite, amorphous calcium aluminate

ABSTRACT

Mineral foam technology, despite being known for decades, has faced limitations in use due to technical challenges. The main issues include slow setting and hardening, low mechanical performance at early age, particularly in low-density foams, as well as shrinkage problems, and limited application range.

To address these challenges, an ettringite accelerator (EA) based on amorphous calcium aluminate and calcium sulfate has been developed. Temperature monitoring, rheological measurements under oscillatory conditions, mechanical characterisations, and dimensional variation measurements are employed to understand the mechanisms involved. It has shown promising results in improving performance: such as structure development and hardening kinetics, enhanced mechanical strength and lower residual moisture. Thermal expansion appears to be a key parameter to master dimensional change, a compromise has to be found. The enhanced foams show potential for applications in thermal insulation and lightweight system, high-rise construction and to contribute to more efficient and sustainable construction practices.

INTRODUCTION | BACKGROUND

Improving building thermal efficiency is a global priority. While organic foams and mineral wools dominate the market, they face challenges regarding flammability, environmental footprint, and recyclability. Cementitious mineral foams offer a promising non-combustible and recyclable alternative, with applications ranging from load-bearing blocks (400-800kg/m^3) to high-performance insulation (<200 kg/m^3). However, pure Ordinary Portland Cement (OPC) foams are limited by slow setting kinetics - causing fresh-state instabilities like coalescence and drainage - and drying shrinkage leading to early-age cracking[1].

In dense mortars, these reactivity and dimensional issues are successfully mitigated by incorporating calcium aluminate cements and calcium sulfates in propriatory binders such as LEAP FIT to trigger rapid ettringite formation[2]. It therefore seems logical to extrapolate these results and apply this solution to improve performance of mineral foams. A major scientific uncertainty exists: the drastic reduction in solid matter (from 2000kg/m^3 in dense mortars to 70kg/m^3 in insulating foams) fundamentally modifies the reaction environment. This research aims to evaluate the performance of amorphous calcium aluminate and calcium sulfate system as an ettringite-based accelerator (EA) to control setting kinetics and compensate for shrinkage within these lightweight structures.

*jeannoel.bousseau@imerys.com

RAW MATERIALS | FORMULATIONS | METHODS

Mineral foam production: the principle is to mix mineral slurry with a foamed solution. Mineral slurries are mixed with a Gertec CIM30E during 4min at 1700RPM. Two slurries (d=2040kg/m^3) are produced. The first is 100% OPC based: 100 parts OPC CEM II B LL 42.5R (Holcim SPLC), 0.09 parts Conpac 500 (PCE) and 35 parts water. The second slurry is composed of 85 parts OPC, 15 parts LEAP FIT (EA: amorphous calcium aluminate and anhydrite Al_2O_3=23%, CaO=42%, SO_3=30% from Imerys), 0.4 parts Na_2CO_3, 0.4 parts tartaric acid, 0.09 parts Conpac 500 and 35 parts water). The foamed solution (d=45kg/m^3) is generated with a Gertec SBL (95 parts water and 5 parts Isocem SB – animal protein + compressed air). The slurry and foamed solution are assembled in the mixing chamber of the Gertec SBL with a volume's ratio slurry/foam solution/air of 20/4/76 to achieve a 440kg/m^3 mineral foam wet density. Final targeted dry density is 400kg/m^3, the 100 OPC containing 299.2kg/m3 of OPC, the 85OPC/15EA containing 254.3 and 44.9kg/m3 of respectively OPC and EA.

Oscillatory mode rheology: Anton Paar MCR 302 rheometer, vane geometry and a cylindric cup are used. A Time scan is carried out through a G' and G" sweep over time: $\dot{\gamma}$ = 0.1%, f =1Hz (strain below the visco-elastic domain limit, material is not irreversibly destroyed). G' (storage modulus) and phase angle (δ) are collected to describe structuration from liquid to solid state (hydraulic set).

Dimensional change: Walter&Baï method allows continuous measurements during plastic phase and beyond. Moulds (triangular, 6.5 x 6.5 x 6.5cm cross-section, 36cm length) are poured with mineral foam, a plastic film is placed at the surface to initiate endogenous conditions during two days and then removed.

KEY FINDINGS

The use of an ettringite accelerator (EA) based on amorphous calcium aluminates in mineral foams has a significant impact on the kinetics of mechanical structuration kinetics during the liquid-to-solid states, compared to pure OPC. Rheological measurement (oscillatory mode – Fig. 1) allows for a precise description of the evolution of structure development from the liquid to the solid state (hydraulic setting) through measurements of the storage modulus G' (how high is the "strength level") and the phase angle δ (how quick the solidification is δ=0°). The addition of EA allows reaching a pure solid state in 1h30min with a G' of 85000Pa, compared to 5h for pure OPC with a G' of 46000Pa.

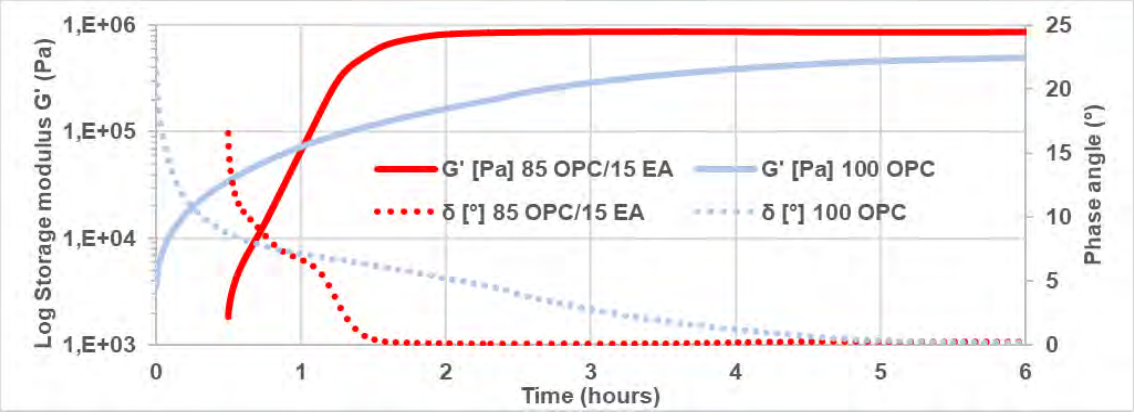

Figure 1: 2 Storage modulus (G': full line) and phase angle (δ: dotted line) evolution over time of 100% OPC (blue) and 85% OPC/15% EA: red) mineral foams (440 kg/m^3 wet)

The addition of EA, thanks to its faster mechanical structure development, gives mineral foam superior short- and long-term mechanical strength compared to 100% OPC foam (Tab 1). No strength development is observed after 2 and 3h with pure OPC mineral foam; for longer durations, the mechanical strength of the EA-based foam is better.

Table 1. Compressive strength measurements (440 kg/m3 wet) - carried out on a RP-50 Syntris (3R) Press on 12x12x11.5 cm cubes according to the DIN EN 826 standard.

, -# ./ $00"1$2P4$ngth T89 : ;						
!"# $	2h	3h	24h	48h	*+	%)+
!""# A%C'	"	"	690	*+"	),"	!"+"
-.# %C' /!.# 0 1	+,"	,""	1040	!+""	1400	1400

An improved mechanical strength is observed regardless of the mineral foam density (Fig. 2). After 24 h, the mechanical strength of the EA-based systems reaches the same performance level as that of the pure OPC system after 7 days. After 7 days, the compressive strength (CS) of the EA-based mineral foam is 1.5 times greater than that of the pure OPC mineral foam (precise correlation for each density tested – $R^2 = 0.99$ – not shown on the graph below).

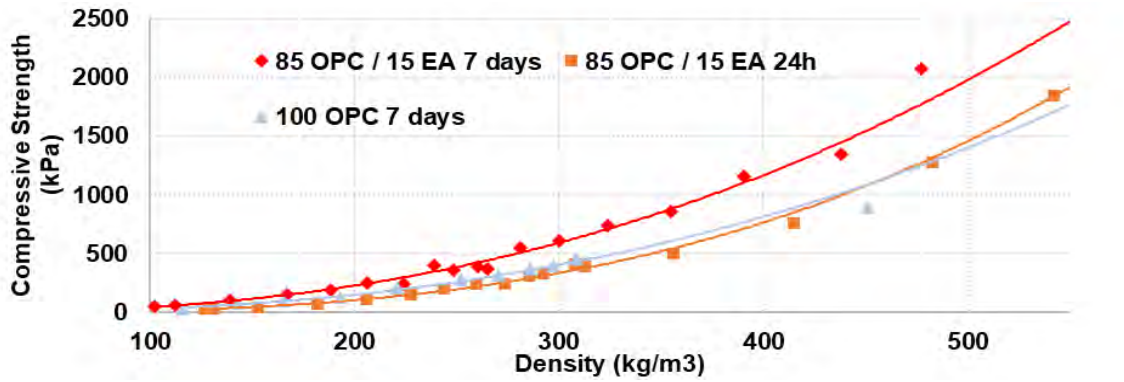

Figure 3: Compressive strength evolution over mineral foam dry density of 100% OPC formulation (light blue ▲) after 7 days, 85% OPC/15% EA formulation after 7 days (red full line ♦) and after 24 h (orange full line ■)

One way to explain these improvements in mechanical strength with the addition of EA is likely due to the early generation of ettringite, as suggested by the temperature evolution of the mineral foams over time (type K thermocouple in a 11.5 × 12 × 12 cm polystyrene cube filled with foam).The 100 OPC exhibits a single temperature peak after 6h (26°C), whereas the 85 OPC/15 EA exhibits two peaks, 1st after 1.5h (48°C), followed by 2nd at 6h (28°C). 1st peak is interpreted as early ettringite formation, 2nd peak mainly C3S hydration. The EA-based mineral foam generates hydrates more rapidly than OPC mineral foam, promotes faster mechanical structuration, and stabilizes the bubble network. A secondary benefit is to accelerate drying. To achieve a residual moisture (measured by carbide bomb method) of 60 kg/m3 (equivalent of 3% for a dense mortar of 2000 kg/m3) it takes 1.5 days for 85 OPC/15 EA versus 11 days for 100

OPC, these times are increased to 7 and 28 days respectively to reach 40 kg/m3 (equivalent to 2%) of residual moisture.

Dimensional variation measurements (Fig 3) show significant shrinkage for 100 OPC, whereas 85 OPC/15 EA exhibit expansion. Final expansion will be moderate, but early expansion on endogenous conditions is very strong reaching 6000µm/m.

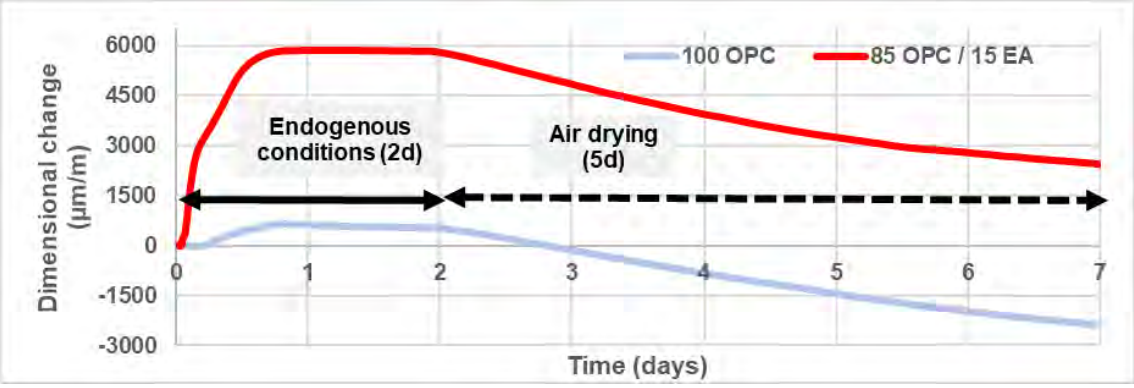

Figure 3: Dimensional change (full line) of mineral foams (440 kg/m3 wet) during 7 days (2 days endogenous, 5 days air drying)

For conventional (high-density) mortars, expansion is mainly due to the crystallization pressure induced by ettringite, but also, to a lesser extent, to thermal expansion. For mineral foams, thermal expansion could have a significant impact on dimensional changes. In this case, the intrinsic mechanical strength is much lower (on the order of kPa) and the material is also very porous (76% air by volume), unlike conventional mortars where this effect can be compensated for by a higher intrinsic mechanical strength (on the order of MPa) and lower porosity. This point will need to be studied in more detail.

CONCLUSIONS

This study demonstrates that amorphous calcium aluminate accelerator EA (LEAP FIT) optimize cementitious foams by enhancing hardening kinetics, mechanical strength, and moisture management. Success probably hinges on balancing heat release from hydration with structuration rates to ensure dimensional stability. These findings gives promising technical solutions for advanced thermal insulation and lightweight structural applications for the future of construction.

REFERENCE

[1] Y. Liu, Z. Zhao, M. Amin, B. Ahmed, K. Khan, S. Arifeen, F. Althoey, Foam concrete for lightweight construction applications: A comprehensive review of the research development and material characteristics, Rev. Adv. Mater. Sci. 63 (2024) 20240022.

[2] S. Berger, D. Tourlakis, S. Perrot, Ettringite accelerator in Portland cement dominated systems: A comparison of different calcium aluminate technologies, in: C.H. Fentiman, R.J. Mangabhai (Eds.), Calcium Aluminates: Proc. Int. Conf., Cambridge, UK, 2022, pp. [147]

International Conference on Calcium Aluminates 2026

FAST AND STABLE: CALCIUM ALUMINATE CEMENTS AS ACCELERATORS IN HIGHLY HEAT-INSULATING MINERAL FOAMS

Laub, Klemens[1], Höchst, Attila[2], GerlicherTobias[2], Tatarin, René[2], Landmann, Mirko[2], Fetter, Robert[2]

[1]Weimar Institute of Applied Construction Research (IAB), Über der Nonnenwiese 1, 99428 Weimar, Germany, k.laub@iab-weimar.de,
[2]Weimar Institute of Applied Construction Research (IAB), Über der Nonnenwiese 1, 99428 Weimar, Germany

Keywords: mineral foam, insulation, acceleration of cement hydration, setting behaviour, rheology, material testing and properties

ABSTRACT

In recent years, the increasing requirements for thermal insulation in building construction and society's growing environmental awareness have led to the increased development of highly thermally insulating, recyclable cement-based mineral foams with low thermal conductivities ($\lambda_{10°C,\,dry} \leq 0{,}035$ W/(m·K)) and low dry densities ($\rho \leq 70$ kg/m³). Their production and application are associated with several challenges. One of the main ones is the stabilization of the pore structure through early and rapid structure formation, which can be solved by using CAC as an accelerator system.

Through extensive research and development work in cooperation with its partners, the IAB investigated different rapid binder systems with different combinations of ordinary Portland cements (OPC) and calcium aluminate cements (CAC). It was found that laboratory tests are already sufficient to estimate and monitor the foam stability and setting behaviour of industrially produced mineral foams. First and foremost, rheometric measurements to characterise the setting behaviour of the binder slurries and the mineral foams should be mentioned here.

The knowledge gained contributes both to resource efficiency in mineral foam production and to the wider application of this technology, which has the potential to sustainably increase the energy efficiency of buildings.

INTRODUCTION | BACKGROUND

The IAB has developed a patented manufacturing process for mineral foam in which two mineral foams are continuously and controllably mixed [1]. While the binder of one mineral foam can be an OPC, the second mineral foam is based on a CAC. By combining the two mineral foams in a targeted manner, the start of the structure formation can also be adjusted during the manufacturing process depending on the building materials to be filled and the ambient conditions. The user of this process is free to select the raw materials independently, but this requires specific expertise and suitable methods.

*email address of corresponding author

Therefore, specific requirements must be defined, above all a processing window for the begin of the setting under real production conditions. Figure 1 shows the overall specifications for the filling of bricks with accelerated mineral foam.

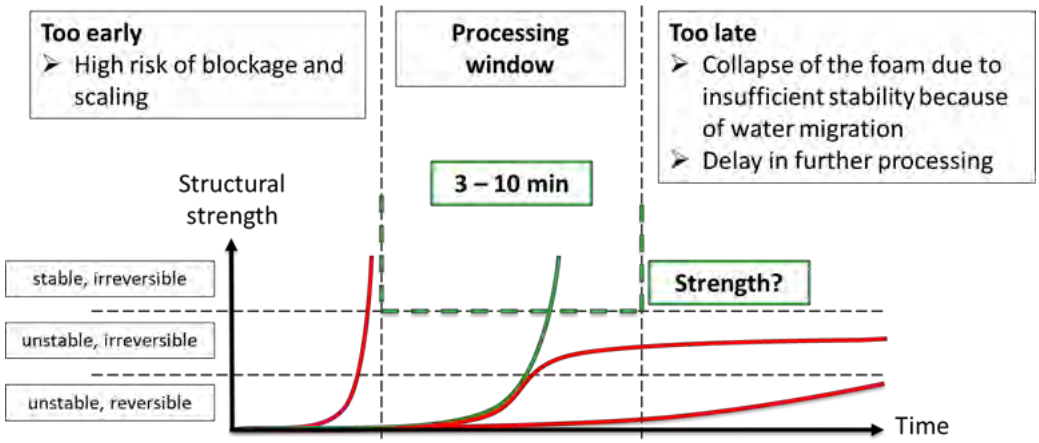

Figure 1. Processing window for accelerated mineral foam for filling bricks

During the industrial production and filling several more challenges must be considered, which are specific to mineral foam. If these challenges, as shown in Table 1, are not taken into account, problems such as the following may arise: Large bubbles, cracks or collapsing.

Table 1. Challenges for mineral foam during industrial production

Water migration/drainage	**In-process handling**	**Coalescence/Ostwald-ripening**
▪ Suction of porous materials ▪ Drainage caused by gravity	▪ Movement ▪ Shocks/bumps ▪ Lifting	▪ Thermodynamically driven spontaneous processes

In order to ensure the high quality of the manufactured products, the raw materials must be tested for usability in advance and during production. The focus here is on the used binders (OPC/CAC).

METHODS

Characterising the setting behaviour is the key. The Viskomat NT was chosen as the preferred method to measure on the slurries of the which the mineral foam is produced. Rheometric measurements using a VANE geometry at very low speeds allowed the increase in torque and shear stress to be observed. This measurement method is hereinafter referred as ‘shear test’ and was chosen due to the following constraints: very high water/solid ratios (1.5 - 2.0) of the slurries, high temporal resolution and sensitivity of the measurements during setting within 15 minutes, temperature insensitivity of the measuring equipment and the possibility of using the determined shear stresses in the physical unit Pascal for modelling. In addition, it is possible to transfer the results of the slurries to those of the mineral foams, which can be characterised rheometric using the same or similar equipment in future.

KEY FINDINGS

To determine whether the shear test is a suitable tool for predicting the setting behaviour of mineral foams, various combinations of OPC and CAC were investigated. The challenges here were, on the one hand, to test at comparable temperatures and, on the other hand, to determine the begin of the setting of the mineral foams. This was done manually and was therefore subjective and inaccurate. To test the practical suitability of the mineral foams produced using a foam generator, several vertically perforated bricks were filled.

One general finding is, that all tested CAC slurries were foamable, which is a essential requirement for the foam generator tests.

In order to examine the various combinations, the same basic recipe consisting of binder, filler, water, foaming agent and hydrophobic agent was used, with only the binders being replaced 1:1 in mass. The ratio OPC/CAC = 3.7 and the temperature of the slurries was between 25 °C and 26 °C, which was in the range of the produced foams. Table 1 shows three examples of combinations of different OPCs and CACs, which were tested with the shear test and the foam generator.

Table 2. Comparison of the shear test and foam generator test of three different combinations of OPC and CAC

Example 1 **OPC1 + CAC1**	**Example 2** **OPC1 + CAC2**	**Example 3** **OPC2 + CAC1**
Shear test		
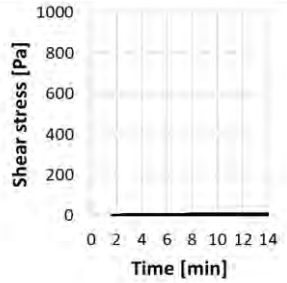	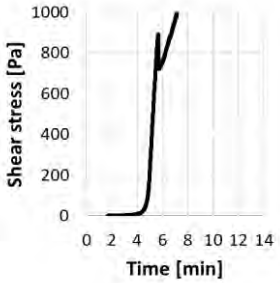	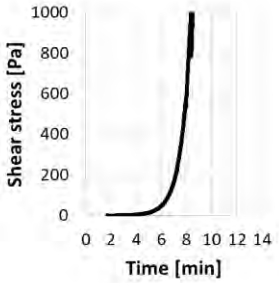
time@10Pa: N/A	time@10Pa: 4.14 min	time@10Pa: 4.72 min
Foam generator test		
		
No begin of setting could be detected. Due to slight collapse of foam, no ρ_{dry} and $\lambda_{10°C,\ dry}$ were tested.	Begin of setting: 6.5 min ρ_{fresh} = 122 kg/m³ ρ_{dry} = 61 kg/m³ $\lambda_{10°C,\ dry}$ = 34.1 mW/(m·K)	Begin of setting: 5.5 min ρ_{fresh} = 115 kg/m³ ρ_{dry} = 52 kg/m³ $\lambda_{10°C,\ dry}$ = 35.1 mW/(m·K)

The results shown here indicate that it is possible to distinguish between setting and non-setting combinations. However, due to the inadequacy of manual testing, it is currently difficult to make accurate predictions based on the shear test regarding the setting behaviour of mineral foam itself. Results are currently available for eight different CACs that were combined with different OPCs, which show, that the shear test is a suitable screening method. The results also show that CACs can work different depending on the used OPCs. The differences consist of whether structure formation takes place at all in the intended processing window, when setting begins and how quickly it progresses. In special cases, a plateau may form, i.e. early setting can be detected, but then the setting process stops, so that no further structure formation takes place. This scenario poses a particular challenge with the testing methods currently available in foam production: Setting can be detected manually, but the structure strength that has been built up and remains is not sufficient to prevent the mineral foam from collapsing as a result of progressive water migration.

FUTURE RESEARCH NEEDS

The construction industry's demand for a higher degree of automation is raising new questions regarding mineral foam application in terms of material optimisation and adaptation, measurement technology options (inline/offline) and process engineering implementation. This extended abstract emphasises that clarification of the differences between the setting behaviour of suspensions (shear test) and the foams produced from them is a pressing issue. Furthermore, measurement methods need to be developed to characterise the setting behaviour of mineral foams. At the same time, the process engineering development of large-scale solutions for the automated production and filling of mineral foam must be carried out.

CONCLUSIONS

Fundamental knowledge was gained about the rapid binder system in terms of methodology, cement chemistry and measurement technology. As part of research projects [2,3], a measuring method was developed that enables the characterisation of the setting behaviour of the rapid binder system in a quick and uncomplicated way. The developed shear test offers a range of further options for analysing rapidly setting binder systems. The patented manufacturing process and mineral foam formulations developed for this purpose based on CAC offer a wide range of applications. First and foremost, among these is the filling of ceramic and cementitious wall building materials. Another area of application is the precast concrete industry.

REFERENCES

[1] EP 3 156 383 B1: Method for producing an inorganic foam., Inventor: Höchst, A., Applicant: IAB - Institute of Applied Construction Research gGmbH, 2017

[2] K. Laub, A. Höchst, Entwicklung von klinker- und CO2-effizienten Schnellbindersystemen zur Herstellung von schnellerhärtenden Mineralschäumen und Anwendung in der Fertigteiltechnologie, Projektabschlussbericht, BMWK-Programm INNO-KOM, Fdg. 49VF210029, IAB Weimar gGmbH, 2024.

[3] K. Laub, A. Höchst, Entwicklung von Qualitätsmessverfahren zur Inline-Bestimmung der Mineralschaumeigenschaften während der Produktion, Projektabschlussbericht, BMWK-Programm INNO-KOM, Fdg. 49MF220234, IAB Weimar gGmbH, 2025.

International Conference on Calcium Aluminates 2026

PERFORMANCE ASSESSMENT OF SPECIALTY CEMENTS FOR MANHOLE CONSTRUCTION IN AUSTRALIAN SEWER INFRASTRUCTURE

Valix, Marjorie, Polczynski, Christopher, and Chunyang Deng

The University of Sydney, Sydney, NSW, 2006, Australia

Keywords: manhole construction, calcium aluminate cement, geopolymer, sewer infrastructure, durability assessment

ABSTRACT

Civil infrastructure assets such as underground pipes, manholes, access chambers, and pumping stations are frequently exposed to aggressive environments including sulphates, chlorides, and biogenic sulphuric acid. Traditional general-purpose (GP) and blended (GB) cements often lack the chemical resistance required, resulting in reduced service life and higher maintenance costs. This study evaluates commercially available specialty binders—calcium aluminate cements (CAC) and geopolymers—as durable alternatives for precast sewer infrastructure, with potential to support lower-carbon construction compared with conventional GP systems. Assessment followed Australian standards AS 4198 and AS 3600, together with WSAA specifications WSA 160 and WSA 161. Durability was evaluated through in-situ exposure across sewer corrosivity environments and complementary accelerated corrosion testing. Casting suitability was assessed using mixes representative of Australian precast supply chains. Results demonstrate that selected specialty binders satisfy both durability and casting requirements across multiple sewer environments, supporting their application in resilient and lower-carbon wastewater infrastructure.

INTRODUCTION | BACKGROUND

Sewer infrastructure is highly susceptible to microbiologically induced corrosion (MIC), driven by sulphur-oxidising bacteria that generate sulphuric acid on concrete surfaces.[1–3] These conditions are particularly severe in manholes and access chambers due to gas-phase exposure and cyclic wetting environments. Conventional GP and GB cement concretes often exhibit limited resistance, leading to premature deterioration and increased lifecycle costs.[3, 4] Recent work has proposed classification of sewer gas-phase corrosivity based on environmental parameters such as H_2S concentration, temperature, and humidity, enabling differentiation of exposure severity and improved linkage between environmental conditions and material durability. Specialty binders such as calcium aluminate cement

*marjorie.valix@sydney.edu.au

(CAC) and geopolymer systems offer enhanced resistance to acidic environments due to stable hydration products and modified microstructures.[5–7] In addition to durability benefits, improved service life may contribute to reduced lifecycle carbon impacts compared with conventional GP systems. This study evaluates specialty binders for manhole construction across sewer corrosivity environments while assessing compatibility with precast manufacturing requirements.

.

METHODS

Standards, Exposure Classification, and Compliance

The evaluation was conducted in accordance with AS 3600 and AS 4198, with sewer durability aligned to WSAA specifications WSA 160 and WSA 161.[8,9] Durability assessment was structured using a sewer gas-phase corrosivity classification framework (Table 1), where environments were categorised based on measured H_2S, CO_2, temperature, and relative humidity—parameters known to drive microbiologically induced corrosion.[1–3] This classification enables comparison of material performance across exposure severities and links durability outcomes to service-life relevance.

Table 1. Sewer gas-phase corrosivity classification (C1–C5 severity levels)

Environmental Conditions				Predicted Depth of Corrosion (mm)		Corrosion Impact	Corrosion Classification
H_2S (ppm)	CO_2 (ppm)	T_g(°C)	RH (%)	10 years of service	100 years of service		
>155	<2500	15-30	95-99	>30	>180	Very High	C5
135-155	2500-4400	15-30	95-99	21-30	166-180	High	C4
70-135	4400-7600	15-30	95-99	14-21	120-166	Medium	C3
15-70	7600-9400	15-30	95-99	6.7-14	55-120	Low	C2
0-15	>9400	15-30	95-99	<6.7	<55	Very Low	C1

Durability Assessment

Durability was evaluated using both field and laboratory methodologies structured around the corrosivity classification. In-situ exposure trials were conducted in operational sewer assets representing multiple severity classes, supported by accelerated acid exposure testing.[2,3] Durability assessment considered chemical stability, microstructural integrity, mechanical performance, and acid resistance.

Corrosion model

To relate durability results to service-life relevance, a semi-empirical corrosion model was applied:

$$t_i = fn(k_{tiG}\ C_{ti}\ F_{tiG}) \qquad (1)$$

where environmental corrosivity (C_{ti}) reflects gas-phase drivers such as H_2S, CO_2, humidity, and temperature, and the material term (F_{ti}) captures

binder chemistry and microstructure. The model was used to interpret durability differences between binder systems across corrosivity classes.

Casting Compliance

Casting suitability was evaluated using precast-representative mixes, focusing on workability, early strength, demoulding, and handling performance.

KEY FINDINGS

Durability Across Corrosivity Classes

Both CAC and geopolymer binders demonstrated improved resistance compared with conventional GP systems (Figures 1 and 2). Performance differentiation increased with corrosivity severity. CAC binders exhibited strong resistance across moderate to high severity environments, attributed to stable alumina-rich hydrates and reduced calcium hydroxide availability.[5], [6] Geopolymer systems showed formulation-dependent behaviour influenced by binder chemistry and microstructural densification[7]. Microstructural stability emerged as a key determinant of corrosion resistance across corrosivity classes. The observed durability trends were consistent with corrosion model predictions, with CAC systems exhibiting longer estimated initiation periods under equivalent exposure conditions.

.

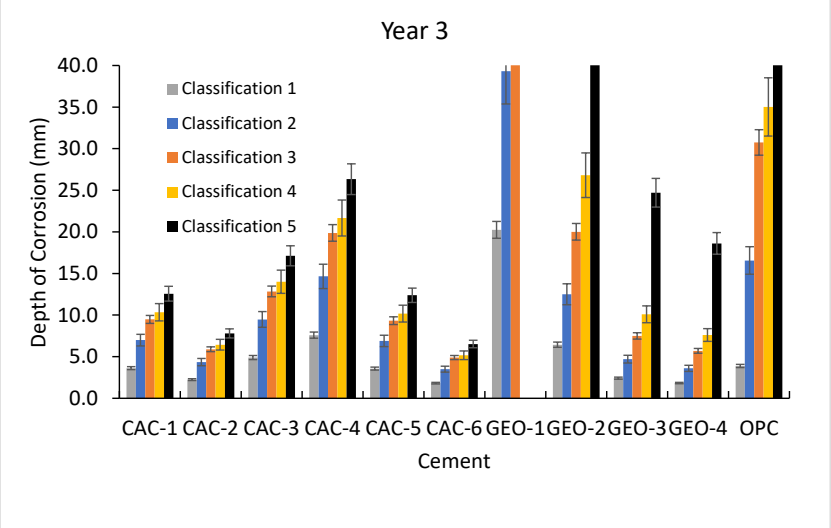

Figure 1. Comparative corrosion depth of CAC, geopolymer, and OPC systems after 3 years across sewer corrosivity classifications

Casting Compliance

Specialty binder mixes demonstrated production characteristics consistent with precast manufacturing requirements, including workability, early strength development, and demoulding behaviour. Observations are reported qualitatively due to confidentiality constraints but indicate compatibility with conventional precast workflows. Representative precast access chambers produced using specialty binders are shown in Figure 2, illustrating compatibility with standard casting and handling practices.

Figure 2. Precast access chambers manufactured using specialty binder concrete during pilot-scale casting trials.

IMPLICATIONS FOR MANHOLE CONSTRUCTION AND CONCLUSIONS

The combined durability and casting results indicate that specific specialty binders met both performance and manufacturability requirements across sewer corrosivity environments. Selected calcium aluminate cement (CAC) and geopolymer systems demonstrated improved resistance compared with GP cement while remaining compatible with precast manufacturing workflows, supporting practical implementation.

REFERENCES

1. Parker, C.D., 1945. The corrosion of concrete: The isolation of a bacterium associated with the corrosion of concrete exposed to atmospheres containing hydrogen sulphide. *Australian Journal of Experimental Biology and Medical Science* 23, 81–90.
2. Davis, J.L., Nica, D., Shields, K., Roberts, D.J., 1998. Analysis of concrete from corroded sewer pipe. *International Biodeterioration & Biodegradation* 42, 75–84.
3. Hudon, E., Mirza, S., Frigon, D., 2011. Biodeterioration of concrete sewer pipes: State of the art and research needs. *Journal of Pipeline Systems Engineering and Practice* 2, 42–52.
4. WSA-201, 2017. *Manual for Selection and Application of Protective Coatings*. Water Services Association of Australia, Melbourne.
5. Scrivener, K., John, V.M., Gartner, E., 2018. Eco-efficient cements: Potential economically viable solutions for a low-CO_2 cement-based materials industry. *Cement and Concrete Research* 114, 2–26.
6. Glasser, F.P., Marchand, J., Samson, E., 2008. Durability of concrete—Degradation phenomena involving detrimental chemical reactions. *Cement and Concrete Research* 38, 226–246.
7. Provis, J.L., Bernal, S.A., 2014. Geopolymers and related alkali-activated materials. *Annual Review of Materials Research* 44, 299–327.
8. WSA 160, 2020. *Sewer Linings Code of Practice*. Water Services Association of Australia.
9. WSA 161, 2021. *Alkali-Activated Materials for Sewer Infrastructure*. Water Services Association of Australia.

International Conference on Calcium Aluminates 2026

UNDERSTANDING BIODETERIORATION MECHANISMS OF A CALCIUM ALUMINATE–BASED COATING AFFECTED BY SUBSTRATE CRACKING

Hoballah, Reem[1,2], Peyre Lavigne, Matthieu[2], Patapy, Cédric[1], Lacarriere, Laurie[1], Toumi, Ahmed[1], Aboulela, Amr[3], Bertron, Alexandra[1]

[1] Université de Toulouse, UPS, INSA, LMDC, 135 Avenue de Rangueil, 31077 Toulouse Cedex 4, France
[2] Université de Toulouse, CNRS, INRA, INSA, TBI, 135 Avenue de Rangueil, 31077 Toulouse Cedex 4, France
[3] Imerys Technology Center, 1 Rue Le Chatelier, Vaulx-Milieu 38090, France

Keywords: wastewater treatment plant, calcium aluminate cement, biodeterioration, durability, cracking.

ABSTRACT

Calcium aluminate cement (CAC)-based coatings have demonstrated superior resistance to microbially-induced concrete deterioration (MICD) in wastewater infrastructures and are widely used to protect Portland cement-based concrete. However, in the penalizing case of cracking within the underlying substrate, cracks might propagate into the coating and act as pathways for aggressive agents. This study investigates the behavior of a thin sprayed CAC-based coating in the presence of cracks to understand the mechanisms that govern the coupling of cracks and biodeterioration.

Representative cracks were generated in coated mortar specimens using a displacement controlled three-point bending test, producing different crack width ranges: 150-200 µm (complying the Eurocode 2 recommendations) and beyond 700 µm. These specimens were exposed to the Biogenic Acid Concrete (BAC) test, which reproduces the aggressive conditions encountered in sewer networks. During the exposure period, the leaching solutions collected from the exposed surfaces were analysed followed by microstructural and chemical analyses of the structure using coupled SEM-EDS analysis.

Results show that the leaching of calcium was not significantly impacted in the presence of cracks. SEM-EDS observations revealed the formation of newly precipitated phases within the crack openings. These phases are suggested as a potential physical barrier, limiting the penetration of aggressive agents and contributing to the crack sealing of the coating in the stated conditions of exposure.

INTRODUCTION | BACKGROUND

Wastewater treatment facilities are constructed mainly using cement-based materials that undergo progressive degradation throughout their service life.

* hoballah@insa-toulouse.fr

Approximately 10% of their concrete deterioration has been attributed to biodeterioration processes arising from coupled biological and chemical activity[1]. This form of degradation is primarily associated with the production of hydrogen sulfide (H_2S) and its subsequent biological oxidation to sulfuric acid (H_2SO_4) by sulfur-oxidizing microorganisms.

Calcium aluminate cements (CAC) have shown superior resistance to microbially-induced concrete deterioration (MICD) in wastewater infrastructures[2,3] and are widely used in coatings to protect Portland cement-based concrete. The key factor in this resistance lies in its chemical and microstructural nature. However, cracks develop in the protected structure and might propagate into the coating, serving as preferential pathways for the ingress of aggressive agents into the underlying concrete[4].

In this context, this paper studies the behavior of a thin CAC-based coating, developed by Imerys, in the presence of cracks to improve the understanding of the mechanisms that govern the coupled effect of cracks and biodeterioration. Using a controlled 3-point bending test, cracks of different crack width ranges were initiated: 150-200 µm and more than 700 µm. These specimens were exposed to BAC test during which the leaching solutions collected from the exposed surfaces were analyzed and coupled microstructural and chemical analyses were performed.

METHODS

Fiber-reinforced mortars were cast into the substrate formulation using CEM III/A 42.5 N-LH cement, suitable for exposure class XA3 according to EN 206, and amorphous metallic fibers in 7 cm x 7 cm x 28 cm molds, with a water-to-cement ratio (w/c) of 0.47. The prisms were submerged in water for 14 days then covered in plastic bags at 20°C for 14 days.

The coating is based on calcium aluminate cement and calcium aluminate synthetic aggregates. It was mixed with 14% by mass water using a portable mixer and then sprayed onto one face of the substrate prisms with a target thickness of 5 mm. The composite specimens were then kept for 7 days in the lab in ambient temperature then cracks were introduced into the substrate-coating composite specimens using a three-point bending test on a servo-hydraulic press under displacement control.

To evaluate the influence of cracking on the coating's protective performance, different surface crack-width ranges were investigated: a crack width between 150 and 200 µm falling below the Eurocode 2 crack-width limit and a crack width exceeding 700 µm.

Biodeterioration was studied using the BAC test, developed at INSA Toulouse[5], which simulates sewer conditions through biofilm inoculation and continuous feeding with a reduced sulfur source ($K_2S_4O_6$). The exposed specimens included uncoated substrates (CEM III) and CAC-coated substrates with different ranges of crack width. Biodeterioration was monitored through analysis of the leached solutions using ICP-OES analyses for the quantification of the cementitious leached cations and acid (H^+) calculations were based on sulfate and sulfite quantification using HPIC. These analyses were followed by SEM-EDS microstructural and chemical characterization after the end of the exposure period.

KEY FINDINGS

The standardized calcium leaching results are presented in Figure 1 in which the results are presented for a CEM III-uncoated substrate, a CAC-coated uncracked substrate and cracked substrates with two ranges of surface crack width: one between 150 and 200 µm and one whose width exceeds 700 µm. The cumulative leached calcium was normalized[6] by its initial content in the material per unit surface area of the exposed surface as a function of the quantity of acid produced on the exposed surface calculated from the quantified sulfite and sulfate.

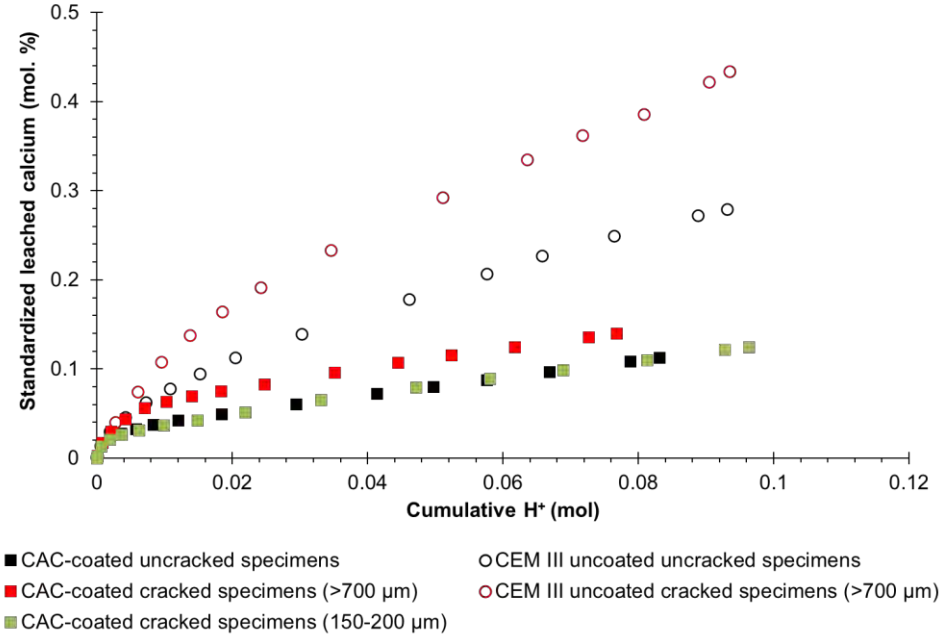

Figure 1. Evolution of the standardized leached calcium as a function of acid production during the 3-month exposure period

The presence of the CAC-based coating on the CEM III-based substrate, reduced calcium leaching by up to three times compared to the uncoated substrate, demonstrating the coating's superior resistance relative to the underlying material. Among the crack-width ranges in the coated specimens, the one between 150 and 200 µm, which complies with Eurocode 2, had no impact on calcium leaching. In contrast, although wider cracks (>700 µm) increased calcium leaching, the coating's performance was not fully compromised as leaching remained substantially lower than in uncoated specimens. Moreover, this range of cracks significantly increased the leaching of calcium in CEM III uncoated cracked specimens.

At the end of the exposure period, SEM-EDS analyses were performed on specimens from different experimental campaigns. In all coated samples, a newly-formed phase was detected near the exposed surface and within the crack openings (Figure 2). While it partially clogs a crack of width between 400 and 600 µm, it appears to completely fill the smaller crack (150-200 µm). Its presence likely contributes to the enhanced performance of the coating even in the presence of cracks. In contrast, this phase was not observed in CEM III-based cracked substrates (>700 µm).

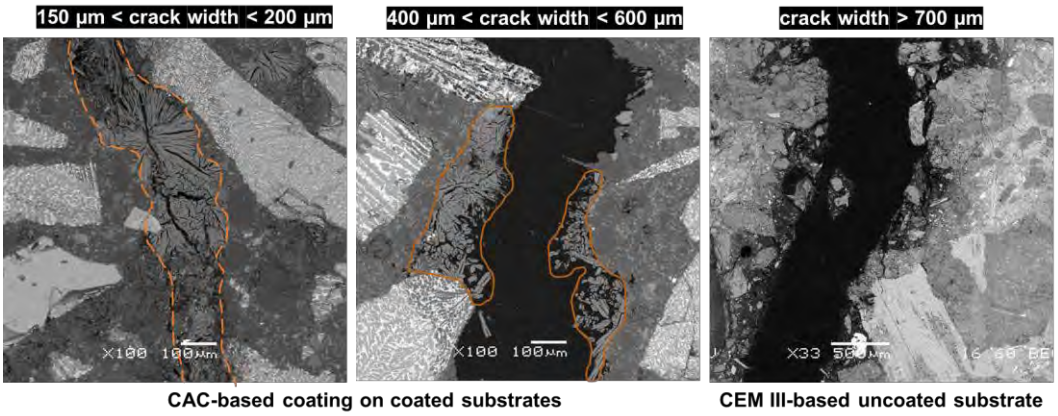

Figure 2. SEM images showing the newly-formed phases (in orange) in the crack opening

CONCLUSIONS

This study investigated the biodeterioration mechanisms of calcium aluminate cement-based (CAC) coatings spray-applied onto CEM III-based substrates under simulated sewer conditions using the BAC test in the presence of cracks. The results demonstrated that the application of this CAC coating significantly reduced calcium leaching compared to uncoated CEM III substrates, confirming its protective performance and the reliability of the BAC test in evaluating biodeterioration of complex coating systems. While cracks compatible with Eurocode 2 limitations (150–200 µm) showed negligible impact on calcium leaching, wider cracks (>700 µm) increased leaching without completely compromising the protective function. SEM-EDS analyses revealed the formation of a phase near the surface and within cracks in the coating, which likely contributes to its superior resistance to biodeterioration. These results suggest the potential of the CAC coating to engage self-healing mechanisms under such aggressive conditions.

REFERENCES

1. Kaempfer, W. & Berndt, M. Estimation of Service Life of Concrete Pipes in Sewer Networks Concrete Pipes in Sewer Networks. in (1999).
2. Herisson, J., van Hullebusch, E. D., Moletta-Denat, M., Taquet, P. & Chaussadent, T. Toward an accelerated biodeterioration test to understand the behavior of Portland and calcium aluminate cementitious materials in sewer networks. *International Biodeterioration & Biodegradation* **84**, 236–243 (2013).
3. Alexander, M. G. & Fourie, C. Performance of sewer pipe concrete mixtures with portland and calcium aluminate cements subject to mineral and biogenic acid attack. *Mater Struct* **44**, 313–330 (2011).
4. Grengg, C. *et al.* Advances in concrete materials for sewer systems affected by microbial induced concrete corrosion: A review. *Water Research* **134**, 341–352 (2018).
5. Aboulela, A. *et al.* Laboratory Test to Evaluate the Resistance of Cementitious Materials to Biodeterioration in Sewer Network Conditions. *Materials* **14**, 686 (2021).
6. Aboulela, A., Peyre-Lavigne, M., Patapy, C. & Bertron, A. Evaluation of the resistance of CAC and BFSC mortars to biodegradation: laboratory test approach. *MATEC Web Conf.* **199**, 02004 (2018).

International Conference on Calcium Aluminates 2026

A FRAMEWORK FOR CLASSIFYING SEWER GAS-PHASE CORROSIVITY BASED ON MATERIAL RESPONSE

Valix, Marjorie[1], Polczynski, Christopher[1], In, Ye Jun[1], Cherdphong Seedao[1], Gardner, James[2]

1. The University of Sydney, Sydney, NSW, 2006, Australia
2. The Water Services Association of Australia, Melbourne, Victoria, 3008, Australia

Keywords: corrosivity, sewer infrastructure, concrete durability, protective coatings and material degradation

ABSTRACT

Concrete and protective materials deteriorate under biologically induced corrosive conditions commonly found in sewer systems. Understanding corrosivity—the severity of corrosion in a given environment—is essential for selecting materials, designing mitigation strategies, and estimating service life and lifecycle costs. This study examines corrosion of concrete sewer infrastructure, including large-diameter pipes, access chambers, and wet wells, where degradation is driven by microbial generation of sulphuric acid under specific environmental conditions. A quantitative classification of sewer gas-phase corrosivity was developed using field data from ordinary Portland cement (OPC) assets in service for 17–81 years across Australian utilities. Corrosivity was correlated with environmental parameters including H_2S, CO_2, temperature, and relative humidity, which served as surrogate indicators. To validate the framework, commercially available materials, including calcium aluminate and geopolymer cement-based systems, were deployed in sewers representing different corrosivity classes. Comparative observations demonstrated clear differences in material performance across exposure severities, confirming the framework's practical relevance. The proposed classification enables improved alignment between environmental exposure and material selection, supporting enhanced durability, optimised lifecycle costs, and more resilient wastewater infrastructure.

INTRODUCTION | BACKGROUND

Concrete and protective materials in sewer environments are vulnerable to biologically induced corrosion driven by microbial sulphuric acid formation under aggressive gas-phase conditions.[1–3] Corrosion severity varies widely depending on environmental exposure and directly influences durability, service life, and lifecycle cost. Despite this variability, sewer environments are often classified generically as "severe," limiting differentiation of

*marjorie.valix@sydney.edu.au

exposure conditions and optimisation of mitigation strategies.[4,5] Corrosivity, defined as the severity of corrosion under a given environment, is a key parameter for material selection and asset management. However, quantitative frameworks linking environmental parameters to field corrosion outcomes remain limited. This study presents a field-based classification of sewer gas-phase corrosivity developed under the CRC-P Smart Lining program. The framework links measurable environmental parameters to long-term corrosion observations and provides a practical basis for durability-informed decision-making in wastewater infrastructure.

.

METHODS

Field Assets and Environmental Monitoring

The classification was developed from field investigations of ordinary Portland cement (OPC) sewer assets in service for 22–81 years across Australian utilities. Assets representing a wide range of deterioration levels were selected to capture diverse corrosive environments. Environmental monitoring followed WSAA protocols[6] and included hydrogen sulphide (H_2S), carbon dioxide (CO_2), gas temperature, and relative humidity—key drivers of biogenic corrosion.[3,7]

Corrosion Assessment and Normalisation

Cores extracted from representative locations were analysed for depth of corrosion. A semi-empirical dose–response approach was used to normalise corrosion rates and enable comparison across assets with different exposure histories.

Validation Using Protective Materials

To validate the framework, commercially available protective mortars—including calcium aluminate cement (CAC) and geopolymer systems—were installed in live sewer environments spanning a range of corrosivity levels. Periodic inspection and coring over up to three years were used to evaluate relative material degradation.

CLASSIFICATION OF SEWER GAS-PHASE CORROSIVITY

Biogenic corrosion results from interactions between microbial communities, environmental conditions, and cement chemistry.[3] Field observations identified H_2S concentration, moisture availability, temperature, and gas-phase chemistry as dominant drivers of corrosion progression.[7] Using normalised corrosion data and environmental measurements, sewer gas-phase conditions were categorised into five corrosivity classes (C1–C5), representing increasing severity from very low to very high corrosion potential (Table 1). The classification was anchored to observed corrosion depths in OPC assets and corresponding environmental ranges, enabling differentiation of sewer environments using measurable exposure parameters rather than generic severity assumptions. Field observations also suggest that extremely high H_2S conditions may not always correspond to proportionally higher corrosion rates, highlighting the

importance of multi-parameter classification. The framework is therefore adaptive and can be refined as additional field data become available.

Table 1. Proposed classification of sewer gas-phase corrosivity (C1–C5) based on field-normalised OPC corrosion data

Environmental Conditions				Predicted Depth of Corrosion (mm)		Corrosion Impact	Corrosion Classification
H_2S (ppm)	CO_2 (ppm)	T_g(°C)	RH (%)	10 years of service	100 years of service		
>155	<2500	15-30	95-99	>30	>180	Very High	C5
135-155	2500-4400	15-30	95-99	21-30	166-180	High	C4
70-135	4400-7600	15-30	95-99	14-21	120-166	Medium	C3
15-70	7600-9400	15-30	95-99	6.7-14	55-120	Low	C2
0-15	>9400	15-30	95-99	<6.7	<55	Very Low	C1

VALIDATION AND IMPLICATIONS

Exposure trials using CAC and geopolymer mortars demonstrated degradation trends consistent with the proposed classification (Figures 1 and 2). Materials installed in higher corrosivity classes exhibited greater corrosion depths compared with those in lower classes, confirming that the framework captures meaningful differences in environmental severity.

While CAC systems generally showed lower degradation than geopolymer mortars, the objective was not comparative material ranking but validation of classification sensitivity. The results demonstrate that environmental classification can be used to predict relative material performance and guide targeted deployment of protective systems.

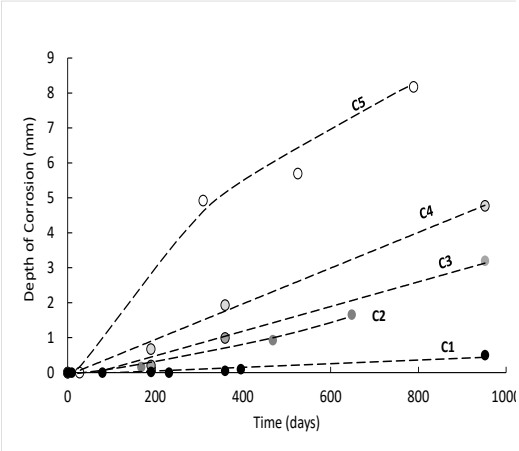

Figure 1. Corrosion depth of calcium aluminate mortars across sewer environments classified as C1–C5

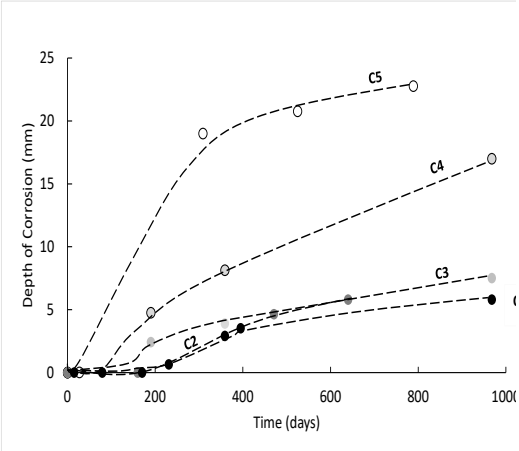

Figure 2. Corrosion depth of geopolymer mortars across sewer environments classified as C1–C5

IMPLICATIONS FOR ASSET MANAGEMENT

The proposed classification provides a practical tool for aligning material selection and rehabilitation strategies with environmental exposure conditions. By linking measurable environmental parameters to corrosion outcomes, the framework supports improved asset prioritisation, risk-based maintenance planning, and optimisation of lifecycle costs. The classification also enables more informed selection of corrosion-resistant materials and protective linings, contributing to improved durability and resilience of wastewater infrastructure. Given its field-based foundation, the framework is readily transferable across sewer networks and can be refined through continued monitoring and integration of long-term corrosion datasets.

CONCLUSIONS

A quantitative classification framework for sewer gas-phase corrosivity was developed based on long-term field observations of OPC sewer assets. Corrosivity was shown to correlate with measurable environmental parameters including H_2S, CO_2, temperature, and relative humidity, enabling classification into five exposure categories (C1–C5). Validation using CAC and geopolymer mortars demonstrated degradation trends consistent with the proposed framework, confirming its practical relevance. The classification provides a robust basis for linking environmental exposure to material performance and supports improved durability planning for wastewater infrastructure. Future refinement is expected through integration of additional long-term monitoring data and broader material validation.

REFERENCES

1. Parker, C.D., 1945. The corrosion of concrete: The isolation of a bacterium associated with the corrosion of concrete exposed to atmospheres containing hydrogen sulphide. *Australian Journal of Experimental Biology and Medical Science* 23, 81–90.
2. Davis, J.L., Nica, D., Shields, K., Roberts, D.J., 1998. Analysis of concrete from corroded sewer pipe. *International Biodeterioration & Biodegradation* 42, 75–84.
3. Hudon, E., Mirza, S., Frigon, D., 2011. Biodeterioration of concrete sewer pipes: State of the art and research needs. *Journal of Pipeline Systems Engineering and Practice* 2, 42–52.
4. Knotková, D., 2007. Corrosivity of atmospheres – derivation and use of information. In: Moncmanová, A. (Ed.), *Environmental Deterioration of Materials*. WIT Press, Southampton, pp. 73–102.
5. WSA-201, 2017. *Manual for Selection and Application of Protective Coatings*. Water Services Association of Australia, Melbourne.
6. Valix, M., 2021b. *Environmental Monitoring*. Water Services Association of Australia, Melbourne.
7. Joseph, A.P., Keller, J., Bustamante, H., Bond, P.L., 2012. Surface neutralization and H_2S oxidation at early stages of sewer corrosion: Influence of temperature, relative humidity and H_2S concentration. *Water Research* 46, 4235–4245.

International Conference on Calcium Aluminates 2026

Sustainable Calcium Aluminate Cement Formulations: Partial Clinker Replacement with Activated Chemicals

Polat, Buket[1*] , Wolf, Julian[2,] Avcioğlu, Berrak[2] ; [1] ÇİMSA ÇİMENTO SANAYİ VE TİCARET A.Ş, TOROSLAR MAH. TEKKE CAD. YENİTAŞKENT – AKDENİZ, Mersin, 33013, TÜRKIYE[2]Sabanci Technology Center GmbH, Freisinger Landstraße 50, Garching bei München, 85748, Germany *b.polat@cimsa.com.tr

Reducing the clinker content in calcium aluminate cement (CAC) is crucial for improving environmental sustainability. This study investigates the partial replacement of CAC clinker with activated pumice to optimize setting time and mechanical strength. Experiments were conducted by gradually decreasing the clinker content and replacing it with varying proportions of activated pumice. The hydration kinetics, setting behavior, compressive strength, and microstructural evolution were analyzed.

Results show that, despite a significant reduction in clinker content, early and long-term strength values were maintained when using properly activated pumice. Additionally, the setting time was found to depend on the surface activity and chemical composition of the pumice.

This study demonstrates that clinker substitution in CAC-based systems is feasible, and mechanical performance can be preserved using activated pumice as a supplementary material. The findings provide a foundation for developing low-carbon cement formulations. Future research should explore the effects of different activators and curing conditions.[1]

INTRODUCTION | BACKGROUND

The cement industry significantly contributes to global CO_2 emissions due to energy-intensive clinker production. While sustainability efforts have primarily focused on Portland cement, strategies for reducing the environmental impact of calcium aluminate cement (CAC) remain limited. CAC is widely used in refractory applications, rapid repair systems, and chemically resistant environments because of its rapid strength development and high-temperature performance.[1] However, its clinker production requires alumina-rich raw materials and elevated burning temperatures, resulting in considerable environmental impact.

Natural pumice (tras) represents a promising supplementary material due to its high silica content and porous structure, although its reactivity is generally limited without activation. Mechanical activation through fine

grinding enhances surface area and exposes reactive silica phases, increasing its potential contribution to hydration reactions.[2]

Methods

Commercial CAC and mechanically activated pumice were used. Chemical compositions were determined by XRF (Table 1). The Blaine fineness of CAC was 3350 cm²/g, while activated pumice reached 9070 cm²/g after 20 minutes of ball milling. Mortars (4×4×16 cm) were prepared with 5% and 10% clinker replacement at constant water content (28%) and cured at 20°C and 96% RH.

Table 1.Chemical composition of CAC and activated pumice (% by mass)

Oxides	***CAC 40***	***Activated Pumice***
Al_2O_3	40.6	12.53
SiO_2	3.72	64.96
CaO	36.38	5.5
Fe_2O_3	15.82	2.64
MgO	0.5	1.2

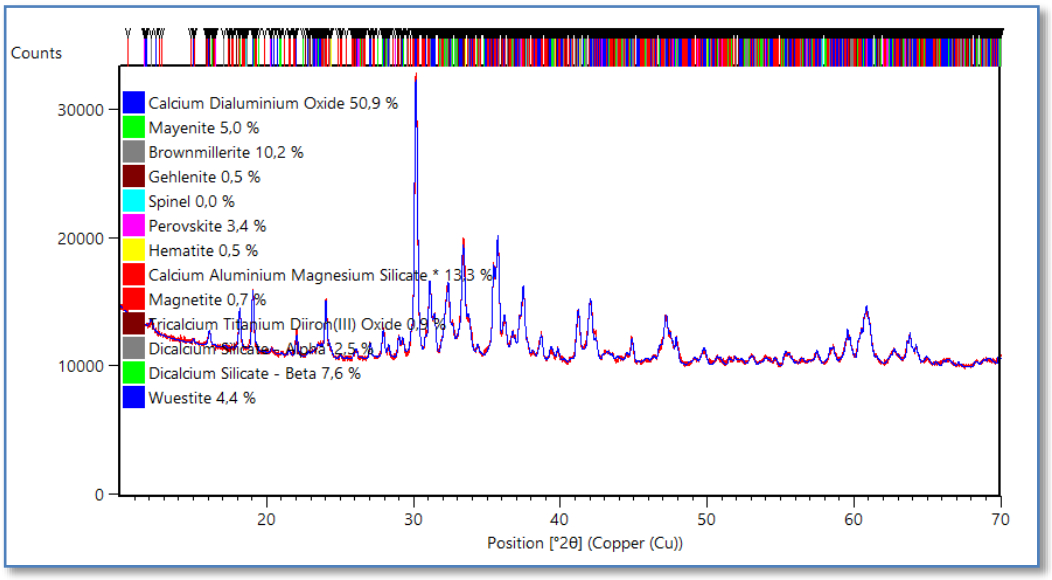

Figure 1. XRD pattern of the CAC clinker

Mechanical Activation

The pumice was mechanically activated using a ball mill for 20 minutes. The activation process aimed to increase the specific surface area. After grinding, particle size distribution analysis indicated a D45 value of 18.85 µm.

Mixture Design

Partial replacement of CAC with activated pumice was performed at different substitution levels. The reference mixture contained 100% CAC,

while other mixtures included 5%, 10%replacement of CAC by activated pumice.

Table 2. Mix proportions and replacement levels

Mix ID	***CAC (%)***	***Activated Pumice (%)***
Reference	100	0
P5	95	5
P10	90	10

* The water content was kept constant at 28%.

Test Methods

Setting time was determined according to the Vicat method. Mechanical and physical tests are done accordingly EN 197-1 to check standard cement sample performance.

Compressive strength tests were performed at 6 hours and 24 hours using a universal testing machine. The performance of pumice-substituted cement was evaluated in self-levelling mortar formulations.

CONCLUSIONS

The setting time and compressive strength results of the reference and pumice-substituted mixtures are summarized in Table 3. The reference CAC mixture exhibited initial and final setting times of 260 and 285 minutes, respectively. In contrast, mixtures incorporating mechanically activated pumice showed a significant acceleration in setting behaviour. The P5 mixture (5% pumice replacement) reached setting times of 150/230 minutes, while the P10 mixture (10% replacement) demonstrated even shorter values of 145/175 minutes. This marked reduction in setting time suggests that finely ground pumice particles enhance early hydration kinetics, likely by increasing nucleation sites and accelerating dissolution processes in alumina-rich systems. Compressive strength results further highlight the beneficial effect of pumice substitution, particularly at early ages. At 6 hours, the reference mixture achieved a strength of 35 MPa, whereas the P5 and P10 mixtures reached 48.8 MPa and 47 MPa, respectively, corresponding to approximately 39% and 34% improvement compared to the reference system. This significant enhancement demonstrates that mechanically activated pumice does not behave merely as an inert filler but actively participates in hydration reactions contributing to early microstructural development.

Table 3. Setting time and compressive strength results of reference and pumice-substituted CAC mixtures

At 24 hours, the reference mixture reached 70 MPa, while the P5 and P10 mixtures achieved 67 MPa and 61 MPa, respectively. Although a moderate reduction in 24-hour strength is observed with increasing pumice content, the values remain within a high-performance range suitable for practical applications.

Mix ID	***Pumice Replacement (%)***	***Setting Time (min.)***	***6h Compressive Strength (MPa)***	***24h Compressive Strength (MPa)***
REF	0	260/285	35	70
P5	5	150/230	48.8	67
P10	10	145/175	47	61

Table 4. Effect of partial clinker replacement on setting behavior and early-age strength of CAC-based self-levelling underlayment (SLU) formulations

Mix ID	***Setting time(min.)***	***3h Compressive Strength (MPa)***	***6h Compressive Strength (MPa)***
REF.	40/50	11.2	16.2
P5	30/50	10.6	16
P10	35/50	11.5	15

The performance of pumice-substituted cement was additionally evaluated in self-levelling mortar formulations. The incorporation of activated pumice allowed a reduction in CAC content within the application recipe while maintaining high early strength and appropriate setting behaviour. Consequently, clinker consumption in the final formulation was reduced, leading to a more sustainable binder design with lower embodied carbon. These findings demonstrate that clinker reduction in CAC systems can be successfully implemented not only at laboratory paste level but also in practical self-levelling applications.

REFERENCES

[1] Bentsen, S. Effect of microsilica on conversion of high alumina cement. In Calcium Aluminate Cements; Chapman and Hall: London, UK, 1990; p. 294.

[2] 22. Parker, K.M. Refractory calcium aluminate cements. Trans. Br. Ceram. Soc. 1982,82, 35–42

International Conference on Calcium Aluminates 2026

BEYOND POZZOLANICITY: METAKAOLIN IS KEY TO THE SURFACE ASPECT OF SUSTAINABLE FLOORING MORTARS BASED ON TERNARY BINDERS

Franceschini*, Alexandre, Imerys, Vaulx-Milieu, France; Wu, Hailong, Imerys, Tianjin City,China; Chen, HongFang, Imerys, Singapore; Taquet, Pascal Imerys, Vaulx-Milieu, France

Keywords: Fooptint, Metakaolin, Surface, Self-Levelling, LEAP

ABSTRACT

Specialty binders for premium drymix products commonly consist of a “ternary” blend of calcium aluminate, calcium sulfate and Portland cement. Target performance for each application is achieved by carefully tuning the relative proportions of these constituents together as well as the type & dosage of several set regulators. Simple substitution of CEM I by a blended Portland cement to lower carbon footprint therefore perturbs this balance and can be counterproductive — altering paste rheology, surface appearance and early strength that are critical for drymix formulations — unless the mix design is re-optimized.

Because the clinker content of the overall drymix largely governs its carbon footprint, we present several low-clinker mix designs that preserve or improve key functional properties while reducing footprint by 35%–40% relative to reference formulations.

We further investigate the effect of metakaolin (MK) on these mix-designs, beyond its pozzolanic contribution, and demonstrate a direct beneficial effect of MK on surface quality and abrasion resistance of self-leveling compounds formulated with these designs. Microstructural and phase analyses combined with rheological characterization elucidate the role of MK and its influence on early-age properties, workability and strength development. The results indicate viable pathways to substantially lower clinker content in premium drymix products, while improving the set of performance of the ternary binders.

INTRODUCTION | BACKGROUND

Metakaolin is successfully used to decrease the carbon footprint of concrete, and mortars, especially tile adhesive, thanks to the pozzolanic reaction[1] [REF]. Unfortunately, this reaction between MK & Portlandite is not adapted to decrease the carbon footprint of specialty binders used in drymix. These binders are blends of mainly Portland cement, Ettringite precursor (eg. CAC & Calcium Sulfate), and setting regulators (eg. Tartaric acid, Sodium carbonate, Lithium Sulfate…). In these binders, upon hydration, once Ettringite has massively precipitated in the early age, Portlandite and even water are sufficiently depleted to significantly

*alexandre.franceschini@imerys.com

hinder the pozzolanic reaction. Here, we show that a better strategy to decrease the carbon footprint, is (i) to use the right Ettringite precursor, with the least impact on Portland hydration and (ii) Substitute a high proportion of Portland Cement by limestone filler, as much less Portland Clinker will be needed to reach the desired strength target. Using this strategy, we decreased the carbon footprint of a specialty binder by 40%.

Then, we design two Self Levelling Compounds, one based on this low carbon binder and one based on a CAC-Rich formulation. We show that in both cases, Metakaolin brings an added value with regards to surface aspect & abrasion resistance, which are important benefits for such application.

MATERIALS & METHODS

LEAP® Fit (LF): Ettringite precursor with d50=7µm, 50% ultra-reactive, amorphous calcium aluminate (molar ratio CaO/Al_2O_3 = 1.8) & 50% calcium sulfate anhydrite. TERNAL® FONDU (CAC) is a well known fused calcium aluminate binder, with Calcium Monoaluminate as its major phase and Mayenite as a minor phase. We note CAC+C$ the Ettringite precursor composed of 66% of CAC and 33% of natural Calcium Sulfate Anhydrite (C$). TERNAL® White (TW) is a high-alumina sintered calcium aluminate, manufactured with Calcium Monoaluminate as major phase and Dicalcium Aluminate as minor phase. We note TW+C$ the Ettringite precursor made with 73% of TW and 26% of Natural Anhydrite. The grey Portland Cement used here is CEM II/A-LL, 52.R from Holcim and the white Portland is a CEM I 52.5N from Dyckerhof. Argical M1000 (MK) is a metakaolin with a Chapelle value of 1100 mg/g, a R3 Value of 900 J/g, and with d50=6µm.

Self-Leveling Compound (SLC): it is a fluid, cementitious product used to level out shallow dips and humps in a floor. Most of the time, these formulations are used as an underlayment, prior to installing a finished floor covering (e.g. PVC or tile). SLC with the highest performances can be used as an overlayment and remain visible. SLCs are covered by the norm EN 13813 and local reference documents, e.g. CSTB QB11-2 in France. The measures done in this article are compliant with the above documents, with the mechanical strength measured on 2x2x16 cms samples, covered for 24h in the mold, then cured in air at 23°C, 50%RH for the remaining 27d.

KEY FINDINGS

We work on a model drymix in order to optimize the carbon footprint of formulation with respect to mechanical strength (Fig1 left.) Portland Cement is the main component of the binder. Keeping the setting regulators constant, we decreased the amount of Portland from 20% down to 10% (by weight of formulation). In all cases, we used 5% of ettringite precursors, either CAC+C$ or LF. The target compression strength for such model formulation is 5MPa at 4h and 30MPa at 28d (Fig1 right). On one hand, 5% of the tested Ettringite precursors is enough to pass the 4h strength threshold. On the other hand, we see that contrary to LF, CAC+C$ has a detrimental effect on the 28d strength.

	CEM	LEAP	CAC	Eco
CEM II/A-LL 52.5 R	25	20	20	10
Filler $CaCO_3$				10
LEAP® Fit		5		5
CAC + C$			5	
Set Regulators		0.2	0.2	0.2
AFNOR Sand	75	75	75	75
% water	12.5%	12.5%	12.5%	12.5%

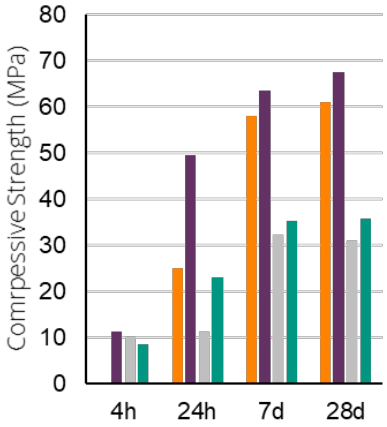

Figure 1: Compositions of model drymix. The set regulators are 0.1% Sodium carbonate, 0.05% tartaric acid, and 0.05% Lithium Sulfate. The three formulations on the left have a carbon footprint close to 180kgCO_2/T, while the one on the right has a footprint of 100kgCO_2/T. Mechanical strength is measured on 2x2x16 samples, covered for 24h and then cured at 23°C, 50%RH.

This is consistent with the poor C_3S hydration (40% at 28d, down from 70-90% otherwise) observed specifically when CAC+C$ is used. As a consequence, when LF is used, it is possible to reach 30MPa at 28d with half the Portland Cement needed when CAC+C$ is used.This drastically reduces the amount of clinker in the formulation, and the carbon footprint of the formulation drops to 100kgCO_2/T, down from 180kgCO_2/T.

All subsequent trials to further decrease the carbon footprint while maintaining the mechanical performance, by adding MK or by using a Portland with less clinker (eg. CEM IIB, CEM IIIB…), have all been unsuccessful due to one or more of the following reason: (i) there is not enough Portlandite, (ii) there is not enough water remaining as samples are cured in air, (iii) further reduction of clinker creates a lack of calcium at early age, which is detrimental to the 4h strength threshold.

We used this study to design a SLCs with a low carbon footprint, with and without 5% of MK. The formulations obtained are consistent with what is expected in terms of flowability (150mm flow spread for more than 20min) and setting time (60min). These formulations reach 30MPa at 28d. The carbon footprint of this binder is around 165kgCO_2/T, down from 240kgCO_2/T of most SLCs binders within this class of performance (Fig.2). The effect of MK is also evaluated on premium SLC based on TW.

For both formulation logic In order to keep the same fluidity, the use of metakaolin implies a small reformulation - 0.04% decrease in cellulose ether and a 0.04% increase in PCE. In both cases, as discussed above, the pozzolanic reaction is not significant enough for MK to play a role with regard to the mechanical strength. Nonetheless, it generates a strong improvement of the surface aspect, observable with a binocular microscope. In the cas of the SLC with TW, it also improves the Taber abrasion by 15%, and yields a much smoother surface (Fig 3). This confirms what was seen elsewhere on other formulation logic[2].

	LEAP	L+MK	TW	T+MK
CEM II/A-LL 52.5R	17	17		
White OPC			3.6	3.6
LEAP® Fit	7	7		
TW + C$			24.8	24.8
MK		5		5
Additives	2.3	2.3	2.3	2.3
Set Regulators	0.37	0.37	0.18	0.18
Sand <600µm	45	45	45	45
Filler $CaCO_3$	30	25	24	19
% water	24%	24%	24%	24%

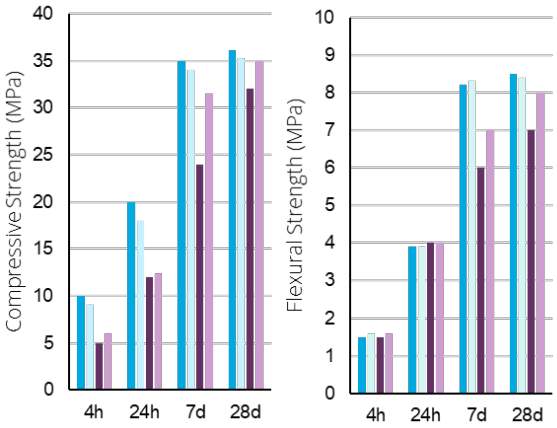

Figure 2: Compositions of SLCs. The set regulators for LEAP & L+MK formulations are 0.12% Sodium carbonate, 0.08% tartaric acid, 0.12 citric acid, and 0.05% Lithium Sulfate. The set regulators for TW & T+MK formulations are 0.15% tartaric acid, and 0.03% Lithium Sulfate.The mechanical strength is measured on 2x2x16 samples, covered for 24h and then cured at 23°C, 50%RH.

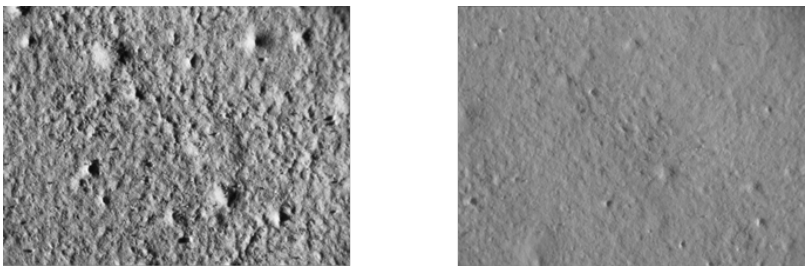

Figure 3: Surface aspect with binocular microscope of the surface of TW (left) and T+MK (right) at 28d.

CONCLUSION

For rapid specialty binders with a strength requirement at 4h, the pozzolanicity of MK does not help with regard to carbon footprint or clinker reduction. A much more efficient carbon footprint reduction is achieved by using LF as an Ettringite precursor, and reducing the Portland cement amount. Nonetheless, we show here that MK plays a direct role in improving the surface aspect & abrasion resistance of flooring compounds. This improvement is a key progress for SLC dedicated to serve as overlayments, as the abrasion resistance is an important criteria to pass

REFERENCES

[1] Benevenuti, B., Fryda, H., Perrot, S., Tichit, E. (2025). Improving the Early Age Strengths of LC3 Using a Mineral Accelerator System Based in Calcium Aluminates. In: Scrivener, K., Sharma, M., Zunino, F. (eds) Calcined Clays for Sustainable Concrete . ICCCSC 2022. RILEM Bookseries, vol 57. Springer, Cham.

[2] A. Franceschini, H. Chen, H. Wu, P. Taquet.Pozzolanicity & beyond: Performance of Metakaolin in Drymix in: Drymix Info Yearbook 2025

International Conference on Calcium Aluminates 2026

CALCIUM ALUMINATE CEMENTS IN CONTEXT: DURABILITY MECHANISMS AND TRANSPORT-CONTROLLED PERFORMANCE FOR CONVENTIONAL CONCRETE APPLICATIONS

Kurtis*, Kimberly E., Georgia Institute of Technology, Atlanta, Georgia USA
Alapati, Prasanth, Furno Materials, South San Francisco, California, USA
Burris, Lisa, The Ohio State University, Columbus, Ohio, USA
Ley, M.Tyler, Oklahoma State University, Stillwater, Oklahoma, USA
Peery, J., Oklahoma Dept. of Transportation,Oklahoma City, Oklahoma, USA
Hajibabaee, Amir, Ozinga, Chicago, Illinois, USA
Behravan, Amir, Virginia Dept of Transportation, Richmond, Virginia, USA
Khanzadeh Moradllo, Mehdi, Temple University, Philadelphia, Pennsylvania, USA
Berke, N., Tourney Consulting Group, Kalamazoo, Michigan, USA
Moser, Robert, U.S. Army Engineer Research and Development Center (ERDC), Vicksburg, Mississippi, USA

Keywords: durability, alkali-silica reaction, corrosion, carbonation, CAC, CAC blends

ABSTRACT
Calcium aluminate cements (CACs) are often treated as specialty binders, but recent work suggests their performance merits broader consideration. Here, the performance of CAC and CAC blends is evaluated in the context of other alternative cementitious materials (ACMs) - including calcium sulfoaluminate (CSA) cements, alkali-activated binders, magnesium phosphate cements, and blended systems - and benchmarked against ordinary portland cement (OPC). The work emphasizes durability-critical behaviors relevant to transportation and other infrastructure applications, including resistance to chemical sulfate attack, alkali–silica reaction (ASR), and transport-controlled deterioration. Microstructural characterization is used to interpret observed durability trends and to clarify the roles of hydration and conversion products, pore solution composition, and pore connectivity. While CACs are well known for rapid strength development and sulfate resistance, results drawn from a broader experimental dataset demonstrate that well-designed CAC systems can also exhibit favorable resistance to ASR expansion and chloride ion penetration relative to OPC. At the same time, the findings reinforce that no single binder system is universally optimal. Instead, this study identifies application contexts in which CACs and other ACMs may offer meaningful durability advantages in conventional concrete construction.

*kkurtis@gatech.edu

INTRODUCTION

Growing interest in alternative cementitious materials is driven by both sustainability objectives and the need for improved durability in aggressive service environments. Calcium aluminate cements occupy a unique position within this landscape: they are commercially mature, well understood in specialty applications, yet rarely considered for conventional reinforced concrete construction.

A recently published US Federal Highway Administration report[1] evaluated and compared the performance of CACs and other ACMs to PC, examining mechanical behavior, dimensional stability and durability. This extended abstract presents previously unpublished long-term durability data, together with transport-based and microstructural interpretations that enable more confident differentiation of CAC, CAC blend, and other ACM performance relative to OPC**.** The focus here is durability-relevant findings most pertinent to infrastructure applications, including sulfate resistance, ASR mitigation, and transport-controlled deterioration mechanisms.

METHODS

Tested systems included an ASTM C150 Type I/II OPC, and multiple compositions of CAC, CSA, and magnesium phosphate cements, and alkali-activated binders. Cement compositions and concrete mixture designs have been previously reported[1-2]. Durability-focused testing included:

- Chemical sulfate resistance, using standard testing (ASTM C1012), and constant-pH sulfate exposure coupled with strength retention and microstructural analysis;
- ASR assessment, incorporating both accelerated tests (ASTM C1260) and long-term concrete prism tests (ASTM C1293) extending to two years;
- Transport characterization, including formation factor (*F*), sorptivity, and resistivity-based indicators of pore connectivity, as well as direct measures of chloride migration;
- Microstructural analysis, including OM, SEM, and TGA used to interpret hydration products, bound water evolution, and phase stability.

Mixture designs emphasized compatibility with conventional batching and placement practices, allowing durability trends to be interpreted in a construction-relevant context.

KEY FINDINGS AND DISCUSSION

For brevity, only results showing resistance to constant-pH sulfate attack, ASR (via two-year concrete prism testing), and transport are included.

Sulfate Resistance

Changes in compressive strength during accelerated sulfate exposure at constant pH (Fig. 1) reveals that sulfate resistance in ACMs is governed not simply by bulk composition, but by the formation and chemistry of near-surface reaction layers and the permeability of the underlying matrix. Ettringite-based systems, including CSA cements and CAC blends (CACT), develop a dense, aluminum-rich (C,N)-A-S-H “armoring” layer that limits

sulfate ingress, suppresses internal damage, and promotes retention of compressive strength. In contrast, converted CAC systems exhibit rapid degradation due primarily to increased porosity associated with conversion, which facilitates sulfate transport and extensive ettringite formation throughout the matrix. Together, these findings demonstrate that sulfate sulfate in ACMs depends critically on coupled phase chemistry, microstructural evolution, and transport phenomena, rather than on sulfate exposure alone.

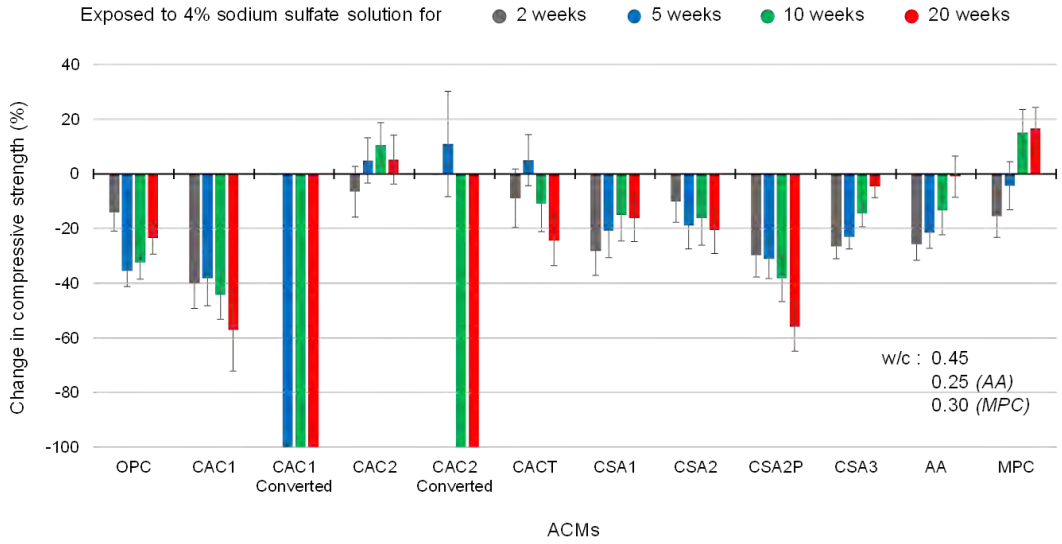

Figure 1. Average change in compressive strength, relative to strength prior to the exposure, for OPC and ACM paste cubes, exposed to a 4% (w/w) sodium sulfate solution. A 100% strength loss indicates the sample integrity was so compromised it could not be tested.

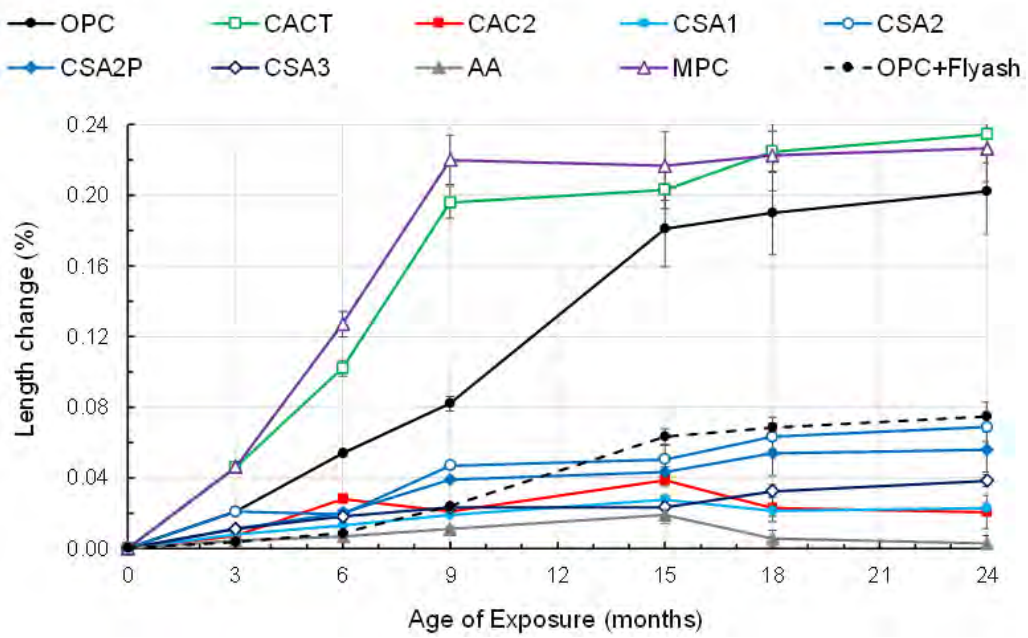

Figure 2. Comparison of expansion of ASTM C1293 concrete prisms prepared with different ACMs, compare with OPC and OPC with 50% Class C fly ash at 2 years.

Alkali–Silica Reaction Mitigation

Two-year concrete prism test data (Fig. 2) demonstrates that CAC concrete experienced less expansion relative to OPC when tested with a reactive aggregate. These findings are consistent with the lower pore solution alkalinity and alkali availability in CAC compared to OPC. However, a blended CAC (i.e., CACT) experienced higher expansion than OPC, attributable to increased pore connectivity combined with sufficient alkali availability from the OPC component.

Transport Properties

As shown in Fig. 3, CAC and CACT mortars generally exhibit lower formation factors than OPC at comparable total porosity (ϕ), indicating a more transport-efficient pore network despite similar void fractions. This trend is consistent with paste sorptivity performed at varying w/b, which show higher total water sorption in CAC and CACT at similar w/b compared to OPC. Of the ACMs examined, sorptivity in CACT also showed the greatest sensitivity to variations in w/b. These results demonstrate that total porosity alone is insufficient to assess durability, and that transport metrics capturing pore connectivity and tortuosity are required.

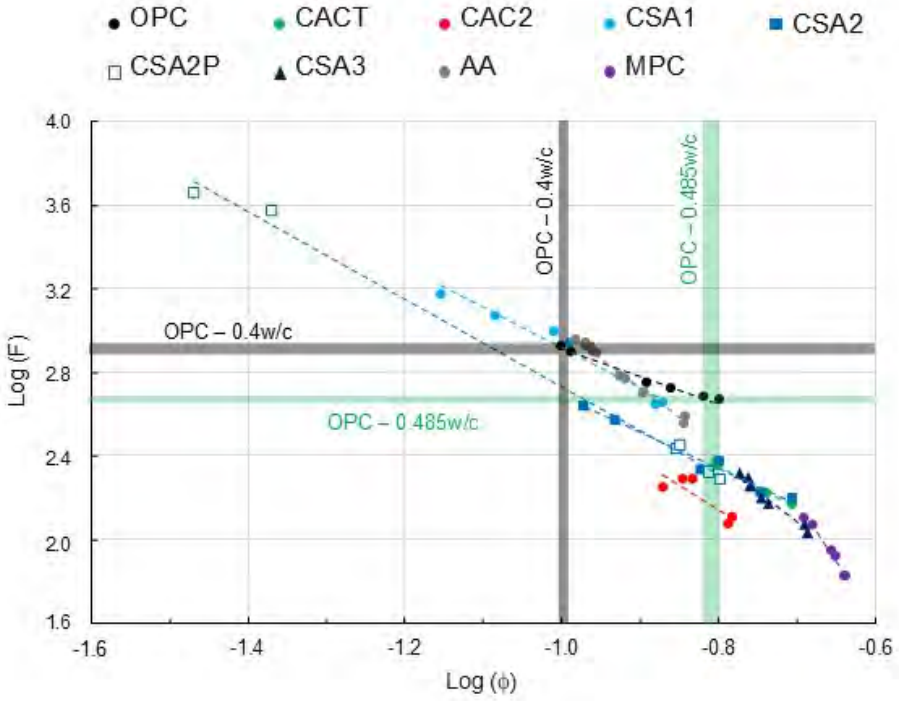

Figure 3. Formation factor (F) versus total porosity (Φ) in ACM mortar mixtures compared to that of OPC at varied water-to-binder ratios (w/b).

REFERENCES

1. Kurtis, K.E., Alapati, P., Burris, L.E., Ley, M.T., Peery, J., Hajibabaee, A., Behravan, A., Khanzadeh, M., Berke, N.S., Moser, R., *Novel Alternative Cementitious Materials for Development of the Next Generation of Sustainable Transportation Infrastructure*, FHWA-HRT-24-012, Federal Highway Administration, Turner-Fairbank Highway Research Center, Washington, DC, 2024. https://doi.org/10.21949/1521792
2. Alapati, P., *Multiscale Investigation of Alternative Cementitious Material Systems*, Ph.D. Thesis, Georgia Institute of Technology, Atlanta, GA, 2020.

International Conference on Calcium Aluminates 2026

ULTRA-RAPID HARDENING REPAIR MORTAR WITH AMORPHOUS CALCIUM ALUMINATES FOR FREEZER FLOOR APPLICATIONS AT –25 ℃

Katagiri*, Tomoki, MU MATEX Co., Ltd., Ube-City, Japan;
Nishimura, Kouichi, MU MATEX Co., Ltd., Ube-City, Japan;
Kimoto, Daisuke, MU MATEX Co., Ltd., Ube-City, Japan;
Nukita, Makoto, MU MATEX Co., Ltd., Ube-City, Japan

Keywords: amorphous calcium aluminates, ultra-rapid hardening, freezer repair, self-leveling underlayment, cold temperature mortar

ABSTRACT

Repairing damaged flooring in commercial freezer warehouses presents significant challenges due to the extremely low temperatures, often below –25 ℃, where continuous forklift traffic and localized freeze–thaw actions near the entrance area accelerate surface deterioration. This study describes the development of a self-leveling, ultra-rapid-hardening mortar designed specifically for subzero applications. The binder system is based on amorphous calcium aluminates (ACA), which exhibit high reactivity and excellent early-age performance in low-temperature environments. The formulation was optimized to ensure adequate flowability and high early strength without the need for external substrate heating.

Laboratory tests evaluated hydration kinetics, setting time, and mechanical properties of the mortar at –25 ℃. Results demonstrated that the ACA-based system achieved the initial set within 10 minutes and compressive strength exceeding 30 MPa after 3 h, even under freezing conditions. The product was successfully applied in a real-world industrial freezer setting, confirming its practical applicability.

This paper highlights the potential of ACA as a next-generation binder for cold-environment infrastructure repair and contributes to expanding the scope of high-performance calcium aluminate-based materials.

INTRODUCTION

At −25 °C, freezer warehouse floor repair is typically challenging. This is due to the constraints of continuous operation, and conventional mortars fail because of immediate freezing, resulting in strength from ice rather than hydration [1]. Organic-based materials are unsuitable in food environments due to food safety compliance. Amorphous calcium aluminates (ACA) offer a promising alternative, as their rapid dissolution and highly exothermic hydration enable reaction even under subzero conditions [2–4]. This study develops and evaluates an ultra-rapid-hardening ACA-based mortar for freezer floor repair and compares its

* *tomoki.katagiri@mu-cc.com*

performance with that of a ternary system composed of calcium aluminate cement (CAC), ordinary Portland cement (OPC), and anhydrite.

METHODS

Materials

Two repair mortar systems were evaluated under subzero conditions:

ACA-based system

The ACA-based system consists of the following: anhydrite blended with ACA, lithium carbonate, polycarboxylate ether (PCE) superplasticizer, retarder (oxycarboxylic acid), redispersible polymer powder, and defoamer. The dry mix had a binder content of 60 wt% and a water-to-powder ratio of 20.0%.

Ternary system (as a reference fast-setting mortar)

The ternary consists of crystalline CAC + anhydrite + rapid OPC, lithium carbonate, PCE superplasticizer, retarder (oxycarboxylic acid), redispersible polymer powder, and defoamer. The dry mix had a binder content of 61 wt% and a water-to-powder ratio of 18.8 wt%.

Aggregates consisted of standard oven-dry silica sand. The water used was tap water.

Mix design & batching

Powder components were preconditioned at 10 °C. Mixing water was preheated to 30 °C. Slurries were mixed at a temperature of ~10 °C.

Compressive strength

Compressive strength was measured at −25 °C after 1 h, 3 h, 7 days, and 28 days (φ50 × 100 mm cylinders; demolding at each curing time).

Substrate and environment

All specimens were cast on frozen concrete paving slabs (300 × 300 × 60 mm) and stored at −25 °C.

Temperature profiling of slurry

Thermocouples were installed on a concrete pavement slab at the center (casting point), mid-span (~75 mm), and edge (~113 mm) to capture lateral gradients. Additional thermocouples were embedded at depths corresponding to the surface (~2 mm), mid-depth (~12 mm), and bottom (~25 mm).

Field simulation

A refrigerated truck maintained at −25 °C was used for pouring and troweling, covering an area of approximately 1200 mm × 1800 mm with a 25 mm thick mortar layer.

KEY FINDINGS AND CONCLUSIONS

Figure 1 compares the compressive strength development of the ACA-based mortar and the ternary rapid system under −25 °C. The ACA system achieved an initial set within approximately 10 min and exceeded 30 MPa after 3 h, thereby meeting trafficability requirements for freezer warehouses. In contrast, the ternary system exhibited almost no setting at an early age, reaching only approximately 0.9 MPa after 1 h. The subsequent strength increase was largely attributed to freezing rather than hydration, with the strength reaching only approximately 25 MPa even after 28 days.

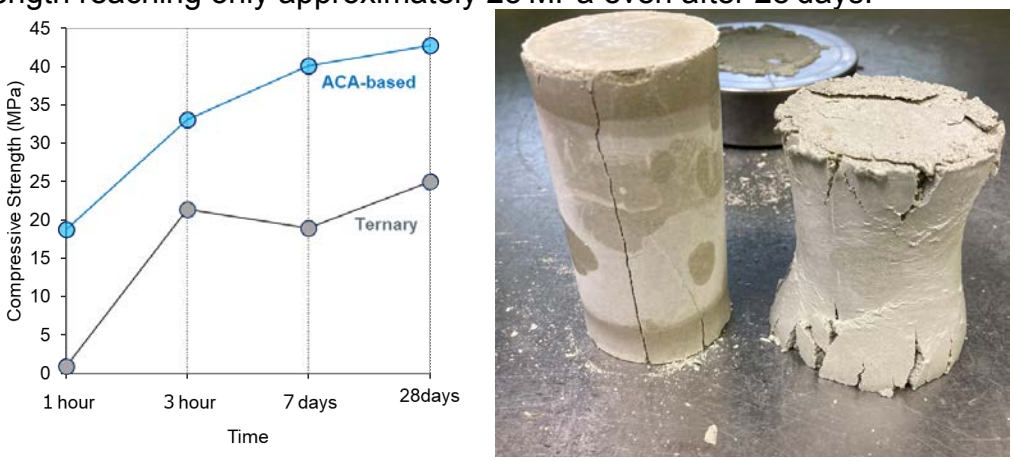

Figure 1. Compressive strength development at −25 °C for ACA-based and ternary systems (graph), with corresponding failure modes after testing: hydrated ACA mortar (left) and frozen conventional mortar (right).

Figure 2 illustrates the temperature evolution of the mortar at −25 °C. The left panel captures lateral (in-plane) gradients from the casting point to the edge, whereas the right panel captures vertical (through-thickness) profiles at three depths. Hydration heat originated at the center surface and propagated both depth-wise and laterally, sustaining reactions in the colder bottom and edge regions of the substrate.

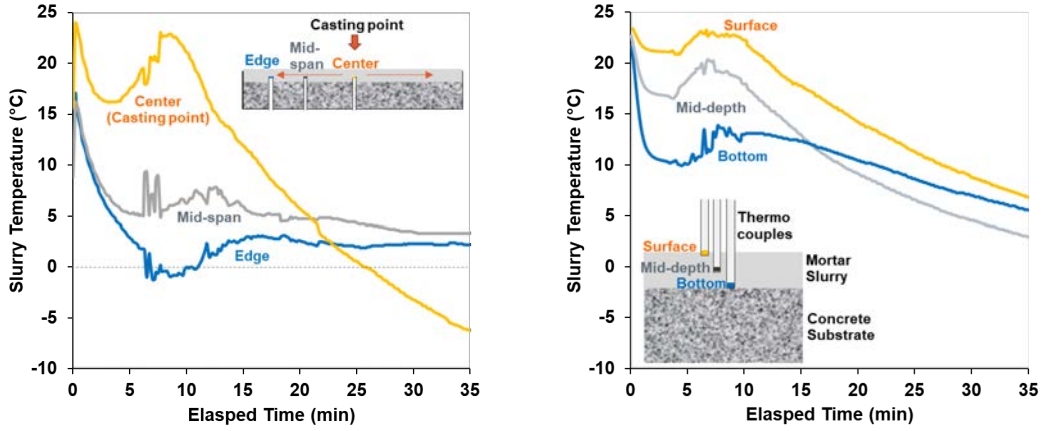

Figure 2. Temperature evolution at −25 °C: lateral gradients (left) and depth profiles (right). Lateral gradients at center (casting point), mid-span (~75 mm), and edge (~113 mm); depth profiles at surface (~2 mm), mid-depth (~12 mm), and bottom (~25 mm).

Field application trials confirmed the practical feasibility of this approach (Figure 3). The mortar was successfully poured and troweled inside a refrigerated truck without external heating, demonstrating that the system can be applied under real operational constraints.

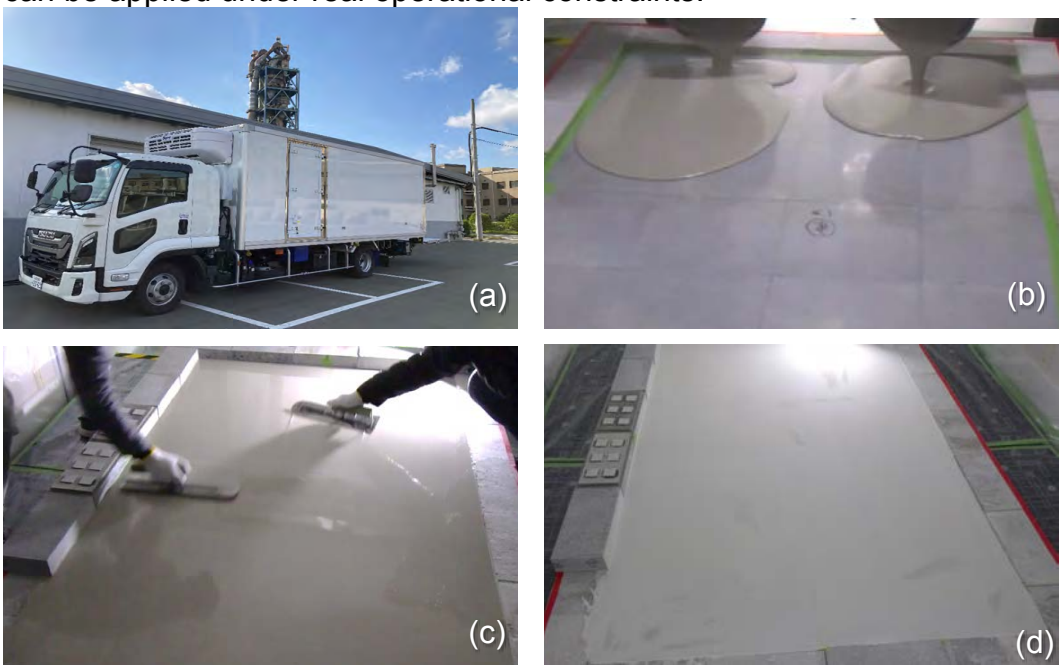

Figure 3. Field application trial inside a refrigerated truck at −25 °C: (a) test environment (refrigerated truck), (b) mortar slurry placement, (c) troweling operation, and (d) finished surface without external heating.

Overall, these results underscore the potential application of ACA-based binders for ultra-rapid repair in extreme cold environments. Future studies should address large-area placement strategies and the management of hydration heat in thick sections, as current formulations exhibit very high reactivity that may lead to excessive thermal gradients in massive pours.

REFERENCES

[1] J.J. Petrovic, Review Mechanical properties of ice and snow, J. Mater. Sci. 38 (2003) 1–6, https://doi.org/10.1023/A:1021134128038.

[2] K. Nakagawa, I. Terashima, K. Asaga, M. Daimon, A study of hydration of amorphous calcium aluminate by selective dissolution analysis, Cem. Concr. Res. 20 (1990) 655–661, https://doi.org/10.1016/0008-8846(90)90108-A.

[3] A. Das, J.N. Bousseau, N. Maach, R.J. Flatt, Effect of Temperature on Performance of Calcium Aluminate Cement Based Accelerator, Proc. 16th Int. Congr. Chem. Cement 4 (2023) 26-29, https://doi.org/10.3929/ethz-b-000656329.

[4] A. Franceschini, C. Nalet, P. Taquet, U-Technology, a Specialty Binder – Pushing further the Synchronisation of Ettringite formation, Drymix Mortar Yearbook (2021) 28–37.

International Conference on Calcium Aluminates 2026

DURABILITY OF CONCRETE CONTAINING ETTRINGITE ACCELERATORS

Benevenuti, Barbara ; Aboulela, Amr ; El Housseini, Sarra
Imerys, 1 Rue le Chatelier, Vaulx-Milieu, France

Keywords: Durability, concrete, accelerator, ettringite, calcium aluminate

ABSTRACT

Previous research[1,2] has demonstrated the successful use of ettringite-based accelerators to enhance the early-age strength of conventional and low-carbon binders without compromising long-term mechanical properties. The present study investigates their effect on the durability, a crucial factor for their use in concrete, by evaluating key durability indicators including chloride permeability, water porosity, and carbonation, in concrete mixes with and without ettringite-based accelerators.

Results indicate that partial replacement of Portland cement with the accelerator significantly reduced the chloride permeability and had minimal effect on other parameters such as carbonation.

While initial water porosity measurements showed an increase of porosity in accelerated systems, this is likely an artifact which can be attributed to the standard testing method, which involves drying of the concrete at 105°C. At this temperature the ettringite formed during the hydration of the accelerator is partially decomposed, leading to an artificially increased porosity of the cementitious matrix. Alternative testing performed with a 50°C drying temperature revealed significantly lower porosity levels.

These findings suggest that the addition of the ettringite accelerator does not have a deleterious effect on the durability of concrete, despite the expected modifications to the hydrate assemblage, thereby supporting their potential use in concrete applications.

INTRODUCTION | BACKGROUND

Ettringite accelerators (EA), based on a combination of calcium aluminate and calcium sulfate, have been utilized for many years to accelerate the strength development of Portland cement-based mortars[1,2], but their application in concrete remains limited. The increasing need to boost productivity in the concrete industry, particularly with the expanded use of supplementary cementitious materials (SCMs)—which often negatively impact early-age strength[3]—creates an opportunity for using such accelerators. However, this raises the critical question of their impact on long-term durability.

Literature examining the durability of concrete containing EA as an accelerator for Portland-based binders is scarce, with most studies focusing on pure calcium aluminate-based concretes. Nevertheless, some PhD studies have

*barbara.benevenuti@imerys.com

addressed this topic[4,5,6]. These studies indicate that accelerators composed of ettringite precursors do not compromise durability.

The present study complements this existing data set by evaluating the durability performance of a CEM II-A-based concrete incorporating an ettringite accelerator.

METHODS

Three concrete mixes were tested in this investigation. The reference mix contained 350 kg/m³ of CEM II-A and was designed to satisfy the C40/50 XF1 SF1 Dmax12 criteria. Two derivative accelerated compositions were prepared by replacing 50 kg/m³ and 100 kg/m³ of the CEM II-A with an ettringite accelerator, composed of amorphous calcium aluminate and calcium sulfate.

All concrete compositions maintained an effective water/binder ratio of 0.5, corresponding to 175kg/m3 of water. A polycarboxylate ether (PCE) superplasticizer was included, with the dosage adjusted to ensure comparable consistencies across all mixes. The accelerated systems additionally contained setting regulators.

Compressive strength measurements were performed according to EN 12390-3 and the durability tests were performed following the Performance-Based Approach (PBA) described in the French Technical Report FD P 18-480, which employs durability indicators to ensure a concrete mix is appropriately formulated to achieve its expected service life within a specific operating environment.

KEY FINDINGS

Compressive strengths

The strength results, displayed in Figure 1, show that the EA significantly improves early-age strengths, from 6h to 48h, while having no significant impact on the later-age strengths (7 days and beyond). The magnitude of the early-age strength increase was proportional to the replacement rate of Portland cement with the accelerator.

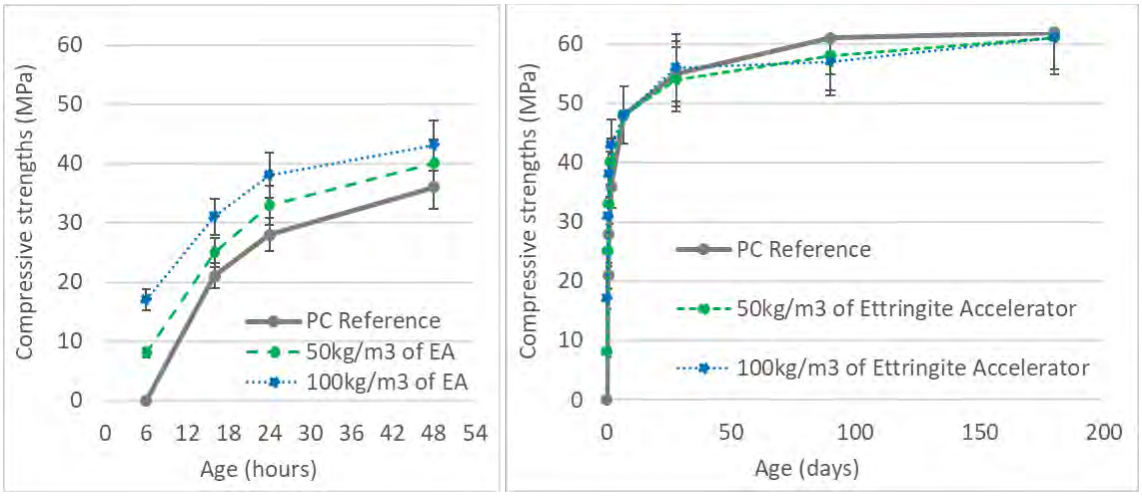

Figure 1: Early (left) and late (right) age strengths of concrete mixes

The fast-forming ettringite generated by the accelerator[7] contributes to the increase in early-age strengths without preventing the subsequent reaction of Portland cement at later ages and the continued filling of the system's porosity.

The observed late-age strengths indicate that the hydrates formed from the accelerator contribute to the densification of the matrix porosity to an extent comparable with the hydrates formed by an equivalent amount of Portland cement.

Durability performance

The durability performance indicators for the three concrete mixes are summarized in Table 1. The results indicate that the partial replacement of Portland cement by the ettringite accelerator does not alter the durability of the concrete.

Regarding electric resistivity and chloride ion diffusion velocity, accelerated systems exhibited superior performance compared to the reference mix, suggesting enhanced resistance to the penetration of deleterious agents. Similar observations have been reported in previous studies[7], and may be linked to a densification of the hydrate matrix and alterations in its chemical composition, particularly an increase in alumina content, which can favor the formation of Friedel's salt.

Carbonation depths measured across all mixes were extremely low. Quantifiable carbonation was observed only in the system with 100kg/m^3 of accelerator, though the extent remained minimal, probably due to the very low porosity of the concrete formulations.

The measured water absorption and porosity to water of the accelerated mixes are superior to the reference. However, this gap is more likely caused by the method of drying the samples than by intrinsic differences between the systems. Ettringite is known to be sensitive to the temperature[8], and the drying at 105°C, as prescribed by the standard testing procedure, will potentially degrade a portion of the ettringite present in the concrete and generate additional porosity. As the accelerated systems likely contain a higher volume of ettringite, they are expected to present a more pronounced increase in the porosity after the drying at 105°C.

By reducing the drying temperature to 50°C, below dehydration temperature of ettringite, a significant reduction in the measured porosity to water was observed. Unfortunately, a direct comparison of the systems' intrinsic porosity is not possible, as the reference mix was not dried under 50°C.

Table 1: Durability indicators of concrete mixes

		PC Reference	50kg/m3 of ettringite accelerator	100kg/m3 of ettringite accelerator
Electric resistivity @28 days	Ω.m	58	57	58
Electric resistivity @90 days	Ω.m	84	111	95
Water absorption @28d (105°C)	%	5,7	6,8	6,9
Porosity to water @90d (105°C)	%	9,0	15,0	15,7
Porosity to water @90d (50°C)	%	Not measured	10,1	10,4
Chloride ions diffusion @90d	10^{-12} m²/s	8,8	6,3	6,7
Accelerated carbonation coef. @90d	mm/d$^{1/2}$	0,00	0,00	0,27

CONCLUSIONS | FUTURE RESEARCH NEEDS

The experimental results for this concrete composition demonstrate that the partial substitution of Portland cement by the ettringite accelerator has a negligible impact on overall durability, despite the expected modification in the proportions of ettringite and calcium-silicate-hydrate (C-S-H) within the formed hydrates, compared to the non-accelerated PC system[7,9].

Further investigation is required to quantitatively evaluate the extent of the changes in the hydrate assemblage.

The high drying temperature required by the current testing standards to carry out some of the measurements seems to be not well suited for systems with significant ettringite content. This methodological limitation can lead to an overestimation of water absorption and porosity, which is not reflective of the true durability performance of such systems.

The concrete composition chosen in this study was revealed to be too dense to allow significant carbonation. It would be beneficial to repeat the study with a composition more prone to carbonation in order to better evaluate the impact of the EA.

A relevant topic for future work is the evaluation of the ettringite accelerator effect on the durability of low carbon systems, incorporating SCM, which themselves influence durability performances.

REFERENCES

1. J. H. Ideker, K. L. Scrivener, H. Fryda, B. Touzo, 12 - Calcium Aluminate Cements, Editor(s): Peter C. Hewlett, Martin Liska, Lea's Chemistry of Cement and Concrete (Fifth Edition), Butterworth-Heinemann, 2019, Pages 537-584.
2. J. Nehring, J. Neubauer, S. Berger, F. Goetz-Neunhoeffer, Acceleration of OPC by CAC in binary and ternary systems: The role of pore solution chemistry, Cement and Concrete Research, Volume 107, 2018, Pages 264-274
3. M. Antoni, J. Rossen, F. Martirena, K. Scrivener, Cement substitution by a combination of metakaolin and limestone, Cement and Concrete Research, Volume 42, Issue 12, 2012, Pages 1579-1589
4. S. Lamberet, Durability of ternary binders based on Portland cement, Calcium Aluminate Cement and Calcium Sulfate, PhD Thesis, EPFL, 2004.
5. E. G. Moffatt, Durability of rapid-set (ettringite-based) concrete, PhD Thesis, University of New Brunswick, 2011.
6. R. D. Lute, Durability of calcium-aluminate based binders for rapid repair applications, PhD Thesis, The University of Texas at Austin, 2016.
7. S. El Housseini, Hydration and durability of fast hardening binders incorporating supplementary cementitious materials, PhD Thesis, EPFL, 2022.
8. H.Y. Ghorab, & U. Ludwig, On the stability of calcium aluminate sulphate hydrates in pure systems and in cements, Proceedings of the 7th International Congress on the Chemistry of Cement, Paris, Vol. IV, pp. 496-503
9. S. El Housseini, B. Benevenuti, H. Fryda, M. Chambon, Understanding the strength development of self-compacting concrete formulation incorporating ettringite accelerator as strength booster, Proceedings of the International Conference on Calcium Aluminates, Lausanne, 2026.

International Conference on Calcium Aluminates 2026

COMPARISON OF DURABILITY OF CALCIUM ALUMINATE AND SULPHOALUMINATE CEMENTS (CAC, CSA AND HB-CSA) FOR AGGRESSIVE ENVIRONMENT

Binwal*, Bishwjeet, School of Chemical and Biomolecular Engineering, The University of Sydney, Australia; Valix, Marjorie, School of Chemical and Biomolecular Engineering, The University of Sydney, Australia

Keywords: CAC, CSA, HB-CSA, Acid resistance, Alkali-silica reactivity

ABSTRACT

Concrete made with traditional Portland cement in the sewer system is subject to severe corrosion. This leads to deterioration of Portland cement, reducing sewer pipe life and increasing maintenance and repair costs. This research addresses a pertinent issue by evaluating three types of specialty cements: calcium aluminate cement (CAC), calcium sulphoaluminate cement (CSA), and high-belite calcium sulphoaluminate cement (HB-CSA). These materials underwent durability tests under conditions that simulate the environment of sewer systems, utilising laboratory-based methodologies. The findings were unexpectedly significant; in the accelerated corrosion tests conducted in the laboratory, CAC demonstrated superior performance compared to the other types. The results indicate that CAC exhibits enhanced durability in acidic environments, significantly outperforming Portland cement. CAC offers the densest and most chemically inert matrix, making it particularly suitable for the most challenging conditions. In comparison, HB-CSA provides moderate acid resistance. In addition to this test, sorptivity, compressive strength, alkali-silica reactivity (ASR-AMBT), and water absorption were measured. In CAC and HB-CSA, water absorption was around 5%, whereas for CSA, it was slightly higher, around 7%. For sorptivity, all three binder systems were within the <6mm/√h range. Strength development for this study was recorded at 1 and 28 days for mortar and concrete samples.

INTRODUCTION | BACKGROUND

Sewer concrete systems are constantly exposed to biogenic sulfuric acid corrosion, where H_2S generated in the sewer is oxidised to H_2SO_4, leading to rapid acidification. Due to this deterioration of concrete, the global annual maintenance cost is progressively increasing. Corrosion outcomes depend significantly on the testing method and exposure conditions [1,2]. Thus, a reproducible and standardised approach is necessary when comparing binders for server environments. Research indicates that CAC outperforms Ordinary Portland Cement (OPC) in both field and laboratory settings, largely due to its unique hydration chemistry and superior neutralisation capacity [3,4]. However, for CSA and HB-CSA, it has been proposed that

*bishwjeet.binwal@sydney.edu.au

these binders can be used as alternatives [5]; however, there is still a need for a direct comparison among all three using a proper test protocol covering fresh, mechanical, and durability properties.

METHODS

The test plan for this study was organised into two stages. The first stage focused on analysing the physical and fresh properties of concrete made with three different binders. It also evaluated their mechanical, durability, and transport properties. In the second stage, the tests primarily assessed these binders under aggressive sewer conditions. To achieve this, a widely used research method was employed: a lab-based testing protocol designed to mimic the effects of concrete exposure to biogenic acids present in the sewer environment, using CAC, CSA, and HB-CSA binders. [2,6,7].

KEY RESULTS AND CONCLUSIONS

A. Fresh properties indicate that concrete made with HB-CSA and CSA sets the fastest, taking less than 30 minutes at a w/c ratio of 0.35. CAC was the only binder that remained workable at a w/c ratio of 0.35. However, at a w/c ratio of 0.3, all binders set within 25-35 minutes.
B. CAC and CSA concretes developed a high early strength at Day-1; however, HB-CSA was at 10.1. At Day 28, all three were above 50 Mpa, and CAC was the highest among all (Figure 1).
C. None of the three binders showed any expansion when used with reactive sand, and HB-CSA performed best among the three.
D. CAC and HB-CSA have lower water absorption than CSA (Table 1). Sorptivity revealed that HB-CSA's initial and final absorption were lower than those of the other two binders (Figure 2).
E. Strength loss during acid immersion for CAC and CSA was similar, ranging from 55% to 58% decrease by 35 days; however, for HB-CSA, it was the lowest, around 41%.
F. Mass loss recorded during acid immersion was lowest in CAC, followed by HB-CSA.
G. Depth of corrosion indicates that CAC showed the least amount of acid permeation, which was 7.4, followed by HB-CSA at 10.5. However, CSA showed a depth of corrosion of 20.5, even higher than OPC at 13.5 (Figure 3).

Table 1. Water absorption of concrete made CAC, CSA and HB-CSA

Binders	Immersed Absorption; Ai (%)	Boiled Absorption; Ab (%)
CAC	5.06 ± 0.02	5.43 ± 0.01
CSA	7.19 ± 0.07	7.26 ± 0.07
HB-CSA	5.75 ± 0.07	5.78 ± 0.07

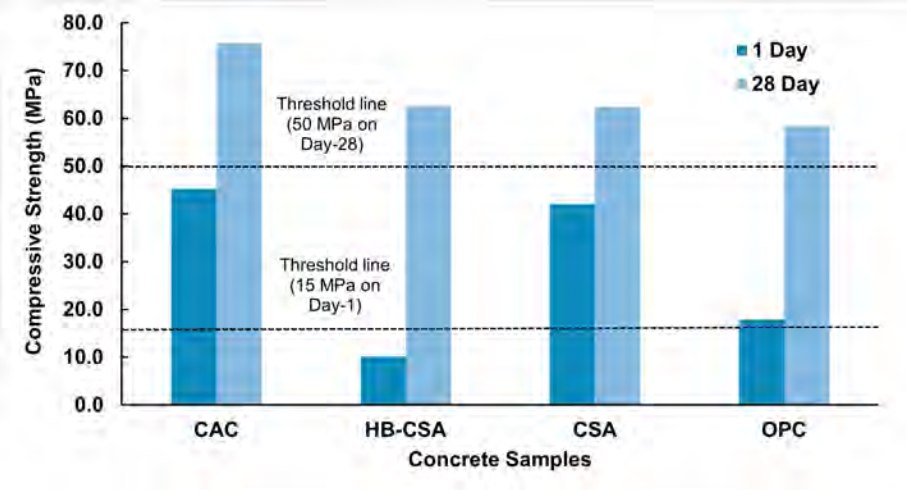

Figure 1. Strength comparison of CAC, CSA and HB-CSA with OPC at Day-1 and Day-28

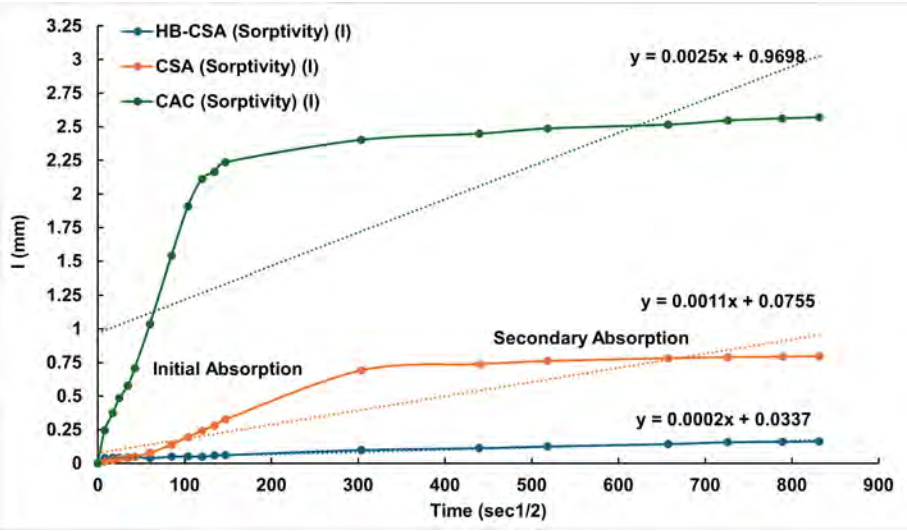

Figure 2. Initial and secondary absorption of CAC, CSA and HB-CSA

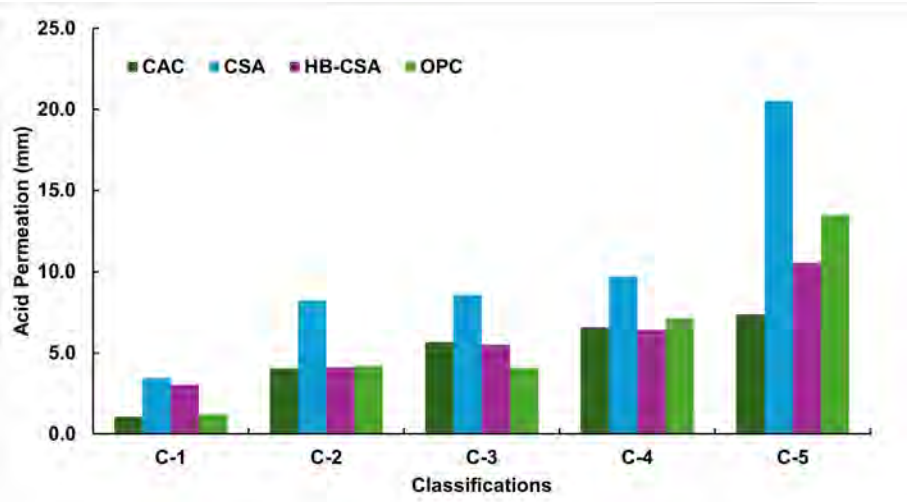

Figure 3. Depth of corrosion of CAC, CSA and HB-CSA at different classifications from C1 to C5 compared with OPC

FUTURE RESEARCH

The experimental program described here is a specific part of a larger thesis framework. In this framework, CAC, CSA, and HB-CSA have been evaluated using standardised protocols to establish a strong performance baseline across key indicators of fresh properties, mechanical properties, and durability. Building on this foundation, the next phase will apply the same testing matrix to newly developed low-carbon binders and directly compare their performance against CAC, CSA, and HB-CSA under the same curing and exposure conditions.

REFERENCES

[1] S.K. Pramanik, M. Bhuiyan, D. Robert, R. Roychand, L. Gao, I. Cole, B.K. Pramanik, Bio-corrosion in concrete sewer systems: Mechanisms and mitigation strategies, Science of The Total Environment 921 (2024) 171231. https://doi.org/10.1016/j.scitotenv.2024.171231.

[2] C. Grengg, F. Mittermayr, N. Ukrainczyk, G. Koraimann, S. Kienesberger, M. Dietzel, Advances in concrete materials for sewer systems affected by microbial-induced concrete corrosion: A review, Water Res. 134 (2018) 341–352. https://doi.org/10.1016/j.watres.2018.01.043.

[3] M.W. Kiliswa, K.L. Scrivener, M.G. Alexander, The corrosion rate and microstructure of Portland cement and calcium aluminate cement-based concrete mixtures in outfall sewers: A comparative study, Cem. Concr. Res. 124 (2019). https://doi.org/10.1016/j.cemconres.2019.105818.

[4] H.A. Khan, A. Castel, M.S.H. Khan, A.H. Mahmood, Durability of calcium aluminate and sulphate resistant Portland cement based mortars in aggressive sewer environment and sulphuric acid, Cem. Concr. Res. 124 (2019). https://doi.org/10.1016/j.cemconres.2019.105852.

[5] A.T. Bakera, A. Aboulela, M.G. Alexander, A. Bertron, M. Peyre Lavigne, S. Meulenyzer, C. Patapy, Performance of Sewer Concretes with Calcium Sulpho-Aluminate Cement and Portland Cement Blends: Field and Laboratory Studies, Materials (Basel). 18 (2025). https://doi.org/10.3390/ma18061256.

[6] P. Sturm, G.J.G. Gluth, C. Jäger, H.J.H. Brouwers, H.C. Kühne, Sulfuric acid resistance of one-part alkali-activated mortars, Cem. Concr. Res. 109 (2018) 54–63. https://doi.org/10.1016/j.cemconres.2018.04.009.

[7] H.A. Khan, M.S.H. Khan, A. Castel, J. Sunarho, Deterioration of alkali-activated mortars exposed to natural aggressive sewer environment, Constr. Build. Mater. 186 (2018) 577–597. https://doi.org/10.1016/j.conbuildmat.2018.07.137.

International Conference on Calcium Aluminates 2026

UTILIZATION OF GRANULATED SLAG AS AGGREGATE AND ALUMINA-BEARING SCM IN CEMENTITIOUS SYSTEMS

Faucher, Santiago, President, Rockwood, Ontario, Canada;
*Lau, Kelly, Intermediate Metallurgist, Rockwood, Ontario, Canada

Keywords: Calcium aluminates, supplementary cementitious materials (SCM), platinum slag, alkali-silica reactivity (ASR) mitigation, sustainable construction

ABSTRACT

This study explores the valorization of a water-granulated platinum slag (GPS) as both a fine aggregate replacement and a supplementary cementitious material (SCM) in mortar formulations. The slag, a byproduct of platinum smelting operations, contains high amorphous content and elevated MgO and Al_2O_3 levels—making it a potential contributor to cement chemistry when properly processed.

The GPS was tested in two ways. First, as a sand substitute (0-100%) sand replacement, and second, ground to make ground granulated platinum slag (GGPS) as a 30% Ordinary Portland Cement (OPC) replacement. Three mortar systems were developed: (A) OPC-only, (B) OPC with 30% fly ash, and (C) OPC with 30% GGPS. Mixes were evaluated for workability, compressive strength, alkali-silica reactivity (ASR), and autoclave expansion.

ASR testing showed that GPS used as sand replacement resulted in excessive expansion (>0.2%), but this was effectively mitigated with the addition of fly ash, enabling up to 100% sand replacement without compromising performance. Autoclave expansion remained within acceptable limits in all cases, indicating mineralogical stability despite high MgO content. The GGPS exhibited a Blaine fineness of 441 m²/kg and was found to be chemically active, with favorable ASR suppression and strength comparable to control mixes.

These results support the use of alumina-bearing GPS and GGPS as promising, industrially sourced SCMs that can help cement manufacturers reach their sustainability and decarbonization goals. Ongoing work is focused on optimizing hybrid binder systems (e.g., fly ash + GGPS) for improved performance in durable and resource-efficient calcium aluminate-based systems.

*kelly@insight-rnd.com

INTRODUCTION | BACKGROUND

Reducing clinker content while maintaining mechanical and durability performance is central to cement decarbonization. Supplementary cementitious materials (SCMs), such as fly ash and slag, enhance mechanical and durability properties of cementitious composites while contributing to sustainability objectives [1-3].

SCMs can react with calcium hydroxide released during Portland cement hydration to form additional calcium silicate hydrate (C-S-H) phases, thereby densifying the microstructure and improving binder performance in blended systems [1,2]. Their latent hydraulic or pozzolanic behavior depends on chemical composition, glass content, and fineness, which govern reaction kinetics and long-term strength development [1].

Several mechanisms explain why fly ash and slag mitigate alkali-silica reaction (ASR) expansion, including alkali binding within hydration products, reduced pore solution alkalinity, refined pore structure leading to lower permeability, and reduced silica dissolution rates [4,5]. Experimental studies indicate that fly ash and slag replacements reduce ASR expansion even in high-alkali systems and represent effective mitigation strategies [4-6].

Granulated platinum slag (GPS), produced through rapid quenching of molten slag, contains a high proportion of amorphous aluminosilicate phases. The GPS material evaluated in this work contains approximately 54 wt% SiO_2, 5 wt% Al_2O_3, 11 wt% Fe_2O_3, and 21 wt% MgO, with measured glass content between 85–88%. Although elevated MgO levels may raise concerns regarding delayed expansion, autoclave testing confirms mineralogical stability of magnesium phases in this system.

This study evaluates two valorization strategies:

- GPS as a fine aggregate replacement
- Ground granulated platinum slag (GGPS) as a 30% OPC replacement

METHODS

Raw Material Characterization

Granulated slag was sieved to obtain the <0.5 mm fraction for aggregate substitution studies. GGPS was produced by ball milling to a Blaine fineness of 441 m²/kg, exceeding that of OPC (341 m²/kg) and fly ash (365 m²/kg). Specific gravity of GGPS was measured at 2.84.

Mix Design

Three mortar series were prepared:

- **Series A:** OPC binder with 0–100% sand replacement by GPS
- **Series B:** 70% OPC + 30% fly ash binder with GPS sand replacement
- **Series C:** 70% OPC + 30% GGPS binder with GPS sand replacement

Water-to-binder (W/B) ratios were adjusted to meet ASTM C1437 flow requirements.

Performance Testing

Mortars were evaluated according to ASTM standards:

- Compressive strength (ASTM C109)
- Autoclave expansion (ASTM C151)
- Alkali-silica reactivity (ASTM C1260)
- Setting time (ASTM C191)
- Bleeding and workability

KEY FINDINGS | CONCLUSIONS

MgO Stability

Despite MgO levels of ~21 wt% , autoclave expansion ranged from 0.01-0.04%, well below the ASTM C150 limit of 0.80%. This confirms mineralogical stability of MgO and absence of deleterious delayed expansion.

Compressive Strength

The OPC control achieved approximately 39 MPa at 56 days. Replacement of 30% OPC with GGPS achieved comparable strength of 38 MPa, demonstrating that GGPS functions effectively as a supplementary cementitious material.

Moderate GPS sand substitution (up to approximately 50%) increased compressive strength in OPC-based systems. At 100% sand replacement, strength declined, likely due to particle segregation rather than intrinsic material limitations.

Alkali-Silica Reactivity

GPS used as sand replacement without SCM mitigation resulted in ASR expansion exceeding 0.2%, indicating potentially deleterious behavior.

Incorporation of 30% fly ash effectively suppressed ASR expansion below deleterious thresholds, even at high GPS substitution levels. GGPS provided partial ASR suppression but was insufficient alone at high aggregate replacement levels.

Overall Technical Implications

GGPS can replace 30% OPC while meeting strength and expansion requirements. Fine aggregate can be fully replaced by GPS when paired with fly ash for ASR mitigation.

These findings demonstrate a viable pathway for clinker reduction and the development of alumina-bearing, sustainable cementitious systems.

A summary of mortar performance can be seen in Table 1.

Table 1. Summary of mortar performance incorporating GPS as sand replacement and GGPS or fly ash as SCMs. Shown are 56-day compressive strength and 21-day ASR expansion values, highlighting technically viable mix designs and ASR mitigation effects.

Binder System	Mix ID	GPS as Sand (%)	Total GPS (wt%)	W/B	56-Day Strength (MPa)	Autoclave Expansion (%)	ASR at 21 Days (%)
OPC (100%)	A1	0	0	0.6	38.89	0.03	0.13
	A3	50	35	0.5	46.63	0.01	0.6
	A5	100	69	0.6	34.71	0.01	0.7
OPC (70%) + Fly Ash (30%)	B1	0	0	0.6	28.21	0.01	0.02
	B3	50	35	0.6	35.89	0.01	0.04
	B5	100	69	0.7	27.65	0.01	0.07
OPC (70%) + GGPS (30%)	C1	0	9	0.6	37.81	0.01	0.1
	C3	50	43.9	0.6	43.43	0.04	0.56
	C5	100	78.6	0.6	25.67	0.01	0.65

REFERENCES

1. M.C.G. Juenger, R. Snellings, S.A. Bernal, Supplementary cementitious materials: new sources, characterization, and performance insights, *Cem. Concr. Res.* 122 (2019) 257-273.
2. J. Skibsted, R. Snellings, Reactivity of supplementary cementitious materials (SCMs) in cement blends, *Cem. Concr. Res.* 124 (2019) 105799.
3. K.L. Scrivener, V.M. John, E.M. Gartner, Eco-efficient cements: potential economically viable solutions for a low-CO_2 cement-based materials industry, *Cem. Concr. Res.* 114 (2018) 2-26.
4. J. Lindgård, Ö. Andiç-Çakir, I. Fernandes, T.F. Rønning, M.D.A. Thomas, Alkali-silica reactions (ASR): literature review on parameters influencing laboratory performance testing, *Cem. Concr. Res.* 42 (2012) 223-243.
5. M.D.A. Thomas, The effect of supplementary cementing materials on alkali-silica reaction: a review, *Cem. Concr. Res.* 41 (2011) 1224-1231.
6. M.H. Shehata, M.D.A. Thomas, The effect of fly ash composition on the expansion of concrete due to alkali-silica reaction, *Cem. Concr. Res.* 30 (2000) 1063-1072.

International Conference on Calcium Aluminates 2026

THE EFFECT OF CARBONATION ON CALCIUM ALUMINATE CEMENT WITH THE ADDITION OF SLAG AND CALCINED CLAY

Bašić, Alma-Dina[1] , Gerz, Alexandra[2], Serdar, Marijana[1]
[1] University of Zagreb, Faculty of Civil Engineering, Department of Materials, Fra Andrije Kačić-Miošić 26, 10000 Zagreb, Croatia, [2]Calucem d.o.o., Revelanteova 4, 52100 Pula, Croatia

Keywords: accelerated carbonation, supplementary cementitious materials, microstructure, pore structure

ABSTRACT

The durability of calcium aluminate cement in aggressive environments is considered one of its competitive advantages. A property that is attracting additional attention in concrete research today is resistance to carbonation, as cement-based materials play a role as carbon sinks in the carbon neutrality strategy. Previous studies have shown that CAC concrete has a faster carbonation rate compared to OPC concrete. However, there are no consistent conclusions on the effects of carbonation on the properties of CAC and limited knowledge on how SCMs affect the carbonation process when mixed with CAC. The present study focuses on the evaluation of the carbonation resistance of mortar based on CAC without and with the addition of slag and calcined clay. The influence of carbonation was investigated on non-conversion-promoted (cured at 20°C) and conversion-promoted samples (cured at 38°C). The experimental results show that accelerated carbonation has different effects on the microstructure and mechanical properties of CAC without and with the addition of slag or calcined clay.

INTRODUCTION | BACKGROUND

The durability of calcium aluminate cement is often cited as the greatest advantage of this material[1]. One of the durability properties raising additional attention in concrete research is resistance to carbonation, due to the implication cement-based materials as carbon sinks have in the carbon neutrality strategy[2]. In CAC cement, according to the literature, the reaction with CO_2 leads to the formation of $CaCO_3$ and AH_3 gel, irrespective of the hydrates present[1]. Alapati and Kurtis[3] demonstrated that CAC concrete exhibits a faster carbonation rate in comparison to OPC concrete. Additionally, they showed that the decomposition of primary hydration products due to carbonation can lead to a considerable decrease in compressive strength and capillary porosity. On the contrary, studies of CAC exposed to carbon dioxide during curing at early age showed that it is possible to overcome conversion process by exposing samples to critical

*marijana.serdar@grad.unizg.hr

carbonation (100% of CO_2) or by early carbonation curing[4]. Studies showed formation of stable hydrates without causing an increase in the porosity of the cement matrix. Overall, however, there is an absence of uniform conclusion on the effect of carbonation on CAC and a limited knowledge about how SCMs impact the carbonation process when incorporated with CAC.

This research is focused on evaluating the carbonation resistance of mortar based on CAC cement without and with the addition of slag and calcined clay. For this purpose, three mixtures were made.

MATERIALS AND METHODS

The studied samples were produced using calcium aluminate cement with 52.67% of Al_2O_3 produced by Calucem company from Pula, Croatia. The slag used in this study was industrially milled with a Blaine size 4580 cm^2/g, while clay was received as raw material without prior processing. Prior to mixing, the clay was first dried for 24h at 60°C to remove the moisture, then ground (for 90 s) to Blaine size of 5980 cm^2/g, and finally calcined at 850 °C for one hour. According to the mass loss (%) from 350 – 600 °C, the calcined clay had 40% kaolinite/illite.

To ensure quantifiable changes in the microstructure of CAC cement, 30% of cement was replaced by GGBFS or calcined clay. Therefore, three mortar mixtures were prepared. One reference mixture with 100% of CAC cement (labelled CAC100), second mixture with 30% replacement with GGFS (labelled CAC70S30) and third mixture with 30% replacement by calcined clay (labelled CAC70C30). The mixtures were prepared according to EN 14647. The influence of carbonation was evaluated on conversion non-promoted (cured at 20°C) and conversion promoted samples (cured at 38°C).

Resistance to carbonation was tested according to EN 12390-12. The depth of carbonation was measured with a phenolphthalein indicator. To assess the impact of carbonation on the mechanical properties, the compressive strength of the samples was tested before and after 56 days of carbonation. To correlate changes in the compressive strength to conversion and phase assemblage changes, microstructure studies were performed by thermogravimetric analysis (TGA) – results showed in the extended abstract, and mercury intrusion porosimetry (MIP), and X-ray diffraction (XRD) – results not shown in the extended abstract.

RESULTS

Carbonation depth was monitored over 56 days of exposure to CO_2. Results obtained from carbonation depth measurement are shown in Figure 1. Mixture CAC70C30 20°C exhibited the highest carbonation ingress throughout all testing periods. Mixtures cured at 38°C before carbonation have an overall lower carbonation depth than mixtures cured at 20°C.

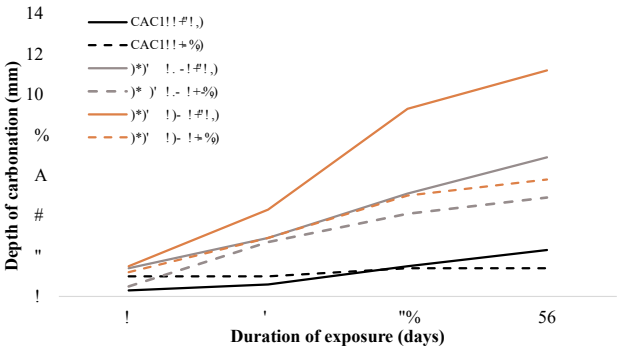

Figure 1 Carbonation depth values for all mixtures

This difference also can be seen in, Figure 2, where samples sprayed with phenolphthalein after 56 days of exposure to CO_2 are presented. Both GGBFS and calcined clay samples show smaller carbonation depth in the case of samples cured at higher temperature which also can be seen from samples sprayed with phenolphthalein.

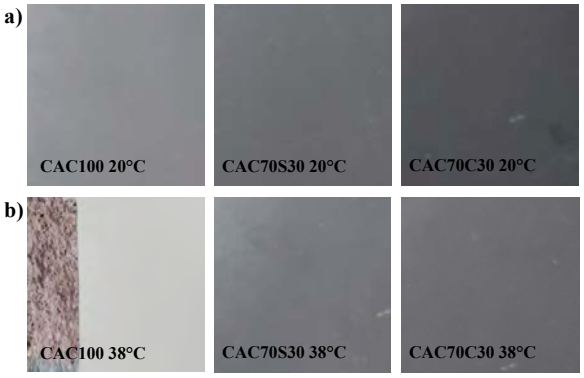

Figure 2 Samples sprayed with phenolphthalein after 56 days of exposure for all three mixtures: a) 20°C, b) 38°C

Accelerated carbonation had the greatest impact on the change in the compressive strength of the reference mixture for both curing temperatures, Figure 3.

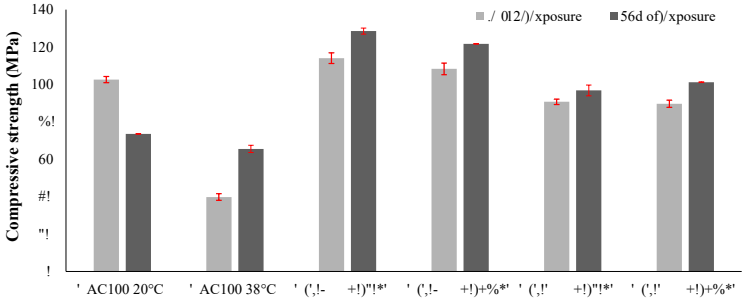

Figure 3 Compressive strength values before and after 56 days of carbonation compared to compressive strength prior to carbonation

While the compressive strength of non-converted reference mixture cured at 20°C decreased for almost 30% after 56 days of carbonation, the same mixture, which was converted due to curing at 38°C, experienced an increase in compressive strength for almost 40% after carbonation. In the case of mixtures with slag and calcined clay, a slight increase in strength

was recorded for all mixtures after 56 days of carbonation, regardless of curing conditions prior to carbonation. Figure 4 shows dTG curves for CAC100, CAC70S30 and CAC70C30 mixture cured at 38°C after 56 days of carbonation.

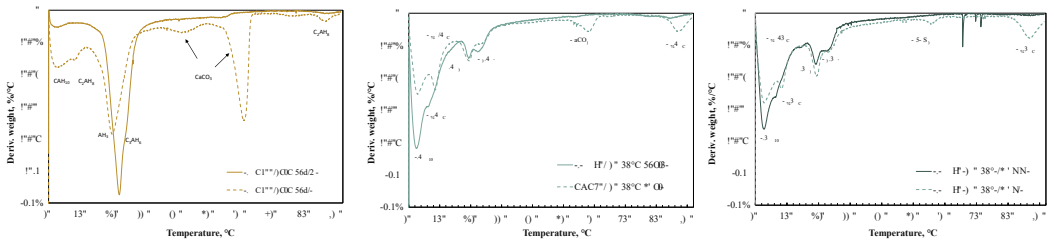

Figure 4 DTG curves of carbonated CAC100, CAC70S30 and CAC70C30 mixture cured at 38°C after 56 days of exposure

In the case of CAC100 mixture cured at 38°C after 56 days of carbonation, there was a decrease in the peak attributed to stable C_3AH_6 and AH_3 hydrate. For CAC70S30 and CAC70C30 cured at 38°C, lower peak intensity was detected for CAH_{10} after exposure to CO_2, while more C_2AH_8, decomposing at lower and higher temperatures, was detected after carbonation. In this case, more C_3AH_6 hydrate was also detected after carbonation, as well as $CaCO_3$ and AH_3 hydrate.

KEY FINDINGS

Curing at 38°C for mixtures incorporating slag and calcined clay to CAC based mortar improved resistance to carbonation compared to those samples cured at 20°C. Only a plain CAC reference sample cured at 20°C experienced decrease in compressive strength after 56 days of carbonation, while compressive strength of samples with slag and calcined clay increased after 56 days of exposure to CO_2. Mixtures with slag and calcined clay addition did not experience major changes in microstructure after carbonation, which makes these mixtures more stable, in relation to compressive strength, compared to the reference mixture.

REFERENCES

[1] Ideker, J.H., Scrivener, K.L., Fryda, H. and Touzo, B.: “Calcium aluminate cements (Chapter)”, Lea`s Chemistry of Cement and Concrete (ur. Hewlett, P., Liska, M.), England: Elsevier Science Publishers Ltd., 2019.

[2] Lippiatt, N., Ling, T. C., and Pan, S. Y., Towards carbon-neutral construction materials: Carbonation of cement-based materials and the future perspective, J. Build. Eng., vol. 28, p. 101062, 2020, doi: 10.1016/j.jobe.2019.101062.

[3] Alapati, P., Kurtis, K.E., Carbonation in Alternative Cementitious Materials: Implications on Durability and Mechanical Properties, Sixth Int. Con. Dur. Concr. Struct ICC02, (2018).

[4] Park, S. M., Jang, J. G., Son, H. M., and Lee, H. K., Stable conversion of metastable hydrates in calcium aluminate cement by early carbonation curing, Journal of CO2 Utilization, vol. 21. pp. 224–226, 2017, doi: 10.1016/j.jcou.2017.07.002.

International Conference on Calcium Aluminates 2026

DEEP-SEA PERFORMANCE OF HIGH-PURITY CALCIUM ALUMINATE CEMENT: DURABILITY UNDER 980 M IN-SITU EXPOSURE

Takahashi*, Keisuke, Kagawa University, Takamatsu, Japan; Kawabata, Yuichiro, Port and Airport Research Institute and Tohoku University, Yokosuka, Japan; Yio, Marcus, Imperial College London, London, UK; Chen, Yining, Imperial College London, London, UK; Wong, Hong, Imperial College London, London, UK

Keywords: high-purity calcium aluminate cement, deep sea, durability, in-situ exposure, phase transformation

ABSTRACT

Calcium aluminate cement (CAC) has demonstrated exceptional durability under deep-sea conditions. Previous investigations at 1887 m depth revealed that high-purity CAC (70% alumina) maintains structural integrity through the stability of aluminium hydroxide (AH) as the binding phase. This study extends the exposure duration to two years at 980 m depth to evaluate long-term performance. Microstructural analysis confirms the persistent stability of the hydrate assemblage. Results demonstrate that calcium aluminate hydrates selectively uptake chloride from seawater to form Friedel's salt, while the AH matrix remains chemically stable. This mechanism prevents the decomposition of hydrates due to leaching of alkali metal and/or alkaline earth metal, typically observed in Portland cement systems under seawater ingress, distinguishing CAC as a promising binder for deep-sea infrastructure applications.

INTRODUCTION | BACKGROUND

The authors have systematically investigated the durability of cementitious materials under deep-sea conditions. Among various binder systems examined, high-purity CAC has exhibited superior resistance to deep-sea environments[1]. Previous research at approximately 1887 m depth for one year demonstrated remarkable stability of the hydrate assemblage.

The fundamental distinction between CAC and Portland cement (PC) systems lies in their binding phases and dissolution behaviour under seawater attack. In PC systems, calcium silicate hydrate (C-S-H) exhibits significant solubility under low-pH conditions induced by alkali leaching due to seawater ingress, leading to microstructural deterioration[2]. Conversely, CAC systems feature AH as the binding phase, which demonstrates exceptional stability even under prolonged seawater exposure[1]. This study investigates specimens exposed for two years at 980 m depth.

*takahashi.keisuke@kagawa-u.ac.jp

METHODS

Exposure site

Field exposure was conducted at 980 m depth offshore Shimizu, Japan, for two years. Environmental conditions closely resembled those at 1887 m, with seawater temperatures of 2–3 °C throughout the year. The seafloor consisted of muddy sediments. Specimens (φ50 mm × 100 mm, water-to-cement ratio of 0.50, sealed-cured for three months) were positioned on a platform elevated approximately 20 cm above the seabed (Fig. 1).

Figure 1. Deep-sea exposure site at 980 m depth showing specimen placement. Photographs courtesy of the Japan Agency for Marine–Earth Science and Technology.

Microstructural characterization

Retrieved specimens were solvent-dried, vacuum-impregnated with low-viscosity epoxy resin and polished with diamond paste. Microstructural examination used a JSM-IT-300 (JEOL) scanning electron microscope (SEM) with backscattered electron (BSE) detector and energy-dispersive X-ray spectrometer (EDS) at 15 kV accelerating voltage and 10.0 mm working distance. EDS spot analyses were performed on at least 100 randomly selected points within 0–1 mm, 4 mm, and 20 mm from the exposed surface, avoiding cracks and large voids. Results were compared against non-exposed specimens sealed-cured for 3 years. X-ray diffraction (XRD) and thermodynamic modelling were carried out to complement SEM-EDS.

KEY FINDINGS

Based on the XRD analysis, the hydrate assemblage in CAC comprises calcium aluminate layered double hydroxides (Ca-Al LDHs) including CAH_{10}, C_2AH_8, and C_3AH_6, together with AH as the binding phase. Non-exposed replicate specimens show residual unreacted monocalcium aluminate (CA) clinker present in significant quantities. SEM revealed a porous microstructure wherein granular Ca-Al LDHs particles are embedded within the AH binding phase with numerous voids visible (Fig. 2).

Thermodynamic equilibrium calculations established that AH remains stable with increasing seawater ingress, whereas Ca-Al LDHs undergo anion exchange by incorporating Cl and S from seawater, transforming into Friedel's and Kuzel's salts (Fs/Ks), followed by ettringite (Ett) formation[1].

Comparative analysis between the sealed-cured specimen (Fig. 2, right) and the 980 m exposed specimen (Fig. 3, left) demonstrates Fs formation from chloride uptake. EDS elemental mapping (Fig. 3, right) confirms that chloride incorporation occurs exclusively within Ca-Al LDHs phases, while AH remains unaffected. Given the porous microstructure observed in Figs. 2 and 3—with AH surrounding large Ca-Al LDHs grains—expansion induced by crystallization pressure is unlikely to occur significantly in this CAC system.

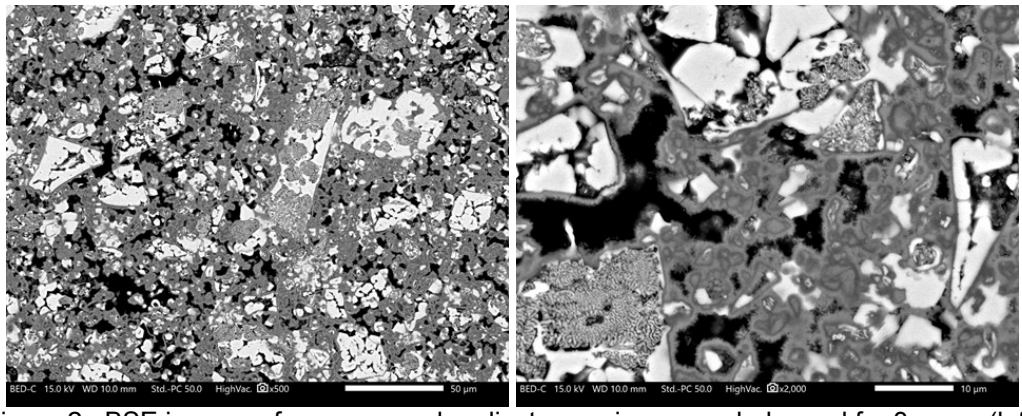

Figure 2. BSE images of non-exposed replicate specimens sealed-cured for 3 years (left: 500 ×, right: 2000 ×)

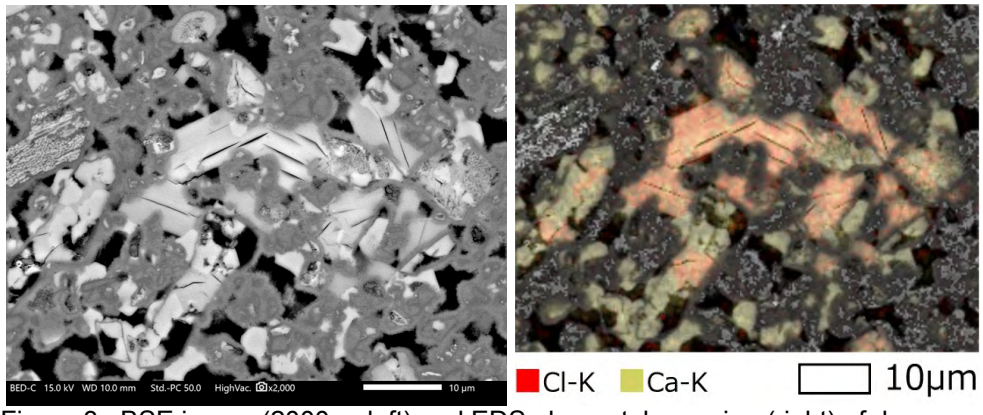

Figure 3. BSE image (2000 ×, left) and EDS elemental mapping (right) of deep-sea specimen exposed at 980 m for 2 years; 20 mm depth from exposure surface.

Figure 4 presents EDS point analysis results at depths of 0-1, 4, and 20 mm from the exposed surface. The appearance of point clusters linking AH and Ca-Al LDHs (including calcium aluminate hydrates and Fs/Ks) indicates intimate phase mixing. At the surface layer, a cluster extending from AH was observed with moderately reduced Cl/Al ratios, potentially indicating partial Fs decomposition. However, sulfur was minimally detected (S/Ca < 0.01), suggesting that subsequent Ett formation had not yet occurred.

Although detailed data are not presented here due to space constraints, several additional observations merit discussion regarding chloride uptake and phase changes. EDS analysis revealed no substantial difference in chloride uptake between deep-sea and laboratory exposed specimens in low-temperature seawater (2 °C) for two years. However, XRD analysis

indicated notably higher peak intensities of Fs in the 980 m deep-sea specimens.

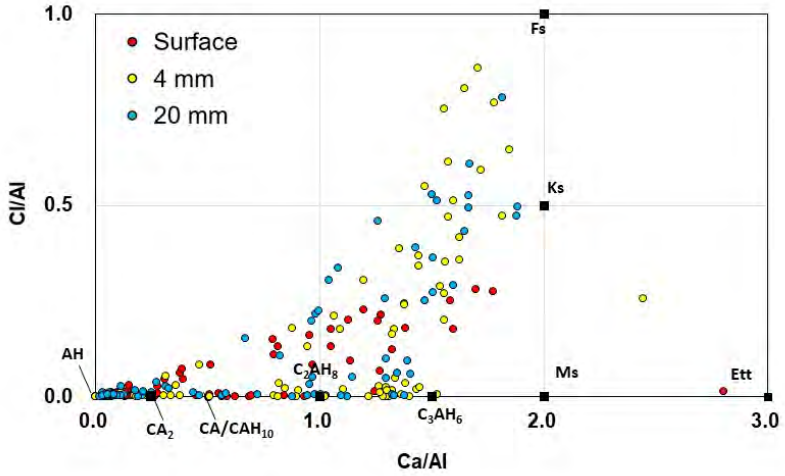

Figure 4. EDS point analysis of deep-sea specimen exposed at 980 m for 2 years showing Ca/Al versus Cl/Al atomic ratios at different depths.

FUTURE RESEARCH NEEDS | CONCLUSIONS

After two years of deep-sea exposure at 980 m depth, the hydrate phases in high-purity CAC systems demonstrate exceptional stability. This durability stems from two synergistic mechanisms: (1) selective chloride uptake by Ca-Al LDHs to form Friedel's salt, which prevents extensive conversion of calcium aluminate hydrates and maintains relatively stable dimensions, and (2) inherent stability of the AH binding phase. Although not detailed in this study, comparable stability has also been observed in specimens exposed under more severe conditions—three years at 3515 m depth—with results to be published in a forthcoming paper.

Extended exposure investigations are necessary to determine whether phase assemblages progressively evolve toward thermodynamic equilibrium states. The minimal leaching observed in CAC systems provides opportunities to investigate interactions between specimen surfaces and deep-sea sediments. Furthermore, comprehensive evaluation of mechanical properties under sustained deep-sea hydraulic pressure remains essential for advancing practical applications in extreme marine environments.

To address these challenges, the authors have initiated a new research programme, DuRACS (Durable and Resilient Advanced Cementitious materials for deep Sea infrastructure), which will continue systematic investigations in the coming years with support from the UK Research and Innovation and Japan Society for the Promotion of Science.

REFERENCES

[1] K. Takahashi, T. Akitou, M. Kobayashi, Changes in the physicochemical properties of calcium aluminate cement paste with high alumina content under deep seas, Constr. Build. Mater. 398 (2023) 132495.

[2] K. Takahashi, Y. Kawabata, M. Kobayashi, T. Kasaya, S. Miyamoto, H.S. Wong, Durability of cementitious binders with blast furnace slag in deep sea

conditions: Analysis of microstructure and phase transformation, Cem. Concr. Res. 196 (2025) 107942.

International Conference on Calcium Aluminates 2026

Long-Term Evaluation of Rapid Concrete Repair Systems

Lute, Racheal[1], Drimalas, Thano[1], Folliard, Kevin J. [1,] Alt, Chuck[2]

[1]The University of Texas at Austin, 10100 Burnet Road, Austin, Texas, 78758, [2]Imerys, 1316 Priority Ln, Chesapeake, VA 23324

Keywords: CAC, Concrete Durability, Alkali-Silica Reaction, Sulfate Attack

Extended Abstract:

This study presents long-term durability findings for various rapid repair concrete systems subjected to over a decade of outdoor exposure in diverse environmental conditions. The systems evaluated include Calcium Aluminate Cement (CAC), blended CAC–Portland cement systems, and Calcium Sulfoaluminate (CSA) cement, benchmarked against conventional Portland cement concrete. Key durability mechanisms monitored were alkali-silica reaction (ASR), external and physical sulfate attack, delayed ettringite formation (DEF), steel reinforcement corrosion, and carbonation. Results demonstrate that each alternative binder system exhibited distinct performance advantages under specific conditions. Overall, the findings highlight the potential of alternative cementitious systems to outperform traditional portland cement in targeted repair applications, emphasizing the importance of selecting repair materials based on anticipated environmental exposures.

In recent years, blended cement systems incorporating both CAC and calcium sulfate (gypsum) with portland cement (PC) have been developed to utilize the rapid hardening characteristics of CAC but at a reduced cost. While the durability of CAC is well researched and documented, the durability of these new blended systems was not yet fully understood at the onset of this study. The focus of this research was to evaluate the performance and long-term durability of various blended systems which utilize CAC or CSA to attain rapid hardening.

Long-term durability of concrete systems is best evaluated through outdoor exposure monitoring. The University of Texas at Austin established their first large-scale outdoor exposure site in 2001 to investigate viable techniques for preventing expansion and cracking due to ASR and/or DEF. In the decades since, the on-site capabilities were expanded to include long-term evaluation of external sulfate attack, physical sulfate attack and carbonation. In 2014, a marine exposure site was established along the Texas coast capable of evaluating steel reinforcement corrosion. The various UT exposure sites have been employed in this study for over a decade and monitoring will continue indefinitely.

The main conclusions of this study are as follows:

Alkali-Silica Reaction

Calcium aluminate cement provides superior protection against ASR compared to OPC concrete. When calcium aluminate cement is blended with OPC or CSA, the durability of the concrete system is reduced, but still performs superior to pure OPC concrete systems

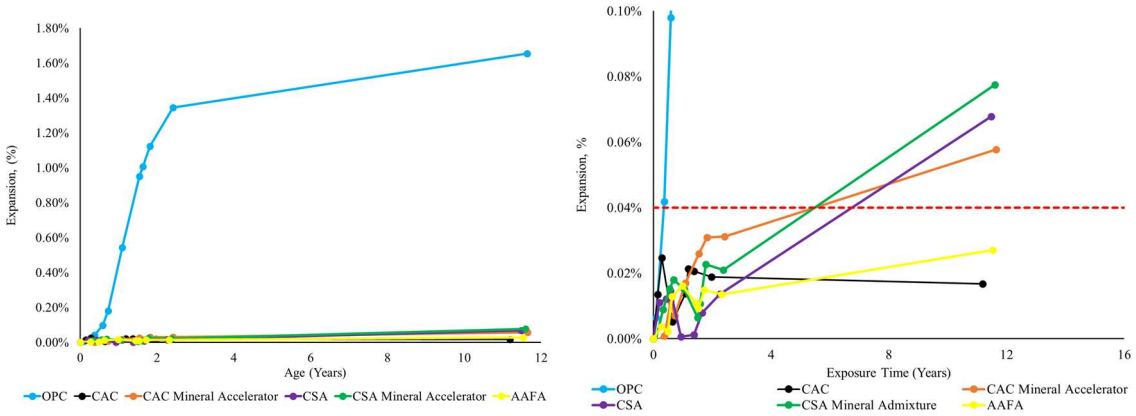

.

Figure 1: (a) Long-term expansion of ASR exposure blocks and (b) ASR exposure block expansion results shown with a 0.10% maximum expansion

External and Physical Sulfate Attack

As expected from historical documentation, pure CAC concrete systems perform well in sulfate-rich environments. Conversely, blended CAC systems may not be appropriate for use when exposed to high sulfate conditions. Blended OPC|CAC and OPC|CSA based concrete systems and pure CSA base concrete systems fully deteriorated within 3 years when exposed to 0.89% and 5.0% sodium sulfate in outdoor exposure due to external sulfate attack. The OPC control concrete also deteriorated within a similar time-frame, but at a significantly higher level of expansion. Figure 2 shows the CAC system after 10 years in outdoor sodium sulfate conditions.

Figure 2: Outdoor vertically placed CAC concretes in 5% Sodium Sulfate Soils

Delayed Ettringite Formation (DEF)

CAC concrete systems have not shown to be susceptible to DEF; however, significant expansion is observed with CAC blended systems. Though significant, the levels of expansion observed in blended systems are roughly half that observed in pure OPC concrete systems at 12 years.

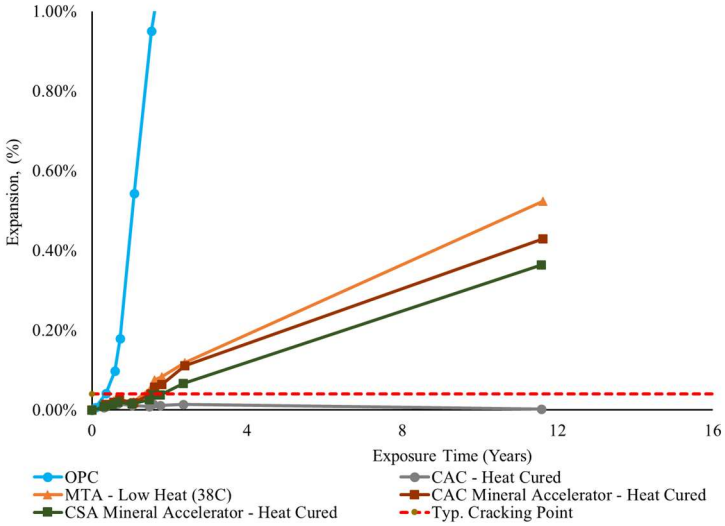

Figure 3: DEF Exposure Block Expansions

Steel Reinforcement Corrosion

Exposure blocks were lost due to Hurricane Harvey in 2017 and long-term measurements are not available for these blocks

Carbonation

Concrete systems that employ 100% OPC offer superior carbonation resistance compared to CAC and CSA blended systems, for the same curing conditions and w/cm ratios. The maximum depth of carbonation for the OPC control concrete reached 2-mm at 11 years; whereas, maximum depth of carbonation for the blended systems ranged between 9-mm and 14.5-mm at 11 years.

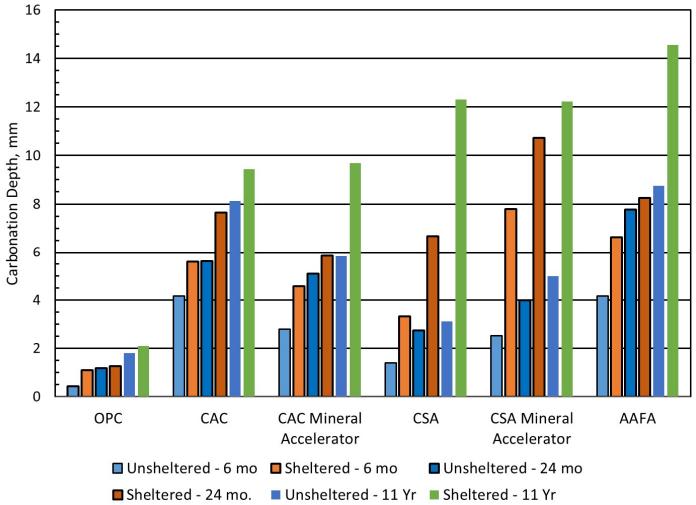

Figure 4: Carbonation depth observed in concrete samples